Fakultät für Medizin

Institut für Molekulare Immunologie

The role of IKKα in macrophage polarization to energy metabolism during development of pancreatic cancer

Çiğdem Atay

Vollständiger Abdruck der von der Fakultät für Medizin der Technischen Universität München zur Erlangung des akademischen Grades eines

Doctor of Philosophy (Ph.D.)

genehmigten Dissertation.

Vorsitzende: Univ.-Prof. Dr. Agnes Görlach

Prüfer der Dissertation:

1.Univ.- Prof. Dr. Florian R. Greten

2. Univ.-Prof. Dr. Jürgen Ruland

Betreuerin: Priv.-Doz. Melek Canan Arkan-Greten, Ph.D.

Die Dissertation wurde am 10.05.2013 bei der Fakultät für Medizin der Technischen Universität München eingereicht und durch die Fakultät für Medizin am 31.07.2013 angenommen.

TABLE OF CONTENTS

LIST OF FIGURES

LIST OF TABLES

ABBREVIATIONS

A/B	acrylamide/bisacrylamide
ADM	acinar to ductal metaplasia
ADP	adenosine diphosphate
AIB1	amplified in breast cancer 1
α-SMA	α-smooth muscle actin
Ang-2	Angiopoietin-2
APC	Adenomatous polyposis coli
APS	ammonium persulphate
ATP	adenosine triphosphate
Bcl	B-cell CLL/lymphoma
bHLH-PAS	basic helix-loop-helix-Per-ARNT-Sim
BMI	Body mass index
BPB	bromophenol blue
BRCA2	Breast Cancer 2
BSA	bovine serum albumin
c-FLIP	FLICE-inhibitory protein
c-IAP	cellular inhibitor of apoptosis
Ca	calcium
CAFs	cancer associated fibroblasts
CCL	chemokine (C-C) ligand
CD	cluster of differentiation
CDK	cyclin-dependent kinase
CDKN2A	cyclin-dependent kinase inhibitor 2A
CoA	Coenzyme A
COX	cyclooxygenase
CP	chronic pancreatitis
CRI	cancer-related inflammation
CSC	cancer stem cell
CSF1	colony-stimulating factor 1
CXCL	chemokine ligand C-X-C motif
Cyt c	cytochrome c
DC	dendritic cells
DEC1	differentially expressed in chondrocytes 1
DEPC	Diethylpyrocarbonate
DHAP	Dihydroxyacetone phosphate
Dhh	Desert
dl	deciliter
DLBCL	diffuse large B-cell lymphoma
DMEM	Dulbecco’s modified eagle medium
DNA	deoxyribonucleic acid
DPC4	Deleted in pancreatic carcinoma 4

DR5	death receptor 5
DTT	Dithiothreitol
DUSP6	dual specificity phosphatase 6
ECM	extracellular matrix
EDTA	ethylenediaminetetraacetic acid
EGF	epidermal growt factor
EGFR	epidermal growth factor receptor
EGTA	ethylene glycol tetraacetic acid
EMA	ethidium monoazide
EMT	epithelial-to-mesenchymal transition
EpCAM	epithelial cell adhesion molecule
ER	oestrogen receptor
ER	endoplasmic reticulum
ETC	electron transport chain
EtOH	ethanol
F-1,6-BP	Fructose 1,6-bisphosphate
F6P	Fructose 6-Phosphate
F6Pase	Fructose 6-Phosphatase
FACS	fluorescence activated cell sorting
FAD	flavin adenine dinucleotide
FADH	flavin adenine dinucleotide hydride
FAMMM	Familial atypical mole-multiple melanoma
FAP	Familial adenomatous polyposis
FAP	fibroblast activation protein
FBPase1	fructose 1,6-biphosphatase
FCCP	carbonylcyanide-p-trifluoromethoxyphenyl hydrozone
FCS	fetal calf serum
FDG-PET	fluorodeoxyglucose positron emission tomography
FGF	fibroblasts growth factor
FMN	flavin mononucleotide (oxidized)
FMNH	flavin mononucleotide (reduced)
FSP-1	fibroblast specific protein-1
G6P	glucose 6-phosphate
G6Pase	glucose 6-phosphatase
G6pd2	glucose-6-phosphate dehydrogenase 2
GAP	glyceraldehyde 3-phosphate
GAPDH	glyceraldehyde 3-phosphate dehydrogenase
GBS	gram positive human pathogen group B Streptococcus
GLUT	glucose transporter molecules
GM-CSF	granulocyte macrophage-colony stimulating factor
G-MDSC	granulocytic myeloid-derived suppressor cells
GLT1	glutamate transporter 1
GLS	glutaminase
Gpi1	glucose phosphate isomerase 1

GS	glutamine synthetase
GTPase	guanosin triphosphatase
H_2O	water
H_2O_2	hydrogen peroxide
HCl	hydrochloric acid
HGF	hepatocyte growth factor
Hh	hedgehog
HIF	hypoxia inducible factor
HK	hexokinase
HNPCC	Hereditary nonpolyposis colon cancer
ICAM	intercellular adhesion molecule
IFN	interferon
IGF	insulin-like growth factor
IHC	immunohistochemistry
Ihh	Indian
IκB	inhibitors of NF-κB
IKK	IκB kinase
IL	interleukin
INK4	inhibitors of CDK4
iNOS	inductible nitric oxide
IP	intra peritoneal
IPMN	intraductal papillary mucinous neoplasms
IRS-1	insulin substrate substrate-1
kg	kilogram
K-ras	Kirsten-ras
LDH	lactate dehydrogenase
LPS	lipopolysaccharide
m^2	square meter
MACS	magnetic activated cell sorting
MALT	mucosa-associated lymphoid tissue
MCP	monocyte chemotactic protein
M-CSF	macrophage colony stimulating factor
MDSC	myeloid-derived suppressor cell
mg	miligram
MHC	major histocompatibility complex
min	minute
MIP	macrophage inflammatory protein
ml	mililiter
MMP	matrix metalloproteinase
mRNA	messenger RNA

MSCs	mesenchymal stem cells
mTOR	mediator mammalian target of rapamycin
MYB	myeloblastosis
Myc	myelocytomatosis oncogene
NaCl	sodium chloride
NAD	nicotinamide adenine dinucleotide
NADH	nicotinamide adenine dinucleotide hydride
NADPHox	NADPH oxidase
NCOA3	nuclear receptor coactivator 3
NE	neutrophil elastase
NEMO	NF-κB essential mediator
NF-κB	Nuclear Factor kappa B
ng	nanogram
NIK	NF-κB inducing kinase
NK	natural killer
NLS	nuclear localization signal
nm	nanometer
NO	nitric oxide
NSAIDs	non-steroidal anti-inflammatory drugs
OAA	oxaloacetate
OAT	ornithine aminotransferase
OPN	osteopontin
PAD	protein assay diution
PanIN	pancreatic intraepithelial neoplasia
PAR1	Prader-Willi/Angelman region-1
PBS	phosphate buffered saline
PBS-T	phosphate buffered saline-tween
PC	pancreatic cancer
PDAC	pancreatic ductal adenocarcinoma
PDC	Pyruvate dehydrogenase complex
PDGF	platelet derived growth factor
PDGFR	platelet-derived factor receptor
PDH	pyruvate dehydrogenase
PDK1	pyruvate dehydrogenase kinase 1
PEP	phosphoenolpyruvate
PFA	paraformaldehyde
PFK	phosphofructokinase
PGF	placental growth factor
PGK	phosphoglycerate kinase
PGM	phosphoglycerate mutase
Pi	inorganic phosphate
PI3K	phosphatidylinositol-3 kinase
PMSF	Phenylmethylsulfonyl Fluoride
PPP	pentose phosphate pathway

Prps1	phosphoribosyl pyrophosphate synthase 1
PTCH	Patched
PTEN	phosphatase and tensin homolog
PyMT	polyoma middle T
RANKL	receptor activator of NF-κB ligand
RARβ	retinoic acid receptor β
RAS	rat sarcoma
RBC	red blood cell
Rbks	ribokinase
RCR	respiratory control ratio
RHD	REL homolog domain
RMA	Robust Multi-Array Analysis
RNA	ribonucleic acid
ROS	reactive oxygen species
Rpe	ribulose-5-phosphate-3-epimerase
Rpia	ribose 5-phosphate isomerase A
rpm	revolutions per minute
RT	room temperature
RT-PCR	real time-polymerase chain reaction
SCC	squamous cell carcinomas
scRNA	scrambled RNA
SCO2	synthesis of cytochrome c oxidase 2
SDF	stromal cell-derived factor
SDS	sodium dodecyl sulfate
SEM	standard error of the mean
SERPINB5	serpin peptidase inhibitor, clade B
Shh	Sonig
siRNA	small interfering RNA
SKP2	S-phase kinase-associated protein 2, E3 ubiquitin protein ligase
SMRT	silencing mediator for retinoid or thyroid-hormone receptors
SMO	Smoothened
SOCS1	suppressor of cytokine signaling 1
SOS	son of sevenless
SPARC	secreted protein, acidic rich in cysteine
Spp	secreted phosphoprotein
SRC-1	steroid hormone receptor coactivator-1
STAT	signal transduction and activator of transcription
Stra13	stimulated by retinoic acid 13 homolog (mouse)
Taldo1	transaldolase 1
TAE	Tris-Acetate EDTA
TAM	tumor-associated macrophage
TAN	tumor-associated neutrophil
TCA	Tricarboxylic acid
TCR	T-cell receptor

TEM	Tie2-expressing monocyte
TEMED	Tetramethylethylenediamine
TGF	transforming growth factor
Th	T helper
TIGER	TP53-induced glycolysis and apoptosis regulator
Tkt	transketolase
TLR	Toll-like receptor
TME	tumor microenvironment
TNFα	tumor necrosis factor α
TP53	tumor protein 53
TPI	triose phosphate isomerase
TPP	thiamine pyrophosphate
TRAF3	TNF receptor-associated factor 3
Tregs	regulatory T cells
TUNEL	Tdt-mediated dUTP-biotin nick end labeling
VCAM	vascular cell adhesion molecule
VEGF	vascular endothelial growth factor
VEGFR	vascular endothelial growth factor receptor
VHL	Von Hippel Lindau
WB	western blot
Wnt	mouse homolog of wingless
1,3-BPG	1,3-bisphosphoglycerate
2,3-BPG	2,3-bisphosphoglycerate
2-DG	2-Deoxy Glucose

ABSTRACT

Pancreatic ductal adenocarcinoma (PDAC) is a very lethal type of exocrine pancreas cancer and constitutive activation of *K-ras* was suggested to initiate PDAC development. Furthermore, NF-κB signaling was shown to be involved in *K-ras*-driven PDAC progression. This pathway is essential for the regulation of immune and inflammatory responses, and involved in pathogenesis of chronic inflammatory and autoimmune diseases. The activation of NF-κB is orchestrated by IκB kinase, consisting of IKKα, IKKβ and IKKγ. Among them, IKKα is required for lymphoid organogenesis, adaptive immune responses and resolution of acute inflammation. Thus, based on its importance, we investigated the role of IKKα in *K-ras* induced PDAC. To that end, Ikkα$^{F/F}$-p48-Kras mouse model in which *K-ras* is constitutively activated and *Ikkα* deleted in pancreas was used. Importantly, loss of *Ikkα* resulted in accelerated pancreatic tumor progression in p48-Kras mice. Moreover, not only embryonic but also post-natal *Ikkα* deletion accelerates the formation of *K-ras* induced premalignant lesions. Furthermore, exacerbated inflammation and fibrosis is observed in the pancreas of Ikkα$^{F/F}$-p48-Kras mice, suggesting that tumor microenvironment might have a role during fast PDAC progression. Importantly, expression of M2 polarized macrophage markers and cytokines by myeloid cells are increased, suggesting that IL4/IL13 signaling pathway is important during PDAC development. However, whole body *Stat6* deletion did not reverse the phenotype of Ikkα$^{F/F}$-p48-Kras mice showing that accelerated PDAC development is independent from Stat6 signaling. In addition, IKKα ablation results in increased expression of glycolytic enzymes, decreased number and respiration rate of mitochondria in Ikkα$^{F/F}$-p48-Kras mice, proposing that glycolytic switch might regulate accelerated tumor development. Thus, Ikkα$^{F/F}$-p48-Kras mice were treated with 2-Deoxy Glucose (2-DG) to inhibit glycolysis. However, the treatment displays partial effects and although pancreas distortion is similar to untreated animals, tumor incidence is reduced in 2-DG treated mice. Besides, 2-DG treatment decreases expression of M2 macrophage markers and increases expression of pro-inflammatory cytokines by CD11b^{+} cells. Moreover, expression of several genes involved in glycolysis and pentose phosphate pathway (PPP) is altered in pancreas derived CD11b^{+} cells, suggesting that 2-DG treatment does not only affect macrophage polarization but also energy metabolism in Ikkα$^{F/F}$-p48-Kras animals.

1. INTRODUCTION

1.1. Epidemiology and Etiology of Pancreatic Cancer

Pancreatic cancer (PC) is a sporadic type of cancer and composes 2.2 % of all cancer cases in 2008 (Ferlay *et al*., 2010). The frequency of pancreatic cancer is relatively low and changes according to different geographic regions. For instance, age-adjusted frequencies are about 6-12/100.000 per year in Western countries and generally show elevated pattern in developed countries including North America, Europe and Japan (Zavoral *et al*., 2011). This might not only be due to racial differences but also to better health services and early detection possibilities. Although the number of pancreatic cancer patients is relatively lower than other cancer types, it is still one of the main causes of cancer lethality in developed countries (Maisonneuve and Lowenfels, 2010). The reason behind is the difficulty of its diagnosis, which is usually not possible before the advanced stages. Thus, survival time for patients is strictly based on its early diagnosis. In general, less than 5% of tumors are possible to be removed surgically when they are diagnosed, and average survival rate differs from 13 to 21 months. If surgery is not possible, median survival decreases drastically to 2.5-8 months (Genkinger *et al*., 2009). Furthermore, incidence of pancreatic cancer is higher in men than women suggesting a possible link between female hormones and PC progression. Nevertheless, Wahi *et al.* reported that there is no connection between PC and female hormones (Wahi *et al.,* 2009) proposing that the variety of risk between men and women might derive from various other reasons, such as smoking or different diet.

The major risk factors for pancreatic cancer include smoking, increased age, family history, genetic predisposition, several diseases such as diabetes, glucose intolerance, overweight and obesity, and long-term chronic pancreatitis (CP).

Cigarette smoking augments the risk of PC similar to the other types of cancer (Iodice *et al*., 2008; Boffetta *et al*., 2008). According to the International Pancreatic Cancer Cohort Consortium's study in which 1481 pancreatic cancer cases and 1539 controls are evaluated, current smoking increases pancreatic cancer risk around 80 % (Lynch *et al*., 2009). Furthermore, a meta-analysis in which 82 different studies were analyzed to display the connection of smoking and pancreatic cancer showed that the predicted pancreatic cancer risk is 1.74 (95% CI, 1.61–

1.87) for current smokers and 1.20 (95% CI, 1.11–1.29) for former smokers in comparison to non-smokers. Although the smoking is quitted, the risk is still higher during at least the next 10 years. If the smoking is terminated more than 10 years ago, then the risk is lower than that for current smokers' (Iodice *et al*., 2008). Additionally, consuming non-cigarette tobacco including cigar, pipes or smokeless tobacco have been shown to elevate pancreatic cancer risk as well (Baker *et al*., 2000; Henley *et al*., 2004; Boffetta *et al*., 2005; Shapiro *et al*, 2000; Alguacil *et al*., 2004; Hassan *et al*., 2007).

Similar to smoking, there is a known relationship between chronic inflammatory diseases and cancer development. As stated in several reports, especially long term inflammation in organs might underlie tumorigenesis. Consistently, chronic pancreatitis (CP) is shown to correlate with PC. However, it is not one of the essential risk factors since only 5% of PC patients had CP before detection and Lowenfels *et al*. showed that at least five years enduring CP increases PC risk. On the other hand, the major risk group consists of the patients who have hereditary pancreatitis and trophical pancreatitis that might enhance the risk of PC at least 50 fold more (Lowenfels *et al*., 2001; Raimondi *et al*., 2010). If people with hereditary pancreatic cancer smoked, development of PC is accelerated and the detection might be possible up to 20 years earlier than in non-smokers (Zavoral *et al*., 2011).

Genetic background is an important factor for cancer development and some genetic abnormalities/diseases are established to increase the pancreatic cancer risk, including germline mutations of *BRCA2* (breast-ovarian familial cancer), *CDKN2A* (familial atypical mole-multiple melanoma (FAMMM)), the mismatch repair genes (hereditary nonpolyposis colon cancer (HNPCC) or Lynch Syndrome), *TP53* (Li-Fraumeni syndrome), *APC* (familial adenomatous polyposis (FAP)) (Murphy *et al*., 2002; Goggins *et al*., 1996; Klein *et al*., 2001; Lynch *et al*., 2002; Giardiello *et al*., 2000; Lim *et al*., 2004; Cowgill *et al*., 2003; Giardiello *et al*., 1993).

Overweight and obesity has been shown to constitute a major risk for PC development since a positive correlation between high BMI values (Body mass index: individual's body mass by square of his/her height (kg/m^2)) and increased risk of pancreatic cancer has been established by several studies (Berrington de Gonzales *et al*., 2003; Larsson *et al*., 2007; Renehan *et al*., 2008). However, the level of correlation changes according to the region. For instance, in Japan, being an obese does not increase the risk of cancer (Otsuki *et al*., 2007) whereas in Western countries there is a great correlation between obesity and cancer (Berrington de Gonzales *et al*.,

2003; Giovanni and Michaud, 2007; Howe and Burch, 1996; Michaud and Fuchs, 2005). In this correlation, central obesity is suggested to be the key factor because it is related with glucose intolerance and insulin resistance, and high insulin levels are proposed to affect the incidence of pancreatic cancer (Jiao and Li, 2011). Gapstur *et al.* have reported that postload plasma glucose levels and BMI were positively correlated with PC mortality for men, but not for women. Risk of PC mortality was 2.2 fold higher for people whose postload plasma glucose levels were ≥200 mg/dl at baseline compared with those whose levels were ≤119 mg/dl. Furthermore, men with BMI; ≥ 26 kg/m^2, had a 3-fold higher risk of PC mortality compared to men with lower BMI (Gapstur *et al*, 2000). In addition, type II diabetes and pancreatic cancer risk have been explored by several meta-analyses and it has been discovered that pancreatic cancer risk is higher for patients who have diabetes longer than 5 years. Moreover, patients with long term diabetes (≥5 years) displayed 50% lesser risk of pancreatic cancer in comparison to patients who had recently detected diabetes (<4 years) (Everhart *et al*., 1995; Huxley *et al*., 2005).

Increased age is another risk factor for PC. In general, the frequency of PC is very low in three first decades of life but afterwards the incidence strikingly heightens and diagnosis is the highest after the age of 50, with a mean value of 65-72 years (Zavoral *et al*., 2011; Jiao and Li, 2010). In addition, Li *et al*. reported that only 10% of the patients are diagnosed before 50 years of age (Li *et al*., 2009).

Apart from these major risk factors, there also several other factors, which might take part in enhancing PC progression including alcohol consumption, special diet, allergy, occupational risks such as being exposed to petrochemical products, use of non-steroidal anti-inflammatory drugs (NSAIDs), and viral infections.

1.2. Histological, Genetic and Molecular Changes in Pancreatic Cancer Development

There are several types of pancreatic cancer showing different histological features, consisting of adenosquamous carcinoma, colloid carcinoma, hepatoid carcinoma, medullary carcinoma, undifferentiated carcinoma with/without osteoclast-like giant cells, solid pseudopapillary carcinoma, and pancreatoblastoma (Xiong and Abbruzzese, 2002). The proper description of the neoplasm is important since they show different pathogenesis and prognosis.

On the other hand, it is also possible to classify pancreatic cancers into two groups; endocrine and exocrine type of pancreatic cancers. Exocrine pancreatic neoplasms include pancreatic intraepithelial neoplasias (PanINs), intraductal papillary mucinous neoplasms (IPMNs), mucinous cystic tumors and serous cystic tumors. They are frequent types of pancreatic cancers and although there are discussions, it is believed that they stem from pancreatic ducts and acinar cells. On the other hand, endocrine pancreas cancers including pancreatoblastoma, pancreatic acinar cell carcinoma and solid pseudopapillary tumor are the tumors of islet cells. In comparison to exocrine pancreatic cancers, their incidence is rare.

Pancreatic cancer progression is a multistep process. Before tumor develops, several types of precursor lesions occur in pancreas such as pancreatic intraepithelial neoplasia (PanIN), the mucinous cystic neoplasm and the intraductal papillary mucinous neoplasm (IPMN). Among them, PanINs are the most common types that lead to invasive pancretic cancer; pancreatic ductal adenocarcinoma (PDAC). They are classified as PanIN-1, PanIN-2 and PanIN-3 according to their histological differences and altered genetic/molecular structures. During tumor development, several accumulating genetic changes induce the differentiation of normal epithelial cells into malignant ones. Early genetic alterations include *K-ras* mutations and telomere shortening, whereas in intermediate stage loss of *p16/CDKN2A* is commonly seen. In the late stage, inactivation of other tumor suppressor genes including *DPC4/SMAD4*, *TP53*, and *BRCA2* are observed. Instead of molecular changes, histological changes are also observed according to the stage of lesions. At the beginning, normal cuboidal epithelial cells differentiate into long- columnar epithelium, followed by loss of epithelial cell polarity, forming papillary folding and shedding into the lumen and finally forming precursor lesions.

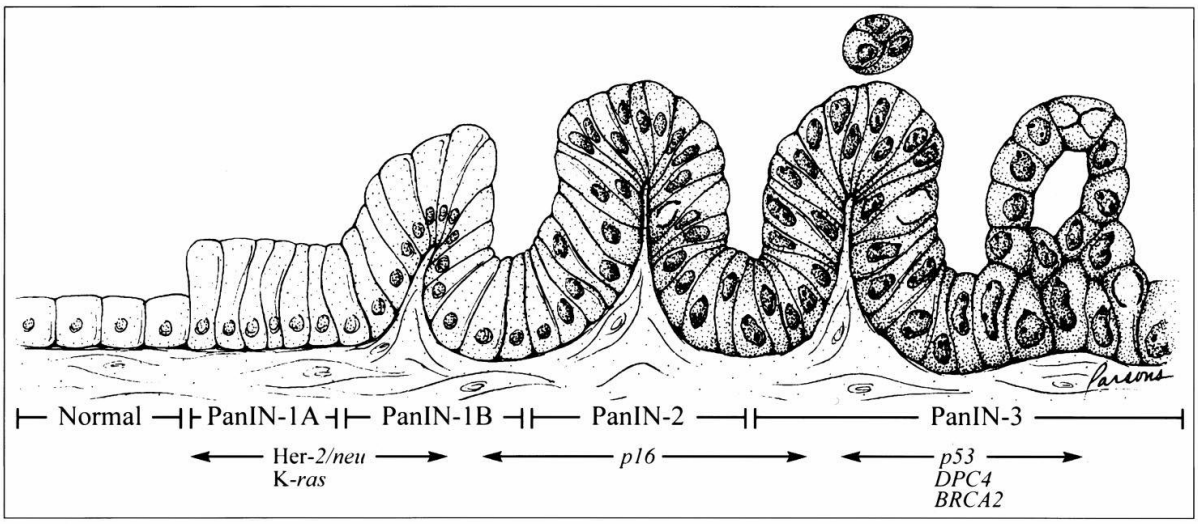

Figure 1.1. Histological changes in the normal epithelium of pancreas during PanIN development (Taken from Hruban *et al*., 2000). These alterations are correlated with genetic changes which are seen specifically in the different stages of PanIN formation.

PDAC is one of the lethal pancreatic cancer type and 95% of patients have activating mutation in *K-ras* (Caldas and Kern, 1995). *K-ras* proto-oncogene is a member of small GTPase protein family called RAS, which is required for cellular signal transduction regulating cell proliferation, differentiation and survival. Activating mutations delete the GTPase function of K-ras protein, which results in constitutive activation of Ras pathway and intracellular signalling (Maitra and Hruban, 2008) that may lead to unlimited cell proliferation. The activating point mutations generally take place in codon 12 and 13, whereas other codons such as 59, 61, 63 might rarely be mutated in PC (Deramaudt and Rustgi, 2005). In addition, *K-ras* mutations are not specific for PDAC since several mutations have already been shown in other types of pancreatic cancers, chronic pancreatitis, and even in the autopsy of normal pancreas tissues without any pancreatic disease history (Tabata *et al*., 1993; Hruban *et al*., 2000; Tada *et al*., 1996). Furthermore, as the *K-ras* mutations have been established in PanINs, it is suggested that these mutations are necessary for the initiation of tumorigenesis but further changes such as loss of *p16* are required for progression (Aguirre *et al*., 2003; Hingorini *et al*., 2003; Bardeesy *et al*., 2006; Ijichi *et al*., 2006; Fleming *et al.,* 2005). Apart from *K-ras* mutations, some other proto-oncogenes have been also established to play an important role for pancreatic cancer development including *c-Myc, MYB, AIB1/NCOA3,* and *EGFR (*Novak *et al.,* 2005*;* Aguirre *et al.,* 2004*;* Bashyam *et al.,* 2005*).*

Regulation of the expression of several tumor suppressor genes including *p16/CDKN2* (also known as *INK4*), *TP53*, *Deleted in pancreatic carcinoma 4* (*DPC4*; also known as *SMAD4*) is also considerable for pancreatic cancer progression. *p16/CDKN2* is a cyclin-dependent kinase

inhibitor, which orchestrates cell cycle through CDK-4 and-6. Similar to *K-ras, p16* inactivation is found in 90% of PC patients. Another tumor suppressor, *TP53,* as its nickname 'the guardian of the genome' implies, has essential functions in the regulation of cell proliferation and apoptosis, and is lost in 50-75% of pancreatic cancers. Since it is important for the regulation of cell death, its disruption also results in the accumulation of abnormal genetic alterations (Maitra and Hruban, 2008). *DPC4/SMAD4* loss generally occurs in PanIN-3 lesions and around 55% of PC cases show loss/inactivation of this tumor suppressor gene. It is involved in TGF-β pathway, which has inhibitory function on cell growth. Thus, when there is no functional *SMAD4* in pancreatic cancer cells, TGF-β pathway can not keep on its suppressive function anymore, which in turn leads to the unlimited growth of pancreatic cancer cells (Siegel and Massague, 2003). Inactivation of all these tumor suppressor genes is not only achieved by mutations or chromosomal rearrangements, but also by epigenetic mechanisms. Epigenetic regulations in pancreatic cancer consist of hypermethylation of genes, which are essential in cell homeostasis including p16 (*p16*; cyclin-dependent kinase inhibitor), retinoic acid receptor β (*RARβ*; cell growth control), Cyclin D2 (*Cyclin D2*; cell cycle control), suppressor of cytokine signaling 1 (*SOCS1*; inhibitor of JAK/STAT pathway), and dual specificity phosphatase 6 (*DUSP6*; negative regulator of MAPK pathway), and hypomethylation of several genes including *14-3-3σ* (sigma) (also known as *stratifin*; p53 induced G2/M cell cycle arrest), *Maspin* (also known as *SERPINB5*; cell motility and cell death regulation), *Claudin 4* (Cell adhesion and invasion), *Mesothelin* (Cell adhesion), and *S100A4* (Cell motility and invasion) (Sato and Goggins, 2006). Furthermore, telomerase rearrangements and micro RNAs (miRNAs) have been established to be involved in several steps during pancreatic carcinogenesis.

In addition to molecular changes affecting only one single gene, activation/reactivation of several signaling pathways contributes to pancreatic cancer development including Notch, Hedgehog, TGFβ signaling and Wnt/β-catenin pathway. Furthermore, these signaling pathways have been shown to cooperate with mutant *K-ras* during pancreatic cancer development.

Notch signaling is an essential pathway for the development and differentiation of pancreas. Miyamoto *et al*. have reported that expression of Notch signaling pathway components are increased in PanIN lesions and invasive cancer both in human and mouse. Furthermore, EGF receptor (EGFR) activation results in activation of Notch signaling pathway in exocrine pancreas and is involved in differentiation process of epithelium by TGFα suggesting that Notch is required in TGFα-induced malignant epithelium formation (Miyamoto *et al*., 2003). Other

reports also established the presence of correlation between Notch overexpression and pancreatic cancer (Hingorini *et al*., 2003).

Hedgehog signaling is an important pathway for embryonic development and abnormal activation of the pathway has been shown to cause cancer such as breast, colon and prostate cancer (Maitra and Hruban, 2008). In this pathway, three secreted ligands, called Sonig (Shh), Desert (Dhh) and Indian (Ihh) hedgehog take part and activate the pathway by binding 12-transmembrane Patched (PTCH) receptor. This leads to the activation of Smoothened (SMO) receptor, which in turn pushes the accumulation of hedgehog (Hh) transcription factors; glioma associated oncogene homolog I family members (GLI1, GLI2, and GLI3) and translocation of these factors into the nucleus for the expression of target genes. It has been already established that abnormalities in Hh signaling pathway are found in chronic pancreatitis, PanIN lesions and PC (Maitra and Hruban, 2008). Thayer and colleagues have reported that high expression of Hh components was observed in PanINs and invasive lesions, but not in normal ductal epithelium in human. Moreover, abnormal expression of Shh caused the formation of some structures in mice, which are similar to human PanINs (Thayer *et al.*, 2003). In addition, Pasca di Magliano *et al.* have showed that epithelium-specific activation of the Hh pathway led to cancer in mice, which is unlike the human tumors, independent of PanIN lesions. When these mice were crossed to another model in which *K-ras is* mutated (K-ras^{G12D} mutation), PanIN formation was observed suggesting that only in the presence of mutated *K-ras*, abnormal Hh signaling can promote tumor development that is similar to those in humans (Pasca di Magliano *et al*., 2006).

Inactivation of TGFβ signaling by mutation or loss of *DPC4* has been detected in PDAC patients suggesting that TGFβ might play a tumor suppressor role. Consistently, in the presence of oncogenic *K-ras*, deficient TGFβ signaling based on the loss of *SMAD4* accelerated PDAC development in a mouse model (Bardeesy *et al*., 2006; Ijichi *et al*., 2006). Moreover, TGFβ signaling is related with desmoplasia. Löhr *et al.* reported that overexpression of TGFβ1 in transfected pancreatic tumor cells enhanced not only the expression of matrix proteins and growth factors, but also the formation of a dense stroma after their transplantation into the pancreas of nude mouse (Löhr *et al*., 2001).

Abnormal β-Catenin/Wnt Pathway signaling has been shown in PanINs and PDAC by several studies. Enhanced β-Catenin expression and accumulation in the nucleus of advanced PanIN lesions (mainly PanIN-2) and adenocarcinoma was detected in human (Al-Aynati *et al*,

2004). Consistently, another report established that total β-Catenin amount was intensified and Wnt/β-Catenin pathway was activated in 65% of human PDAC although most of them did not show β-Catenin mutations (Zeng *et al*., 2006). Recently, Morris *et al*. have explained the role of β-Catenin in oncogenically activated *K-ras* driven acinar to ductal metaplasia (ADM) and PanIN development. According to their study, β-Catenin is required for acinar cell regeneration and sustained β-Catenin expression inhibits ADM and PanIN formation induced by mutant *K-ras* expression. On the other hand, β-Catenin expression is increased when the precursor lesion numbers start to be dominant in the epithelium suggesting that the balance between β-Catenin and mutant K-ras signaling pathways is important for the determination of acinar cells' fate (Morris IV *et al.*, 2010).

1.3. The Effect of Tumor Microenvironment in Cancer Progression

Tumorigenesis is a multistep event in which presence of genetic/epigenetic modifications result in alterations of cell biology, giving extraordinary abilities to normal cells and pushing them to become malignant. According to Hanahan and Weinberg, there are six general characteristics that most of the cancer types share, the so-called 'six hallmarks of cancer'. These hallmarks are: resistance to anti-growth signals, self-stimulation for cell growth, insensitivity to cell death inducing signals (apoptosis), limitless replication ability, continuous production of blood vessels (angiogenesis), and invading local tissue and spreading to other organs (metastasis) (Hanahan and Weinberg, 2000). Recently, a seventh hallmark is added to this list by Colotta and colleagues; that is cancer-related inflammation (CRI) (Colotta *et al*., 2009) (Figure 1.2).

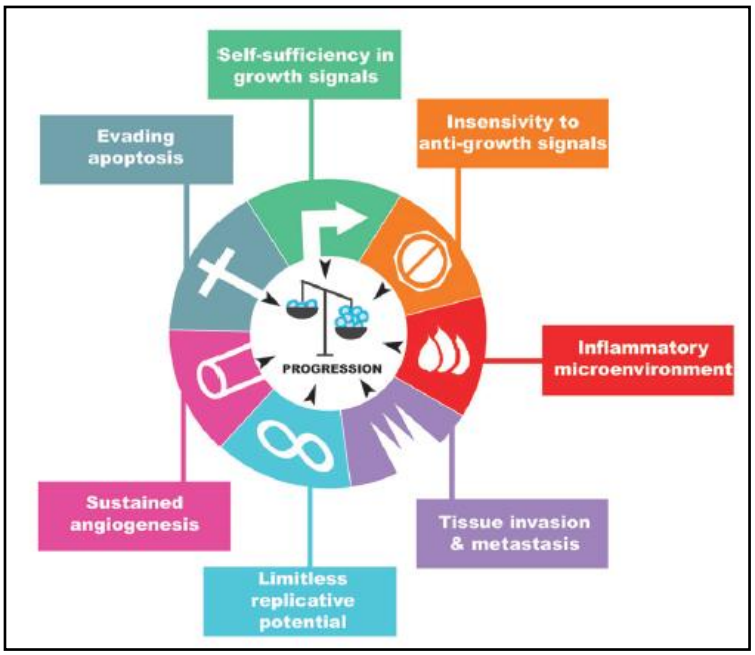

Figure 1.2. The hallmarks of cancer (Taken from Colotta *et al*., 2009). The six hallmarks of cancer are explained by Hanahan and Weinberg, and the seventh hallmark, inflammation, is added to this list by Mantovani.

Carcinomas are the largest group of human cancers, which generally develop from the epithelial cell layers of organs. Instead of transformed epithelial cells, supportive connective tissue (stroma) of the organ is also involved during carcinoma progression. However, the exact mechanism explaining how cancer progress in the cooperation of tumor and stromal cells is not known. Two mechanisms have been suggested for it: first suggestion is that stromal changes might happen and push epithelial cell transformation and second suggestion is that stromal cells might be activated by transformed epithelia in a paracrine loop (R.A. Weinberg, 2007; Bissell and Radisky, 2001; Polyak and Weinberg, 2009). Supporting connective tissue (stroma) creates 'tumor microenvironment' and based on its involvement in carcinogenesis, research on tumor microenvironment can be valuable to enlighten the molecular pathway of tumorigenesis. Tumor microenvironment consists of several cell types including endothelial and smooth muscle cells and pericytes, fibroblasts, and tumor infiltrating myeloid cells including dendritic cells, macrophages, neutrophils (Räsänen and Vaheri, 2010). Although it is not still completely known how tumor microenvironment supports tumor formation, it is suggested that the main function behind is the secretion of several cytokines, growth factors, angiogenic factors and matrix metalloproteases (MMPs) (Backwill *et al*., 2001; Coussens *et al*., 2002).

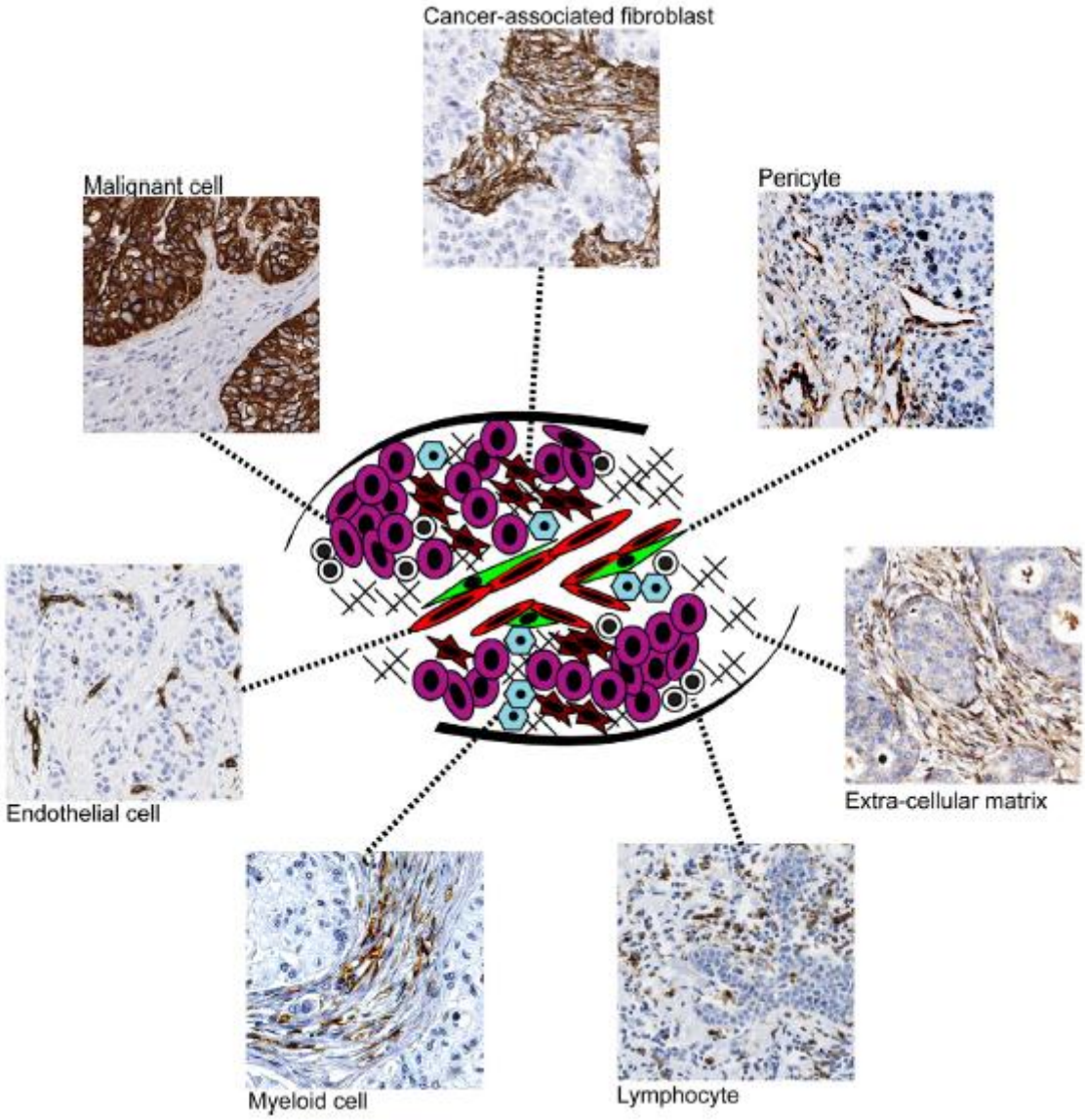

Figure 1.3. The components of tumor microenviroment (Taken from Pietras and Östman, 2010). The figure shows different representative pictures for the components of TME. Immunohistochemical staining was performed to display them and those markers are used specifically for each cell types: Malignant cells, cytokeratin 14; Cancer-associated fibroblasts, α-SMA; Pericytes, PDGF receptor-β; Extracellular matrix, collagen-1a1; Lymphocytes, CD45; Myeloid cells, CD11c; Endothelial cells, CD34.

1.3.1. Fibroblasts

Fibroblasts are the most prominent cells in connective tissues and they shape the stroma by producing extracellular matrix (ECM) components including fibronectin and collagens. Under normal conditions, fibroblasts are in an inactive quiescent phase. Upon an abnormal situation such as wound healing and fibrosis, they are activated and called as myofibroblasts, as first described by Giulio Gabbiani in 1971. Since cancer is evaluated as a wound that never heals, fibroblasts become activated too but they are not removed by a special type of cell death program, called nemosis, likewise the end of wound healing process (Eyden *et al*., 2009;

Räsänen and Vaheri, 2010). Activated fibroblasts, which are recruited into tumor stroma and affect tumorigenesis are named as cancer associated fibroblasts (CAFs) (Kalluri and Zeisberg, 2006; Hanahan and Weinberg, 2011). A variety of markers are used to differentiate CAFs from other cell types including α-smooth muscle actin (α-SMA), fibroblast specific protein-1 (FSP-1; also known as S100A4), fibroblast activation protein (FAP; also known as seprase), and platelet-derived factor receptor α/β (PDGFR α/β). Although the source of CAFs is not completely comprehended, they are supposed to stem from variable origins including local fibroblasts, bone marrow-derived mesenchymal stem cells (MSCs) and epithelial cells (Cirri and Chiarugi, 2011).

CAFs are highly found in tumor stroma, especially in breast, prostate and pancreatic cancer (Kalluri and Zeisberg, 2006; Pietras and Ostman, 2010) and have a complex role in tumor progression. Like inflammatory immune cells, they show inhibitory effects at the early stages of tumor development, whereas in later stages, they stimulate tumor growth and progression. In later stages of tumorigenesis CAF subgroups might promote tumorigenesis in different ways depending on tissue localization and their specific functions. For instance, CAFs can enhance cancer cell proliferation by secreting several growth factors, cytokines and hormones including hepatocyte growth factor (HGF), some epidermal growth factor (EGF) family members, insulin-like growth factor-1 (IGF-1), and stromal cell-derived factor-1 (SDF-1, also known as CXCL12) (Cirri and Chiarugi, 2011; Erez *et al*., 2010; Franco *et al*., 2010; Kalluri and Zeisberg, 2006; Orimo *et al*., 2005; Rosen and MacDougald, 2006; Spaeth *et al*., 2009). Activated fibroblasts can attract and recruit inflammatory immune cells into the tumor microenvironment by secreting a variety of pro-inflammatory molecules (Hanahan and Coussens, 2012; Erez *et al*., 2010), and enhance vascularization in several tumor types via producing pro-angiogenic signaling molecules, such as vascular endothelial growth factor (VEGF), FGF2, interleukin 8 (IL8; also known as CXCL8), and platelet derived growth factor-C (PDGF-C). In addition, CAFs facilitate storage and secretion of pro-angiogenic factors by producing ECM proteins and ECM-degrading enzymes, such as MMP-9, -13,-14 (Kalluri and Zeisberg, 2006; Pietras and Ostman, 2010; Räsänen and Vaheri, 2010). Production of MMPs does not only degrade ECM, but also aids cancer cell invasion. Lederle *et al*. showed that MMP-13 secretion by CAFs stimulates tumor angiogenesis by releasing VEGF from ECM, thereby causing elevated invasion of squamous cell carcinoma (Lederle *et al*, 2010). MMP-1 has also been reported to stimulate cancer cell invasiveness via PAR1-dependent Ca^{+2} signals (Boire *et al*., 2005) In addition, CAFs can also increase migratory capacity and invasion of cancer cells by orchestrating epithelial-to-mesenchymal transition (EMT) via secretion of TGF-β (Chaffer and Weinberg, 2011).

A variety of studies have showed tumor growth and cancer cell apoptosis are restricted by CAFs (Kalluri and Zeisberg, 2006; Loeffler *et al*., 2006; Pietras and Ostman, 2010) via secreting diffusible paracrine survival factors such as IGF-1, IGF-2 and by producing ECM molecules and ECM-remodeling proteases that contribute to formation of a neoplastic ECM, distinctive from normal tissue stroma, that provides nondiffusible survival signals (e.g., ligands for antiapoptotic integrins). Lu *et al.* already exhibited that CAF-derived ECM take part in regulating cancer cell survival (Lu *et al*., 2011).

1.3.2. Dendritic cells (DCs)

Tumor microenvironment includes several types of immune cells, such as natural killer (NK) cells, gamma delta T and natural killer T (NKT) cells, dendritic cells (DCs), and adaptive immune system components B- and T-cells. Among them, DCs orchestrate activation of T, B, NK and NKT cells and their cytokine secretion (Gao *et al*., 2003; Borg *et al*., 2003; Smyth *et al*., 2001; Hildner *et al*., 2008; Crowe *et al*., 2002; Shankaran *et al*., 2001; Banchereau *et al*., 1998; Shortman *et al*., 2002; Chaput *et al.*, 2008). DCs are very important for initiation of adaptive responses. They are found in peripheral tissues where they pick up antigens and then migrate to the draining lymph nodes where they present processed antigens to naïve T cells via major histocompatibility complex (MHC) class I and II, and CD1d antigen presenting molecules (Shortman *et al*., 2002). As a result of activation, DCs enhance T cell proliferation and differentiation into helper and effector cells. Conversely, they also show inhibitory effects on T and NK cells via producing regulatory T cell development and/or enhancing immune tolerance by inactivating mature T cells and regulating deletion of self-reactive thymocytes (Chaput *et al*., 2008). Thus, the effect of DCs on cancer progression is still puzzling. Moreover, although DCs take place in tumor microenvironment (TME), it is suggested that TME endanger their differentiation, maturation and survival. For instance, Ménétrier-Caux *et al.* showed that in renal carcinoma, precursor cells are induced to differentiate into macrophages rather than DCs (Ménétrier-Caux *et al*., 1999). Additionally, it is reported that DCs are obstructed in an immature stage, with a low antigen-presenting ability in breast, head, neck, and lung cancers (Almand *et al*., 2000; Coventry *et al*., 2002). It is suggested that TME achieves this by secreting a variety of pro-inflammatory molecules including CXCL8, M-CSF/IL6, VEGF, TGFβ, indoleamine, extracellular adenosine, and 2, 3-deoxygenase, which principally and eventually activates the signal transduction and activator of transcription 3 (STAT3) (Gabrilovich *et al*., 1996; Zou, 2005; Novitsky *et al*., 2008; Pardoll and Allison, 2004; Kortylewski *et al*., 2005; Cheng *et al*,

2003). Other reports have shown that tumor-infiltrating mature DCs have also been detected in many solid tumors such as gall bladder (Furihata *et al*., 2005), melanoma (Movassagh *et al*., 2004; Vermi *et al*., 2003), breast (Bell *et al*., 1999), and colorectal carcinomas (Schwaab *et al*., 2001).

1.3.3. Neutrophils

Another cell types, which are essential in immune system are neutrophils. They compose the biggest population of circulating leukocytes in human and have drastic functions in host defense including phagocytosis and killing the pathogens by producing several cytokines, toxic substances, reactive oxygen species (ROS), and proteases (Brinkmann and Zychlinsky, 2012; Fridlender and Albelda, 2012). Instead of their host protective roles, it is also shown that tumor-associated neutrophils (TANs) and their precursors including granulocytic myeloid-derived suppressor cells (G-MDSCs) take part in cancer development. Based on their subtype and the tissue/tumor they infiltrate, they show variable effects during carcinogenesis. Neutrophils are induced to be polarized by several factors such as TGFβ and differentiate into N1 and N2 neutrophils. N1 neutrophils exhibit pro-inflammatory, anti-tumorigenic roles, whereas N2 neutrophils behave for the benefit of cancer and can induce tumorigenesis via secreting angiogenic factors, suppressing immune response against tumors, pushing tumor cell invasion and metastasis (Schmielau *et al*., 2001; Shojaei *et al*., 2008; Huh *et al*., 2010; Fridlender *et al*., 2009).

MMP-9 secretion by neutrophils was shown to induce tumor growth. However, according to microarray analysis performed by Fridlender *et al*., expression of MMP-9 by TANs is lower than naïve neutrophils proposing that MMP-9 expression has essential roles during the early stages of tumor progression rather than late stages (Fridlender *et al.*, 2012). Furthermore, similar to the macrophages, elevated accumulation of neutrophils promote vascularization through MMP-9 and there is a correlation between MMP-9 and VEGF (Nozawa *et al*., 2006; Kuang *et al*., 2011). Nozawa *et al*. reported that transient depletion of neutrophils stopped angiogenic switch in early stage of tumorigenesis by inhibiting VEGF binding to its receptor VEGFR in pancreatic islet carcinogenesis (Nozawa *et al*., 2006).

Neutrophil elastase (NE) secreted by neutrophils also play important roles in angiogenesis, extravasation of tumor cells and metastasis. In human and mouse lung adenocarcinoma, it was

shown that NE degrades insulin substrate substrate-1 (IRS-1), which leads to enhanced activation of Akt/PI3K pathway toward tumor cell proliferation (Houghton *et al*., 2010). This enzyme is also reported to be involved in tumor invasion by breaking ECM structure (Sun *et al*., 2004). Moreover, Doi *et al*. showed that ischemia-reperfusion induced hepatic cell metastasis was lowered via use of NE inhibitor ONO-5046 Na in rat colon adenocarcinoma model (Doi *et al*., 2002).

1.3.4. Macrophages

Tumor microenvironment orchestrates accumulation of macrophages around tumor area by secreting a variety of chemokines such as CCL2,-5,-7,-8, CXCL12 (also known as stromal-derived factor-1; SDF-1), as well as cytokines including VEGF, PDGF, and M-CSF. These factors enhance gathering of blood monocytes at tumor microenvironment where they further differentiate into tissue resident macrophages. As a result of the functional plasticity, tumor type and its local microenvironment, tissue resident macrophages are converted into M1 and M2 macrophages, which show functional differences (Ruffell *et al*., 2012). M1 macrophage polarization is induced by lipopolysaccharide (LPS), interferon gamma (IFNγ), and engagement of Toll-like receptors (TLRs). The classically activated M1 macrophages are required in the responses of type I helper T (Th1) cells against pathogens. This macrophage subgroup has immune-stimulatory Th1-orienting characteristics and shows high expression of major histocompatibility complex (MHC) class II, interleukin 12 (IL12), tumor necrosis factor α (TNFα). They are able to kill cells and pathogens, produce nitric oxide (NO) and reactive oxygen species (ROS) (Mantovani *et al*., 2005; Chomarat *et al*., 2000). On the other hand, alternatively activated M2 macrophages suppress Th1 adaptive immunity and take part in the responses of type II helper T (Th2) cells such as wound healing and humoral immunity (Gordon, 2003). M2 polarization is induced mainly by interleukin 4 (IL4) and 13 (IL13) and this subgroup show elevated interleukin 10 (IL10) expression (Figure 1.4).

Macrophages are shown to have multifaceted role during tumorigenesis. According to several studies, macrophages prevent cancer development, whereas some other studies establish that they promote tumor development. As reported by Kim *et al*., high macrophage numbers are correlated with augmented survival in pancreatic cancer patients (Kim *et al*., 2008). On the contrary, Bingle *et al*. established that more than 80% of studies reveal a correlation between macrophage density and poor patient prognosis (Bingle *et al*., 2002).

Macrophages which are abundant in tumor microenvironment are referred as tumor-associated macrophages (TAMs) and show M2 polarization features. They show pro-tumorigenic effects by affecting angiogenesis, tumor cell invasion, metastasis, and immune modulation. It is already established that TAM induces angiogenesis directly via production of VEGF-A or indirectly by producing MMP-9 and placental growth factor (PGF). MMP-9 can stimulate angiogenesis by releasing VEGF-A from extracellular storages and eventually increasing its bioavailability in some tumor models (Giraudo *et al*. 2004; Du *et al*., 2008). Rolyn *et al.* showed that a homolog of VEGF-A, PGF, enhances vascularization by binding VEGF receptor1 (VEGFR1) (Rolyn *et al*., 2011). In lung cancer, TAM is shown to induce tumor growth via angiogenesis by secreting platelet derived growth factor (PDGF) (Ruffell *et al*, 2012).

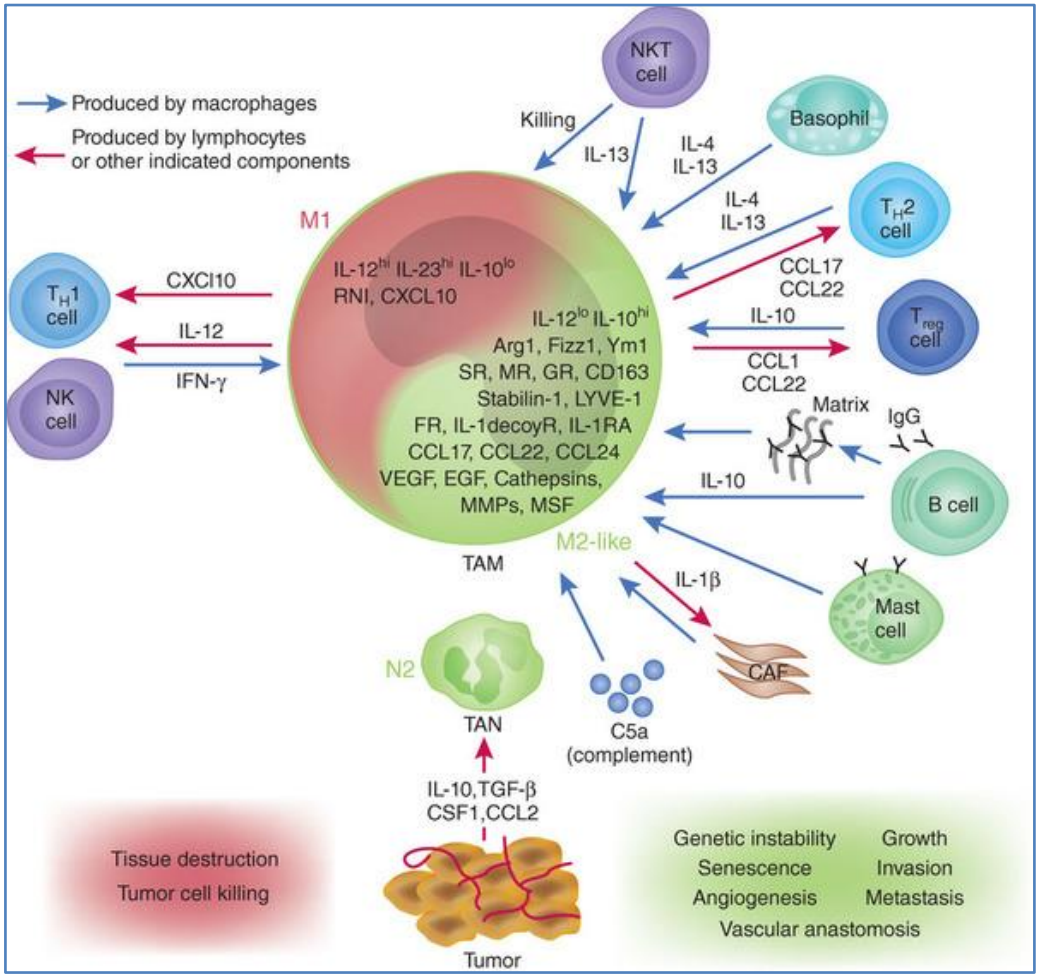

<u>Figure 1.4.</u> Macrophage polarization and general features of M1 and M2 macrophages (Taken from Biswas and Mantovani, 2010).

In TME, TAMs can modulate immune responses via suppressing $CD8^+$ T cells or inducing the recruitment of regulatory T cells (Tregs) by secretion of CCL22 (Curiel *et al*., 2004). The inhibition of $CD8^+$ T cell proliferation by TAMs is partially dependent on L-arginine metabolism

via arginase-1 or iNOS (Doedens *et al*., 2010; Movahedi *et al*., 2010, Lu *et al*., 2011b; Molon *et al*., 2011) in mouse cancer models. On the other hand, L-arginine metabolism is not essential for the suppression of $CD8^+$ T cells by TAMs in humans (Kryczek *et al*., 2006).

One of the main mechanisms that macrophages use to promote malignancy is facilitating invasion and metastasis of cancer cells. It is shown that a paracrine loop signaling between macrophages and tumor cells is important for invasion of malignant cells into ectopic tissue. In this signaling loop, cancer cells secrete colony-stimulating factor 1 (CSF1; also known as macrophage colony-stimulating factor (MCSF)), which attracts macrophages into tissue. As a result of CSF1 binding to its receptor CSFR1 on resident macrophages and macrophage precursors (CSFR1 receptor is restricted to macrophages), some mechanisms including macrophage proliferation, survival and tissue recruitment is promoted (Pollard, 2009). Importantly, this interaction also induces EGF secretion by macrophages and binding of EGF to its receptor ErbB1 on tumor cells that in turn enhances tumor cell migration. Inhibition of either the EGF or CSF-1 signaling pathways leads to inhibition of migration and chemotaxis of both cell types (Condeelis *et al.*, 2006; Wyckoff *et al.*, 2004; Wyckoff *et al.*, 2007). It is also reported that loss of CSF-1 sharply decreases accumulation of macrophage in tumors, weakens tumor malignancy, and prevents metastasis in the polyoma middle T (PyMT) oncoprotein mouse model of breast cancer (Lin *et al*., 2001), and in an osteosarcoma xenotransplant model (Kubota *et al*, 2009). Moreover, deletion of the Est-2 transcription factor, a direct effector of the CSF-1 pathway, in myeloid cells inhibits metastasis in both PyMT and orthotopic transplant breast cancer models (Zabuawala *et al.*, 2010). CSF-1 is regulated by steroid hormone receptor coactivator-1 (SRC-1) in PyMT tumor model and loss of SRC-1 results in disrupted macrophage recruitment and tumor cell intravasation, and inhibition of metastasis (Wang *et al*, 2009). Furthermore, Cheng *et al*. reported that knockdown of osteopontin (also known as SPP1) leads to loss of motility in tumor cells, which can be compensated by macrophages (Cheng *et al*., 2007).

Another way that macrophages use to enhance invasion and metastasis of cancer cells is to produce and secrete a variety of proteases, including serine proteases, matrix metalloproteinases, and cathepsins (Egeblad and Werb, 2002; van Kempen *et al*., 2002; Kessenbrock *et al*., 2010) in TME, which regulates proteolytic devastation of the matrix, tumor cell migration through the stroma and their invasion into ectopic tissue. This also results in production of ECM fragments with proinvasive signaling activities. For instance, MMP-2 produced by macrophages cleaves laminin-5 γ2 chains, which results in the release of cryptic ECM fragments that induce tumor

cell motility and invasion via mimicing EGF receptor (Giannelli *et al*., 1997; Pirilä *et al*., 2003). In addition, elevated invasiveness of the malignant cells by macrophages via TNFα dependent MMP induction was indicated in co-culture experiments (Pollard, 2004). In PyMT model, cathepsin B and S depletion from macrophages leads to deacresed tumor cell invasion and inhibition of metastasis (Goncheva *et al*., 2010; Vasilijeva *et al*., 2006). A kind of serine protease, Urokinase/Plasminogen activator (uPA), is also mostly produced by macrophages, and in the PyMT model its loss prevents metastasis (Almholt *et al.*, 2005). Sangaletti *et al.* reported that macrophages synthesize SPARC (secreted protein, acidic rich in cysteine; also known as osteonectin), which is important for collagen IV removal, and invasion of tumor cells (Sangaletti *et al*., 2008).

According to DNA microarray experiments, in which the transcriptome of the macrophages that promote tumor cell invasion were investigated, indicated that this invasive subgroup is not similar to general TAM or a reference population of splenic macrophages. It is discovered that the invasive macrophages show similar features to those found during embryogenesis and they are improved in developmental pathways, especially in the Wnt signaling pathway (Ojalvo *et al*., 2010). As already established, angiogenesis is promoted by macrophage derived Wnt signaling during development (Lobov *et al*., 2005). It is hypothesized these invasive macrophages correlate with angiogenesis and tumor invasion.

1.3.5. Other inflammatory cells

Instead of tumor associated macrophages (TAMs), Tie2-expressing monocytes (TEMs) and myeloid-derived suppressor cells (MDSCs) also have important roles in tumor promotion and metastasis. In hypoxic area of solid tumors, TEM infiltration is increased in response to Angiopoietin-2 (Ang-2) that is upregulated in hypoxic vascular cells of tumors. In addition, with the help of tumor microenvironment signals such as hypoxia, Ang-2 induces the angiogenic activity of TEMs (Murdoch *et al*., 2007).

MDSCs are immature myeloid cells and can suppress T cell function. Under normal conditions, these cells are found in bone marrow. However under pathological conditions, they can be found in high numbers in spleen, blood and lymph nodes. Some cytokines and growth factors like VEGF, GM-CSF, IL3, M-CSF, and IL6 are known to promote this recruitment process. Furthermore, MMP-9 enzyme is necessary for VEGF secretion by MDSCs and an

inhibitor of this enzyme can decrease VEGF concentrations and the number of circulating MDSCs in mice that have mammary tumors (Melani *et al*., 2007). In addition, the pro-inflammatory cytokine IL1β also stimulates MDSC production (*Ostrand-Rosenberg and Sinha, 2009*).

1.4. Inflammation and Cancer Link

The link between inflammation and tumor development was first suggested by Virchow in 1863. He proposed that chronic inflammation might push cancer development based on the observation that tumors generally evolve at the chronic inflammation area in organs. Further studies confirmed this observation by reporting the obvious correlation of chronic inflammatory diseases and cancer progression, including chronic pancreatitis-pancreatic cancer, inflammatory bowel disease-colon cancer, and *Helicobacter pylori* infection-gastric cancer, proving that chronic inflammatory diseases enhance cancer development (Colotta *et al*., 2009). According to literature, this link is explained by two ways; extrinsic and intrinsic pathways. In extrinsic pathway, long term inflammation prepares the suitable conditions for tumor development, whereas in intrinsic pathway, genetic alterations such as proto-oncogene activation, tumor suppressor deactivation via mutagenesis are required. These two pathways cause the stimulation of several transcription factors in tumor cells, most importantly Nuclear Factor kappa B (NF-κB; nuclear factor kappa-light-chain-enhancer of activated B cells) and STAT3. These transcription factors enhance the production of inflammatory molecules including cytokines and chemokines, which in turn leads to the accumulation of inflammatory cells and eventually development of tumor microenvironment. In addition, these inflammatory mediators further enhance the activation of the same transcription factors in the cells that compose the tumor microenvironment including inflammatory cells, stromal cells and fibroblasts. To sum up cells, which are affected by intrinsic and extrinsic pathways activate distinct transcription factors, produce proinflammatory molecules to create an inflammatory microenvironment, which then facilitates tumorigenesis (Karin and Greten, 2005; Mantovani *et al*., 2008; Colotta *et al*., 2009).

1.4.1. Components and activation of the NF-κB Signaling Pathway

NF-κB protein family is composed of ubiquitously expressed transcription factors, which are important for the regulation of several cellular processes; including development, immune responses, cell growth and apoptosis. Thus, it is not astonishing that these factors have been

established to function in different diseases, including inflammatory diseases, neoplastic disorders, Alzheimer's disease, and cancer. NF-κB family consists of five members; RelA (p65), RelB, c-Rel, NF-κB1 (p105), and NF-κB2 (p100), which can build variable homo-/ hetero- dimers to orchestrate the expression of multiple genes via binding to DNA. All NF-κB proteins have a highly conserved N-terminal REL homolog domain (RHD), consisting of approximately 300 amino acids, which is responsible for DNA binding and dimerization. Intead of RHD domain, RelA (p65), RelB, and c-Rel has a C-terminal transactivation domain. In the absence of an activation signal, these proteins are kept inactive in the cytoplasm by the inhibitors of NF-κB ptoteins (IκB proteins; IκBα, IκBβ, IκBε). Basically, IκB proteins bind to RHD domain of these proteins to hide the nuclear localization signal (NLS) and prevent their transfer to nucleus. On the other hand, in the presence of an activation stimulus, IκB proteins are phosphorylated by IκB kinase (IKK) complex, and then ubiquitinylated for the proteosomal degradation, which in turn leads to nuclear localization of NF-κB homo- and heterodimers. IKK complex includes three different subunits; IKKα (IKK1), IKKβ (IKK2) and IKKγ (also known as NF-κB essential mediator; NEMO). In the complex, IKKα and IKKβ functions as catalytic kinase subunits, whereas IKKγ regulates the function of complex by detecting the activator signal and integrating it for the activation of IKKα and IKKβ. Other two members of NF-κB family, NF-κB1 (p105) and NF-κB2 (p100), are produced as precursor proteins, which have C-terminal ankyrin repeat sequences. For the activation, repetitive sequences are removed to generate p50 and p52, respectively. These active forms, both p50 and p52 homodimers, can bind to another IκB family member, Bcl3, which behaves as a transcriptional co-activator in the nucleus (Perkins, 2007; Wong and Tergaonkar, 2009; Perkins, 2012).

There are two activation pathways of NF-κB: canonical (or classical) and non-canonical (or alternative) pathway. Canonical pathway is induced by several factors including the pro-inflammatory cytokines (TNFα and IL1β), bacterial products (LPS) or T-cell receptor (TCR) engagement. Upon the detection of activating stimuli, Ser32 and Ser36 residues of IκBα are phosphorylated by IKKβ for its further ubiquitination and degradation by 26S proteosome (Hayden and Ghosh, 2004). Canonical NF-κB pathway is essential for innate immunity, immune responses, development and maturation of innate and adaptive immune cells. On the other hand, non-canonical (or alternative) NF-κB pathway is activated by different effectors; cytokines belong to TNF family such as B-cell activating factor (BAFF), CD40, lymphotoxin-β receptor, and receptor activator of NF-κB ligand (RANKL) (Wong and Tergaonkar, 2009). In the presence of an activation signal, the inhibitory protein TRAF3, c-IAP1 and c-IAP2 are degraded, NF-κB

inducing kinase (NIK) is stabilized and it directly activates IKKα via phosphorylation. After activation, IKKα homodimer phosphorylates the C-terminal region of p100 for its proteolytic cleavage to generate p52, which in turn creates the active p52-RelB complex. Active p52-RelB dimmer translocates into the nucleus to induce gene expression. Activation of non-canonical NF-κB pathway is important for growth of secondary lymphoid organs including spleen, Peyer's patches, mucosa-associated lymphoid tissue (MALT), the lymph nodes, B-lymphocyte development, as well as formation of bone matrix (osteoclastogenesis) (Nabel and Verma, 1993; Gilmore, 2006; Perkins, 2007; Wong and Tergaonkar, 2009).

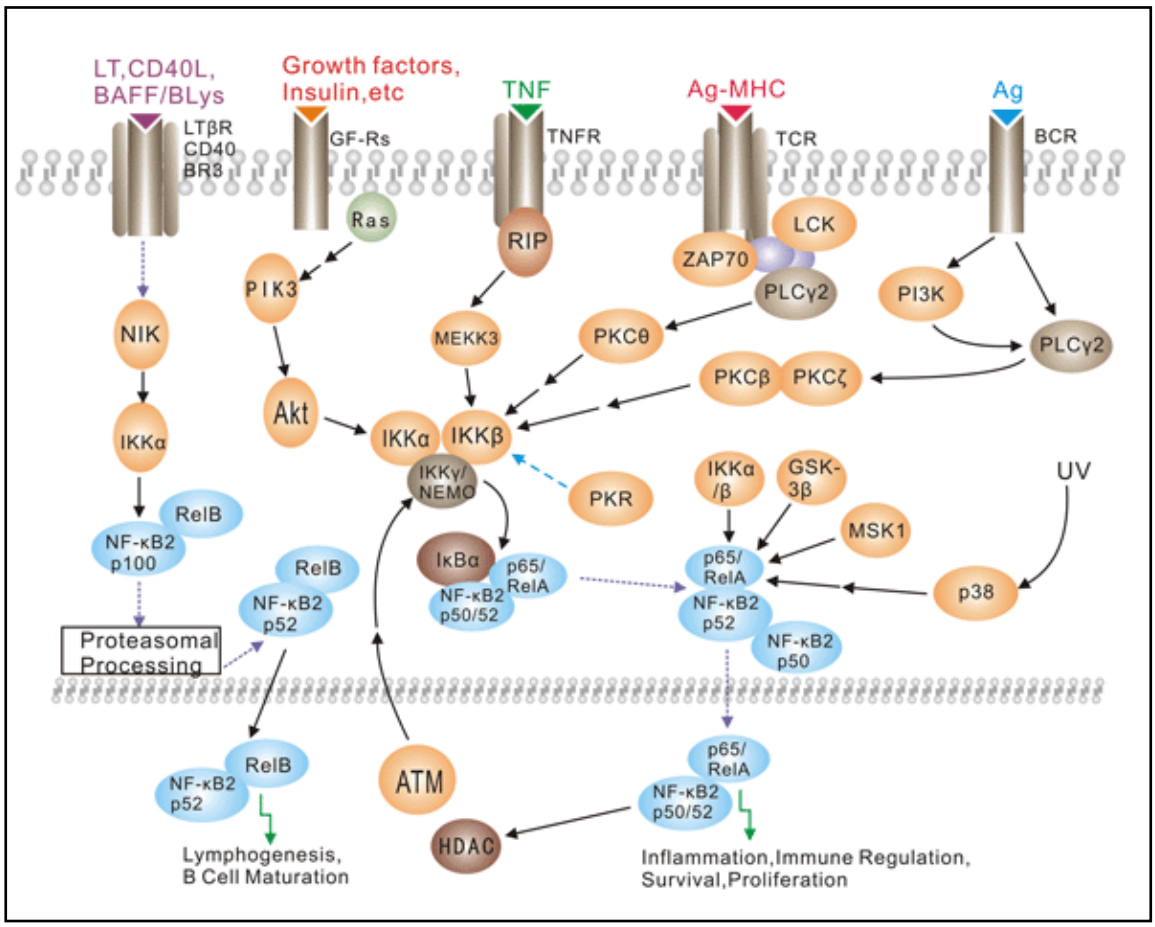

Figure 1.5. NF-κB Pathway (http://www.biobest.com.au/sab/products_al98dc.html?id=45).

1.4.2. The NF-κB Pathway in Cancer Development

Aberrant activation of NF-κB pathway is known to be considerable in cancer development and is already noticed in several types of solid tumors including breast and PDAC, and haematological malignancies including T- and B-cell lymphomas. For instance, increased levels of nuclear RelB and p52 were detected both in vivo (breast cancer, prostate cancer, oral cancers)

and in vitro (breast, pancreatic and prostate cancer cell lines) (Chandler *et al*., 2004; Dejardin *et al*., 1995; Dejardin *et al*., 1999; Lessard *et al*., 2005; Lessard *et al*., 2007; Mishra *et al*., 2006). Abnormal activation of NF-κB signaling might occur due to the genetic alterations in the upstream elements of NF-κB pathway, or less frequently in NF-κB components (Intrinsic pathway). In multiple myeloma cell lines and patients, activating/deactivating mutations in several genes containing *TRAF3*, *CYLD*, *CD40*, *NIK*, *NF-κB1*, and *NF-κB2* have been reported to cause abnormal activation of NF-κB pathway (Annunziata *et al*., 2007; Keats *et al*., 2007). Another study detected that a mutant form of TLR adaptor protein MyD88 (L265P MyD88) led to the spontaneous activation of NF-κB via IRAK1/IRAK4 protein complex, which in turn activated the STAT3 transcription factor by Jak kinase and IL6, IL10 and IFN-β secretion at activated B-cell-like subtype of diffuse large B-cell lymphoma (DLBCL) (Ngo *et al*., 2011). As this study implies, several other factors might be involved in NF-κB induced oncogenesis, such as STAT3. As being a transcription factor, STAT3 was reported by several studies that it took part in NF-κB enhanced tumorigenesis (Bollrath *et al*., 2009; Griennikov *et al*., 2010; Iliopoulas *et al*., 2009).

Since NF-κB transcription factor family orchestrates the expression of a wide range of genes, it is not surprising that abnormal NF-κB activation might enhance tumorigenesis via affecting crucial cellular processes, such as cell proliferation, cell growth, cell survival, apoptosis, angiogenesis, invasion and metastasis. Some of NF-κB targets have already been established to be related with cancer, including the genes encoding cytokines and chemokines (IL1β, IL2, IL6, IL8, TNFα, GM-CSF, Rantes, MCP-1, MIP-1α), vascularization factors (VEGF), matrix metalloproteases (MMP-9), cell adhesion molecules (ICAM-I, VCAM-I, E-selectin), and anti-apoptotic genes (Bcl-xl, Bcl-2, c-FLIP, c-IAP, AI) (Wong and Tergaonkar, 2009).

NF-κB has been shown to promote tumor development by orchestrating macrophage polarization in tumor microenvironment. It is published that TAM responses to NF-κB inhibition by changing the M2 pro-tumorigenic type to the M1 anti-tumorigenic type (Hagemann *et al*., 2008). According to literature, p50 is very important for M2 promoted inflammatory reactions. In chemically induced murine fibrosarcoma model, M2 polarized TAMs were found to be related with defective NF-κB activation (Biswas *et al*., 2006), and overexpression of p50 was shown to silence TAM against M1 inflammatory responses in a murine fibrosarcoma and human ovarian carcinoma (Saccani *et al*., 2006). Consistently, p50 suppressed M1 polarization of TAM, and

mice lacking p50 had intensified M1-driven inflammation and showed impaired M2-driven inflammatory responses (Porta *et al*., 2009). Furthermore, Hagemann and colleagues have discovered that IKKβ is fundamental for IL1R and MyD88 enhanced immunosuppressive M2 phenotype, and IKKβ blockage pushed TAMs to convert their phenotype from M2 to anti-tumorigenic M1 in ovarian cancer (Hagemann *et al.*, 2008). Instead of TAMs, another component of tumor microenvironment; CAFs can be also modified by NF-κB in order to increase pro-inflammatory gene expression, angiogenesis, macrophage recruitment and eventually tumor growth (Erez *et al*., 2010).

NF-κB signaling pathway is also correlated with the tumor suppressor p53. NF-κB and p53 can regulate the expression of several genes in a co-operate manner since genes such as *SKP2*, *KILLER/DR5* have binding sites for these two transcription factors. Weisz *et al*. showed that in the presence of mutant p53, NF-κB activation was enhanced via the secretion of TNFα in human non-small cell lung carcinoma cell line; H1299 and cancer cells became sensitive to cell death after mutant p53 down-regulation (Weisz *et al*., 2007). In another study, high expression of mutant p53 was shown to cause NF-κB activation via transactivation of *NF-κB2* in H1299 cell line and the overexpression of *NF-κB2* resulted in chemoresistance suggesting that mutant p53-induced NF-κB pathway activation might be related to drug insensitivity in tumor cells (Scian *et al*., 2005). In addition, a common polymorphism of p53 at codon 72 increases the binding of this form of p53 to RelA and enhances the expression of p53 target genes, which also have NF-κB binding domain. For instance, caspase 4/11 is among these genes and it is required for DNA damage proposing that NF-κB signaling is correlated with DNA damage responses (Frank *et al*., 2011). Although there is no abnormal NF-κB activation, DNA damage was reported to promote IKK activation in tumors (Wu and Miyato, 2007; Wu *et al*., 2010; Stilmann *et al*., 2009).

1.4.3. The NF-κB Pathway in Pancreatic Cancer

Mutations in ras genes are generally found in many types of human tumors and NF-κB has been shown to be required for ras mediated oncogenesis (Finco *et al*., 1997; Mayo *et al*., 1997). Finco *et al*. showed that H-ras activates NF-κB pathway via increasing the transcriptional activation of p65/RelA (Finco *et al*., 1997). Consistently, Wang *et al.* reported that RelA was constitutively activated in 67% of pancreatic adenocarcinomas, and dominant negative mutants of IκBα, raf kinase and MAPK were able to suppress NF-κB activation in pancreatic tumor cell lines (Wang *et al*., 1999). Since oncogenic *K-ras* is activated in approximately 80-95% of

pancreatic carcinomas (Sclabas *et al*., 2003), NF-κB pathway might be important for *K-ras* driven pancreatic cancer development. Supporting this hypothesis, Ling and colleagues investigated the role of IKK2/IKKβ in *K-ras* promoted PDAC and found out that mutant *K-ras* activated NF-κB activation via increasing IL1α expression. Furthermore, IKKβ inactivation decreased pre-neoplastic lesion and chronic pancreatitis development and mice did not show PDAC progression over 12 months proposing that IKKβ might be essential in mutant *K-ras* driven PDAC development (Ling *et al*., 2012).

Although the number of studies, which explored the link between NF-κB pathway and oncogenic *K-ras* driven PDAC is limited, there are several reports, which focus on the role of canonical NF-κB pathway in pancreatic cancer development. Chandler *et al.* detected the elevated levels of NF-κB localization in both cytoplasm (IkBα, p50, p52, p65) and nucleus (p50, p52, p65, c-Rel) in PANC-1 and BxPC-3 pancreatic cancer cell lines (Chandler *et al.,* 2004). Fujioka *et al*. showed that inhibition of constitutive NF-κB activity via using a mutant form of IκBα resulted in suppression of tumorigenicity and liver metastasis of pancreatic cell lines in orthotopic nude mouse model, however the responses of the pancreatic cancer cell lines were different. Furthermore, suppression of NF-κB activation attenuated angiogenesis in pancreatic cancer via decreasing the expression of VEGF *in vivo* and *in vitro* (Fujioka *et al*., 2003a; Fujioka *et al*., 2003b).

In comparison to the number of literature about canonical NF-κB pathway, research on non-canonical pathway are not very extensive, however the interest is growing. One of the important studies to enlighten the role of non-canonical pathway was done by Wharry and colleguages. According to their report, expression of non-canonical pathway target genes including *CXCL12*, *CXCL13*, *CCL19*, *CCL21* and *BAFF* were enhanced in human pancreatic cancer cell lines Capan-1, MiaPACA-2, BxPC-3, Panc-1, Hs-766T, PCA-2 and ASPC1. Furthermore, expression of *CXCL12*, *CXCL13* and *BAFF* was decreased in BXPC-3 cell line by using a dominant negative IKKα form suggesting that these genes were over-expressed as a result of non-canonical pathway activation. Consistently, immuno-precipitation experiments using nuclear extracts from BXPC3 and Hs-766T cells resulted in detection of p52-RelB heterodimers confirming that in several human pancreatic cancer cell lines, non-canonical NF-κB is activated (Wharry *et al*., 2009). In addition, RelB-p52 co-localization was detected on the promoter of the S-phase kinase associated protein 2 (skp2) in MiaPACA-2 cells and inhibition of IKKα suppressed their nuclear accumulation (Schneider *et al*., 2006), suggesting that IKKα

might be crucial for PDAC development. However, further *in vivo* data is necessary to confirm this hypothesis. Thus, the role of IKKα in PDAC progression is worth of investigation.

1.4.4. The Role of IKKα in Inflammation and Cancer

IKKs are essential components for NF-κB activation. Nevertheless, as the numbers of studies are growing on this topic, it is understood that IKKs are not just involved in degradation of IκB and eventual activation of NF-κB, but also in the regulation of cellular responses to the initial activating stimulus. Previously, research was more focused on the function of IKKβ, but since several NF-κB independent targets of IKKα have been identified, IKKα has gained more interest (Perkins, 2007).

IKKα is an essential mediator during the lymphoid organ development and B cell maturation through classical and nonclassical NF-κB pathways (Senftleben *et al*., 2001; Lawrence *et al*., 2005). In addition, NF-κB independent IKKα targets have recently been explored. It is found out that IKKα can regulate cell proliferation by orchestrating the expression of cyclin D1 via several NF-κB-independent mechanisms. It can activate cyclin D1 expression by phosphorylating and stabilizing the transcription factor β-catenin (Albanese *et al*., 2003) or activating the estrogen receptor α (ERα) transcription factor and its co-activator protein SRC3 (Park *et al*., 2005). Moreover, it can directly phosphorylate cyclin D1 to promote its degradation (Kwak *et al*., 2005). However, Cyclin D1 is not the only target of IKKα to regulate cell cycle progression because IKKα was also shown to activate the E2F1 transcription factor in order to orchestrate estrogen induced cell-cycle progression in breast cancer (Tu *et al*., 2006). Furthermore, IKKα has been found to be necessary for the SMRT phosphorylation and depression, which results in the activation of NF-κB target gene expression and enhanced cell survival in several cancer cell lines including HEK293T, DU145 and HT29 (Hoberg *et al*., 2006). In addition, Hoshino *et al*. has established that IKKα is involved in TLR7/9 signaling for interferon α (IFNα) production (Hoshino *et al*., 2006).

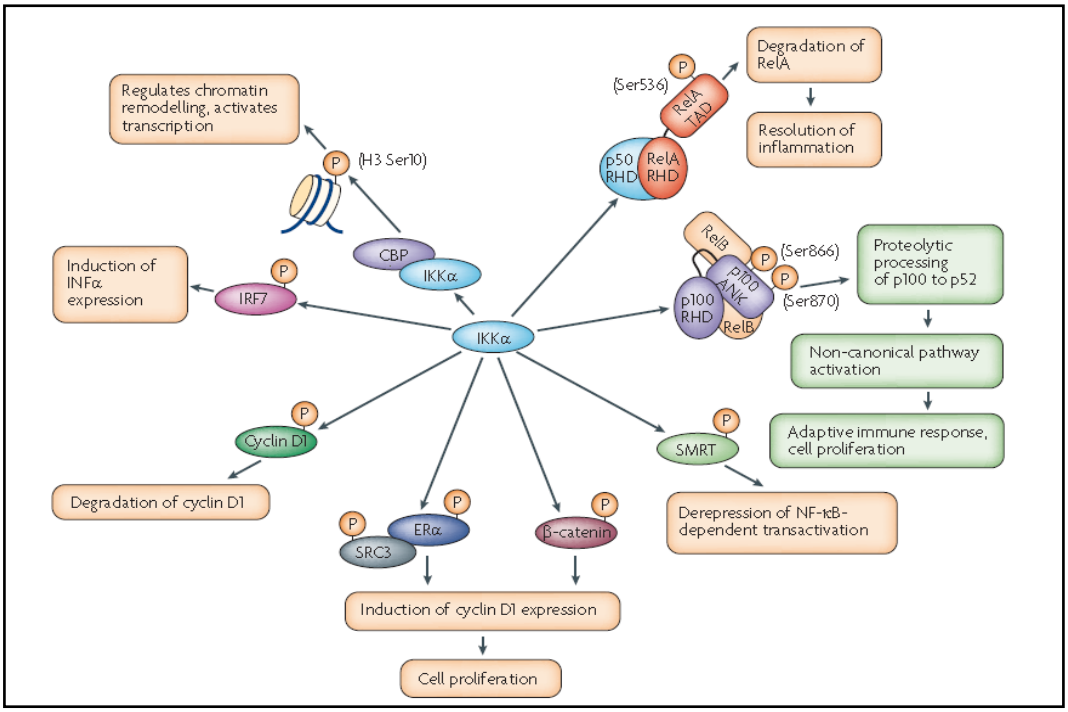

Figure 1.6. IKKα and its NF-κB independent functions (Taken from Perkins, 2007).

Furthermore, Lawrence *et al*. showed that IKKα decreases macrophage activation via controlling the activation of NF-κB subunits; RelA and c-Rel. By using Ikkα$^{AA/AA}$ mouse model in which the kinase activity of IKKα is inactivated, the group showed that upon the Gram positive human pathogen group B Streptococcus (GBS) challenge, Ikkα$^{AA/AA}$ mice had increased immune response with faster bacterial clearance but also showed higher tendency to septic shock. Macrophages from these animals were found out to display low activity against GBS and the expression of NF-κB target genes was decreased in the alveolar and peritoneal macrophages. In addition, RelA and c-Rel turnover was accelerated by IKKα suggesting that IKKα can control immune response and activity of macrophages by regulating the activity of NF-κB subunits (Lawrence *et al*., 2005).

IKKα is important for development. It is found out that IKKα deficient mice die perinatally and *Ikkα*$^{-/-}$ fetuses have defective limb and skin development. The mice displayed hyperplastic epidermal cell structure with aberrant epidermal differentiation suggesting that IKKα is essential for epidermis formation during embryonic development in mice (Takeda *et al.*, 1999; Park *et al*., 2011). Furthermore, nuclear IKKα homodimers were shown to orchestrate epidermal development, keratinocyte maturation and differentiation (Sil *et al*., 2004; Liu *et al*., 2006; Descargues *et al*., 2008). The importance of IKKα was further verified by another study in which

IKKα reduction and *Ikkα* mutations were detected in poorly differentiated human squamous cell carcinomas (SCCs) (Liu *et al*, 2006). Increased expression of IKKα in the epidermis suppressed skin cancer development and metastasis in mice, proposing that IKKα is a considerable inhibitor for the development of SCC (Liu *et al*, 2006). Lack of IKKα has been observed to increase the susceptibility to chemical carcinogen induced skin cancer in mice by enhancing the proliferation of keratinocytes and papilloma formation in a *Ras* cooperation manner (Park *et al*., 2007). The importance of IKKα in skin cancer is further supported by another study in which keratinocyte specific deletion of IKKα in mice was displayed to activate EGFR pathway and inactivation of this pathway blocks the development of epidermal hyperplasia and tumors (Liu *et al*., 2008). Moreover, Zhu *et al*. established that IKKα takes part in epigenetic regulation and orchestrates G2/M cell cycle arrest by preventing the hypermethylation of 14-3-3σ of CpG islands in keratinocytes. 14-3-3σ is involved in cell cycle arrest upon DNA damage, however it is not targeted by IKKα directly in the IKKα-mediated terminal differentiation process (Zhu *et al*., 2007). Additionally, Kwak and colleagues have confirmed that lack of IKKα results in nuclear accumulation of Cyclin D1 in MEFs and discovered that $Ikk\alpha^{-/-}$ cells displayed a neoplastic phenotype by forming colonies in soft agar and promoting tumor development in nude mice. Moreover, IKKα deletion led to an increased expression of anti-apoptotic genes and decreased tumor suppressor genes. Lower IKKα expression was detected in several mouse and human lung cancer cells suggesting that IKKα might inhibit tumor progression by functioning as a tumor suppressor (Kwak *et al*., 2011). However, the mechanism that IKKα uses to suppress cancer is still unknown and further studies are required to explore its roles in different types of tumor development.

1.5. Energy Metabolism and Its Alterations in Cancer Cells

1.5.1. Metabolic Pathways in the Cells

1.5.1.1. Glycolysis

Glycolysis is one of the main energy production pathways in living organisms in which glucose is metabolized to produce energy. Instead of glucose, other monosaccharides including fructose and galactose can be also processed by glycolysis. In eukaryotes, glycolytic reactions progress in the cytoplasm. Glycolysis consists of two main steps. In the first step, the aim is not to produce energy, but to take and keep the glucose molecule in the cytoplasm. First of all,

glucose molecule is carried through the cell membrane via glucose transporter molecules (GLUTs). After transport, it is phosphorylated and converted into Glucose 6-Phosphate (G6P) by hexokinases in the cytoplasm. Hexokinases are one of the main catalyzers of the reaction since the reaction they catalyze is irreversible. Due to its chemical structure, G6P can not go out of the cytoplasm through the cell membrane, thus it is trapped in the cell. Moreover phosphorylation of glucose facilitates its metabolism in further steps since the addition of phosphoryl group on carbon 6 makes the structure of glucose more destabilized. Afterwards G6P, an aldose, is converted into Fructose 6-Phosphate (F6P), a ketose, via an isomerization reaction catalyzed by phosphoglucose isomerase (also known as glucose-6-phosphate isomerase (Gpi). Then, F6P is phosphorylated by phosphofructokinase (PFK) and transformed into Fructose 1,6-bisphosphate (F-1,6-BP). Afterwards, F-1,6-BP is splitted by aldolase in a reversible reaction to generate Glyceraldehyde 3-Phosphate (GAP) and Dihydroxyacetone phosphate (DHAP). At this point, GAP is used for further reactions whereas DHAP not and the loss of DHAP molecule would lead to the loss of ATP that will be produced. Thus, DHAP is further converted to GAP by an isomerization reaction catalyzed by triose phosphate isomerase (TPI). This reaction is the last step of the first part of glycolysis. In the second part, GAP is transformed into 1,3-Bisphosphoglycerate (1,3-BPG) by glyceraldehyde 3-phosphate dehydrogenase. 1,3-BPG is a great energy source since it has high phosphoryl transfer potential. As the next step, phosphoryl groups of 1,3-BPG are transferred to adenosine diphosphate (ADP) by phosphoglycerate kinase (PGK), which leads to the formation of 3-phosphoglycerate and ATP. At this point, since 2 GAP molecules are formed as a result of the activation of aldolase and TPI in the first stage of glycolysis, 2 ATP molecules are formed. However, these 2 ATP molecules only compensate the investment of 2 ATP molecules in the first part of glycolysis. Afterwards, the phosphoryl group of 3-phosphoglycerate is rearranged by phosphoglycerade mutase leading to firstly 2,3-bisphosphoglycerate (2,3-BPG) and following 2-phosphoglycerate formation. Afterwards, 2-phosphoglycerate is dehydrated and converted into phosphoenolpyruvate (PEP), by Enolase. As the final step, phosphoryl group of PEP is transferred to ADP and PEP is converted into a more stabile keton structure, pyruvate, by pyruvate kinase. Since 2 molecules of pyruvate are formed, 2 ATP molecules are also generated concomitantly (Berg *et al*., 2012-Chapter 16) (Figure 1.7).

Glycolysis can be summarized by this formula:

$$\text{Glucose} + 2\ \text{Pi} + 2\ \text{ADP} + 2\ \text{NAD}^+ \rightarrow 2\ \text{Pyruvate} + 2\ \text{ATP} + 2\ \text{NADH} + 2\ \text{H}^+ + 2\ \text{H}_2\text{O}$$

The end product of glycolysis, pyruvate, can be transformed into ethanol and lactate by fermentation in the absence of oxygen. In the presence of oxygen, pyruvate can be directed to Tricarboxylic acid (TCA) cycle and electron transport chain (Berg *et al*., 2012- Chapter 16).

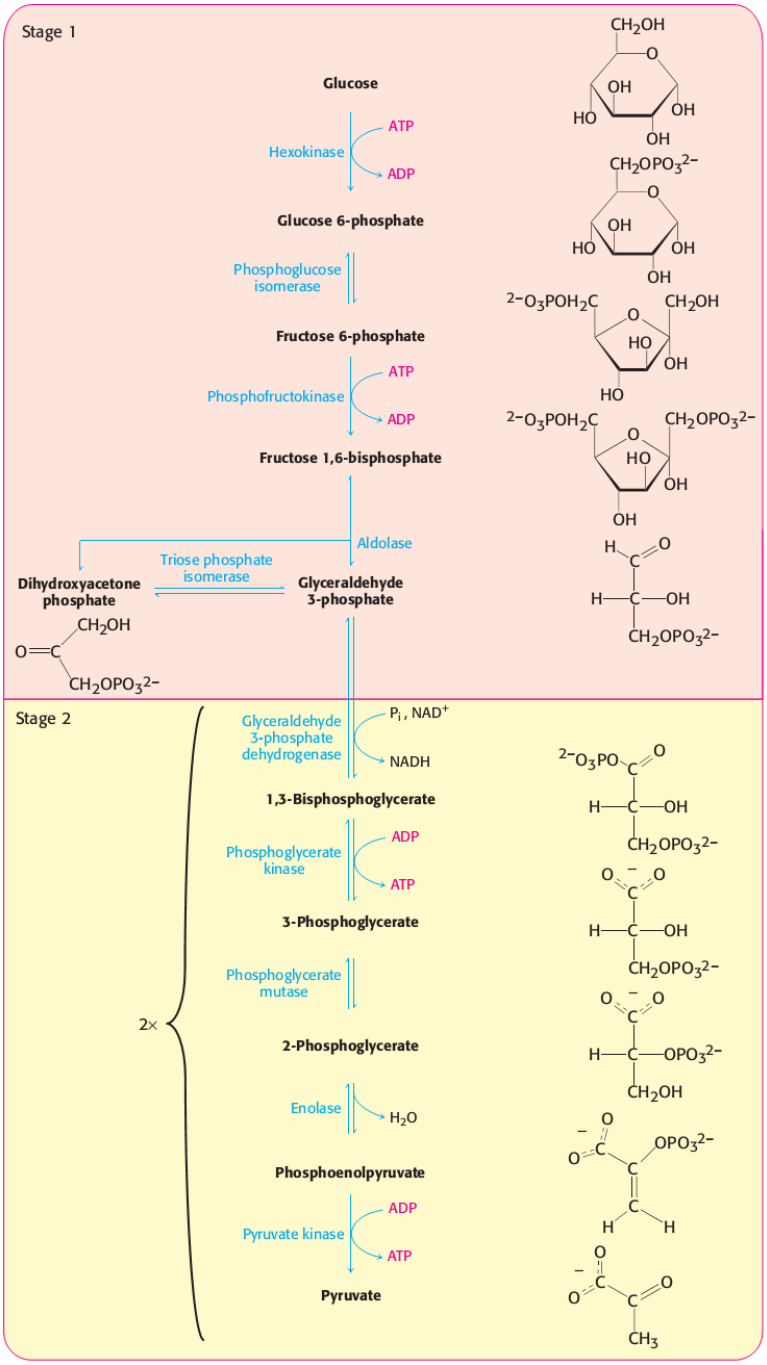

<u>Figure 1.7.</u> Gycolysis (Berg *et al*., 2012- Chapter 16).

1.5.1.2. Gluconeogenesis

Gluconeogenesis is the process in which glucose is synthesized from noncarbohydrate precursors including lactate, amino acids and glycerol. These precursors are either firstly

transformed into pyruvate or used lately in the form of oxaloacetate (OAA) or dihydroxyacetone phosphate for further glucose production. During the long term of starvation or fasting, gluconeogenesis is very essential for providing glucose (Berg *et al*., 2012-Chapter 16).

As the first step, pyruvate is carboxylated by pyruvate carboxylase and converted into OAA in the mitochondria. Among the enzymes involved in gluconeogenesis, only pyruvate carboxylase is mitochondrial whereas the other enzymes are cytoplasmic. Thus, OAA has to be transported to the cytoplasm for further reactions. Since it can be transported in the form of malate, it is reduced by NADH-linked malate dehydrogenase. Upon arrival to the cytoplasm, NAD^+- linked malate dehydrogenase reoxidizes malate to OAA. Afterwards, OAA is decarboxylated and phosphorylated by phosphoenolpyruvate carboxykinase (PEPCK) to form PEP in the cytoplasm. PEP is then metabolized by the same enzymes, which are involved in glycolysis. However, when Fructose 1,6-bisphosphate (F-1,6-BP) is formed, then fructose 1,6-bisphosphatase (FBPase1; also known as fructose bisphosphatase 1) metabolizes it to F6P, which is further transformed into G6P. Generally, gluconeogenesis stops at this point and G6P is not converted to free glucose. However, when free glucose is necessary, G6P is transferred to endoplasmic reticulum (ER). In ER, G6P is converted into glucose by the membrane-bound enzyme glucose 6-phosphatase resulting in the formation of glucose and Pi. For the transport of these molecules to the cytoplasm, transporters are also necessary (Berg *et al*., 2012-Chapter 16).

Glycolysis and gluconeogenesis are strictly regulated pathways and they are organized mutually.

1.5.1.3. Tricarboxylic acid (TCA) Cycle

Tricarboxylic acid (TCA) cycle (also known as Krebs cycle or Citric acid cycle) is an important metabolic pathway for supplying the fuel molecules for energy production or intermediate molecules, which are used to synthesize essential biomolecules including nucleotides and proteins. In eukaryotes, TCA cycle reactions takes place inside of the mitochondria.

In the presence of oxygen, the end product of glycolysis, pyruvate, is converted into Acetyl Coenzyme A (Acetyl CoA) by oxidative decarboxylation. Acetyl CoA is the substrate of TCA cycle. During TCA cycle, acetyl group of Acetyl CoA is oxidized by oxidation-reduction

reactions, and eventually leads to the removal of electrons from Acetyl CoA. During these reactions, six electrons are transferred to 3 molecules of nicotinamide adenine dinucleotide (NAD^+) and two electrons are transferred to 1 molecule of flavin adenine dinucleotide (FAD), resulting in the generation of NADH and $FADH_2$ respectively. These electron carriers, NADH and $FADH_2$, are then oxidized by oxygen during oxidative phosphorylation and release electrons flow through electron transport chain proteins, which are localized in the membrane of mitochondria. As a result, a proton gradient is generated across the membranes leading to the production of ATP from ADP and inorganic phosphate by ATP synthase. This shows that instead of producing abundant amounts of ATP by itself, TCA cycle produces most of the required energy for aerobic cells together with oxidative phosphorylation (Berg *et al*., 2012-Chapter 17).

Pyruvate dehydrogenase complex (PDC) is responsible for the transfer of pyruvate from cytosol to mitochondria and its conversion into Acetyl CoA. This irreversible reaction connects glycolysis to cellular respiration. Pyruvate dehydrogenase complex (PDC) is a very large complex including three different enzymes: Pyruvate dehydrogenase component (E1), Dihydrolipoyl transacetylase (E2) and Dihydrolipoyl dehydrogenase (E3). All these subunits are required for the reaction, together with coenzymes thiamine pyrophosphate (TPP), lipoic acid, FAD, CoA, and NAD^+. The first two reactions, decarboxylation and oxidation of pyruvate, are catalyzed by E1 subunit PDC. The third step, transfer of acetyl group and formation of Acetyl CoA, together with dihydrolipoamide, is processed by E2 subunit of PDC. In order to continue in the cycle, dihydrolipoamide has to be oxidized to lipoamide and this is catalyzed by E3 subunit of PDC. After the generation of Acetyl CoA, OAA reacts with Acetyl CoA and H_2O to produce CoA and citrate, which is catalyzed by citrate synthase. Then, citrate is converted into isocitrate by an isomerization reaction catalyzed by acotinase. This step is necessary for the oxidative decarboxylation of isocitrate, since the chemical structure of citrate is not suitable for the reaction. Then, oxidative decarboxylation of isocitrate is catalyzed by isocitrate dehydrogenase leading to the generation of α-ketoglutarate and NADH. NADH is an important molecule for the reaction since it functions as high-transfer-potential electron carrier. Afterwards, α-ketoglutarate dehydrogenase complex converted α-ketoglutarate into Succinyl CoA by another oxidative decarboxylation reaction. Then, Succinyl CoA is cleaved into succinate by Succinyl CoA synthetase (also known as succinate thiokinase), which is further oxidized to fumarate by succinate dehydrogenase. This step is followed by the hydration of fumarate by fumarase to produce L-malate. The cycle is completed by the oxidation of malate to generate OAA and

NAD^+ as the hydrogen acceptor, which is catalyzed by malate dehydrogenase (Berg *et al*., 2012-Chapter 17).

The sum of the reactions of TCA cycle can be summarized by this formula:

Acetyl CoA + 3 NAD^+ + FAD + ADP + Pi + 2 H_2O → 2 CO_2 + 3 NADH + $FADH_2$ + ATP + 2 H^+ + CoA

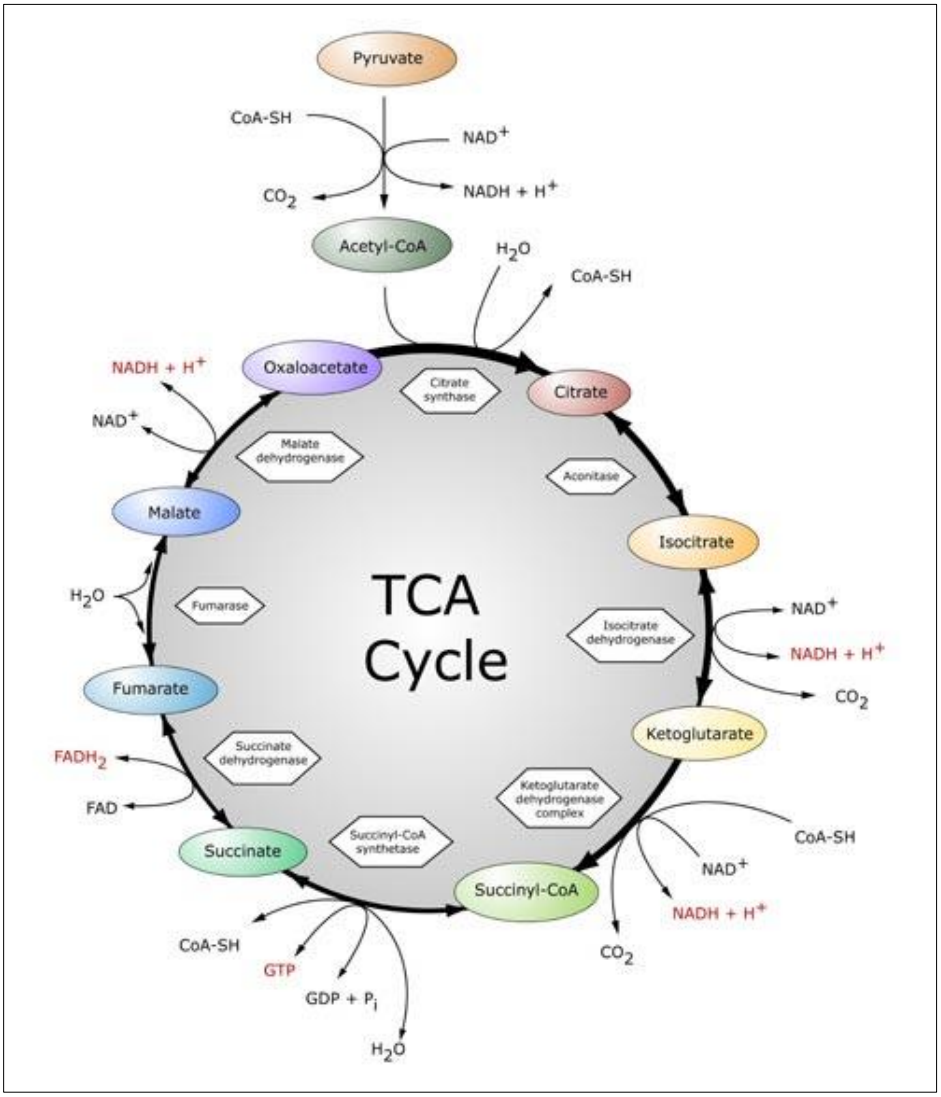

<u>Figure 1.8.</u> TCA cycle (http://25.media.tumblr.com/tumblr_lgtvemTj8o1qg1qzoo1_500.jpg).

1.5.1.4. Oxidative Phosphorylation

As mentioned before, TCA cycle supplies mitochondrial NADH. However, NADH can be also provided by mitochondrial fatty acid oxidation. Furthermore, cytoplasmic NADH can be also transported to mitochondria for the use by the electron transport chain.

Oxidative phosphorylation includes several reactions that lead to ATP production. The first step is the binding of NADH to NADH-Q oxidoreductase (also known as Complex I and NADH dehydrogenase). All of the redox reactions process in the extra membranous part of Complex I, which is a big protein including 46 subunits and is encoded by both mitochondrial and nuclear genome. After binding of NADH to the extra membranous part of Complex I, two electrons of NADH are transferred to a prosthetic group, flavin mononucleotide (FMN) leading to the reduction of FMN to $FMNH_2$. Afterwards, the electrons are transferred from $FMNH_2$ to another prosthetic group of Complex I, a series of iron-sulfur clusters and then to coenzyme Q (ubiquinone), leading to its reduction and conversion into QH2 (ubiquinol). During the transfer of two electrons from NADH to coenzyme Q (reduction of coenzyme Q) via Complex I, four hydrogen ions are pumped out of the mitochondrial matrix leading to the generation of a proton gradient (Berg *et al*., 2012- Chapter 18). The enzymatic reaction catalyzed by Complex I can be summarized as:

$$NADH + Q + 5\ H^+_{\ matrix} \rightarrow NAD^+ + QH_2 + 4\ H^+_{\ intermembrane}$$

The second electron source of the oxidative phosphorylation is $FADH_2$, which is generated as a result of the oxidation of succinate to fumarate by succinate dehydrogenase during TCA cycle. Succinate dehydrogenase is a unique enzyme since it is not only involved in TCA cycle but also a part of Succinate-Q reductase (also known as Complex II). The electrons of $FADH_2$ are transferred to iron-sulfur clusters by the complex and eventually to coenzyme Q, leading to its reduction to QH2. During these reactions, protons are not pumped through the mitochondrial membrane as it is done by Complex I. Thus, energy production by the oxidation of $FADH_2$ is less than the oxidation of NADH (Berg *et al*., 2012- Chapter 18). The enzymatic reaction catalyzed by Complex II can be shown as:

$$Succinate + Q + \rightarrow Fumarate + QH_2$$

The third step of oxidative phosphorylation is catalyzed by Q-cytochrome c oxidoreductase, which is also known as Complex III or cytochrome c reductase. Complex III catalyzes the transfer of electrons from QH2 to cytochrome c (Cyt c) and pumps the protons out of the mitochondrial matrix concomitantly. In mammals, the enzyme functions as dimers and each subunit consists of 11 subunits, an iron-sulfur cluster and three cytochromes (one cytochrome c1 and two cytochromes b, which transfer the electrons and include at least one heme group. The heme groups of Complex III consist of iron atoms, which switch from a reduced ferrous (+2) and oxidized ferric (+3) state during the transfer of electrons through the protein (Berry *et al*., 2000; Crofts, 2004; Iwata *et al*., 1998; Berg *et al*., 2012-Chapter 18).

The function of Complex III is a bit more complicated than other enzymes of oxidative phosphorylation since only one electron can be transferred from QH2 to acceptor Cyt c. Thus the reaction is catalyzed in two steps, which is called as Q cycle (Trumpower, 1990). At the beginning, QH2 is oxidized by the complex III and one electron is transferred to the acceptor Cyt c, followed by the release of two electrons from QH2 that are passed to the intermembrane space. Another substrate of complex III, a bound oxidized Q in a second binding site takes the second electron of QH2, resulting in its conversion to a ubisemiquinone free radical $Q^{\cdot -}$ molecule. In the second step, another QH2 molecule is bound to the complex and its first electron is again transferred to Cyt c, similarly to the first step. On the other hand, second electron of QH2 is transferred to $Q^{\cdot -}$ molecule. Upon the transfer of an electron from second QH2, $Q^{\cdot -}$ accepts two protons from the matrix of mitochondria, leading to the generation of QH2. Importantly, removal of two electrons from mitochondrial matrix results in the generation of proton gradient (Hunte *et al*., 2003; Berg *et al*., 2012- Chapter 18). The reaction catalyzed by complex III can be summarized by this formula:

$$2\ QH2 + Q + 2\ Cyt\ c_{ox} + 2\ H^{+}_{matrix} \rightarrow 2\ Q + QH2 + 2\ Cyt\ c_{red} + 4\ H^{+}_{cytoplasm}$$

After this step, cytochrome c oxidase (also known as complex IV), which consists of 13 subunits, two heme groups and several metal ion cofactors takes place (Tsukihara *et al*., 1996). It transfers electrons from reduced Cyt c to the terminal acceptor oxygen and concomitantly pumps the protons across the membrane (Yoshikawa *et al*., 2006). As a result, oxygen is reduced to water and proton gradient is formed. The reaction catalyzed by Complex IV is:

$$4\ Cyt\ c_{red} + O_2 + 8\ H^{+}_{matrix} \rightarrow 4\ Cyt\ c_{ox} + 2\ H_2O + 4\ H^{+}_{intermembrane}$$

The final step of oxidative phosphorylation is catalyzed by ATP synthase (also known as Complex V). Electron flow through Complex I, II, III and IV resulted in transfer of electrons from the matrix side to the inner membrane of mitochondria. This proton accumulation in the inner membrane forms membrane potential, which is used by Complex V to synthesize ATP from ADP and inorganic phosphate molecules. The reaction catalyzed by Complex IV is:

$$ADP + Pi + 4\ H^+_{\text{intermembrane}} \leftrightarrow ATP + H_2O + 4\ H^+_{\text{matrix}}$$

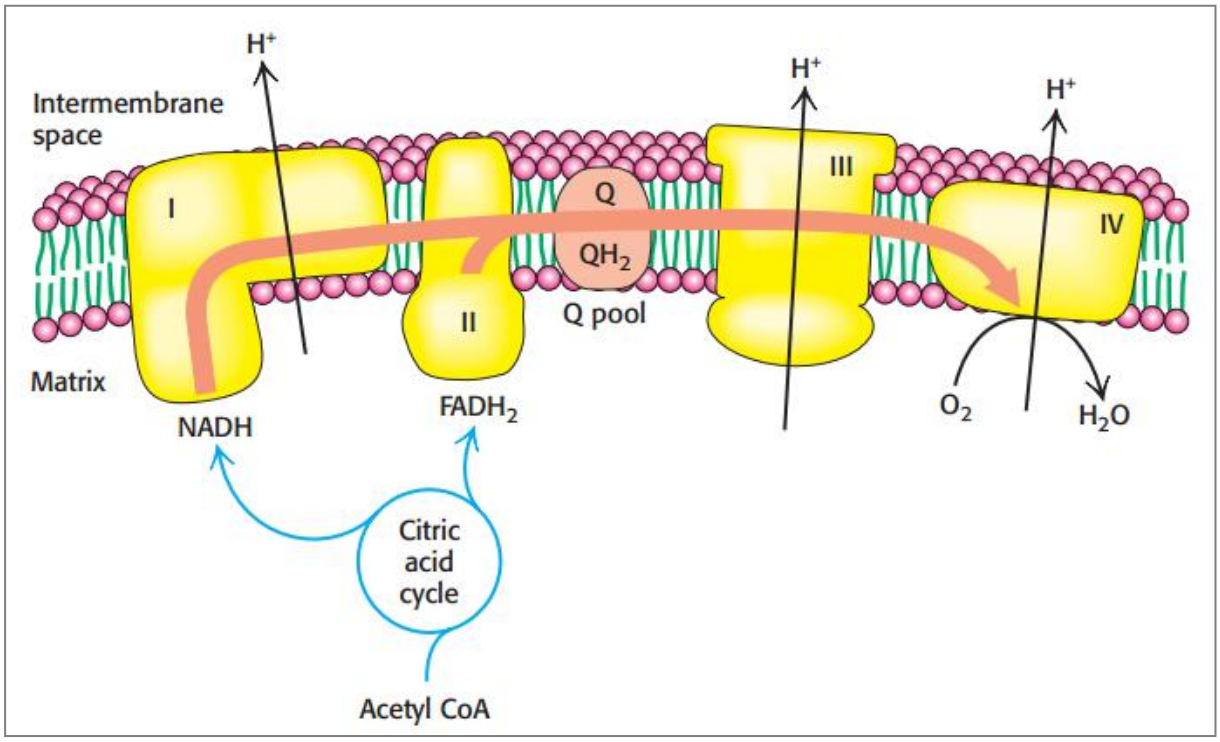

Figure 1.9. Electron transport chain (Berg *et al*., 2012- Chapter 18).

1.5.1.5. Pentose Phosphate Pathway (PPP)

Pentose phosphate pathway (also known as hexose monophosphate pathway, the phosphogluconate pathway or the pentose shunt) is responsible for the oxidation of glucose and generation of NADPH, which functions as a reducing agent in biosynthetic reactions and is important for protection against oxidative stress in the cells. Moreover, the synthesis of pentose sugars for nucleotide biosynthesis is also done by this pathway. The substrate of PPP is Glucose 6-phosphate, which might also be processed in glycolysis. The pathway which will use Glucose 6-P is determined by the cytoplasmic concentration of $NADP^+$ in the cells (Berg *et al*., 2012- Chapter 20).

PPP consists of two main steps and all the reactions catalyzed in the pathway take place in cytoplasm. The first step is the oxidative step that starts with dehydrogenation of glucose 6-phosphate (G6P) by glucose 6-P dehydrogenase, leading to the generation of 6-phosphoglucono-δ-lactone. Afterwards, hydrolysis of 6-phosphoglucono-δ-lactone is catalyzed by lactonase and 6-phosphogluconate is produced. As the last reaction of oxidative step of PPP, oxidative decarboxylation of 6-phosphogluconate is catalyzed by 6-phosphogluconate dehydrogenase and it is converted to ribulose 5-phosphate. In the first oxidative step, oxidization of each glucose 6-phosphate molecule results in the production of two NADPH molecules and one ribulose 5-phosphate molecule. The second step is the non-oxidative step in which sugar molecules are converted. In this step, firstly ribulose 5-phosphate is converted to ribose 5-phosphate by an isomerization reaction catalyzed by phosphopentose isomerase. Then, ribose 5-phosphate and xylulose 5-phosphate is converted into glyceraldehydes 3-phosphate and sedoheptulose 7-phosphate by transketolase, which are further converted into fructose 6-phosphate and erythrose 4-phosphate by transaldolase. At the last step of the non-oxidative branch of PPP, fructose 6-phosphate and glyceraldehyde 3-P is generated from erythrose 4-phosphate and xylulose 5-phosphate by transketolase (Berg *et al*., 2012-Chapter 20).

Among the enzymes involved in PPP, transketolase and transaldolase are important since they catalyze the reactions that link glycolysis and PPP. Moreover, glucose 6-phosphate dehydrogenase is also important because it is the rate-limiting enzyme of PPP.

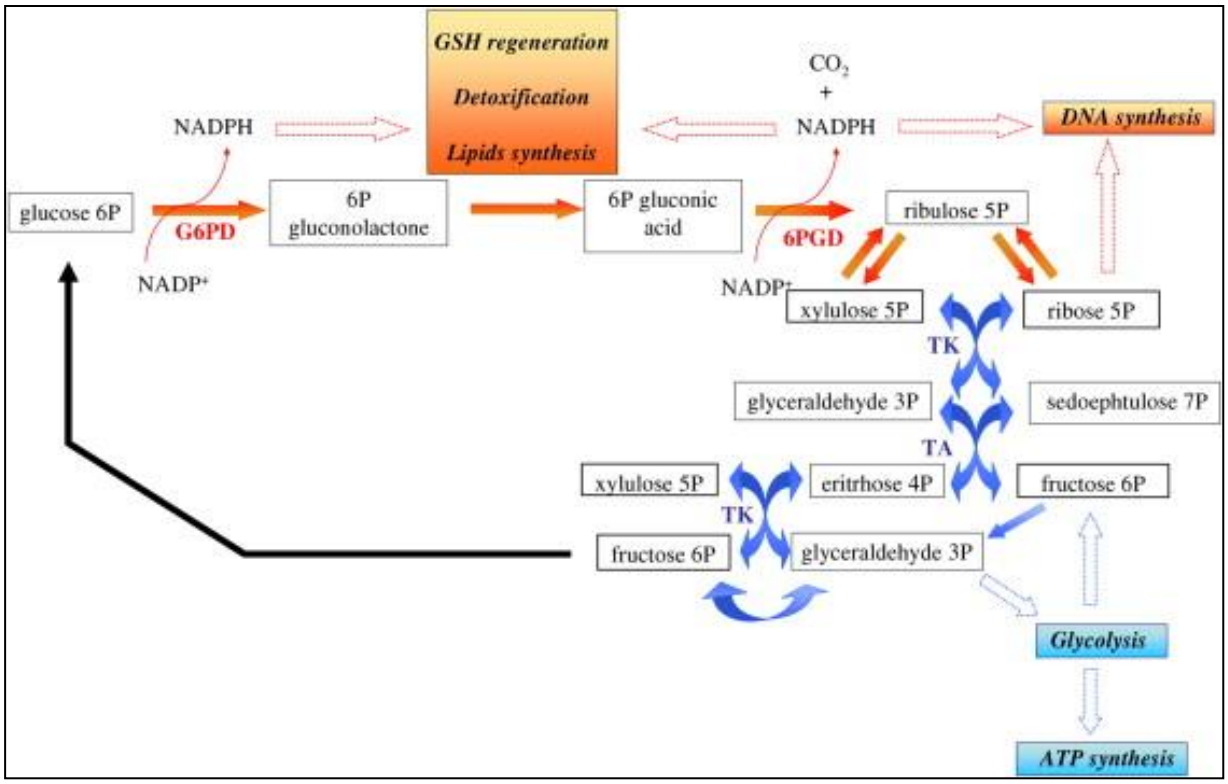

Figure 1.10. Pentose Phosphate Pathway (Riganti *et al*., 2012).

1.5.2. Energy Metabolism in Cancer Cells

It is known since long time that cancer cells have different metabolism than normal untransformed cells. In 1920s, Otto Warburg discovered that even in the presence of oxygen, cancer cells prefer to produce energy via glycolysis rather than mitochondrial oxidative phosphorylation, even in the expense of less ATP production. This hypothesis is known as 'Warburg effect' or 'aerobic glycolysis', and accepted as a hallmark of cancer cell metabolism (Warburg, 1956). This hypothesis further led to the discovery of clinical [^{18}F] fluorodeoxyglucose positron emission tomography (FDG-PET) imaging in which a radio-active glucose analogue is used to detect the organs that uptake high amount of glucose. Since tumor cells have increased metabolic demands, detection of the increased glucose uptake by cancer cells becomes possible by FDG-PET (Gambhir, 2002).

Indeed, the exact reason why cancer cells preferably depend on glycolysis for energy production is not completely understood (Hsu and Sabatini, 2008). It is previously suggested that tumor cells shift to glycolysis due to the defects in mitochondria, which prevents ATP production by oxidative phosphorylation. However, afterwards, it was established that defects in the mitochondria of cancer cells is not very common (Frezza and Gottlieb, 2009). Moreover, an

alternative proposal why this shift happens was the hypoxic area of tumor microenvironment; during which the absence of enough vascularization induces HIF-1, and cells can not continue to produce ATP via oxidative phosphorylation. Another suggestion is that cells can produce ATP at a higher rate by glycolysis than oxidative phosphorylation and since tumor cells have increased and continuous energy demand, increased turnover rates by the glycolytic pathway may appear advantageous. Lastly, it is suggested that glycolysis is not just helpful for ATP production, but also generates high amount of substrates, which are used by cells to produce additional macromolecules including proteins, nucleic acids, carbohydrates and lipids through biosynthetic pathways such as PPP (Cairns *et al*., 2011). Furthermore, activation of oncogenes or loss of tumor suppressor genes is suggested to cause alterations in energy metabolism (Yeung *et al*., 2008).

HIF-1 is a member of basic helix-loop-helix-Per-ARNT-Sim (bHLH-PAS) transcription factor family (Liao *et al*., 2007). Under normal oxygen (normoxic) conditions, Von Hippel Lindau (VHL) tumor suppressor protein binds to HIF-1, which results in its ubiquitination and proteasomal degradation (Maxwell *et al*., 1997; Kallio *et al*., 1990). However, in the presence of hypoxia, HIF-1 is stabilized and regulates the expression of genes involved in the adaptive responses to hypoxia (Manalo *et al*., 2005). Together with c-Myc, HIF-1 can induce the expression of glycolytic enzymes pyruvate dehydrogenase (PDH) and lactate dehydrogenase (LDH) (Brahimi-Horn *et al*., 2007; Yeung *et al*., 2008). These enzymes are very important because their relative activities regulate the switch between glycolysis and oxidative phosphorylation (Brahimi-Horn *et al*., 2007). The activity of pyruvate dehydrogenase (PDH) is orchestrated by pyruvate dehydrogenase kinase 1 (PDK1). PDK1 inhibits the conversion of pyruvate into acetyl CoA and decreases its utilization during oxidative phosphorylation by inhibiting PDH (Gogvadze *et al*., 2008). It is shown that PDK1 expression is upregulated by HIF-1, which leads to inactivation of PDH and the suppression of Krebs cycle and mitochondrial respiration (Kim *et al*., 2006; Papandreaou *et al*., 2006). Another HIF-1 target, LDHA, converts pyruvate into lactate and is over-expressed in several human cancers including colorectal cancer (Goldman *et al*., 2964; Brahimi-Horn *et al*., 2007). In the absence of LDHA, lactate production is blocked and oxygen consumption by oxidative phosphorylation in mitochondria (OXPHOS activity) is elevated in tumor cells, showing the importance of LDHA for glycolysis/respiration balance in tumor cells (Fantin *et al*., 2006). Together with c-Myc and p53, HIF-1 also regulates the expression of Hexokinase 2 (HK2). HK2 is an important enzyme in glycolysis since it phosphorylates glucose into glucose-6-phosphate, which enters into glycolysis for ATP

production or the pentose phosphate pathway for the production of reduced nicotinamide adenine dinucleotide phosphate (NADPH) and /or ribose (Mathupala *et al*., 1997).

HIF-1 is an important molecule for the regulation of energy metabolism in pancreatic cancer. Yoon *et al.* found that in human pancreatic cancer cell line, Capan-2, HIF-1 can induce the expression of hypoxia inducible genes GPI/NLK/AMF (glucose phosphate isomerase/ neuroleukin/autocrine motility factor), HK2 and DEC1/Stra13 (Yoon *et al*., 2001). GPI/NLK/AMF is an important player both in glyconeogenesis and glycolysis. It catalyzes the reversible izomerization of D-glucose-6-phosphate and D-fructose-6-phosphate (Niinaka *et al*., 1998) and may help cancer cells to survive and proliferate in the absence of nutrients and oxygen (Akakura *et al*., 2001). Furthermore, Chen *et al.* suggested that under hypoxic conditions, inhibition of a subunit of HIF-1 (HIF1α) results in decreased glucose uptake and glycolysis in pancreatic cancer cells, which in turn causes the production of less energy and enhanced apoptosis. They showed that in the presence of a dominant negative HIF1α mutant transfectants, the expression of GLUT-1, aldolase A and VEGF is reduced in pancreatic ductal adenocarcinoma cell line (PCI-43), which already has mutated p53. However, *in vivo*, only glucose uptake was suggested to be less than normal, whereas angiogenesis was not decreased (Chen *et al*., 2003).

Abnormal activation of oncogenes or loss and/or inactivation of tumor suppressor genes can derange the energy metabolism in the cells. However, paradoxically, deranged energetic pathways might also cause abnormal activation of signaling pathways. For instance, inactivating mutations of mitochondrial succinate dehydrogenase and fumarate dehydrogenase leads to the accumulation of fumarate and succinate, which are the substrates of Krebs cycle. This accumulation, in turn, causes the inhibition of the prolyl hydroxylases-the enzymes that are involved in VHL-directed HIF-1 degradation. Thus, HIF-1 can be stabilized and directs the cells towards glycolysis in the absence of hypoxia (Isaacs *et al*., 2005; Pollard *et al*., 2005; Selak *et al*., 2005).

Another gene, which has roles in energy metabolism, is TP53. It regulates the expression of enzymes required in energetic pathways including Glucose-6-phosphate dehyrogenase (G6PD) and phosphoglycerate mutase (PGM). The activation of G6PD can diminish the Warburg effect by directing glycolysis into the PPP (Olovnikov *et al*., 2009). On the other hand, active p53 activation induces the degradation of PGM and eventually inhibits glycolysis (Matoba

et al., 2006; Kondoh *et al*., 2005). Furthermore, together with Synthesis of cytochrome c oxidase 2 (SCO2) and TP53-induced glycolysis and apoptosis regulator (TIGAR), p53 orchestrates the balance between mitochondrial oxidative phosphorylation and glycolysis (Bensaad *et al*., 2006; Matoba *et al*., 2006). SCO2 is essential for the assembly of cytochrome c oxidase complex of electron transport chain (ETC), which is involved in mitochondrial respiration and the utilization of oxygen to produce ATP (Bensaad *et al*., 2006; Matoba *et al*., 2006). The expression of SCO2 is regulated in a p53 dependent manner. In normal tissues, p53 induces SCO2 expression to maintain the cytochrome c complex. However, in the presence of p53 mutation, depending on the insufficient expression of SCO2, COX deficiency is observed.

Fructose 2,6-biphosphate is an important regulator of glycolysis and gluconeogenesis. It stimulates glycolysis by affecting PFK-1 and inhibits gluconeogenesis by blocking fructose 1,6-biphosphatase (FBPase1) (Green and Chipuk, 2006). A p53 inducible enzyme TIGAR is a FBPase2, which inhibits glycolysis by decreasing the levels of fructose 2,6-biphosphate and the activity of Phosphofructokinase-1 (PFK-1), whereas induces gluconeogenesis by stimulating the activity of FBPase1 (Bensaad *et al*., 2006). In tumor cells, FBPase1 activity is usually attenuated due to the loss of p53-mediated lower TIGAR expression (Bensaad *et al*., 2006, Green and Chipuk, 2006). As a result, in tumor cells, the level of FBPase1 is generally high and glycolysis is being used as the major energy production mechanism.

Kawaguchi and colleagues showed that in the absence of p53, NF-κB signaling pathway is activated due to increased kinase activity of IKKα and IKKβ. Furthermore, this activation leads to enhanced aerobic glycolysis in cultured cells. However, increased rate of glycolysis was inhibited by p65 deletion. Moreover, a glycolysis inhibitor also blocked the activation of NF-κB pathway, suggesting that the rate of glycolysis might be due to the balance of p53 and NF-κB activation in the cells (Kawaguchi *et al*., 2008).

Apart from the genes mentioned above, K-ras oncogene is also known to be involved in the regulation of energy metabolism. Racker and colleagues published that aerobic glycolysis is increased in rat-1 cells transfected with ras oncogene and they proposed a correlation between the tumorigenicity and elevated aerobic glycolysis in the cells (Racker *et al*., 1985). Consistently, PDAC cell lines were shown to have metabolic alterations including increase in glycolysis, fatty acid synthesis, Ribose-5-phosphate production, and decrease in oxidative phosphorylation and fatty acid β-oxidation (Zhou *et al*., 2011). Recently, Ying and colleagues showed that oncogenic

K-ras activation enhances glycolysis and ribose biogenesis through nonoxidative arm of PPP, whereas inactivation of oncogenic *K-ras* leads to decrease in the activation of G6P, F6P, FBP enzymes accompanied by decreased glucose uptake and lactate production. Moreover, knock out of Rpe and/or Rpia, the enzymes involved in PPP, blocked the clonogenic activity of the tumor cells suggesting that *K-ras* driven increased glucose flux is very important for PPP and inactivation of this pathway inhibits tumorigenesis. Furthermore, MAPK pathways and myc activation is required in *K-ras* driven metabolism reprogramming in PDAC (Ying *et al*., 2012).

2. AIM OF THE STUDY

The most common cancer type of exocrine pancreas is pancreatic ductal adenocarcinoma (PDAC), which is the 4th leading cause of cancer-associated deaths worldwide. The average survival is 4-6 months and 5 year survival rate is lower than 5% showing the high mortality rate of the disease. The reasons of the high mortality are asymptomatic nature of the disease, absence of an efficient detection system and fibrotic structure of the organ in the presence of disease causing the inefficiency of medical treatment.

There are several reasons causing to PDAC development including smoking, viral infections, low-physical activity, diabetes, glucose intolerance, obesity and long-term chronic pancreatitis. Furthermore, genetic abnormalities such as activation of oncogenes and/or absence of tumor suppressor genes have been shown to be related with PDAC. Importantly, oncogenic activation of *K-ras* has been detected in 95% of patients, suggesting that *K-ras* activation might be the initiator factor for PDAC progression.

The correlation between chronic inflammation and cancer is well-known. In addition, Nuclear factor kappa B (NF-κB) transcription factor family, which is an essential regulator of innate and adaptive immune system, has been shown to be involved in mutant *Ras* induced cancers. Thus, it was worth to investigate the function of NF-κB during mutant *K-ras* induced PDAC development. To that end, a well-known PDAC mouse model *p48*^{Cre}-*K-ras*$^{LSL-G12D/+}$ (termed p48-Kras), which had oncogenic *K-ras* activation was used and IκB kinase α (IKKα), which is involved during the activation of canonical and non-canonical NF-κB, was deleted in these mice. Additionally, in order to see the effect of post-natal IKKα deletion on p48-Kras mice, Elastase-Cre system was employed and Ikkα$^{F/F}$-Kras-Ela-Cre mice was analyzed. Furthermore, in order to discover how the ablation of non-canonical NF-κB pathway would affect PDAC development, *Relb* was deleted in Ikkα$^{F/F}$-p48-Kras mice. Since IKKα deletion caused increased immune cell infiltration and fibrosis in the pancreas, the contribution of tumor microenvironment was further analyzed and in order to understand whether the acceleration of PDAC was achieved via increased IL4/IL13 signaling, whole body *Stat6* knock out mice were crossed to Ikkα$^{F/F}$-p48-Kras mice. Furthermore, in order to figure out whether IKKα deletion affected energy metabolism in p48-Kras animals, metabolic pathways were checked and Ikkα$^{F/F}$-p48-Kras

animals were treated with a modified glucose molecule, 2-Deoxy Glucose (2-DG), which inhibits glycolysis.

Since PDAC is a very lethal type of cancer, it is very crucial to explore the molecular mechanism of the disease, which might lead to improvement of more efficient detection techniques and treatment options. Thus, establishing the link between NF-κB-driven inflammation, metabolic changes and PDAC progression will be very crucial.

3. MATERIALS AND METHODS

3.1. Mice

3.1.1. Mouse models

The mice were kept in pathogen-free facility, under 12 hours dark/light cycle and fed with autoclaved rodent chow diet (Rodent Standard Diet, Altromin #1314).

K-ras ^{G12D} (*K-ras* ^{LA})

An activating glycine to aspartic acid mutation at codon 12 (G12D) was introduced to *K-ras* exon 1 with the help of a plasmid vector. The expression of this mutant allele is blocked by a stop codon flanked by LoxP sites. Cre-mediated recombination results in the removal of the stop codon and the expression of mutant K-ras allele, leading to oncogenic activation of K-ras gene (Johnson *et al*., 2001).

P48-Cre

A vector was used to replace the protein encoding region of *P48* with the sequences encoding the recombinase cre. The sequence was also including the neomycin resistance gene flanked by loxP sites. Since the sequence is under the control of *P48* gene promoter, Cre can be expressed in the acinar cells of pancreas (Kawaguchi *et al*., 2002).

Ikkα$^{flox/flox}$

A neomycin cassette fragment with loxP sites was added into intron 6 as well as intron 9 of *Ikkα* gene by using a special targeting vector. When crossed to p48-Cre + mouse, following cre recombination, the neomycin cassette is removed and leads to the deletion of exon 6-8 of *Ikkα* gene, which in turn leads to a frameshift for *Ikkα* (Liu *et al*., 2008).

Elastase-Cre

For generating the *Elastase-CreER*^{TM} construct, a 200 bp enhancer of the *Elastase* gene was fused to a minimal *hsp68* promoter and placed the chimeric promoter upstream of a *CreER*^{TM} coding sequence. In order to induce the activation of *Elastase*-Cre in mice, tamoxifen administration is necessary (Stanger *et al*., 2005).

Stat6$^{-/-}$

A targeting vector was employed to place a neomycin resistance cassette in the place of *Stat6* encoding amino acids 505-584 which encodes the SH2 domain required for Stat dimerization. Thus, mutant protein is unable to dimerize and not functional (Kaplan *et al*., 1996).

Relb$^{-/-}$

Exon 4 of *Relb* gene, which encodes the beginning of Rel homology domain, was replaced with a PGK-neomycin cassette fragment by using a targeting vector (Weih *et al*., 1995).

3.1.2. Genotyping of mice

In order to determine the genotype of the mice, genomic DNA was isolated. For this aim, tail of mouse was cut and lysed in a 190 µl lysis buffer and 10 µl proteinase K (Qiagen) mixture at 60°C overnight. After incubation, the samples were heat inactivated at 95°C (Eppendorf) for 10 minutes in order to stop enzymatic reaction. Then, they were centrifuged at 13200 rpm (radius: 13 cm) for 10 minutes. 10 µl of supernatant was diluted with 90 µl of distilled water (dH_2O). This dilution was used for polymerase chain reaction (PCR).

Tail Lysis Buffer: 1.5 M Tris (pH 8.5) (Roth)
200 mM NaCl (Sigma)
0.2% sodium dodecyl sulfate (SDS) (Fluka)
5 mM Ethylenediaminetetraacetic acid (EDTA) (Fluka)

General PCR mix: Taq PCR Master Mix (Qiagen) 12.5 µl
100 pMol Forward Primer 0.5 µl

100 pMol Reverse Primer	0.5 µl
dH_2O	7.5 µl
DNA	3 µl

Each PCR condition includes an initial denaturation step at 94°C for 5 min and a final elongation step at 72°C for 10 min.

Gene	Primer (F/R*)	Primer Sequence (5'→3')	PCR program
K-ras	F	CCATGGCTTGAGTAAGTCTGCG	94°C 30 sec 60°C 1 min 72°C 1 min } 35 cycles PCR product is~ 550 bp
	R	CGCAGACTGTAGAGCAGCG	
p48 / Cre	370 F	ACCTGAAGATGTTCGCGATTATCT	94°C 30 sec 58°C 30 sec 72°C 30 sec } 35 cycles PCR product is~ 350 bp
	370 R	ACCGTCAGTACGTGAGATATCTT	
αLox	Int5 819 F	GGAATTAGTTCTCCTCTTCTCATATGG	94°C 30 sec 58°C 30 sec 72°C 30 sec } 35 cycles wt 180 bp, mutant 220 bp
	Int5 1027 R	TTAAATTGTTGAAATATCTGTAAAGGAAGG	
RelB	225 F	GGGTATGGCTTATATCCCAGCAG	94°C 30 sec 58°C 30 sec 72°C 30 sec } 35 cycles wt ~165 bp, mutant 200 bp
	328 R	CTGGTGCTTGCTTTAATTTGGTT	
Stat6	oIMR0092	AATCCATCTTGTTCAATGGCCGATC	94°C 30 sec 66°C 30 sec 72°C 1 min } 40 cycles wt~275 bp, mutant~380 bp
	oIMR1822	ACTCCGGAAAGCCTCATCTT	
	oIMR7416	AAGTGGGTCCCCTTCACTCT	

Table 3.1. Primer sequences for each gene, the product sizes and PCR conditions are depicted. * Forward/Reverse, wt: wild type, bp: base pair.

The PCR products were checked on a 2% agarose gel containing ethidium bromide (EtBr) (Invitrogen).

2 % Agarose Gel : 2 % (w/v) Agarose (PEQLab) in 1X TAE Buffer

50X TAE Buffer : 242 gr Tris Base
27.1 ml Acetic Acid
100 ml 0.5 M EDTA
Completed up to 1 lt with dH_2O

1X TAE Buffer : 20 ml 50X TAE Buffer in 1 lt dH_2O

3.1.3. Mouse treatment

3.1.3.1. Tamoxifen Administration

In order to induce Cre expression in $Ikk\alpha^{F/F}$-Kras-ElaCre model, 1 mg tamoxifen (Sigma) was dissolved in 100 µl 10% ethanol/90% sunflower oil mixture and given to mice for 5 consecutive days by oral gavage.

3.1.3.2. 2-Deoxy Glucose (2-DG) Treatment

To block glycolysis in mice, 0,082 mg 2-Deoxy-Glucose (2-DG) (Sigma-Aldrich) was diluted in 1 ml dH_2O and 3 mM/gr 2-DG was administered to two weeks old mice by intra-peritoneal (IP) injection once every 3 days.

3.1.4. Sacrifice of mice

After sacrifice, pancreas and other organs including stomach, muscle, liver, spleen and lungs were harvested. For histological analysis, tissues were transferred to 4% paraformaldehyde (Electron Microscopy Sciences) overnight at 4°C. Subsequently, they were processed in dehydration machine (LEICA ASP300S) overnight and embedded in paraffin blocks. For molecular analysis (RNA and protein analysis) tissues were immediately frozen in liquid nitrogen and stored at -80°C until use.

3.2. Histology

3.2.1. Haematoxylin & Eosing staining (H&E)

H&E staining is one of the basic staining methods to examine the histology of organs. To prepare tissue sections, paraffin embedded tissues were kept at -20°C for 30 min to cool down. The sections were taken in 3-4 μm thickness using a microtome (Leica RM2235) and mounted on glass slides (Thermo Scientific), kept at RT overnight or 37°C for 1-2 hours for drying. The dry sections were first deparaffinized in xylene (X-TRA Solv, Medite) for 10 min to remove paraffin from tissues, and rehydrated in serial EtOH dilutions (Medite) (100%, 95%, 80%, 70%, 50% respectively) for 2 min each. After rehydration, samples were washed in PBS to get rid of excess ethanol and kept in hematoxylin (Vector Laboratories) for 1 min to stain nucleus, washed with dH_2O until the excessive color was gone. The next step was cytoplasm staining with 1% eosin solution. Sections were kept in eosin solution for 10-15 seconds, washed two times with distilled water (dH_2O) and dehydrated by inserting in serial EtOH dilutions (50%, 70%, 80%, 95%, 100% respectively). As a last step, they were put in xylene for 10 min and left at RT for xylene evaporation and drying. Tissues were further mounted with cover slips (Menzel-Gläser) using mounting medium (Vector Laboratories).

Eosin solution: 2.5 gram eosin (Eosin Y disodium salt/Sigma-Aldrich) was dissolved in 250 ml dH_2O, supplemented with 15 drops of acetic acid (Sigma).

3.2.2. Alcian Blue staining

For Alcian blue staining, deparaffinization and rehydration steps were performed as indicated for H&E staining. After rehydration, sections were washed with PBS to get rid of EtOH, stained with Alcian blue solution for 30 min at RT. After incubation, the sections were washed with dH_2O until the excessive color was gone and counterstained with ready-to-use nuclear fast red solution (Vector Laboratories) for 5 min at RT, washed with dH_2O for 1 min, dehydrated in serial EtOH dilutions, kept in xylene for 10min, air-dried and mounted.

Alcian Blue solution: 1 gr Alcian blue, 8GX (Sigma)
100 ml 3% Acetic acid solution
pH is adjusted to 2.5 using Acetic acid (Sigma)

3% Acetic acid solution: 3 ml Acetic acid
97 ml dH_2O

3.2.3. Sirius Red staining

After rehydration as mentioned above, sections were washed with PBS and stained with Sirius red solution for 2 hours at RT, treated with PBS for 1 min, washed with dH_2O for 5 min. The sections were dehydrated, cleaned in xylene and covered as previously explained.

Sirius Red Solution: 0.1 gr Direct Red 80 (Sigma-Aldrich)
0.1 gr Fast Green FCF (Sigma-Aldrich)
Dissolved in 100 ml Picric acid (Sigma)

3.2.4. Immunohistochemical staining (IHC)

IHC staining is done to detect specific localization of proteins of interest in the cells by using antibodies. The preparation of tissues for IHC, deparaffinization, dehydration, and following washing was done as explained previously. Afterwards, sections were treated with 3% Hydrogen peroxide (H_2O_2) (Sigma)/PBS for 10 min at RT to block endogenous peroxidase activity and washed with PBS for 5 min. Antigen retrieval was done by keeping the sections in 2,8 ml antigen unmasking solution (Vector Laboratories) mixed with 300 ml dH_2O and boiled for 20 min in a microwave (Sharp) at 180-360°C. After cooling down at RT for 20 min, each section was treated with 3% BSA (Roth) / PBS with 2 drops of avidin block (Vector Laboratories) for 30 min at RT and then the first antibody was applied in suitable dilutions with 3% BSA/PBS and biotin (Vector Laboratories). Incubation time and temperature was different according to each antibody, thus sections were treated with first antibody either for 1 hour at RT or overnight at 4°C. After incubation, sections were washed 3 times with PBS for 5 min each. Biotinylated secondary antibody (Vector Laboratories), diluted 1:2000 in 3% BSA/PBS, was added onto sections and incubated for 30 min at RT, followed by 3 washing steps for 5 min with PBS. Subsequently, sections were incubated with ABC solution (avidin dehydroxygenase and biotinylated horseradish peroxidase, Vector Laboratories) for 30 min at RT, washed again as previous step and kept in dH_2O. For color development, sections were incubated with DAB solution (3,3'-diaminobenzidine solution; 5 ml dH_2O consisting of 2 drops of buffer stock solution, 4 drops of DAB, 2 drops of H_2O_2) (DAB kit, Vector Laboratories) for 5 sec-3 min. When the positive signal was detected under microscope, DAB reaction was stopped

immediately by putting the sections in dH_2O. Afterwards, sections were counterstained in hematoxylin for 1 min, followed by washing in dH_2O until the excessive color was gone. Dehydration, cleaning with xylene and covering the slides were performed as explained before.

Antibody	**Company**	**Catalog Num.**	**Working Dilution**	**2nd Antibody**
Ki67	Santa Cruz	sc-15402	1:1000	Anti-rabbit
RelA (p65)	Neomarkers	1638-PO	1:750	Anti-rabbit
RelB	Santa Cruz	sc-226	1:200	Anti-rabbit
p53	Novocastra	NCL-p53- CM5p	1:500	Anti-rabbit
β-catenin	Santa Cruz	sc-1496	1:100	Anti-rabbit
c-myc	Santa Cruz	sc-764	1:100	Anti-rabbit

Table 3.2. The details of first antibodies that were used in IHC are depicted.

3.2.5. TUNEL staining (TdT-mediated dUTP-biotin nick end labeling)

TUNEL staining is performed to visualize apoptotic cells using the commercial Kit ApoAlert DNA-Fragmentation Assay (Clontech). The preparation of tissue sections, deparaffinization, and dehydration was performed as indicated for H&E staining. Afterwards, tissues were kept in 0.85% NaCl solution for 5 min. and washed with PBS for 5 min. After washing, sections were fixed with 4% PFA for 15 min at RT, followed by 2 times wash with PBS for 5 min and draining, incubated with 100 µl of 20 µg/ml Proteinase K for 5 min at RT. Subsequently, samples were again fixed with 4% PFA for 5 min, washed with PBS for 5 min. Following washing, each section was treated with 51 µl of mix containing equilibration buffer (45 µl), nucleotide mix (5 µl), and TdT enzyme (1 µl) for 1 hour at 37°C in a dark humidified incubator (MAXQ 4000-Thermo Scientific). The enzymatic reaction was stopped by inserting the samples into 2 X SSC (dH_2O diluted) (Clontech) for 15 min at RT, followed by 2 times washing with PBS for 5 min each. At the end, the sections were covered with DAPI containing anti-fade medium (ProLong Gold, Invitrogen) and kept at 4°C in dark until use.

3.3. RNA Analysis

3.3.1. RNA isolation from tissue and cells

To isolate RNA from tissues, first the frozen tissue was crushed on a cold plate using a pestle. All the equipments that were used to crush tissues were previously cooled down by keeping them in liquid nitrogen. Crushed tissue was taken into a cold, sterile 5 ml polypropylene

round-bottom tube (Becton Dickinson) and 1 ml of Trizol (TRI Reagent® Solution; Ambion) added onto the sample. The tissues were kept on ice and homogenized with Polytron (Polytron-PT1200E), which was previously washed 1 time with 10% SDS/DEPC water, and 2 times with DEPC water, respectively. Homogenized tissues were transferred into a 1.5 ml eppendorf and centrifuged at 24042 g for 10 min at 4°C. Afterwards, supernatant was collected and kept 5 min at RT. 200 µl Chloroform (Merck) was added onto samples and they were shaken forcefully for 15 sec, incubated for 2-3 min at RT, centrifuged at 24042 g for 15 min at 4°C. Subsequently, the transparent aqueous part was collected. 400 µl isopropyl alcohol (Merck) and 400 µl high salt precipitation solution (Molecular Research Center Inc.) was added onto samples and they were incubated for 15 min at RT, centrifuged at 24042 g rpm for 10 min at 4°C. After centrifugation, supernatant was discarded and the pellet was washed with 400 µl of 75% EtOH (diluted with DEPC water). The samples were vortexed, centrifuged at 15027 g for 5 min at 4°C. Supernant was removed and RNA pellet was air-dried. Then, RNA pellet was dissolved in RNAse free water by incubating at 37°C for 5 min. As a last step, concentration of RNA samples was checked using NanoDrop (Thermo Scientific/ PEQLAB) and stored at -80°C (Thermo Scientific).

In order to extract RNA from cells, The RNeasy Mini Kit (Qiagen) was used and all isolation steps were carried out at RT. According to the manufacturer's protocol, RLT buffer supplemented with 1% β-mercaptoethanol (Sigma) was added onto the cell pellet to disrupt the cells. Afterwards, the lysate was transferred into a QIAshedder spin column (Qiagen) and centrifuged at maximum speed for 2 min. The flow-through was kept and mixed with one volume of 70% EtOH, transferred to an RNeasy spin column, centrifuged at ≥ 8000 g for 15 sec. and after this step flow-through was always discarded. Then, 700 µl of Buffer RWI was used to wash the column-bound RNA, centrifuged at ≥8000 g for 15 sec and washed 2 times with Buffer RPE. After this step, the column containing RNA was placed into a clean 2 ml collection tube and centrifuged at full speed for 1 min to get rid of excessive buffer. As a last step, depending on the expected amount of RNA, 30-50 µl RNase-free water was put on the column that was previously placed in a 1.5 ml collection tube, centrifuged for 1 min at ≥8000 g. RNA concentration was measured using NanoDrop. Samples were kept at -80°C (Thermo Scientific).

3.3.2. cDNA Synthesis

As an initial step of cDNA synthesis, RNA concentration and purity was checked using NanoDrop. Generally, 0.5 or 1 µg of total RNA was used for cDNA synthesis. Required amount of RNA was calculated and incubated with 1 µl of Oligo (dT) (50 µM, Invitrogen), 1 µl of dNTP mix (10 mM each, Invitrogen) and dH_2O in a final volume of 12 µl at 65°C for 5 min. Afterwards, the samples were quickly chilled on ice, centrifuged briefly and 7 µl mixture containing 5X First-Strand Buffer (4 µl) (Invitrogen), 0.1M DTT (2 µl) (Invitrogen), RNaseOUT^{TM} (40 units/µl) (1 µl) (Invitrogen) was added onto the samples, and they were incubated at 42°C for 2 min. Subsequently, 1 µl of SuperScript^{TM} II RT (200 units) (Invitrogen) was added and incubated at 42°C for 50 min. The reaction was stopped by keeping the samples at 70°C for 15 min. The final volume was completed up to 100 µl with dH_2O and the samples were kept at -20°C.

3.3.3. RT- PCR

In order to detect the expression of genes of interest, we performed RT-PCR using a StepOne Plus Real Time PCR system (Applied Biosystems). Primers were designed using Primer express 1.0 primer software. SYBR Green Master Mix (Roche) was used to label amplified DNA. 96 well plates (Applied Biosystems) were used for reaction. For each well, a mixture of 10 µl of Syber Green Master Mix, 5 µl of dH_2O, 2 µl of primer mix (final concentration for each primer is 0.5 pmol/µl), and 3 µl cDNA was added. For amplification, a standart program was used: 50°C for 2 min, 95°C for 10 min, followed by 40 cycles of 95°C for 15 sec, 60°C for 1 min and a final melting curve step. The results were analyzed employing the StepOne Software v2.0.2 and normalized according to the expression of housekeeping gene Cyclophylin with the formula $2^{\Delta CT}_{Cyclophilin} - 2^{\Delta CT}_{target\ gene.}$

Gene	Primer (F/R*)	Primer Sequence (5'→3')
ARG-1	F	GTGAACACGGCAGTGGCTTT
	R	GTCCCTGGCTTATGGTTACCC
CD44	F	CTCCTGGCACTGGCTCTGA
	R	CTGCCCACACCTTCTCCTACTATT
CD68	F	CTTCCCACAGGCAGCACAG
	R	AATGATGAGAGGCAGCAAGAGG
Cox7a2	F	CTTGCTCGACGCGCG
	R	AGCGCTAGGAGGGAGTTCCGTTTCC
Cyclophilin	F	ATGGTCAACCCCACCGTGT
	R	TTCTGCTGTCTTTGGAACTTTGTC
DECTIN-1	F	GGCGGGGAATAAAACGGAGCGA
	R	CCTCACGGGCACAAGTCTGGAA
F4/80	F	CTTTGGCTATGGGCTTCCAGTC
	R	GCAAGGAGGACAGAGTTTATCGTG
FBPase	F	CCATCATAATAGAGCCCGAGAAGA
	R	CTTTCTCCGAAGCCTCATTAGC
G6Pase	F	GAAGGCCAAGAGATGGTGTGA
	R	TGCAGCTCTTGCGGTACATG
G6pd2	F	CTGAATGAACGCAAAGCTGA
	R	CAATCTTGTGCAGCAGTGGT
GLS	F	TCAAAGGGTGAAGTCGGTGAT
	R	AATCCCGCTGCTCCATGTC
GLT1	F	TGCTCATCCTCCCTCTTATCATC
	R	GGCCGCTGGCTTTAGCAT
Glys	F	GAGAACGCAGTGCTCTTCGAA
	R	TCGTCTGCAGCACCGTGTAG
Gpi	F	GTGGTCAGCCATTGGACTTT
	R	CTTTCCGTTGGACTCCATGT
GS	F	CGGCCACCGCTCTGAA
	R	ACATTTGCTTGATGCCTTTGTTC
h-ARG-1	F	GGCAAGGTGATGGAAGAAAC
	R	AGTCCGAAACAAGCCAAGGT
h-Cyclophilin	F	ATGGTCAACCCCACCGTGT
	R	TCTGCTGTCTTTGGGACCTTGTC
h-IL1β	F	GTGCACGATGCACCTGTACG
	R	ATCACCAAGCTTTTTTGCTGTG
h-IL4	F	ACATCTTTGCTGCCTCCAA
	R	AGGCAGCGAGTGTCCTTCT

h-IL6	F	ACCCCTGACCCAACCACAA
	R	GTCATGTCCTGCAGCCACTG
h-IL10	F	GATCCAGTTTTACCTGGAGGA
	R	CCTGAGGGTCTTCAGGTTCTC
h-IL13	F	ACAGCCCTCAGGGAGCTCAT
	R	TCAGGTTGATGCTCCATACCAT
h-IL4Rα	F	AGACCCCCAAAATCGTGAACT
	R	GCAACAAGAGGACATGCACCTA
h-IL13Rα1	F	GAAGCAAACCAAGGAGGAAACC
	R	ATCTCCATCACTGAGAGGCTTTCT
h-MRC-1	F	CAGCGGTTGGCAGTGGA
	R	CAGCTGATGGACTTCCTGGTAAG
h-MCP-1	F	CGACATCCTGGAACTGCCCTACC
	R	CACTGTGCCGCTCTCGTTCAC
h-TNFα	F	ATCAATCGGCCCGACTATCTC
	R	TGTTCGTCCTCCTCACAGGG
HK1	F	TCTCCAGAATCATGGACCA
	R	GATCCTGCTCTTAGGCGTTC
HK2	F	AACCGAACAAGCTGGTGTAC
	R	TGCACACATCTATAGGTGGC
IFNγ	F	TTACTGCCACGGCACAGTCA
	R	AGTTCCTCCAGATATCCAAGAAGAGA
IFNGR	F	CAAAGGCTCTGGAGGCTGG
	R	TTTGTGTCGGAGTTGGAGGG
IL1β	F	GTGGCTGTGGAGAAGCTGTG
	R	GAAGGTCCACGGGAAAGACAC
IL4	F	ACAGGAGAAGGGACGCCAT
	R	GAAGCCCTACAGACGAGCTCA
IL4Rα1	F	AGCCTGCTGTCCTCCGCT
	R	CTGGTCATATGTGGGTAACTGGC
IL6	F	GTATGAACAACGATGATGCACTTG
	R	ATGGTACTCCAGAAGACCAGAGGA
IL10	F	GGTTGCCAAGCCTTATCGGA
	R	ACCTGCTCCACTGCCTTGCT
IL12p35	F	CACGCTACCTCCTCTTTTTG
	R	CAGCAGTGCAGGAATAATGTT
IL13	F	GGACCCAGAGGATATTGCATG
	R	GGGAGGCTGGAGACCGTAG
IL13Rα1	F	TGGAGCACGGCACAATTG
	R	TCTAAGATGCCTGTATCCCAGCT

MCP-1	F	GGC TCA GCC AGA TGC AGT TAA
	R	CCT ACT CAT TGG GAT CAT CTT GCT
MRC-1	F	TTGGTGGCAATTCACGAGAG
	R	GGGAAGGGTCAGTCTGTGTTTG
Mttp	F	CAAGCTCACGTACTCCACTGAAG
	R	TCATCATCACCATCAGGATTCTC
Ndufb9	F	CAGAATCAGCATCCTCAGCCGTATATC
	R	AGGTCTGGTCACAATATGCCACCACA
Ndufb10	F	TGTGCCAAGGAACTGGAGCA
	R	GCCTCGCAGCCTTCCTTTCT
OAT	F	GCCCTTTCTGGCGGTTTATAC
	R	TGGTTTAATGGTCAGCATTATCTCA
p16	F	CCCAAGGCCCCGAACTC
	R	TGTGAACGTTGCCCATCATC
PDHb	F	GAAGGAGGCTGGCCACAGT
	R	TTGAACGCAGGACCTTCCAT
Prominin1	F	TCTTTTGTATGTGCCGTTGCTG
	R	GCATGGCGCATTCTGCTT
Prps1	F	TTGATATCCCGGTGGACAAT
	R	AGGGCCAGAAAAGATTCCAT
Rbks	F	AGTGGCTGGAGCAAATCTGT
	R	GCGTGGCCTGTTAAAATCTC
Rpe	F	GGGGAATGGGATGAAGGTT
	R	GCACTGCCAGACACAATCAT
Rpia	F	TGCAGCGAATAGCTGAAAGA
	R	ACAGCCATTCGAAGTTCCAC
SdHa	F	ATGCCAGGGAAGATTACAAAGTGC
	R	GTAACCTTGCCAGTCTTGATGTCC
Spp1 (OPN)	F	TTTGCCTGTTTGGCATTGC
	R	TCTTCTCCTCTGAGCTGCCAG
Taldo1	F	TGACGCTCATCTCTCCCTTT
	R	GCCAGCTTGCTGTTATCCTT
TNFα	F	ACTCCAGGCGGTGCCTATG
	R	GAGCGTGGTGGCCCCT
Tkt	F	TCCACCGTCTTTTACCCAAG
	R	CAAGGCCTCATGCAGAGTTA

Table 3.3. Primer sequences of each gene, which were used for RT-PCR are shown.

3.3.4. RNA microarray analysis

3.3.4.1. Microarray sample labeling, hybridization and processing

Total RNA (1.5 μg) and newly transcribed RNA (280 ng) were amplified and labeled using the Affymetrix One-Cycle Target Labeling Kit. As newly transcribed RNA mainly consists of mRNA, it was amplified and labeled according to the manufacturer's protocol for mRNA. The amplified and fragmented biotinylated cRNA was hybridized to Affymetrix Mouse Gene ST arrays using standard procedures.

3.3.4.2. Microarray data processing and statistical analysis

Data were processed and analyzed with R and Bioconductor (R Development Core Team 2007). Arrays were assessed for quality, RMA-normalized and filtered for low and invariant expression. "Quality assessment" consisted of RNA degradation plots, Affymetrix quality control metrics, sample cross-correlation, data distributions, and probe-level visualizations. Data is normalized for (separately for each RNA type data set) background correction and probe-level summarization by RMA. Differential gene expression between the groups was statistically assessed by SAM28, which repeats permutations of the data to determine if the expressions of any genes are significantly related to the response. Differentially expressed genes between the groups were identified at the p-value (corrected for multiple testing FDR) cutoff of 0.0%.

3.4. Protein Analysis

3.4.1. Protein extraction from tissues

Protein extraction was done using both frozen tissue and cultured cells. Frozen tissue was crushed on a cold plate and transferred into a 1.5 ml eppendorf kept on ice. 100 μl of protein lysis buffer was added onto samples and homogenized with a pellet pestle, followed by centrifugation at 4°C at 24042 g for 20 min. Then, supernatant was collected and protein concentration was measured using NanoDrop. The same procedure was employed for protein extraction from cells.

Protein Lysis Buffer (stock) : 50 mM Tris-HCl (pH 7.5) (Roth)
250 mM NaCl (Sigma)

30 mM EDTA (Fluka)
30 mM EGTA (Sigma)
25 mM sodium pyrophosphate (Sigma)
1% Triton-X 100 (Sigma)
0.5% NP40 (Sigma)
10% Glycerol (Merck)
1 mM DTT (Sigma)
1 tablet of complete protease inhibitor cocktail tablets (Roche) / 50 ml

Protein Lysis Buffer (complete) : 8 ml of stock protein lysis buffer
50 mM β-glycerol 2-phosphate disodium salt hydrate (Sigma)
25 mM sodium fluoride (Sigma)
5 mM sodium pyrophosphate (Sigma)
5 mM sodium orthovanadate (Sigma)
2 nM PMSF (Sigma)

3.4.2. Immunoblot analysis

In order to detect the expression of gene of interest at the protein level, WB using Biorad Mini Protean Gel System (BioRad) was performed. As a first step, protein concentrations were determined by Bradford assay in which 2 µl of protein sample was mixed with 1 ml of 1:5 diluted protein assay dilution (PAD) (BioRad), kept for 5 min at RT, and concentrations were measured according to their absorbance at 595 nm using a spectrophotometer. Afterwards, 10-30 µg of protein was adjusted to a volume of 15 µl with complete lysis buffer, and mixed with 10 µl of Laemmli buffer containing 0.5 µl β-mercaptoethanol (Sigma) mixture, denatured by boiling at 95°C for 5 min. Samples were shortly spinned and the supernatants were loaded on a polyacrylamide gel (7 to 12%) and run in 1X running buffer at 30 mA for 1-1.5 hours at RT.

Running Gel (7-10-12%) : 8.62/ 7.5/ 6.75 ml dH_2O
2.63/ 3.75/ 4.5 ml 40% acrylamide/bisacrylamide (A/B) (Merck)
3.75 ml main gel buffer
112.5 µl 10% ammonium persulphate (APS) (Sigma)

11.25 µl Tetramethylethylenediamine (TEMED) (Sigma)

Stacking Gel : 4.6 ml dH_2O
950 µl stacking gel buffer
950 µl A/B
62.5 µl 10% APS
12.5 µl TEMED

Laemmli Buffer : 3.55 ml dH_2O
1.25 ml 0.5M Tris-HCl (pH 6.8)
2.5 ml Glycerol (Merck)
1 ml 20% SDS (w/v)
0.2 ml 0.5% Bromophenol blue (BPB) (Sigma)

10X Main Gel Buffer (stock) : 181.65 gr Tris (Roth)
20 ml 20% SDS (w/v)
Adjusted to 500 ml with dH_2O, pH 8.8

Stacking Buffer (stock) : 12.11 gr Tris
5 ml 20% SDS (w/v)
Adjusted to 100 ml with dH_2O, pH 7.0

10X Running Buffer : 15.15 gr Tris
72 gr Glycin (Roth)
25 ml 20% SDS (w/v)
Adjusted to 500 ml with dH_2O

1X Running Buffer : 100 ml 10X main gel buffer (stock)
900 ml dH_2O

20% SDS : 20 gr SDS in 100 ml dH_2O (w/v)

Tris-HCl : 6 gr Tris in 100 ml dH_2O (w/v)
pH is adjusted to 6.8 with HCl

APS (10%) : 1 gr APS in 10 ml dH_2O (w/v)

Gels were transferred using the Mini Trans-Blot Cell System (Biorad). The gel was blotted onto a PVDF membrane (Immobilon P, Zefa Laborservice) and transferred in 1X transfer buffer for 2 hours at 250 mA at 4°C. Finally, the membrane was removed from the cassette and incubated in 5% (w/v) skim milk (Fluka)/Phosphate Buffer Saline-Tween (PBS-T) for 1 hour at RT to block unspecific binding. Subsequently, the membrane was incubated with the primary antibody, which was diluted in 3% Bovine Serum Albumin (BSA)/PBS-T or 5% skim milk/PBS-T for 2 hours at RT or 4°C overnight. Afterwards, the membrane was washed 3 times for 5 min each with PBS-T and incubated with the HRP-labeled secondary antibody; mouse (1:3500 diluted with 5% skim milk/PBS-T) or rabbit (1:3000 diluted with 5% skim milk/PBS-T) or guinea-pig (1:5000 diluted with 5% skim milk/PBS-T) (GE Healthcare) for 30 min at RT. In order to remove excess antibody, the membrane was washed with PBS-T 3 times for 5 min each, and dried shortly with a pair of Whatman paper. For detection, 3-5 ml ECL solution (Super Signal West Pico or Super Signal West Femto, Thermo Scientific) was put on the membrane for 5 min. Afterwards, the membranes were dried fastly and exposed to an X-ray film (Thermo Scientific) at dark. Then, the X-ray film was developed using the Hyperprocessor (Amersham Bioscience) and the size of bands were checked in comparison to the protein ladder (Thermo Scientific). For further use, the membrane was sealed in PBS and kept at 4°C.

Transfer buffer stock (10X) : 144 gr Glycin (Roth)
30 gr Tris
Completed up to 1 lt with dH_2O

Transfer buffer stock (1X) : 100 ml 10X Transfer buffer stock
200 ml methanol (Merck)
700 ml dH_2O

PBS-T : 5 ml PBS-T stock in 1 lt of PBS (Invitrogen)

PBS-T (stock) : 10 ml Tween (Sigma)
40 ml PBS

Antibody	Company	Cat. Num.	Dilution	2° Antibody
RelA (p65)	Santa Cruz	sc-372	1:1000 in 5% milk-PBS-T	Anti-rabbit
RelB	Santa Cruz	sc-226	1:500 in 5% milk-PBS-T	Anti-rabbit
c-Rel	Santa Cruz	sc-71	1:500 in 5% milk-PBS-T	Anti-rabbit
p52/p100	Cell Signaling	4882	1:1000 in 5% milk-PBS-T	Anti-rabbit
p50/p105	Santa Cruz	sc-7178	1:750 in 3% BSA-PBS-T	Anti-rabbit
IkBα	Santa Cruz	sc-371	1:500 in 5% milk-PBS-T	Anti-rabbit
phospho-IkBα	Cell Signaling	9241	1:500 in 3% BSA-PBS-T	Anti-rabbit
IKKα (IKK1)	IMGENEX	IMG-136A	1:1000 in 3% BSA-PBS-T	Anti-mouse
Cyclin D1	Santa Cruz	sc-718	1:500 in 5% milk-PBS-T	Anti-rabbit
p16	Santa Cruz	sc-1661	1:500 in 5% milk-PBS-T	Anti-mouse
p16	Santa Cruz	sc-1207	1:250 in 5% milk-PBS-T	Anti-rabbit
p-AKT (S473)	Cell Signaling	9271	1:1000 in 3% BSA-PBS-T	Anti-rabbit
AKT	Cell Signaling	9272	1:1000 in 5% milk-PBS-T	Anti-rabbit
mTOR	Cell Signaling	2983	1:1000 in 5% milk-PBS-T	Anti-rabbit
RICTOR	Cell Signaling	2114	1:1000 in 3% BSA-PBS-T	Anti-rabbit
GβL	Cell Signaling	3274	1:1000 in 3% BSA-PBS-T	Anti-rabbit
p-mTOR	Cell Signaling	2971	1:1000 in 3% BSA-PBS-T	Anti-rabbit
p-mTOR	Cell Signaling	2974	1:2000 in 3% BSA-PBS-T	Anti-rabbit
p38	Santa Cruz	sc-535	1:1000 in 5% milk-PBS-T	Anti-rabbit
OXPHOS	Mitosciences (Abcam)	MS604	1:1000 in 5% milk-PBS-T	Anti-mouse
GAPDH	Cell Signaling	2118	1:1000 in 3% BSA-PBS-T	Anti-rabbit

Table 3.4. The primary antibodies used for WB are shown.

3.5. Cell Culture and Transfection

Human pancreatic cancer cell line, Patu-S, was cultured under standard conditions in RPMI medium containing 10% serum and antibiotics (penicillin/streptomycin) (Invitrogen), whereas mouse pancreatic cancer cells were cultured in DMEM medium containing 10% serum and antibiotics (penicillin/streptomycin).

During transfection, two different mixtures were prepared separately. The first mixture contained 5 µl scrambled RNA (scRNA) or small interfering RNA (siRNA) (1552) for IKKα (final concentration is 100 pmol) and 250 µl Optimem medium (Invitrogen). The second mixture included 5 µl Lipofectamine (Invitrogen) and 250 µl Optimem medium, which was kept for 5 min at RT after preparation. Afterwards, these two mixtures were combined and incubated for 20

min at RT. Just before transfection, the medium of the cells was replaced with 2 ml Optimem medium, and 500 µl final mixture was pipetted onto the cells. The cells were kept in this medium for 6 hours at 37°C in CO_2 incubator. Then, the medium was replaced with RPMI or DMEM accordingly.

3.6. Fluorescence Activated Cell Sorting (FACS)

3.6.1. Cell Isolation

To isolate pancreatic cells, pancreas was minced in digestion buffer containing RPMI 1640 (L-Glutamine) (Gibco) supplemented with Collagenase P (Roche), Dispase II (Roche) and DNAse I (Roche), and transferred to a 50 ml falcon tube. The amount of digestion buffer was added up to 5 ml and the samples were incubated by shaking in a 37°C preheated incubator (MAXQ 4000-Thermo Scientific) for 25 min. After incubation, 100 µl of 0.5 M EDTA (pH 8.0) (Ambion) was added to inactivate enzymatic reaction and samples were kept at RT for 5 min. Afterwards, the samples were passed through 70 µm and 40 µm cell strainers (BD Falcon) respectively to get rid of undigested tissue particles. Subsequently, 10 ml Dulbecco's Phosphate Buffered Saline (PBS) (Gibco) / 2% Fetal Calf Serum (FCS) (Gibco) were added to wash and centrifuged at 1500 rpm for 5 min. The supernant was removed. The cell pellet was dissolved in 1 ml red blood cell (RBC) lysis buffer (Sigma) to lyse the erythrocyte membranes 5 minutes at RT. Then the samples were washed and centrifuged again as above. The supernant was removed and isolated cells were resuspended in %2 FCS/PBS (FACS Buffer).

3.6.2. Staining

After cell isolation, resuspended cells were divided into a 96 well plate, centrifuged in 1500 rpm for 5 min at 4°C. Supernatant was removed and the cells were dissolved in 100 µl of FACS buffer containing 1,5-2 µl ethidium monoazide (EMA) (Sigma) for each well. In order to detect dead cells, the samples were incubated in this dilution on ice for 15 min under bright light. At the end of incubation, cells were centrifuged at 880 g for 5 min at 4°C and then washed using 100 µl of FACS buffer. Subsequently, cells were resuspended in α-CD16/32 blocking antibody (Clone: 2.4G2, BD Pharmingen) at a dilution of 1:100 in FACS buffer and kept on ice for 10 min to prevent unspecific binding of antibodies, followed by centrifugation at 880 g for 5 min at 4°C

and washing with FACS buffer. Afterwards, the cells were resuspended in 100 µl of antibody/FACS buffer dilution and incubated on ice for 20 min at dark. The antibodies used at this step (α-CD11c, α-CD11b, α-F4/80, α-GR-1, α-CD44, α-EpCAM, α-IL-13Ra1 (α-CD213a1), α-fibroblast) were able to detect cell surface markers. After incubation, cells were centrifuged at 880 g for 5 min at 4°C, and washed once in FACS buffer. In order to detect fibroblasts, we performed an indirect staining technique. Thus after first antibody incubation, centrifugation and washing steps, FITC-conjugated rat IgG2a antibody diluted in FACS buffer was added onto the cells and incubated on ice for 30 min under dark. Subsequently, the cells were fixed by incubating with fixation buffer (eBioscience) on ice for 30 min at dark. Following further centrifugation and washing steps, the cells were resuspended in another antibody (α-IL-13-PE, α-IL-4-PE) dilution that required intracellular staining. The antibodies were diluted with 1X permeabilization buffer. After 30 min incubation on ice under dark, the cells were centrifuged and washed once with FACS buffer. Finally, cells were diluted in FACS buffer, filtered using 50 µm filcons (Günter Keul GmbH) and counted using the Gallios Flow Cytometer (10 colors, 3 lasers-Beckman Coulter). Data analysis was done using FlowJo Version 8.8.6 Software.

Antibody	Conjugated Dye	Clone	Dilution	Company
α-CD11c	FITC	HL3	1: 200	BD Pharmingen
α-CD11b	APC-eFluor® 780	M1/70	1: 200	eBioscience
α-F4/80	APC	BM8	1: 200	eBioscience
α-GR-1 (α-Ly-6G)	Alexa Fluor® 700	RB6-8C5	1: 200	eBioscience
α-CD44	APC-eFluor® 780	IM7	1: 200	eBioscience
α-EpCAM (α-CD326)	APC	G8.8	1:200	eBioscience
α-IL-13Ra1 (α-CD213a1)	PE	13MOKA	1:100	eBioscience
α-fibroblast	-	TR7	1:100	Thermo Scientific
FITC-conjugated rat IgG2a	FITC	MARG2a1	1:100	Thermo Scientific
α-IL-13	PE	eBio13A	1:100	eBioscience
α-IL-4	PE-Cy7	BDV6-24G2	1:200	eBioscience

Table 3.5. The antibodies used for FACS analysis, their conjugated dyes, clones, dilution ratios and company names.

3.7. Magnetic Activated Cell Sorting (MACS)

To isolate $CD11b^+$ cell population from pancreas, we performed MACS. The first step of MACS sorting was pancreas digestion and cell isolation, and these steps were performed as explained above. At the end of cell isolation, cell pellets were dissolved in 450 µl MACS buffer

and transferred into a 1.5 ml eppendorf tube. 50 µl CD11b beads (Miltenyi Biotec) were added onto the samples and incubated for 20 min at 4°C on a rotator under dark. Following incubation, 1 ml MACS buffer was added on the samples and centrifugated at 330 g at 4°C, supernatant was discarded and washing was repeated. After discarding the supernatant, the cells were dissolved in 1 ml MACS buffer and kept on ice. The big columns were placed on MACS multistand and 1 ml MACS buffer was loaded for wetting. Subsequently, samples were loaded onto the columns. Once passed, three times washing was performed by applying 1 ml MACS buffer each. At the end of washing, a clean 15 ml falcon was placed under the columns, 1 ml MACS buffer was put onto the columns again and the syringe was applied immediately. The falcon tube was centrifuged at 330 g at 4°C, supernatant was discarded and the $CD11b^+$ cells were further used for protein or RNA isolation.

MACS buffer: 0.5% BSA in PBS (w/v), supplemented with 2 mM EDTA

3.8. Mitochondrial Analysis

3.8.1. Mitochondrial Genome Quantification

Quantification of mitochondrial genome was done by detecting the relative number of mitochondrial genome to nuclear genome copy number by PCR. To that end, DNA was amplified using special primers, which are designed according to the sequences located in the mitochondrial or nuclear genome, and probes, which are indicated in Table 3.6. For PCR, 6 µl of the master-mix and 4 µl genomic DNA (25 ng/ µl) was pipetted into a 96-well plate (Roche, #04729692001). Each sample was pipetted in duplicate. The PCR reaction was performed using LightCycler (Roche, LightCycler® 480 Real-Time PCR System).

General PCR mix:		
	Master Mix (Roche, #04887301001)	5 µl
	Probe	0.2 µl
	Forward Primer	0.2 µl
	Reverse Primer	0.2 µl
	dH_2O	0.4 µl

PCR conditions : 95°C 5 min

95°C 10 sec
60°C 20 sec } 40 cycles
72°C 10 sec

40°C 10 sec

For the quantification, mitochondrial and nuclear genome ct values were raised by 2 and the reciprocal value was taken (1/(2^ct)). Then, the values were multiplied with a factor of 10^6 and the mean mitochondrial DNA amount was divided by the mean nuclear DNA amount.

Mouse nuclear primer pair	F*	5'-TTTACAGGATCTCCAAGATTCAGA-3'	Probe No.26 (Roche, #04687574001)
	R*	5'-GATACACCCATGTGAACAAA-3'	
Mouse mitochondrial primer pair	F	5'-CAAATTTACCCGCTACTCAAC-3'	Probe No.101 (Roche, #04692195001)
	R	5'-GCTATAATTTTTCGTATTTGTGTTTG-3'	

Table 3.6. The primer sequences and probe numbers for PCR analysis are shown. ***Forward, Reverse.

3.8.2. Mitochondria Isolation

To isolate mitochondria, the pancreas was harvested into 5 ml cold isolation buffer and minced in isolation buffer using scissors. Then, the homogenate was transferred into a glass homogenizer (potter) (Sartorius, #BBI-854 2406), and filled up to 15 ml with cold isolation buffer. The cells were separated by moving the teflon plunger (Sartorius, #BBI-854 2805) up and down carefully. The homogenate was transferred into a tube and centrifuged at 800 rpm at 4°C for 10 min to get rid of the cell fragments. Afterwards, the supernatant was transferred into a new tube and centrifuged at 9.000 rpm at 4°C for 10 min. Then the supernatant was discarded and the pellet was resuspended in isolation buffer free of BSA via a brush, transferred into a 1,5 ml tube trough a pipette. The tip was previously cut in order to avoid the disruption of mitochondria due to shear force. As a last step, the concentration of mitochondria was measured via Bradford assay at 595 nm using a BSA standard curve with the concentrations ranging from 0,04 to 0,2 µg/µl.

Isolation Buffer : 192 mM Mannitol (Roth, #4175.1)
58 mM Sucrose (Roth, #4621.1)
2 mM Tris-HCL

0,5 mM EDTA
500 µl Inhibitor Halt™Protease Inhibitor Single-Use Cocktail
(TermoScientific, #78425)
Adjusted to 500 ml with dH_2O
pH is adjusted to 7,2 with 10 M KOH at 4°C

After preparation of the buffer, 100 ml of buffer was separated. Fatty acid free BSA (Sigma, #A3803) was added onto 400 ml of respiration buffer in a final concentration of 2,5%.

Respiration Buffer: 120 mM KCL (Roth, #6781)
5 mM KH_2PO_4 (Roth, # 3904)
3 mM HEPES (Roth, # 9105.4)
1 mM EGTA (Roth, # 3054.2)
5 % BSA
2 mM $MgCl_2$
Adjusted to 500 ml with dH_2O
pH is adjusted to 7,2 with 10 M KOH at RT

3.8.3. Clark Electrode

In order to measure the mitochondrial respiration in the pancreas, the Clark Electrode (Rank Brothers, #Digital model 10) was used. First the Electrode was calibrated with air-saturated assay medium (respiration medium). Then, 1 ml of warm (37°C) respiration buffer was put into the chamber of electrode and 500 µg mitochondria suspension was added. During the measurements, the sample was mixed via a stirrer. In order to measure basal mitochondrial respiration rate, Complex I (NADH dehydrogenase) of the respiration complex was blocked via adding 4 mM rotenone (Sigma, #R8875). Then, as substrate for complex II (Succinate dehydrogenase), 3 mM succinate (Sigma, #S3674) was added and state 2 respiration was measured. Subsequently, 3 mM adenosine diphosphate (ADP) (Sigma, #A2754) was administered to measure the state 3 respiration. Afterwards, the ATP production was inhibited by adding 1 µM oligomycin, which blocks the activation of complex V (ATPase synthase) and state 4 was measured. As a last step, mitochondrial uncoupler carbonylcyanide-p-trifluoromethoxy-phenyl hydrazone (FCCP) was added onto mitochondria and the complex II driven maximum respiration was recorded.

All measurements were performed two times for each mitochondria sample. The respiratory control ratio (RCR), which is the ratio of state 3 to state 4, was calculated for each sample and the median value was considered.

3.9. Statistical Analysis

Data are expressed as mean ± SEM and the differences were analyzed by Student's t-test and one-way ANOVA followed by Bonferroni`s multiple comparison test using Prism5 (GraphPad Software Inc.). Significance of tests are determined according to p-values (* p-value ≤ 0.05, ** p-value ≤ 0.01, *** p-value ≤ 0.001).

4. RESULTS

4.1. Exocrine pancreas-specific deletion of *Ikkα* accelerates pancreatic ductal adenocarcinoma (PDAC) development in p48-Kras^{G12D} mice

Pancreatic ductal adenocarcinoma (PDAC) constitutes of nearly 95% of all exocrine pancreas malignancies. It is an extremely lethal type of cancer as it appears the 4th leading cause of cancer-associated death worldwide (Haq *et al*., 2012). The average survival is 4-6 months. Moreover, 5 year survival rate is less than 5% emphasizing its fast and irrepressible progression (Hingorani *et al*., 2003). The reason for the high mortality rate in PDAC is the absence of an efficient detection system and its resistance to existing chemotherapy. Thus, it is very crucial to explore the molecular mechanisms that underlie the development of PDAC.

The aim of this study was to investigate the role of *Ikkα* during PDAC development. To that end, *Ikkα*$^{F/F}$ mice were crossed to a well established mouse model of pancreatic cancer; *p48*^{Cre}-*K-ras*$^{LSL-G12D/+}$ (termed p48-Kras). Since activating mutations of *K-ras* are seen in nearly 90% of PDAC cases, the use of p48-Kras model in which oncogenic *K-ras* expression is under the control of a pancreas-specific promoter, *p48*, is of relevance to human disease. Moreover, in this model, oncogenic *K-ras* activation leads to the progression of premalignant pancreatic intraepithelial neoplastic lesions (PanINs), which is reminiscent of human PDAC.

By crossing *Ikkα*$^{F/F}$ mice to p48-Kras mice, *Ikkα*$^{F/F}$-*p48*^{Cre}-*K-ras*$^{LSL-G12D/+}$ mice (termed Ikkα$^{F/F}$-p48-Kras), which had simultaneous oncogenic *K-ras* activation and deletion of *Ikkα* only in the exocrine pancreas, was obtained. Pancreas-specific *Ikkα* deletion did not exert any visible phenotype during birth. Ikkα$^{F/F}$-p48-Kras mice were born at an expected Mendelian ratio and bred normally. However, after three weeks of age, Ikkα$^{F/F}$-p48-Kras mice stayed leaner than their control littermates and p48-Kras mice and showed mean survival of 28 days for males (n:21) and 29 days (n:22) for females. Histological sections from the pancreas of 3-4 weeks old Ikkα$^{F/F}$-p48-Kras mice and p48-Kras mice were analyzed and lesion frequency as well as lesion grade was scored. Pancreata from Ikkα$^{F/F}$-p48-Kras mice was completely transformed with PanIN1, 2, 3 lesions, and multifocal cancer areas, which were accompanied with elevated fibrosis and immune cell infiltration (Figure 4.1 A, B). In contrast, age-matched p48-Kras mice showed only diluted ducts and early PanIN1A lesions and the exocrine pancreas was still intact (Figure 4.1 E,

F). This indeed is in accordance with the previous findings that p48-Kras mice do not show pancreatic tumors before 7,5 months unless they are challenged with chronic inflammation (Guerra *et al*., 2007; Khasawneh *et al*., 2008). Indeed when p48-Kras mice were checked at advanced ages (7-14 months) during when they could potentially show focal cancer areas, although there was variation among the animals tested still the distortion, infiltration of fibroblasts and inflammatory cells, and most importantly cancer incidence was not as pronounced as it was for Ikkα$^{F/F}$-p48-Kras mice (Figure 4.1 I, J). In the light of these findings, *Ikkα* deletion was concluded to accelerate tumor development in the pancreas in mice with oncogenic *K-ras* activation. In addition, we observed that the loss of *Ikkα* during cancer development depended on the number of intact alleles since the pancreata from *Ikkα*$^{F/+}$-*p48*^{Cre}-*K-ras*$^{LSL-G12D/+}$ (termed Ikkα$^{F/+}$-p48-Kras) mice did not show advanced PanINs or tumor at the age of 3-4 weeks (Figure 4.1 M, N). Apart from pancreas, other organs did not show any structural or histological abnormalities in Ikkα$^{F/F}$-p48-Kras mice.

Histological evaluation of the pancreata from Ikkα$^{F/F}$-p48-Kras mice showed acinar structure of the pancreas was mostly replaced by PanIN lesions, which was accompanied by a strong stromal reaction. In order to check fibrotic response, Sirius red staining was performed using pancreas sections. Low grade fibrosis was detected around newly forming lesions in the pancreas of 3-4 weeks old p48-Kras mice, whereas most of the pancreatic areas were fibrotic in Ikkα$^{F/F}$-p48-Kras mice and 7-14 months old p48-Kras mice (Figure 4.1 C, G, K). In addition, Alcian blue staining was performed to determine mucin secretion in the pancreas since it is one of the basic characteristics of PanINs. In 3-4 weeks old p48-Kras mice, no mucin secretion was detected. Contrarily, abundant mucin production was observed in p48-Kras, which had PanINs and tumors, and in Ikkα$^{F/F}$-p48-Kras mice in accordance with the increased incidence of cancer (Figure 4.1 D, H, L).

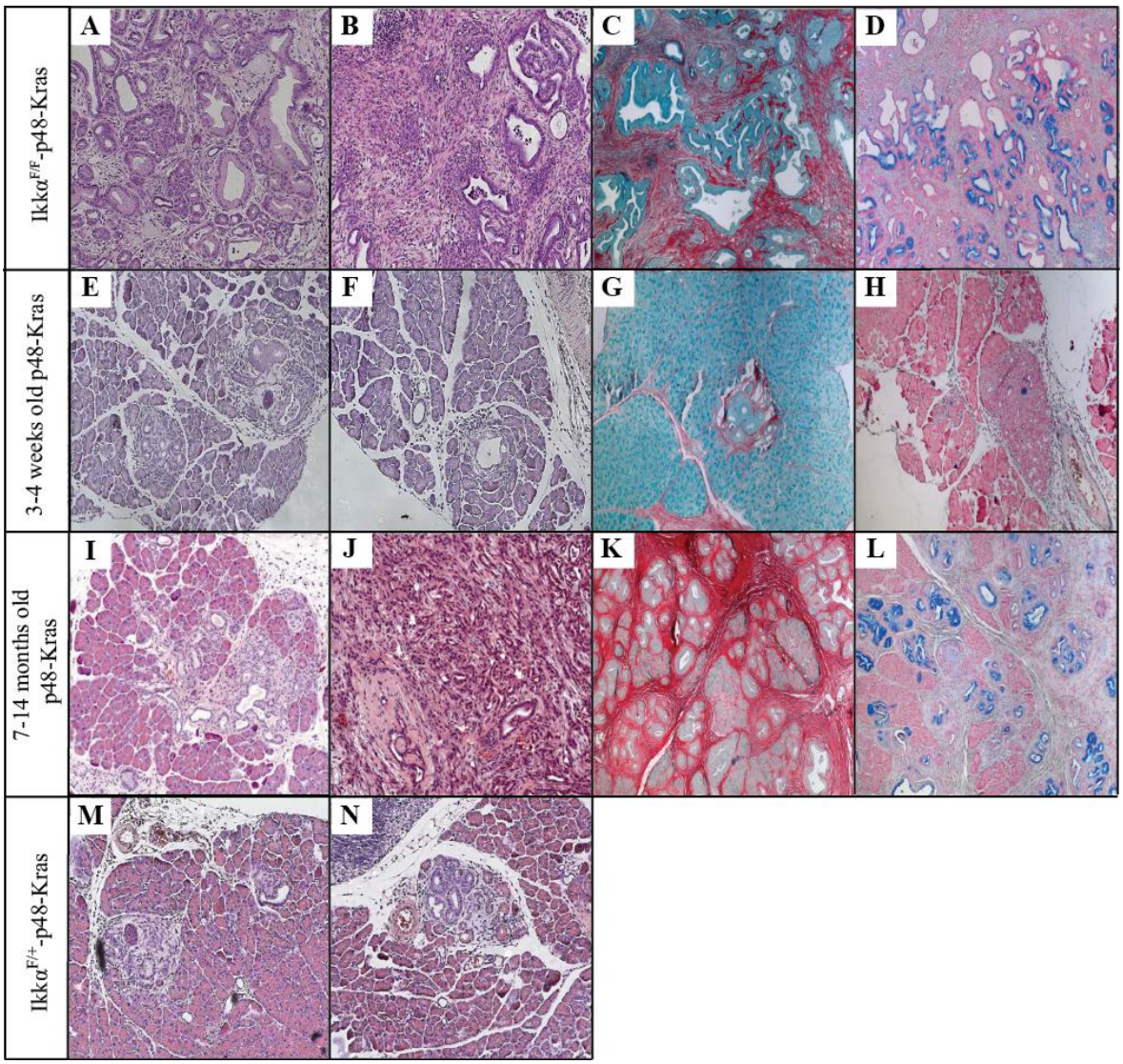

Figure 4.1. Pancreas-specific *Ikkα* deletion accelerates PanIN development and tumor progression accompanied by increased fibrosis and mucin production. (A, B) Haematoxylin and Eosin (H&E)-stained pancreas sections of 3-4 weeks old Ikkα$^{F/F}$-p48-Kras, (E, F) age-matched p48-Kras mice and (I, J) 7-14 months old p48-Kras animals. 3-4 weeks old p48-Kras mice show significantly intact acini, whereas pancreas structure is completely transformed in Ikkα$^{F/F}$-p48-Kras mice. (C, D) Sirius red and Alcian blue staining, respectively, performed on pancreas sections of 3-4 weeks old Ikkα$^{F/F}$-p48-Kras, (G, H) age-matched p48-Kras mice and (K, L) 7-14 months old p48-Kras animals indicating increased fibrosis and mucus secretion in the presence of PanINs and tumors. (M, N) H&E staining on the pancreas sections of Ikkα$^{F/+}$-p48-Kras mice displaying similar histology to 3-4 weeks old p48-Kras pancreata, which show only early-stage PanINs surrounded by normal acini and partially diluted ducts. 10X magnification.

4.2. *Ikkα* deletion in pancreas accelerates oncogenic *K-ras* driven PanIN development not only during embryonic stage but also after post-natal period

Ikkα deletion in pancreas accelerates *K-ras* driven PanIN and tumor development in p48-Kras mice. However, in Ikkα$^{F/F}$-p48-Kras mouse model, *Ikkα* deletion and oncogenic *K-ras* activation occurs as early as 9.5-10.5 days during embryonic stage. To check whether tumor

promotion and progression could be accelerated due to *Ikkα* deletion also in adult mice, another *Cre* system, Elastase-Cre (Ela-Cre), was used as it allows recombination only in adult acinar cells in an inducible manner. To generate Ikkα$^{F/F}$-Kras-Ela-Cre mice, Ikkα$^{F/F}$–Kras mice were crossed to Ela-Cre animals. Approximately 10 µg/µl tamoxifen was administered to 5 weeks old Ikkα$^{F/F}$-Kras-Ela-Cre mice and age matched control littermates for five consecutive days. Animals were sacrificed three months after the last tamoxifen administration. Among six Ikkα$^{F/F}$-Kras-Ela-Cre mice, five of them showed PanIN lesions and one displayed abnormalities in acinar cell structure suggesting IKKα induced *K-ras*-driven PanIN formation is not restricted to embryonic stage but can occur also post-natally (Figure 4.2).

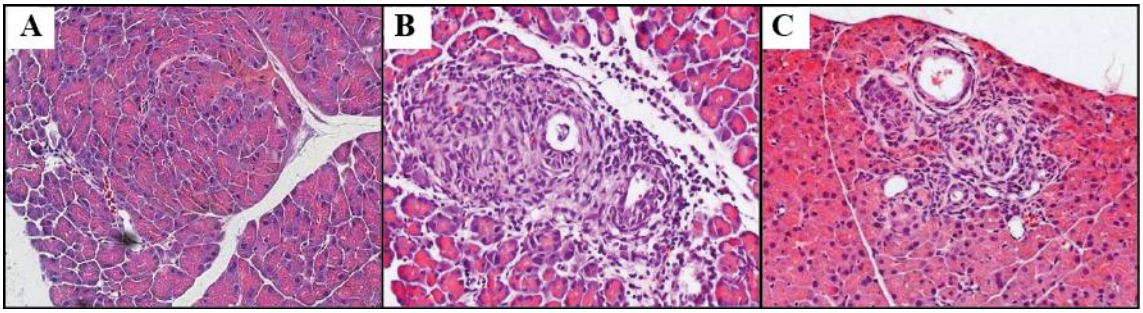

Figure 4.2. Acinar cell-specific *Ikkα* deletion leads to PanIN development not only during embryonic stage of life but also in post-natally. (A) H&E-stained pancreas section of age matched Ikkα$^{F/F}$ mouse and (B, C) Ikkα$^{F/F}$-Kras-Ela-Cre mice. 20X magnification.

4.3. Pancreas-specific deletion of *Ikkα* causes increased proliferation and resistance to apoptosis in p48-Kras mice

During cancer development, several genetic and epigenetic alterations occur to transform normal cells into abnormal tumor cells. As a result, the transformed cells become insensitive to anti-growth signals and proliferate in the absence of growth signals. Further they induce resistance to programmed cell death (apoptosis) and replicate unlimitedly. Moreover, angiogenesis, invasion and metastasis are also enhanced. All together, these characteristics of transformed cells are recently defined as 'six hallmarks of cancer' (Hanahan and Weinberg, 2000). Among these hallmarks, *K-ras* is especially important for cell proliferation in the absence of growth signals because as a part of the SOS-RAS-RAF-MAP kinase cascade, which plays an essential role in releasing the mitogenic signals into cells, oncogenic activation of *K-ras* supply continuous growth signals to the cells. As a proof, abundant number of human tumors has been shown to exhibit oncogenic RAS proteins (Medema and Bos, 1993). To check the proliferation, Ki67 staining was performed using the pancreas. Only the lesion forming cells were observed to

proliferate in the pancreas of 3-4 weeks old p48-Kras mice (Figure 4.3 A, B). On the contrary, in accordance with enhanced tumor progression, highly proliferative cells around lesions, tumors and desmoplastic areas in the pancreas of 7-14 months old p48-Kras and 3-4 weeks old Ikkα$^{F/F}$-p48-Kras mice were observed (Figure 4.3 C, D, E, F). In addition, TUNEL was performed to check apoptotic index in pancreas sections. As a result, only very few apoptotic cells in the pancreas of Ikkα$^{F/F}$-p48-Kras mice were determined in comparison to age-matched p48-Kras pancreata (Figure 4.3 G, H, I, J).

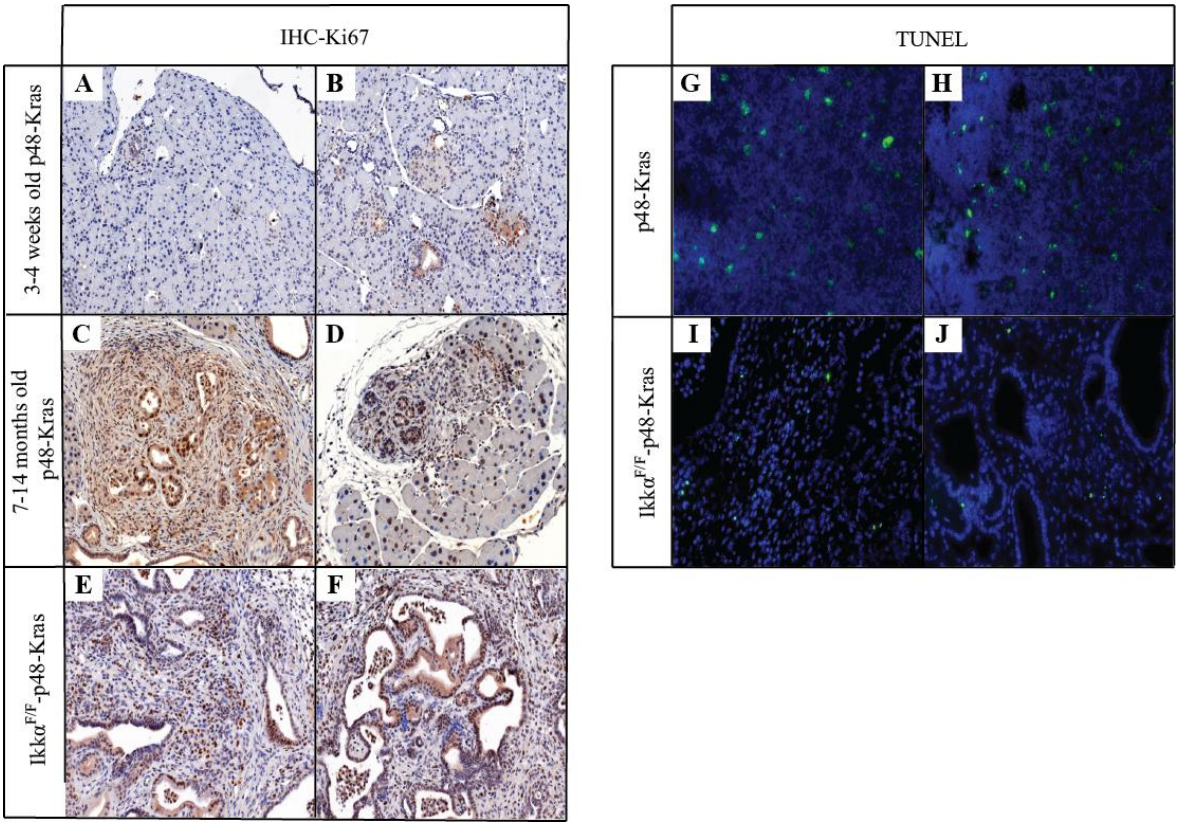

Figure 4.3. ***Ikkα*** **deletion gives rise to increased cell proliferation and decreased apoptosis in the pancreas of 3-4 weeks old p48-Kras mice.** (A, B) Determination of cell proliferation by immunohistochemistry (IHC) staining using anti-Ki67 antibody in the pancreas of 3-4 weeks old p48-Kras, (C, D) 7-14 months old p48-Kras and (E, F) 3-4 weeks old Ikkα$^{F/F}$-p48-Kras mice. (G, H) Evaluation of apoptosis in the pancreas sections of 3-4 weeks old p48-Kras and (I, J) Ikkα$^{F/F}$-p48-Kras mice by TUNEL. 20X magnification.

4.4. *Ikkα* regulates cell cycle progression via controlling the key players involved in G1/S phase transition

Cell cycle consists of four different phases, which are called G1 (Gap 1), S (Synthesis), G2 (Gap 2) and M (Mitosis). All these phases are carried out by cell cycle machinery consisting

of cyclins, cyclin dependent kinases (CDKs) and cyclin dependent kinase inhibitors (CDKIs), which are regulated by a variety of molecules such as *Ras* and *Myc* (Weinberg, 2007). Thus, in order to define in detail the hyperproliferative response of the tumors in Ikkα$^{F/F}$-p48-Kras mice, the expression of Cyclin D1 was checked. Expression of Cyclin D1, required in the G1 phase of the cell cycle, was found to be highly up-regulated in Ikkα$^{F/F}$-p48-Kras mice (Figure 4.4), which is in agreement with the IKKα's function in regulation Cyclin D1 expression.

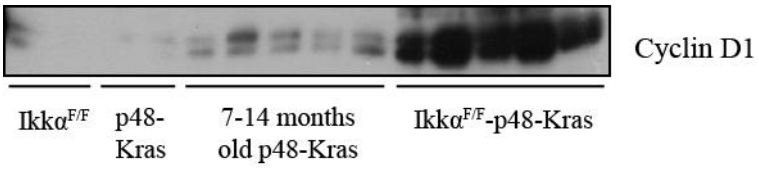

Figure 4.4. Cyclin D1 expression level is significantly increased in Ikkα$^{F/F}$-p48-Kras mice in comparison to 7-14 months old p48-Kras mice. WB analysis exhibiting the expression of Cyclin D1 in the pancreas of 3-4 weeks old Ikkα$^{F/F}$, p48-Kras, Ikkα$^{F/F}$-p48-Kras and 7-14 months old p48-Kras mice.

In addition to Cyclin D1 that takes part in cell cycle, the expression of another CDKI, p16^{INK4A}, was investigated. p16^{INK4A} can halt cell cycle in the G1 phase by inhibiting CDK-4 and-6. Furthermore, its main function is suggested to be the induction of permanent growth arrest, which is called cellular senescence. Cellular senescence is the stage of irreversible cell cycle arrest, which is promoted by several factors including abnormal growth signals or DNA damage. Thus, it is accepted as an important mechanism, which prevents cancer and suppresses tumor development (Ohtani *et al*., 2004). In order to determine p16 expression, WB was performed using proteins from both mouse pancreata and human pancreas biopsies from patients with PDAC. To directly compare the tumors from Ikkα$^{F/F}$-p48-Kras mice to that of p48-Kras mice, p48-Kras animals that were between 7-14 months old were used. Fourteen out of twenty-six Ikkα$^{F/F}$-p48-Kras mice showed similar p16 expression to old p48-Kras animals, whereas twelve samples showed decreased p16 expression (Figure 4.5 A). In addition, p16 expression was further checked by RT-PCR. Indeed, significantly elevated p16 expression was detected in Ikkα$^{F/F}$-p48-Kras in comparison to Ikkα$^{F/F}$ and 3-4 weeks old p48-Kras mice (Figure 4.5 B). On the other hand, p16 expression was detected in %55 of normal human pancreas and % 77 of PDAC samples. In order to check if alterations in IKKα expression is a common phenomenon during human disease and whether there is any correlation with p16 expression, WB was performed using the same human samples. Among PDAC samples tested, IKKα expression appeared to be decreased. Furthermore only two PDAC samples, which were negative for IKKα showed p16 expression (Figure 4.5 C). To further elucidate, *Ikkα* was knocked-down in

pancreatic cancer (PC) cell lines and expression of p16 was detected. For this aim, Patu-S and MiaPaCa human PC cell lines were chosen according to their high and low p16 expression levels (Figure 4.5 D). siRNAs were used to knock-down *Ikkα* in these cells lines (Figure 4.5 E). In MiaPaCa cell line, comparably to two human samples, IKKα loss resulted in elevated p16 protein expression, whereas in Patu-S line, IKKα loss did not alter p16 expression (Figure 4.5 E).

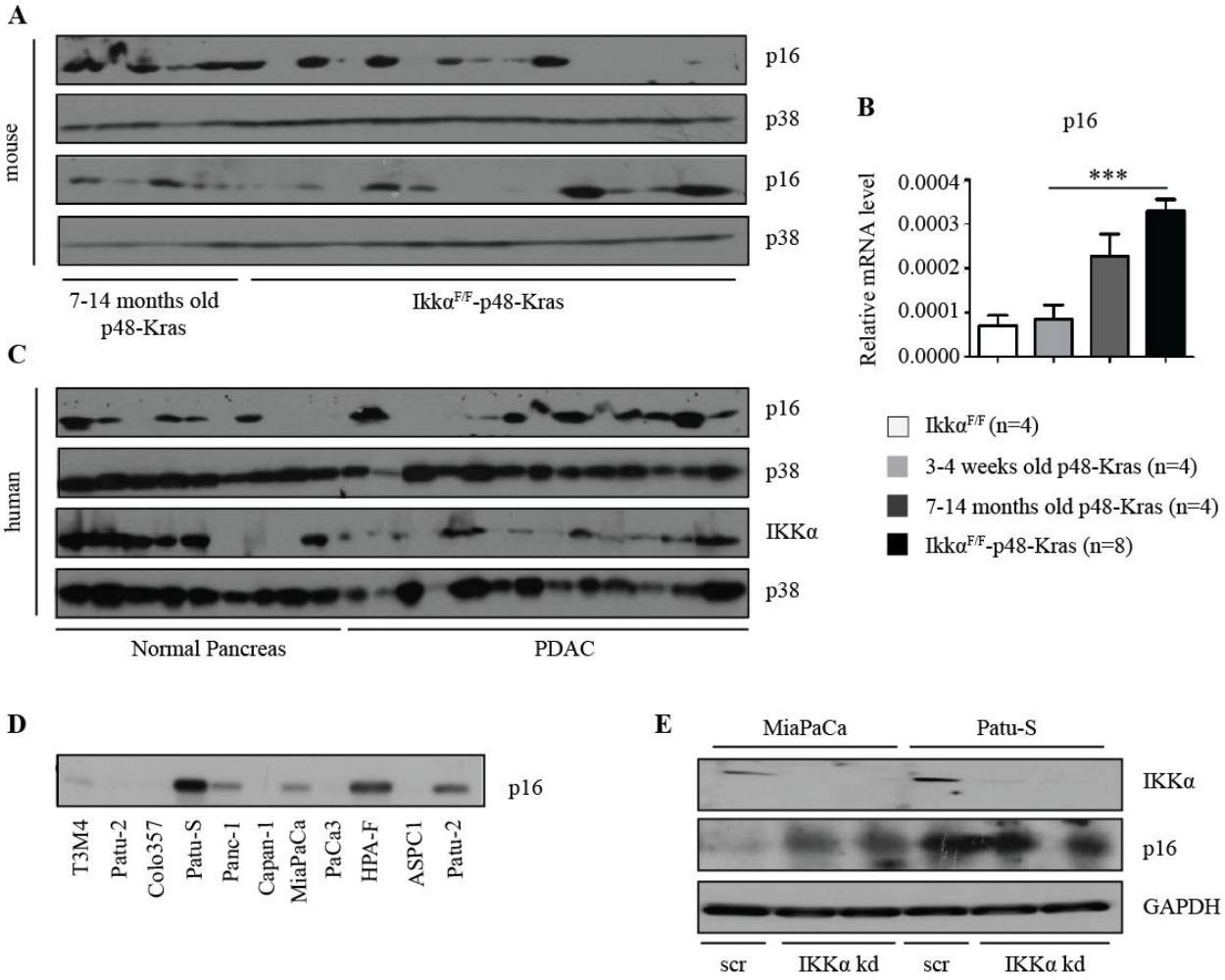

<u>Figure 4.5.</u> p16 expression in the pancreas changes due to the grade of tumors in mouse and human, and *Ikkα* deletion causes increased p16 expression in MiaPaCa cell line. (A) Detection of p16 expression by WB, (B) and RT-PCR in mouse pancreas. (C) Detection of p16 and IKKα expression by WB in normal human samples and samples from PDAC patients. (D) Determination of p16 by WB in human pancreatic cancer cell lines. (E) The effect of *Ikkα* loss on p16 expression was checked by WB level for MiaPaCa and Patu-S human pancreatic cell lines. GAPDH and p38 was used as a loading control. P value was determined by one-way ANOVA followed by Bonferroni`s multiple comparison test. ***$p \leq 0.001$.

c-MYC is a proto-oncogene, which belongs to basic helix-loop-helix (bHLH) transcription factor family. It is known to function as a downstream transcriptional effector of several signaling pathways, which take part in cell growth, differentiation and apoptosis. In addition to its cell growth promoting effects, it has been found that *Ras* and *Myc* oncogenes are

able to cooperate during cell transformation (Weinberg, 2007). Moreover, expression of MYC is deregulated in 15-30% of cancers, which leads to high expression of MYC following abnormal cell growth. Based on its important role during cancer progression, c-MYC localization was checked in pancreas sections from 3-4 weeks old p48-Kras and Ikkα$^{F/F}$-p48-Kras mice. In both animal groups, cytoplasmic and nuclear c-MYC was detected in lesions (Figure 4.6).

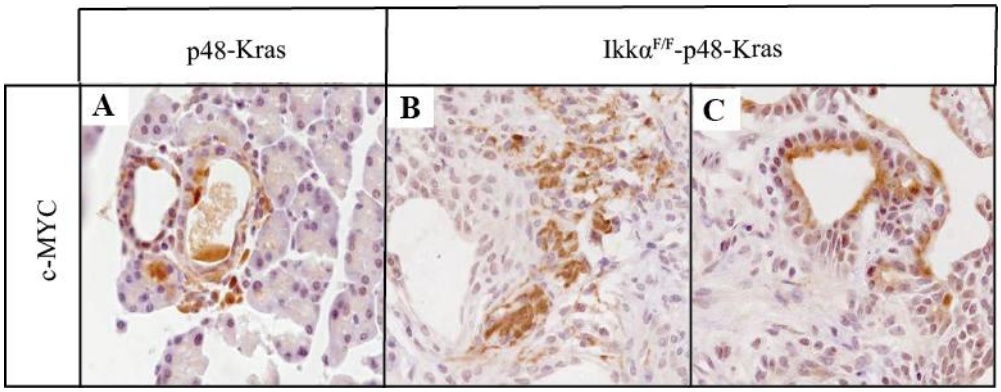

Figure 4.6. Cytoplasmic and nuclear localization of c-MYC is observed in lesions in 3-4 weeks old p48-Kras and Ikkα$^{F/F}$-p48-Kras mice (A) Localization of c-MYC is exhibited via IHC staining using pancreas tissue sections from p48-Kras mice and (B, C) Ikkα$^{F/F}$-p48-Kras mice. 20X magnification.

p53 is a very important tumor suppressor protein that regulates cell proliferation, cell cycle arrest, cell death, DNA repair in the cells and is lost in 50-75% of pancreatic cancers (Maitra and Hruban, 2008). Due to its importance, p53 location was visualized in the pancreas of Ikkα$^{F/F}$-p48-Kras mice. Mostly, the lesions were positive for p53 in p48-Kras and Ikkα$^{F/F}$-p48-Kras mice. Furthermore, p53 was located both in cytoplasm and nucleus in both animal groups (Figure 4.7).

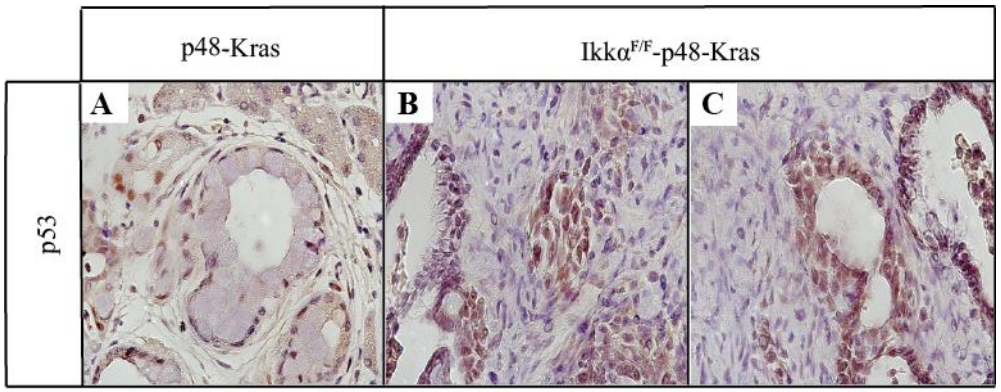

Figure 4.7. Nuclear and cytoplasmic localization of p53 is detected in the lesions in Ikkα$^{F/F}$-p48-Kras mice. (A) Immunohistochemical analysis of p53 using pancreas sections from p48-Kras and (B, C) Ikkα$^{F/F}$-p48-Kras mice. 20X magnification.

4.5. Pancreas-specific *Ikkα* deletion does not induce AKT but elevates mTOR expression in p48-Kras mice

One of the important pathway in PDAC progression is the phosphatidylinositol-3' kinase (PI3K)/AKT-pathway, which is shown to be active in nearly 60% of PDAC patients. The oncoprotein AKT, which is a serine-threonine kinase, is activated by PI3K mutations, inactivation and/or loss of PTEN and several survival signals including oncogenic *K-ras* activation. This activation leads to induced cell proliferation, growth and survival (Bader *et al*., 2005; Dan *et al*., 2008). Furthermore PI3K/AKT signaling has been established to regulate NF-κB (Jones *at al*., 2000). Thus, levels of AKT, its downstream mediator mammalian target of rapamycin (mTOR), GβL and RICTOR were checked. Although total AKT levels were similar, phosphorylated AKT (p-AKT) levels were increased in Ikkα$^{F/F}$-p48-Kras mice in comparison to Ikkα$^{+/F}$-p48-Kras, whereas AKT level was slightly increased in Ikkα$^{F/F}$-p48-Kras animals in comparison to p48-Kras mice (Figure 4. 8). Furthermore, increase in mTOR, phosphorylated mTOR (p-mTOR) and mTOR adaptor protein RICTOR was observed in Ikkα$^{F/F}$-p48-Kras mice suggesting that this pathway might be involved in increased cell proliferation in the pancreas (Figure 4. 8).

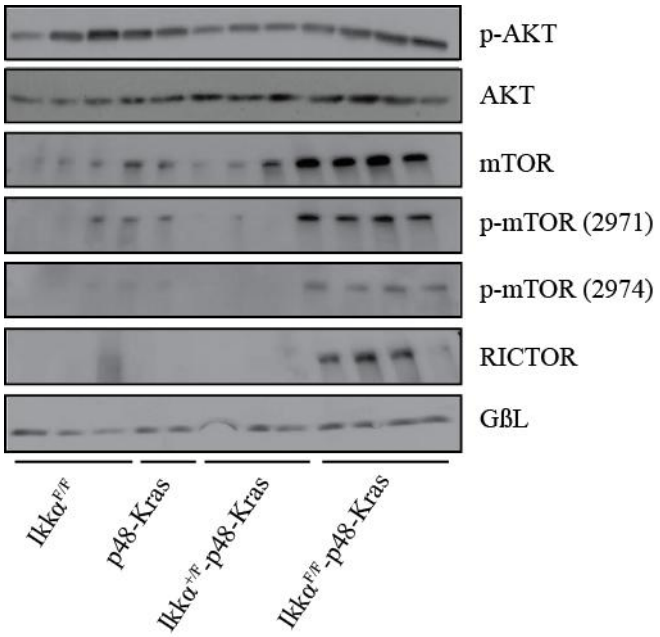

Figure 4.8. mTOR, p-mTOR and RICTOR levels are elevated in Ikkα$^{F/F}$-p48-Kras mice in comparison to age-matched p48-Kras. WB analysis displaying the expression of AKT, p-AKT, mTOR, p-mTOR, RICTOR and GβL in the pancreas of 3-4 weeks old Ikkα$^{F/F}$, p48-Kras, Ikkα$^{+/F}$-p48-Kras and Ikkα$^{F/F}$-p48-Kras mice.

4.6. Pancreas-specific *Ikkα* deletion enhances secretion of pro-inflammatory cytokines

Chronic inflammation is known to be an important initiator for tumor progression. Since as initially proposed by Rudolf Virchow in 1863, many recent studies confirmed the connection between chronic inflammation and cancer development. It has been established that activated oncogene and/or inhibition of a tumor suppressor gene might induce inflammation-related mechanisms. Thus, cancer-associated inflammation can activate transcription factors such as NF-κB, STAT3 and HIF-1α and thereby give rise to the production and secretion of inflammatory mediators including cytokines, chemokines, nitric oxide and prostaglandins (Karin and Greten, 2005; Mantovani *et al*, 2008).

In the light of this information and our observation, which points out to the transformation of intact acinar cells in Ikkα$^{F/F}$-p48-Kras with premalignant lesions and areas with multifocal cancer surrounded by increased inflammatory cells, the expression of inflammatory markers and pro-inflammatory cytokines were investigated via RT-PCR (Figure 4.9). Expression of macrophage surface marker F4/80 showed a tendency towards an increase in Ikkα$^{F/F}$-p48-Kras in comparison to age-matched p48-Kras mice. Consistently, expression of cytokines including interleukin 1β (IL1β) and interleukin 6 (IL6) was also elevated in Ikkα$^{F/F}$-p48-Kras mice in comparison to age-matched p48-Kras mice. However, the expression of F4/80, TNFα and IL1β did not show significant difference between Ikkα$^{F/F}$-p48-Kras and 7-14 months old p48-Kras mice, whereas IL6 level was decreased in Ikkα$^{F/F}$-p48-Kras mice. Thus, in an advanced tumor model such as Ikkα$^{F/F}$-p48-Kras mice, although it is not surprising to detect higher expression levels of these cytokines, yet the presence of an active tumor microenvironment is important (Figure 4.9).

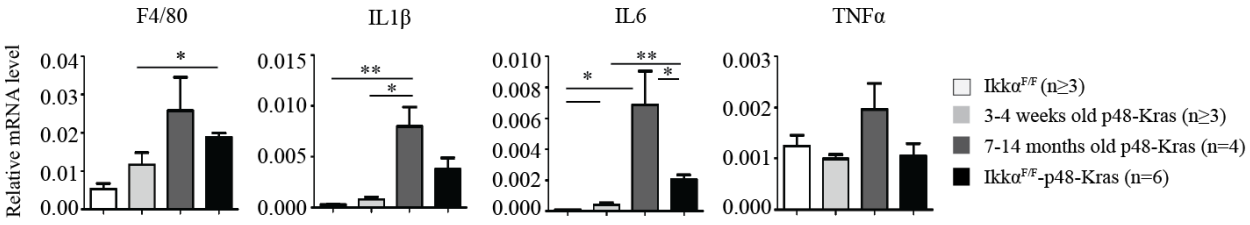

Figure 4.9. Expression of inflammatory cell markers and pro-inflammatory cytokines is increased in Ikkα$^{F/F}$-p48-Kras mice. Expression analysis of genes involved in inflammatory responses in the pancreas of 3-4 weeks old Ikkα$^{F/F}$, p48-Kras, Ikkα$^{F/F}$-p48-Kras and 7-14 months old p48-Kras mice analyzed by RT-PCR. Data are mean values ± Standard error of the mean (SEM), *p ≤ 0.05, **p ≤ 0.01.

In order to detect which cell type constitutes the major inflammatory microenvironment around lesions and tumors in the pancreas of Ikkα$^{F/F}$-p48-Kras mice, the pancreatic cells were sorted via Fluorescence-activated cell sorting (FACS) based on their cell surface markers. The cells were gated according to their double positivity for F4/80-CD11b and CD11b-GR1. Significant increase in macrophage and neutrophil infiltration was observed in the pancreas of Ikkα$^{F/F}$-p48-Kras mice in comparison to 7-14 months old p48-Kras mice (Figure 4.10). Indeed this may suggest elevated inflammatory response might have had a stronger tumor promoting effect in Ikkα$^{F/F}$-p48-Kras mice, which leads to accelerated pancreatic tumor development in this mouse model at the age of 3-4 weeks in contrast to 7-14 months in p48-Kras animals.

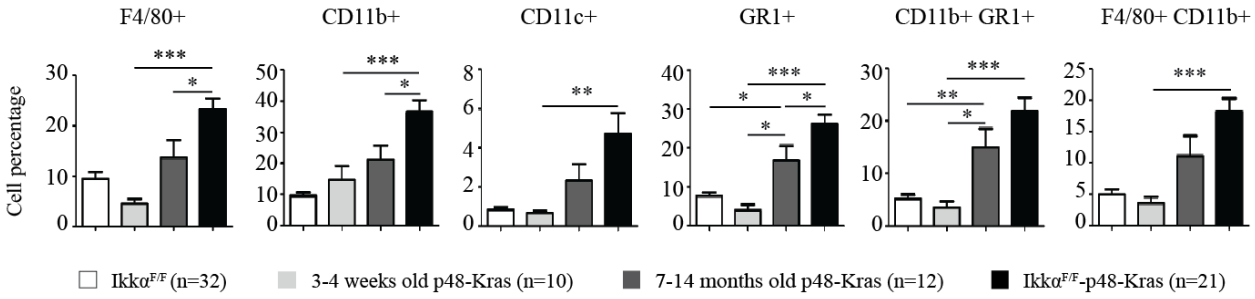

Figure 4.10. Ikkα$^{F/F}$-p48-Kras mice displays increased percentages of inflammatory cell infiltration in the pancreas in comparison to p48-Kras mice. The graphs representing the percentages of F4/80^{+}, CD11b^{+}, CD11c^{+}, GR1^{+}, CD11b^{+} GR1^{+} and F4/80^{+} CD11b^{+} cells in the pancreas of 3-4 weeks old Ikkα$^{F/F}$, p48-Kras, Ikkα$^{F/F}$-p48-Kras and 7-14 months old p48-Kras mice. P value was determined by one-way ANOVA followed by Bonferroni`s multiple comparison test. *p ≤ 0.05, **p ≤ 0.01, ***p ≤ 0.001.

4.7. Although *Ikkα* is absent in the exocrine pancreas, both canonical and non-canonical NF-κB pathways are still active in Ikkα$^{F/F}$-p48-Kras mice

NF-κB is a very important transcription factor, which regulates the expression of genes mainly involved in inflammation and innate immunity. Thus, NF-κB activity might cause drastic changes such as promotion of cancer via enhancing the expression of inflammatory cytokines or enzymes including COX-2 and iNOS. Moreover, NF-κB proteins have been shown to promote the expression of genes required for cell proliferation and apoptosis (Karin, 2006; Courtois and Gilmore, 2006).

IKKα plays a critical role in both canonical and non-canonical NF-κB pathways. Moreover, it has NF-κB independent but nuclear functions in the cells (Huang and Hung, 2013). Further, recent studies suggest a tumor suppressor property for IKKα (Kwak *et al.*, 2011). In our Ikkα$^{F/F}$-p48-Kras mouse model, pancreatic tumor development was accelerated and accompanied

by increased inflammatory cell infiltration. However, whether this was NF-κB dependent or independent and how *Ikkα* deficiency affected the expression of other NF-κB members involved in canonical and non-canonical pathways was not addressed. To that end, expression of NF-κB family members was determined. Additionally, human pancreas samples were analyzed as p48-Kras mouse model closely recapitulates the human PDAC. Importantly, increased expression of RelA, RelB, cRel, p50/p105, p52/p100, IκBα and phosphorylated IκBα (p-IκBα) was detected in 7-14 months old p48-Kras and 3-4 weeks old Ikkα$^{F/F}$-p48-Kras mice in comparison to other animal groups with or without *K-ras* activation. Especially, expression of RelB and cRel were significantly elevated in Ikkα$^{F/F}$-p48-Kras mice in comparison to 7-14 months old p48-Kras mice (Figure 4.11 A). Similarly, increased expression of RelA, cRel, p50/p105, and p52/p100 was detected in CP and PDAC human samples (Figure 4.11 B). On the other hand, lower expression of RelB was detected in CP and PDAC samples, which was contradictory to the findings in the mouse model (Figure 4.11 B).

Since elevated expression of RelA and RelB was detected, their location in the cells was elucidated in pancreas sections (Figure 4.11 C, H). Indeed, RelA and RelB were detected in the nucleus of cells, which give rise to lesions in 3-4 weeks old p48-Kras mice. Moreover, cytoplasmic and nuclear RelA was observed in lesions as well as in the inflammatory and desmoplastic areas in Ikkα$^{F/F}$-p48-Kras and 7-14 months old p48-Kras mice (Figure 4.11 D, E, F, G, I, J, K, L).

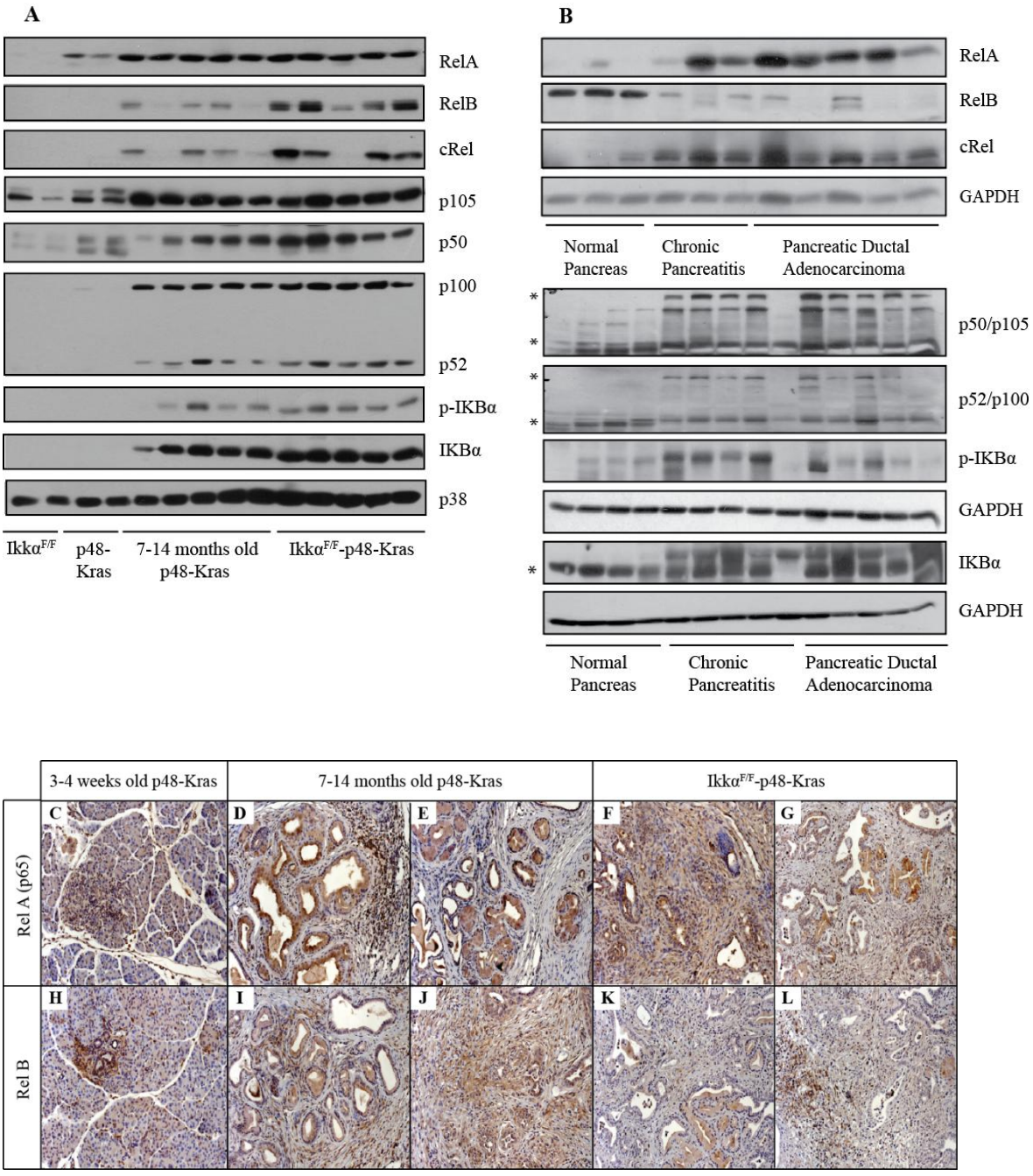

<u>Figure 4.11.</u> Pancreas-specific *Ikkα* deletion changes the expression of NF-κB family members in both mouse and human pancreas. (A) WB pictures representing the expression levels of NF-κB members in mouse pancreas samples and (B) in human pancreas. GAPDH was used as a loading control. Asterisks indicate the corresponding bands. (C, H) Representative pictures of IHC staining for RelA and RelB using pancreas sections from 3-4 weeks old p48-Kras, (D, E, I, J) 7-14 months old p48-Kras and (F, G, K, L) 3-4 weeks old Ikkα$^{F/F}$-p48-Kras mice. 20X magnification.

4.8. Additional *RelB* deficiency in the exocrine pancreas increases inflammation but does not affect tumor progression in Ikkα$^{F/F}$-p48-Kras mice

Increased RELB expression and nuclear localization in inflammatory and transformed cells was observed in the pancreas of Ikkα$^{F/F}$-p48-Kras mice. Since similar to *Ikkα*, *RelB* takes part in the non-canonical pathway, the effect of pancreas-specific deletion of *RelB* on tumorigenesis in Ikkα$^{F/F}$-p48-Kras mice was checked. To that end, RelB$^{F/F}$ was crossed on Ikkα$^{F/F}$-p48-Kras background. RelB$^{F/F}$-Ikkα$^{F/F}$-p48-Kras mice did not show any visible phenotype until birth due to additional pancreas specific *RelB* deletion. Although mice bred normally and RelB$^{F/F}$-Ikkα$^{F/F}$-p48-Kras mice were born at the expected Mendelian ratio, however, they showed increased mortality shortly after birth. Similar to Ikkα$^{F/F}$-p48-Kras mice, RelB$^{F/F}$-Ikkα$^{F/F}$-p48-Kras mice remained smaller than control littermates. Although the pancreas histology of 3 weeks old RelB$^{F/F}$-Ikkα$^{F/F}$-p48-Kras mice was comparable to Ikkα$^{F/F}$-p48-Kras mice, however the inflammatory response was much more exacerbated. Indeed exocrine pancreas structure was completely altered and normal acinar cells were replaced by premalignant lesions, multifocal cancer areas, inflammatory cells and fibroblasts suggesting pancreas-specific inhibition of the non-canonical NF-κB pathway accelerated cancer progression in p48-Kras mice (Figure 4.12).

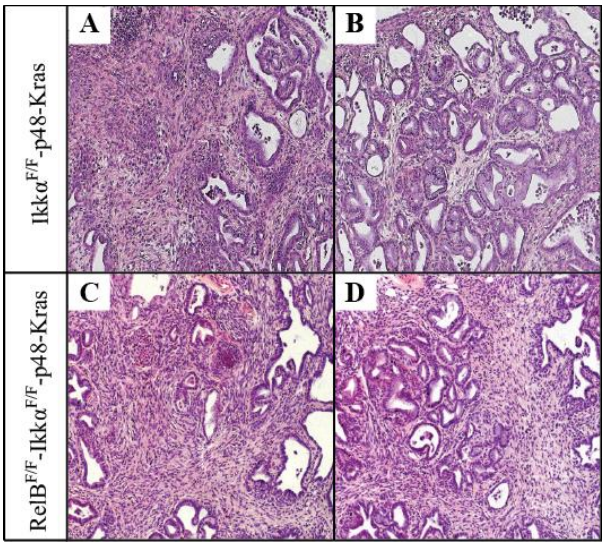

Figure 4.12. Pancreas-specific *RelB* deletion further enhanced inflammation during tumorigenesis in Ikkα$^{F/F}$-p48-Kras mice. (A, B) H&E staining of pancreas section from Ikkα$^{F/F}$-p48-Kras and (C, D) RelB$^{F/F}$-Ikkα$^{F/F}$-p48-Kras mice. 10X magnification.

To further check the increased inflammatory response in the pancreata of RelB$^{F/F}$-Ikkα$^{F/F}$-p48-Kras mice, FACS analysis was performed. Indeed higher numbers of F4/80^{+}-CD11b^{+}

macrophages and CD11b^{+}-GR1^{+} neutrophils were detected in the pancreas of RelB$^{F/F}$-Ikkα$^{F/F}$-p48-Kras mice. Especially F4/80^{+} CD11b^{+} macrophages were increased in RelB$^{F/F}$-Ikkα$^{F/F}$-p48-Kras mice in comparison to Ikkα$^{F/F}$-p48-Kras animals suggesting that in accordance with the pathology, macrophage infiltration in the pancreas was the highest in RelB$^{F/F}$-Ikkα$^{F/F}$-p48-Kras mice. In addition, CD11c^{+} cell infiltration was significantly lower in RelB$^{F/F}$-Ikkα$^{F/F}$-p48-Kras mice in comparison to Ikkα$^{F/F}$-p48-Kras animals proposing that RELB deficiency could accelerate cancer progression in Ikkα$^{F/F}$-p48-Kras mice, possibly through an increase in macrophages and a decrease in dendritic cells that present tumor antigens to adaptive immune cells (Figure 4.13).

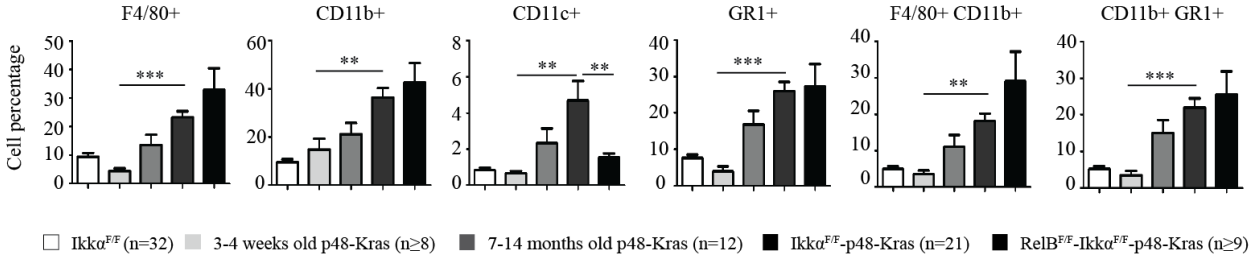

Figure 4.13. RelB$^{F/F}$-Ikkα$^{F/F}$-p48-Kras mice exhibited elevated inflammatory cell infiltration and decreased percentage of CD11c^{+} cells in the pancreas in comparison to Ikkα$^{F/F}$-p48-Kras and p48-Kras mice. The graphs representing the percentage of F4/80^{+}, CD11b^{+}, CD11c^{+}, GR1^{+}, F4/80^{+} CD11b^{+} and CD11b^{+} GR1^{+} cells in the pancreas of Ikkα$^{F/F}$, 3-4 weeks old p48-Kras, 7-14 months old p48-Kras, Ikkα$^{F/F}$-p48-Kras and RelB$^{F/F}$-Ikkα$^{F/F}$-p48-Kras mice. P value was determined by one-way ANOVA followed by Bonferroni`s multiple comparison test. **p ≤ 0.01, ***p ≤ 0.001.

4.9. *Ikkα* deletion increases the expression of genes involved in inflammatory response in p48-Kras mice

To further elucidate the molecular mechanisms involved in pancreatic cancer progression in Ikkα$^{F/F}$-p48-Kras mice in detail, microarray analyses was performed in which 28853 probe sets were used to check the expression of genes. Among 28176 genes, expression of 466 genes was significantly altered; 388 genes were up-regulated in Ikkα$^{F/F}$-p48-Kras mice in comparison to p48-Kras mice while 78 genes were down-regulated. Among the down-regulated genes, 25% of them were involved in metabolism. On the other hand, the highest numbers of up-regulated genes were engaged in cell cycle, growth, proliferation (6.7%), several signal transduction pathways (5.41%), and cell adhesion (5.41%). The rest of the up-regulated genes could be mainly classified under metabolism, angiogenesis, growth and development, transport, transcription, proteolysis and immune response.

Elevated expression of *CyclinD1* (NM_007631) in the pancreas of Ikkα$^{F/F}$-p48-Kras mice was confirmed by microarray analysis. Moreover, some other genes involved in cell cycle process including *CyclinG2* (NM_007635), *p15* (NM_007670), *Pak1* (NM_011035), *p21* (NM_007669) and *Cul1* (NM_012042) were also up-regulated in Ikkα$^{F/F}$-p48-Kras mice in comparison to 3-4 weeks old p48-Kras mice.

Interestingly, up-regulation in *Ctnnb1* (*β-catenin*) (NM_0076149) expression in Ikkα$^{F/F}$-p48-Kras mice in comparison to 3-4 weeks old p48-Kras mice was detected. This up-regulation was further checked on pancreas sections from 3-4 weeks old p48-Kras and Ikkα$^{F/F}$-p48-Kras mice. Indeed, cytoplasmic and nuclear β-catenin expression was detected in lesions in both mouse groups (Figure 4.14).

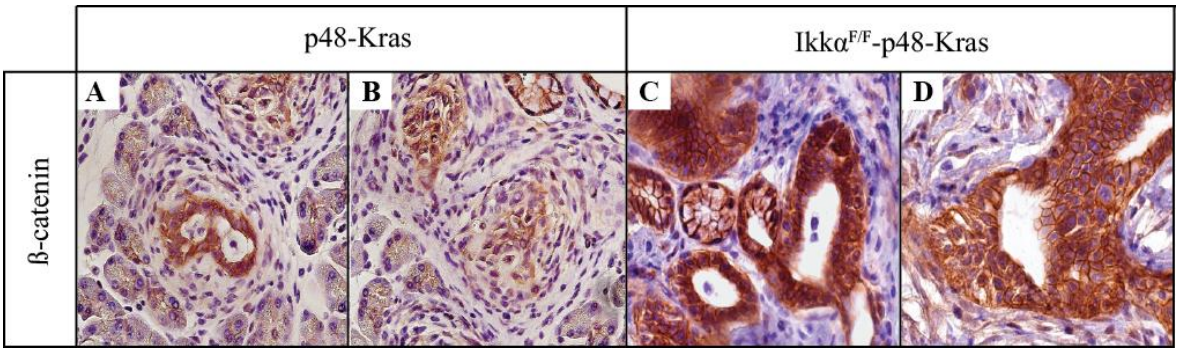

Figure 4.14. Cytoplasmic and nuclear β-catenin expression is detected in the pancreas of Ikkα$^{F/F}$-p48-Kras mice. (A, B) Representative pictures of IHC-β-catenin staining for 3-4 weeks old p48-Kras and (C, D) Ikkα$^{F/F}$-p48-Kras mice. 20X magnification.

According to microarray results, expression of Prominin-1 (*Prom1*) and CD44 (*Cd44*), which are assessed as cancer stem cells (CSCs) markers, were up-regulated in Ikkα$^{F/F}$-p48-Kras mice. This up-regulation was further confirmed by RT-PCR (Figure 4.15 A). Additionally, expression of CD44 was checked by FACS analysis together with a pancreatic cell marker, epithelial cell adhesion molecule (EpCAM), since these two markers are accepted as pancreatic cancer stem cell markers. A significant increase in the percentages of CD44^{+} and CD44^{+} EpCAM^{+} cells was detected in Ikkα$^{F/F}$-p48-Kras mice in comparison to p48-Kras animal groups (Figure 4.15 B).

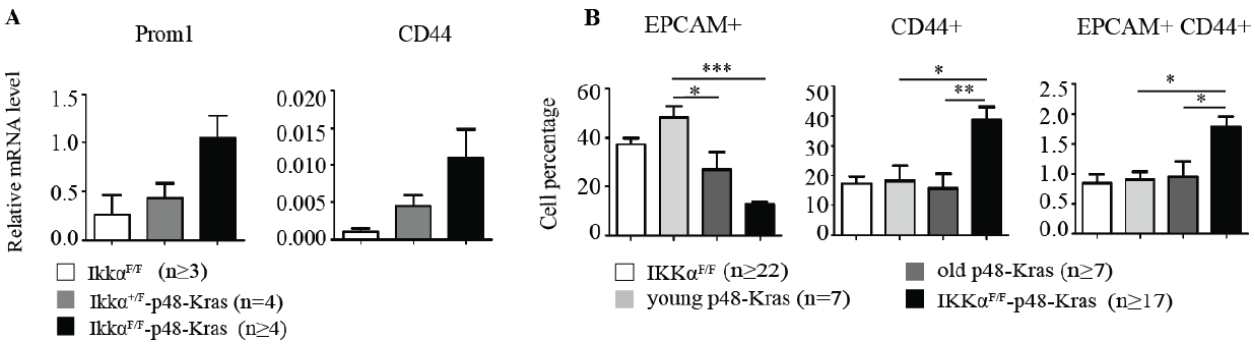

Figure 4.15. Expression of pancreatic cancer stem cell markers Prom1 and CD44 increases in the pancreas of Ikkα$^{F/F}$-p48-Kras mice. (A) Relative mRNA levels of Prom1 and CD44 were checked by RT-PCR using RNA from 3-4 weeks old Ikkα$^{F/F}$, Ikkα$^{+/F}$-p48-Kras, Ikkα$^{F/F}$-p48-Kras mice. (B) EpCAM and CD44 positive cells were determined by FACS using pancreatic cells from 3-4 weeks old Ikkα$^{F/F}$, p48-Kras, Ikkα$^{F/F}$-p48-Kras and 7-14 months old mice. P value was determined by one-way ANOVA followed by Bonferroni`s multiple comparison test. *p ≤ 0.05, **p ≤ 0.01, ***p ≤ 0.001.

Interestingly, the percentage of up-regulated inflammation-related genes was only 3.35% in microarray data. However, the genes known for M2 macrophage polarization including Interleukin 4 receptor α (*Il4rα)*, Interleukin 13 receptor α1 (*Il13rα1)*, Mannose Receptor-1 (*Mrc1*) and Arginase-1 (*Arg1*), together with general macrophage marker, cluster of differentiation 68 (*Cd68*) and multi functional extracellular structure protein secreted phosphoprotein 1 (*Spp1*) (also known as osteopontin; OPN), were significantly increased in Ikkα$^{F/F}$-p48-Kras animals (Figure 4.16 A) and this up-regulation was further confirmed by RT-PCR (Figure 4.16 B). In addition, expression of another M2 polarized macrophage marker, *Dectin1*, and a frequently found chemokine in tumors, Macrophage Chemotactic Protein-1 (*Mcp1*) (also known as chemokine (C-C motif) ligand 2; CCL-2), was also checked by RT-PCR (Figure 4.16 C) and they showed a trend towards an increase in Ikkα$^{F/F}$-p48-Kras mice.

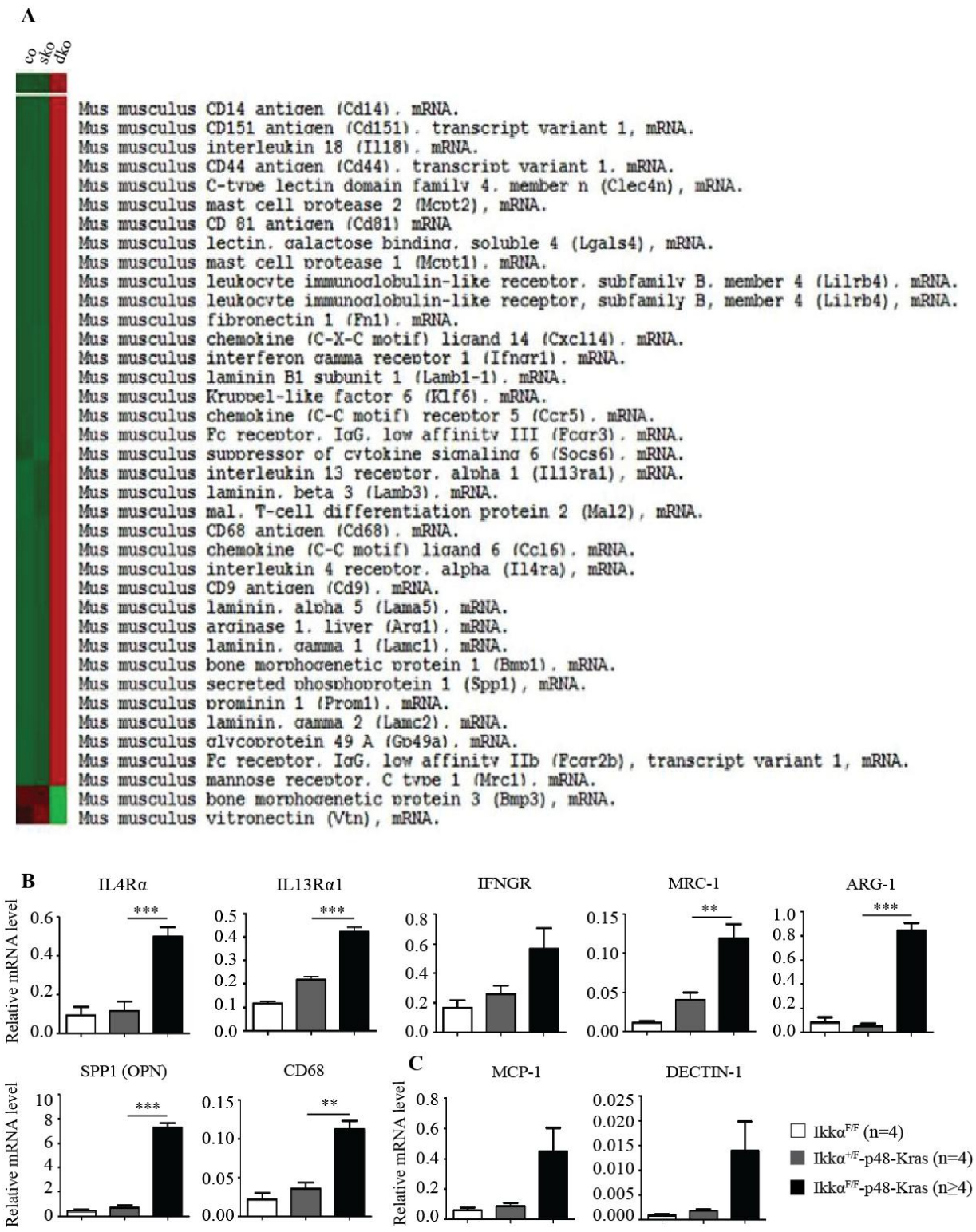

Figure 4.16. M2 macrophage polarization markers are up-regulated in the pancreas of Ikkα$^{F/F}$-p48-Kras mice. (A) Gene expression profiles are shown as a heat-map for 3-4 weeks old Ikkα$^{F/F}$ (co, n:3), p48-Kras (sko, n:2) and Ikkα$^{F/F}$-p48-Kras (dko, n:3). Red color shows up-regulation of the genes whereas green color represents down-regulation. (B) mRNA expression of the genes involved in inflammation and macrophage polarization are further checked in the pancreas of Ikkα$^{F/F}$, Ikkα$^{+/F}$-p48-Kras and Ikkα$^{F/F}$-p48-Kras mice by RT-PCR. (C) M2 macrophage marker, DECTIN-1, expression levels are detected for the pancreas of Ikkα$^{F/F}$, Ikkα$^{+/F}$-p48-Kras and Ikkα$^{F/F}$-p48-Kras mice by RT-PCR. P value was determined by one-way ANOVA followed by Bonferroni`s multiple comparison test. **$p \leq 0.01$, ***$p \leq 0.001$.

When pancreas samples from 7-14 months old p48-Kras mice bearing tumors were used, the genes related to M2 macrophage polarization including *Il4rα*, *Il13rα1*, pro-inflammatory cytokine *Il1β*, and M1 macrophage polarization-related genes *Ifngr1* and *Spp1* were similarly increased in Ikkα$^{F/F}$-p48-Kras animals, except *Arg1* and *Mrc1* that were significantly higher in IKKα-deficient p48-Kras mice. Furthermore, expression patterns of M2 macrophage related cytokines IL4, IL10, IL13 and M1 macrophage related cytokines IL12 and IFNγ were similar in 7-14 months old p48-Kras and 3-4 weeks old Ikkα$^{F/F}$-p48-Kras, and was decreased in comparison to 3-4 weeks old p48-Kras mice. In addition, expression of pro-inflammatory cytokine IL6 and chemokine MCP-1, which recruits inflammatory cells, was increased in 7-14 months old p48-Kras mice in comparison to other animal groups. Lastly, the expression of TNFα was decreased in Ikkα$^{F/F}$-p48-Kras mice(Figure 4.17 A). The up- and down-regulation of these genes was further verified by RT-PCR (Figure 4.17 B). In addition, expression of another M1 polarized macrophage marker, iNOS, and M2 polarized macrophage marker, DECTIN-1, was also checked. iNOS expression was significantly elevated in 7-14 months old p48-Kras mice. Furthermore, the expression of DECTIN-1 was significantly increased in Ikkα$^{F/F}$-p48-Kras mice, overall suggesting increased M2 macrophage polarization in these animals (Figure 4.17 B).

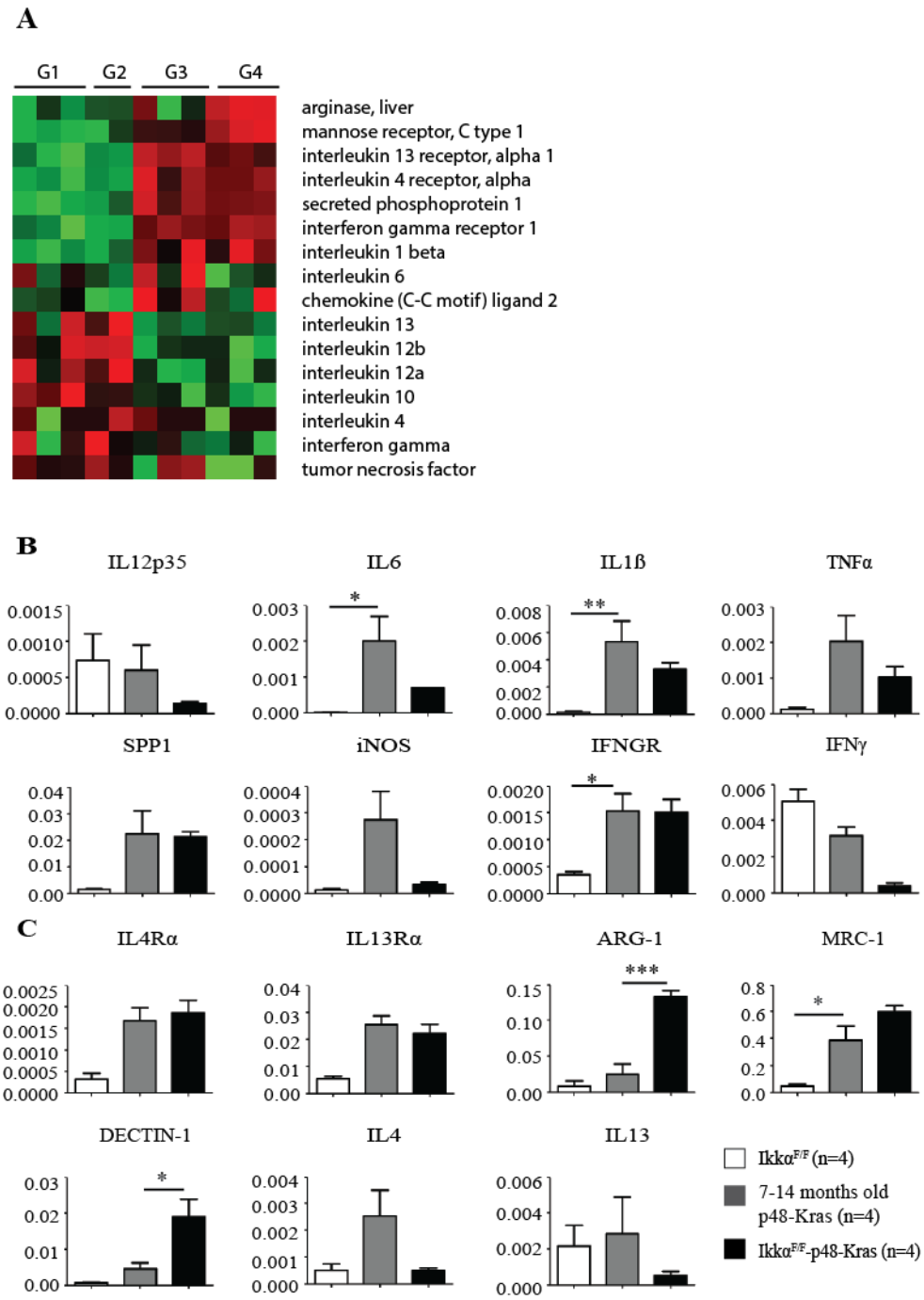

Figure 4.17. M2 macrophage polarization markers are up-regulated in the pancreas of 7-14 months old p48-Kras and 3-4 weeks old Ikkα$^{F/F}$-p48-Kras mice. (A) Gene expression profiles are shown as a heat-map for 3-4 weeks old Ikkα$^{F/F}$ (G1, n:3), p48-Kras (G2, n:2), Ikkα$^{F/F}$-p48-Kras (G4, n:3) and 7-14 months old p48-Kras (G3, n:3) mice. Red color shows up-regulation of the genes whereas green color represents down-regulation. (B) Increased mRNA expression of the genes involved in inflammation and macrophage polarization are further confirmed in the pancreas of 3-4 weeks old Ikkα$^{F/F}$, Ikkα$^{F/F}$-p48-Kras and 7-14 months old p48-Kras mice by RT-PCR. P value was determined by one-way ANOVA followed by Bonferroni`s multiple comparison test. *$p \leq 0.05$, **$p \leq 0.01$, ***$p \leq 0.001$.

Since p48-Kras model closely mimics human PDAC, IKKα protein level was checked in normal human pancreas (NP) and pancreas samples from PDAC patients to elucidate whether loss of IKKα expression is a common phenomenon in pancreatic cancer development (Figure

4.18 A). Among nine NP samples, three of them showed low IKKα expression, whereas among thirteen PDAC samples, eight of them displayed low IKKα expression suggesting that PDAC samples displayed decreased IKKα expression. Furthermore the expression of M2 macrophage markers and pro-inflammatory cytokines were checked using human samples. Similar to the mouse model, the expression of M2 macrophage markers MRC-1 and MCP-1 were significantly increased in PDAC samples. Another M2 marker, ARG-1 and M2 polarized macrophage related cytokines IL4, IL10 and IL13 also showed elevated expression in PDAC samples, however since the variation between samples were high, the difference between groups did not reach significance. Moreover, expression of pro-inflammatory cytokines TNFα, IL1β and IL6 was also increased in PDAC samples (Figure 4.18 B). Taken together, these results suggest that IKKα loss and M2 polarization may be a common feature of human PDAC progression.

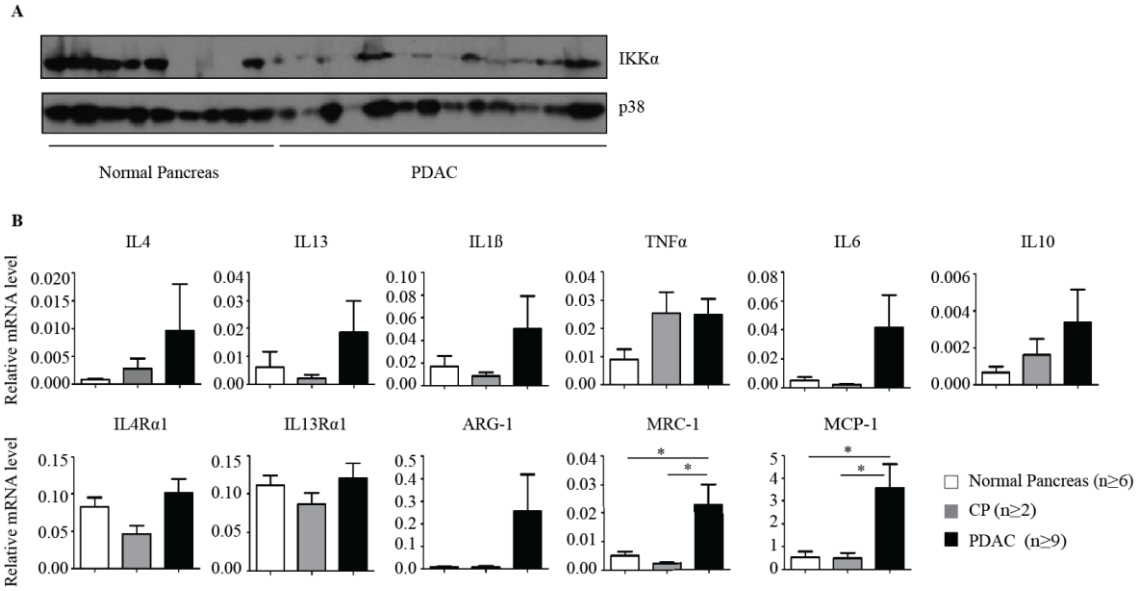

Figure 4.18. IKKα expression is decreased and M2 macrophage polarization markers are up-regulated in the pancreas samples from PDAC patients. (A) Detection of IKKα protein levels by WB using the proteins from normal pancreas and PDAC samples. (B) Determination of mRNA expression of M2 macrophage polarization markers, pro-inflammatory cytokines and the chemotactic factor, Mrc1, in the normal pancreas samples and samples from CP and PDAC patients by RT-PCR. P value was determined by one-way ANOVA followed by Bonferroni`s multiple comparison test. *$p \leq 0.05$. p38 was used as a loading control.

Increased M2 macrophage polarization in Ikkα$^{F/F}$-p48-Kras mice might be critical for the acceleration of pancreatic cancer in this mouse model. In order to investigate this hypothesis, FACS analysis was performed to confirm the increased expression of IL13Rα1 as well as to detect which cell type was responsible for the expression of this receptor. Moreover, secretion and the source of IL4 and IL13 were also determined. Although, no difference was detected in total expression of IL13Rα1 between animal groups, however, when the cells were gated according to their positivity for IL13Rα1 and each cell surface marker together, a significant

increase in the percentage of IL13Rα1 expressing myeloid cells was observed in the pancreas of Ikkα$^{F/F}$-p48-Kras (Figure 4.19 A). Similar to IL13Rα1 results but to a lesser extent, cytokine secreting F4/80^{+}, CD11b^{+}, CD11c^{+} and GR1^{+} cell numbers were elevated in Ikkα$^{F/F}$-p48-Kras in comparison to control groups and tumor bearing mice suggesting a critical role for IL13 and its receptor during enhanced cancer progression (Figure 4.19 B, C).

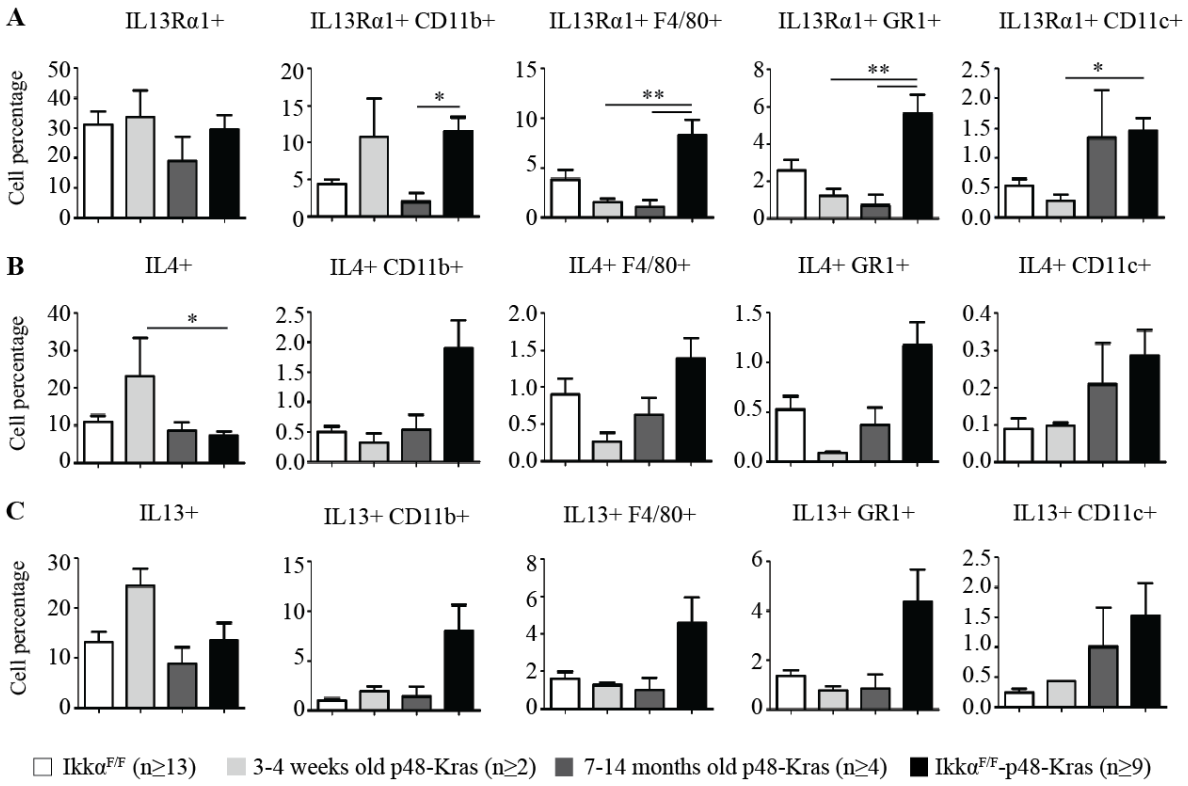

Figure 4.19. The percentage of IL13Rα1, IL4 and IL13 expressing myeloid cells are increased in Ikkα$^{F/F}$-p48-Kras. (A) Graphs representing the percentages of IL13Rα expressing cells (total) and myeloid cells separately, and (B, C) the percentages of IL4 and IL13 secreting (total) and myeloid double positive cells separately in the pancreas of 3-4 weeks old Ikkα$^{F/F}$, p48-Kras, Ikkα$^{F/F}$-p48-Kras and 7-14 months old p48-Kras mice. P value was determined by one-way ANOVA followed by Bonferroni`s multiple comparison test. *$p \leq 0.05$, **$p \leq 0.01$.

As being a component of tumor microenvironment, fibroblasts have already been established to induce tumor development in later stages of carcinogenesis by producing pro-inflammatory cytokines, proangiogenic factors and matrix metalloproteinases (Lederle *et al.*, 2010; Celis *et al.*, 2005; Dirat *et al.*, 2011; Erez *et al.*, 2010). Thus due to the presence of a strong desmoplastic reaction in the pancreas of Ikkα$^{F/F}$-p48-Kras mice, fibroblasts and their contribution to the production of IL13Rα1, IL4 and IL13 were checked. In accordance with histology, the dense fibroblast population in the pancreas of Ikkα$^{F/F}$-p48-Kras mice was confirmed by FACS analysis (Figure 4.20 A). Importantly, IL4 and IL13 secreting fibroblast numbers were increased in Ikkα$^{F/F}$-p48-Kras mice (Figure 4.20 B). Similarly, IL13Rα1 expression in fibroblasts was also significantly elevated in Ikkα$^{F/F}$-p48-Kras mice in comparison

to 3-4 weeks old p48-Kras mice (Figure 4.20 A). These data suggest that in addition to myeloid cells, fibroblasts also contribute to the production of IL4, IL13 and are perhaps more responsive in a feed-back loop due to increased IL13Rα1.

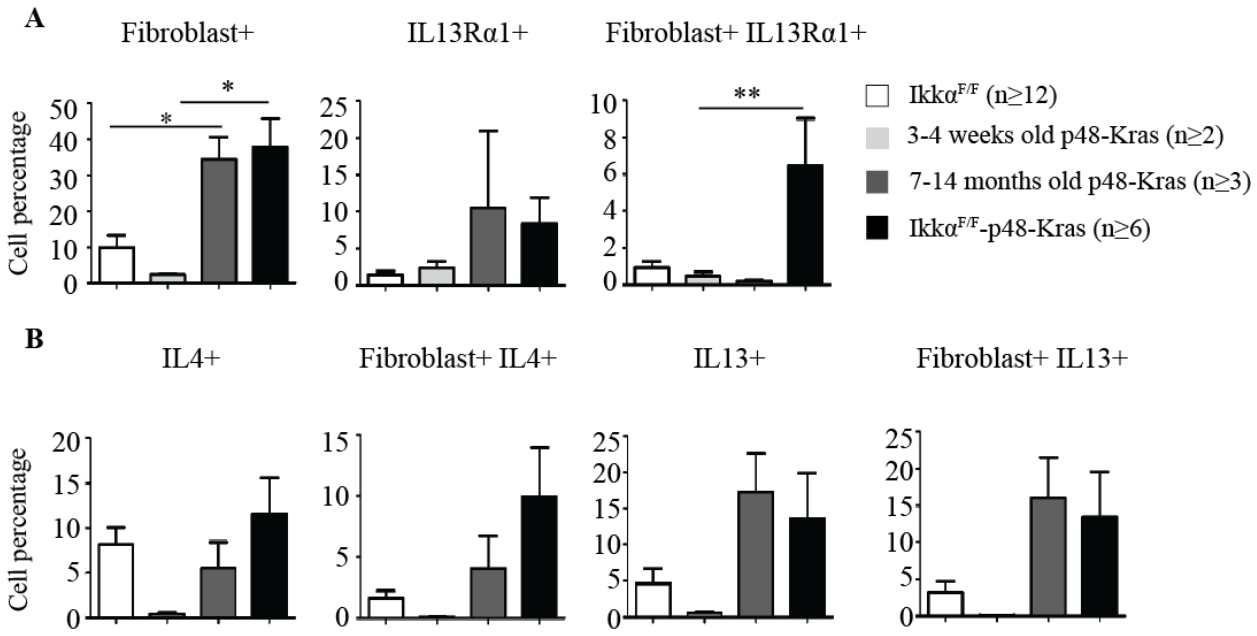

Figure 4.20. Fibroblast expression of IL13Rα1, IL4 and IL13 are elevated in the pancreas of Ikkα$^{F/F}$-p48-Kras mice. (A) IL13Rα1 and (B) IL4, IL13 expressing fibroblast percentages were determined by FACS using pancreatic cells from 3-4 weeks old Ikkα$^{F/F}$, p48-Kras, Ikkα$^{F/F}$-p48-Kras and 7-14 months old p48-Kras mice. P value was determined by one-way ANOVA followed by Bonferroni`s multiple comparison test. *$p \leq 0.05$, **$p \leq 0.01$.

In addition, pancreatic cells were further analyzed to see whether they could serve as a potential source for IL13Rα1, IL4 and IL13 expression. To that end, epithelial cell adhesion molecule (EpCAM) (also known as CD326) was chosen as pancreatic cell marker. As expected due to the major architectural transformation, significant decrease in the number of EpCAM^{+} cells in the pancreas of Ikkα$^{F/F}$-p48-Kras mice was observed (Figure 4.21 A). IL13Rα1, IL4 and IL13 expressing EpCAM^{+} cell numbers were not significantly changed in Ikkα$^{F/F}$-p48-Kras and the percentage of these cells -especially for IL13Rα1- was very low (Figure 4.21 A, B). All together these data suggest fibroblasts and myeloid cells as the major source of IL13 and its receptor expression in Ikkα$^{F/F}$-p48-Kras pancreas.

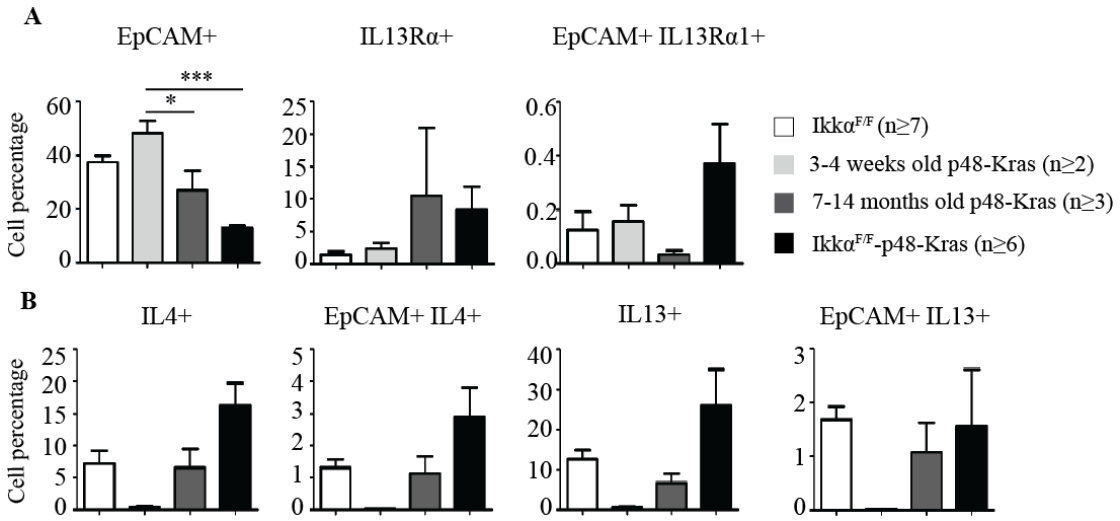

Figure 4.21. Expression of IL13Rα1, IL4 and IL13 by EpCAM$^+$ pancreatic cells is unchanged in Ikkα$^{F/F}$-p48-Kras mice. (A) IL13Rα1, (B) IL4 and IL13 expression by EpCAM$^+$ pancreatic cells in 3-4 weeks old Ikkα$^{F/F}$, p48-Kras, Ikkα$^{F/F}$-p48-Kras and 7-14 months old p48-Kras mice were checked by FACS. P value was determined by one-way ANOVA followed by Bonferroni`s multiple comparison test. *p ≤ 0.05, ***p ≤ 0.001.

4.10. Pancreas-derived CD11b$^+$ cells show M2 macrophage polarization in Ikkα$^{F/F}$-p48-Kras mice

To further characterize the phenotype of pancreas-infiltrating myeloid cells, CD11b$^+$ cell population was isolated from the whole pancreas by magnetic activated cell sorting (MACS) and RT-PCR was performed to determine the expression levels of *Ifnγ*, *Ifngr*, *Il1β*, *Il6*, *Il12*, *Tnfα*, *Spp1 (Opn)*, and *iNOS* as M1 macrophage markers, and *Il13*, *Il4*, *Il10*, *Il13rα1*, *Il4Rα*, *Dectin1*, *Mrc1* and *Arg1* as M2 macrophage markers. There was high expression of IL1β, IL6, and TNFα, which are generally secreted by M1 macrophages (Figure 4.22 A), although the expression of M2 macrophage markers including ARG-1 and DECTIN-1 were significantly increased in CD11b$^+$ positive cells from Ikkα$^{F/F}$-p48-Kras mice (Figure 4.22 B). In addition, another M1 marker iNOS showed elevated expression, whereas IL12 expression was lower in Ikkα$^{F/F}$-p48-Kras mice. Among the genes tested, expression of IFNγ, IFNGR, IL13, IL4 did not show any significant changes between 7-14 months old p48-Kras and Ikkα$^{F/F}$-p48-Kras animals (Figure 4.22 A, B).

The expression of these markers were further checked for the whole pancreas and compared with the results of CD11b$^+$ positive cells. Similar to CD11b$^+$ cells, expression of IFNGR displayed an increase in Ikkα$^{F/F}$-p48-Kras animals in comparison to other groups. IFNγ expression was decreased in the pancreas of Ikkα$^{F/F}$-p48-Kras mice, whereas there was no

significant difference in iNOS expression. Another M1 macrophage marker, IL12, showed a decrease in Ikkα$^{F/F}$-p48-Kras in comparison to 7-14 months old p48-Kras mice. Interestingly, SPP1, IL6 and TNFα expression were not significantly higher in the whole pancreas of Ikkα$^{F/F}$-p48-Kras mice but were especially secreted by CD11b^{+} positive cells in these animals in comparison to 7-14 months old p48-Kras mice (Figure 4.22 A). Importantly, M2 markers IL4Rα, ARG-1 and DECTIN-1, displayed elevated expression in the whole pancreas of Ikkα$^{F/F}$-p48-Kras mice similar to CD11b^{+} cells. Moreover, apart from IL4 and IL13, the other M2 markers displayed higher expression in the whole pancreas of Ikkα$^{F/F}$-p48-Kras mice as well as CD11b^{+} cells (Figure 4.22 B). Altogether these results suggest that although M2 polarized macrophage infiltration in the pancreas of Ikkα$^{F/F}$-p48-Kras is high, still M1 polarized macrophages exist and continue to secrete pro-inflammatory cytokines.

Since abundant amount of fibroblast infiltration was also observed in the pancreas of Ikkα$^{F/F}$-p48-Kras mice, contribution of the fibroblasts in accelerated tumor progression was further checked. For this aim, fibroblasts were isolated from pancreas and afterwards expression of pro-inflammatory cytokines and M2 macrophage markers were determined. A significant increase in the expression of the genes tested was observed in the fibroblasts from Ikkα$^{F/F}$-p48-Kras mice in comparison to Ikkα$^{F/F}$ animals, which was similar to the results of CD11b^{+} cells. This result displays that not only CD11b^{+} cells but also fibroblasts might play an important role in the acceleration of tumor development in Ikkα$^{F/F}$-p48-Kras animals (Figure 4.23).

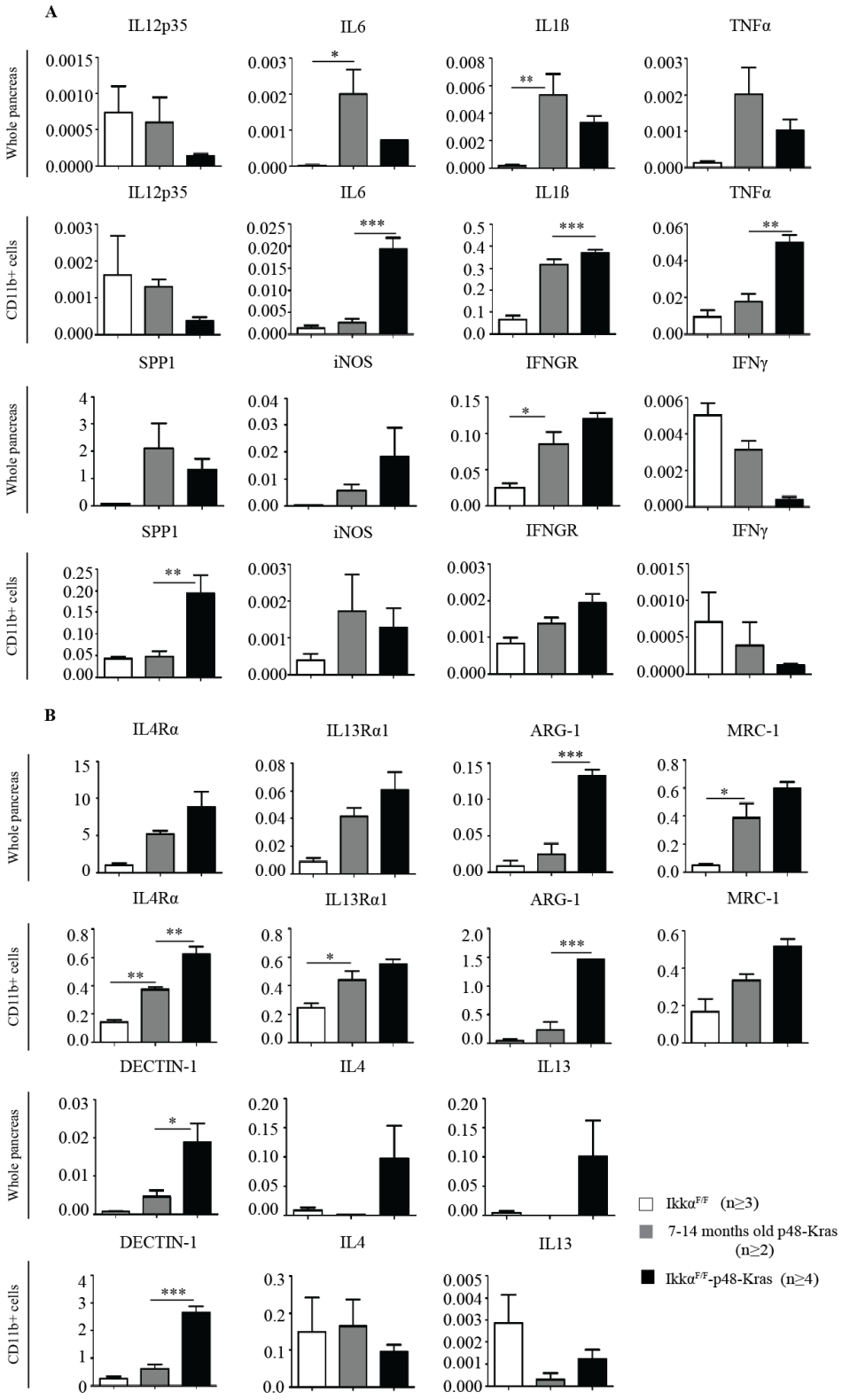

Figure 4.22. Pancreas-specific *Ikkα* deletion increases the expression of M2 macrophage markers and proinflammatory cytokines in whole pancreas and CD11b$^+$ cells that are isolated from the pancreas of Ikkα$^{F/F}$-p48-Kras mice. (A) Relative mRNA levels of the genes important for M1 and (B) M2 macrophage polarization were detected by RT-PCR for 3-4 weeks old Ikkα$^{F/F}$, Ikkα$^{F/F}$-p48-Kras and 7-14 months old p48-Kras mice. P value was determined by one-way ANOVA followed by Bonferroni`s multiple comparison test. *p ≤ 0.05, **p ≤ 0.01, ***p ≤ 0.001.

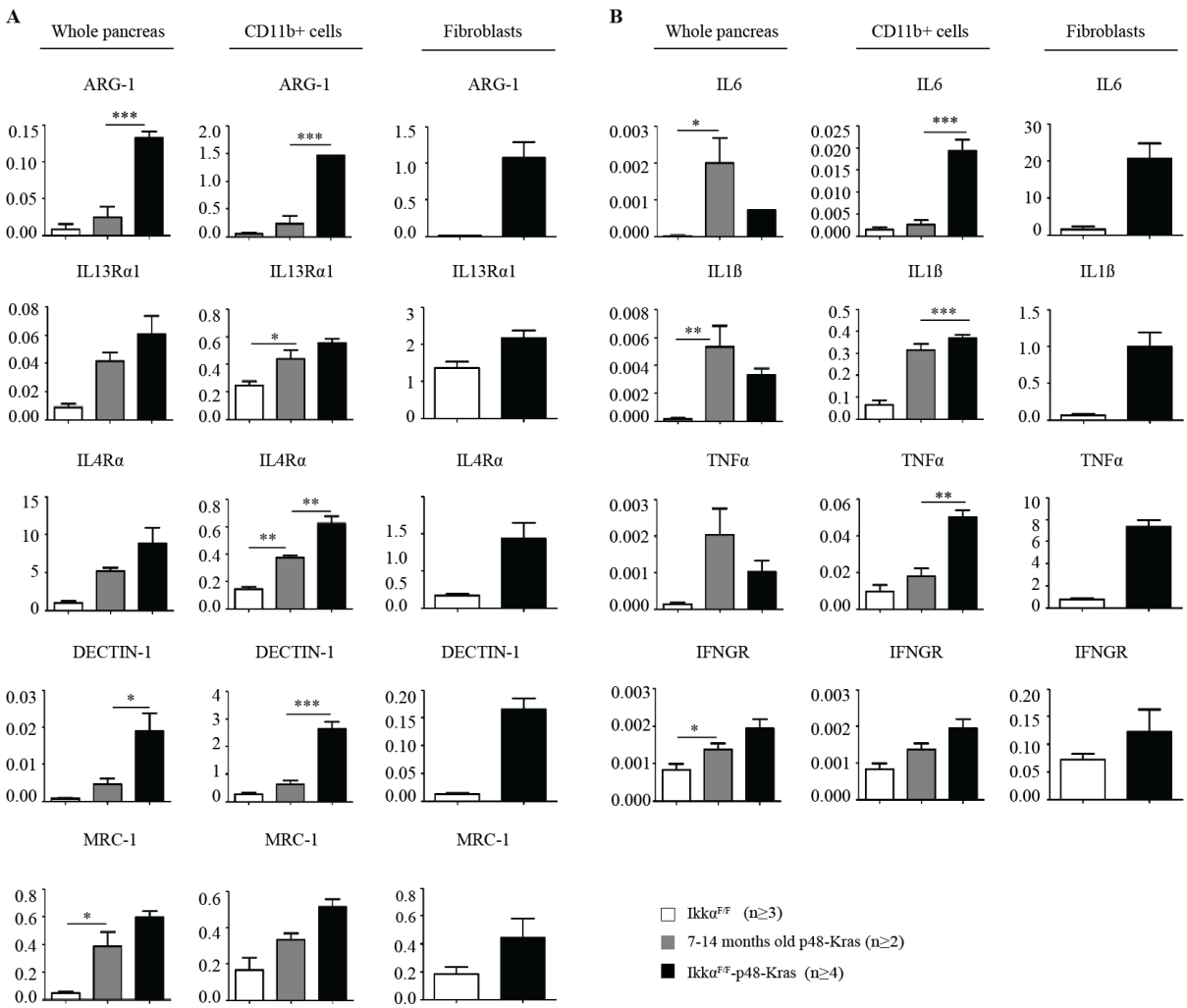

Figure 4.23. ***Ikkα*** **ablation enhances the expression of M2 macrophage markers and pro-inflammatory cytokines not only in CD11b^{+} cells but also in fibroblasts, which are isolated from the pancreas of Ikkα$^{F/F}$-p48-Kras mice.** (A) RT-PCR was used to detect the relative mRNA levels of the genes related to M2 macrophage polarization and (B) pro-inflammatory cytokines and IFNGR for 3-4 weeks old Ikkα$^{F/F}$, Ikkα$^{F/F}$-p48-Kras and 7-14 months old p48-Kras mice. P value was determined by one-way ANOVA followed by Bonferroni`s multiple comparison test. *p ≤ 0.05, **p ≤ 0.01, ***p ≤ 0.001.

4.11. *Stat6* deletion does not block accelerated tumor progression in Ikkα$^{F/F}$-p48-Kras

Stat6 is an essential molecule that functions as a downstream mediator of IL4/IL13 signaling pathway. In order to address whether accelerated tumor progression was conferred by increased M2 polarization, Ikkα$^{F/F}$-p48-Kras mice were crossed to whole body *Stat6* knock-out animals. The mice bred normally and were born at expected Mendelian ratio. However after birth, Stat6$^{-/-}$-Ikkα$^{F/F}$-p48-Kras mice displayed the same phenotypic features as Ikkα$^{F/F}$-p48-Kras mice. Histological evaluation of pancreas sections from 4 weeks old Stat6$^{-/-}$-Ikkα$^{F/F}$-p48-Kras mice showed that pancreas was completely altered. Similar to Ikkα$^{F/F}$-p48-Kras mice,

architectural distortion in Stat6$^{-/-}$-Ikkα$^{F/F}$-p48-Kras mice was nearly 100% with a cell rich stroma and solid tumor cell nests. Taken together these data suggest M2-associated inflammation-induced tumor progression in Ikkα$^{F/F}$-p48-Kras mice was independent of Stat6 signaling (Figure 4.24).

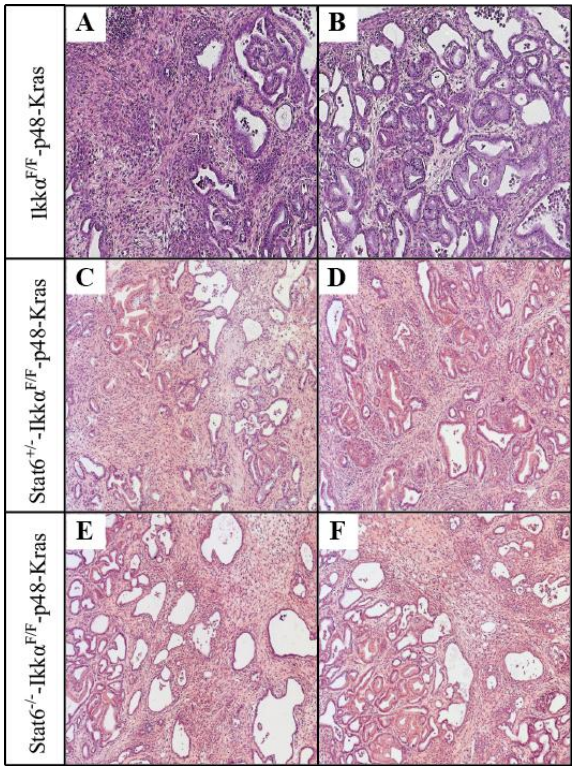

Figure 4.24. Whole body *Stat6* deletion does not confer protection against accelerated tumor progression in Ikkα$^{F/F}$-p48-Kras mice. (A, B) H&E-stained pancreas sections of Ikkα$^{F/F}$-p48-Kras mice (C, D) Stat6$^{+/-}$-Ikkα$^{F/F}$-p48-Kras mice and (E, F) Stat6$^{-/-}$Ikkα$^{F/F}$-p48-Kras mice. 20X magnification.

4.12. Pancreas-specific *Ikkα* deletion alters the expression of genes involved in energy metabolism in p48-Kras mice

Alterations in energy metabolism appear as a hallmark of inflammation-associated cancer. Thus, in order to determine the expression of genes involved in energy metabolism, microarray analysis was performed and particularly gene sets involved in several metabolic pathways including Oxidative phosphorylation, Tricarboxylic acid cycle (TCA cycle) (also known as the Krebs cycle), Glycolysis-Gluconeogenesis, and Pentose Phosphate Pathway (PPP) were analyzed.

Mitochondria are essential organelles, which regulate the production of reactive oxygen species (ROS), energy production via oxidative phoshorylation and TCA cycle, and cell death.

Importantly, abnormalities in mitochondria function, which can be due to the mutations of mitochondrial genome, oncogene activation or hypoxia, might be seen in cancer cells (Solaini *et al*., 2010; Solaini *et al*., 2011).

Oxidative phosphorylation is the major mitochondrial energy production pathway. However, it is already shown that although in the presence of oxygen, oxidative phosphorylation is less preferred by the tumor cells. Thus, expression of 128 genes involved in oxidative phosphorylation was checked by microarray analysis. Overall the gene signatures for Complex I-V of the mitochondria were distinctly separated between Ikk$\alpha^{F/F}$-p48-Kras mice and p48-Kras animals. Indeed several subunits of the mitochondrial complexes were mostly differentially regulated in these two tumor-bearing mouse groups. Although it was difficult to point single gene differences, still these findings suggest altered ATP production in p48-Kras mice with or without IKKα deletion (Figure 4.25).

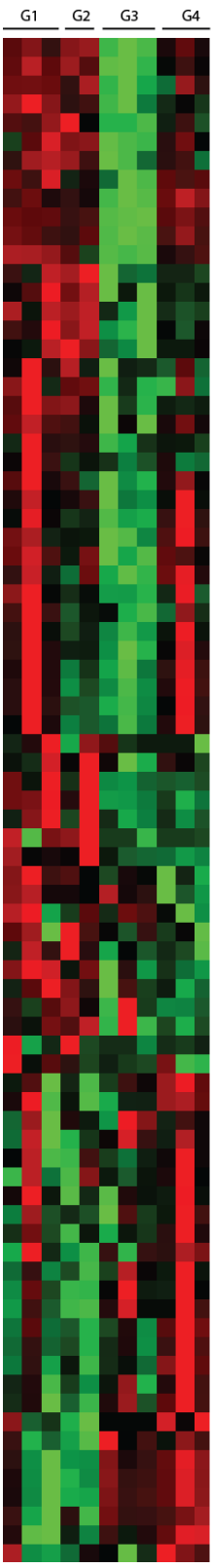

NADH dehydrogenase (ubiquinone) Fe-S protein 6
NADH dehydrogenase (ubiquinone) 1 alpha subcomplex, 1
cytochrome c oxidase, subunit VIIa 2
ubiquinol-cytochrome c reductase, complex III subunit VII
NADH dehydrogenase (ubiquinone) 1 beta subcomplex, 2
NADH dehydrogenase (ubiquinone) 1 alpha subcomplex, 5
ATP synthase, H+ transporting, mitochondrial F1F0 complex, subunit e
ubiquinol-cytochrome c reductase, Rieske iron-sulfur polypeptide 1
NADH dehydrogenase (ubiquinone) 1 alpha subcomplex, 4
NADH dehydrogenase subunit 6
NADH dehydrogenase (ubiquinone) 1 beta subcomplex, 7
ATP synthase, H+ transporting, mitochondrial F1 complex, O subunit
cytochrome c oxidase subunit VIb polypeptide 2
ATPase, H+ transporting, lysosomal V1 subunit G2
cytochrome c oxidase, subunit VI a, polypeptide 2
ATPase, H+ transporting, lysosomal V0 subunit A2
ATPase, H+ transporting, lysosomal V1 subunit E2
NADH dehydrogenase (ubiquinone) Fe-S protein 5
NADH dehydrogenase (ubiquinone) Fe-S protein 5
NADH dehydrogenase (ubiquinone) 1 beta subcomplex, 6
ATP synthase, H+ transporting, mitochondrial F1 complex, epsilon subunit
succinate dehydrogenase complex, subunit B, iron sulfur (Ip)
cytochrome c oxidase subunit VIIb2
NADH dehydrogenase (ubiquinone) 1 alpha subcomplex, 6 (B14)
NADH dehydrogenase (ubiquinone) 1, subcomplex unknown, 1
NADH dehydrogenase (ubiquinone) 1 beta subcomplex, 5
ATP synthase, H+ transporting, mitochondrial F0 complex, subunit F2
ubiquinol-cytochrome c reductase, complex III subunit X
cytochrome c oxidase, subunit Va
NADH dehydrogenase (ubiquinone) 1 alpha subcomplex, 12
NADH dehydrogenase (ubiquinone) 1 beta subcomplex 8
ATP synthase, H+ transporting, mitochondrial F0 complex, subunit g
ATP synthase, H+ transporting, mitochondrial F0 complex, subunit g
ATP synthase, H+ transporting, mitochondrial F0 complex, subunit g
ATP synthase, H+ transporting, mitochondrial F0 complex, subunit g
ATP synthase, H+ transporting, mitochondrial F0 complex, subunit g
ATP synthase, H+ transporting, mitochondrial F0 complex, subunit g
NADH dehydrogenase (ubiquinone) 1 alpha subcomplex, 13
NADH dehydrogenase (ubiquinone) 1 alpha subcomplex, 4-like 2
NADH dehydrogenase (ubiquinone) 1 beta subcomplex, 5
ATPase, H+ transporting, lysosomal V1 subunit B1
ATPase, H+ transporting, lysosomal V1 subunit G3
cytochrome c oxidase, subunit VIIa 1
ATPase, H+ transporting, lysosomal V1 subunit C2
NADH dehydrogenase (ubiquinone) 1 beta subcomplex, 9
NADH dehydrogenase (ubiquinone) 1 beta subcomplex, 11
COX10 homolog, cytochrome c oxidase assembly protein, heme A: farnesyltransferase (yeas
NADH dehydrogenase (ubiquinone) 1 alpha subcomplex 11
cytochrome c oxidase, subunit VIIIb
NADH dehydrogenase (ubiquinone) 1 beta subcomplex, 10
ATPase, H+ transporting, lysosomal V0 subunit E2
ATPase, H+/K+ exchanging, gastric, alpha polypeptide
ATPase, H+/K+ exchanging, beta polypeptide
cytochrome c oxidase, subunit VIIIc
ATPase, H+/K+ transporting, nongastric, alpha polypeptide
NADH dehydrogenase (ubiquinone) Fe-S protein 3
NADH dehydrogenase (ubiquinone) Fe-S protein 3
NADH dehydrogenase (ubiquinone) 1 alpha subcomplex, 2
NADH dehydrogenase (ubiquinone) 1 alpha subcomplex, 3
NADH dehydrogenase (ubiquinone) 1, alpha/beta subcomplex, 1
NADH dehydrogenase (ubiquinone) 1, alpha/beta subcomplex, 1
NADH dehydrogenase (ubiquinone) 1, subcomplex unknown, 1
NADH dehydrogenase subunit 3
ATP synthase, H+ transporting, mitochondrial F0 complex, subunit d
ubiquinol-cytochrome c reductase hinge protein
NADH dehydrogenase subunit 3
ATP synthase F0 subunit 6
ATP synthase F0 subunit 6
cytochrome c oxidase subunit II
cytochrome c oxidase subunit II
cytochrome c oxidase, subunit Vb
ATPase, H+ transporting, lysosomal V1 subunit F
ATPase, H+ transporting, lysosomal V1 subunit F
COX15 homolog, cytochrome c oxidase assembly protein (yeast)
cytochrome c-1
ATP synthase, H+ transporting, mitochondrial F0 complex, subunit C2 (subunit 9)
ATP synthase, H+ transporting, mitochondrial F0 complex, subunit C2 (subunit 9)
ATP synthase, H+ transporting, mitochondrial F0 complex, subunit C2 (subunit 9)
ATPase, H+ transporting, lysosomal V0 subunit D1
ATPase, H+ transporting, lysosomal V1 subunit H
ATP synthase, H+ transporting, mitochondrial F0 complex, subunit B1

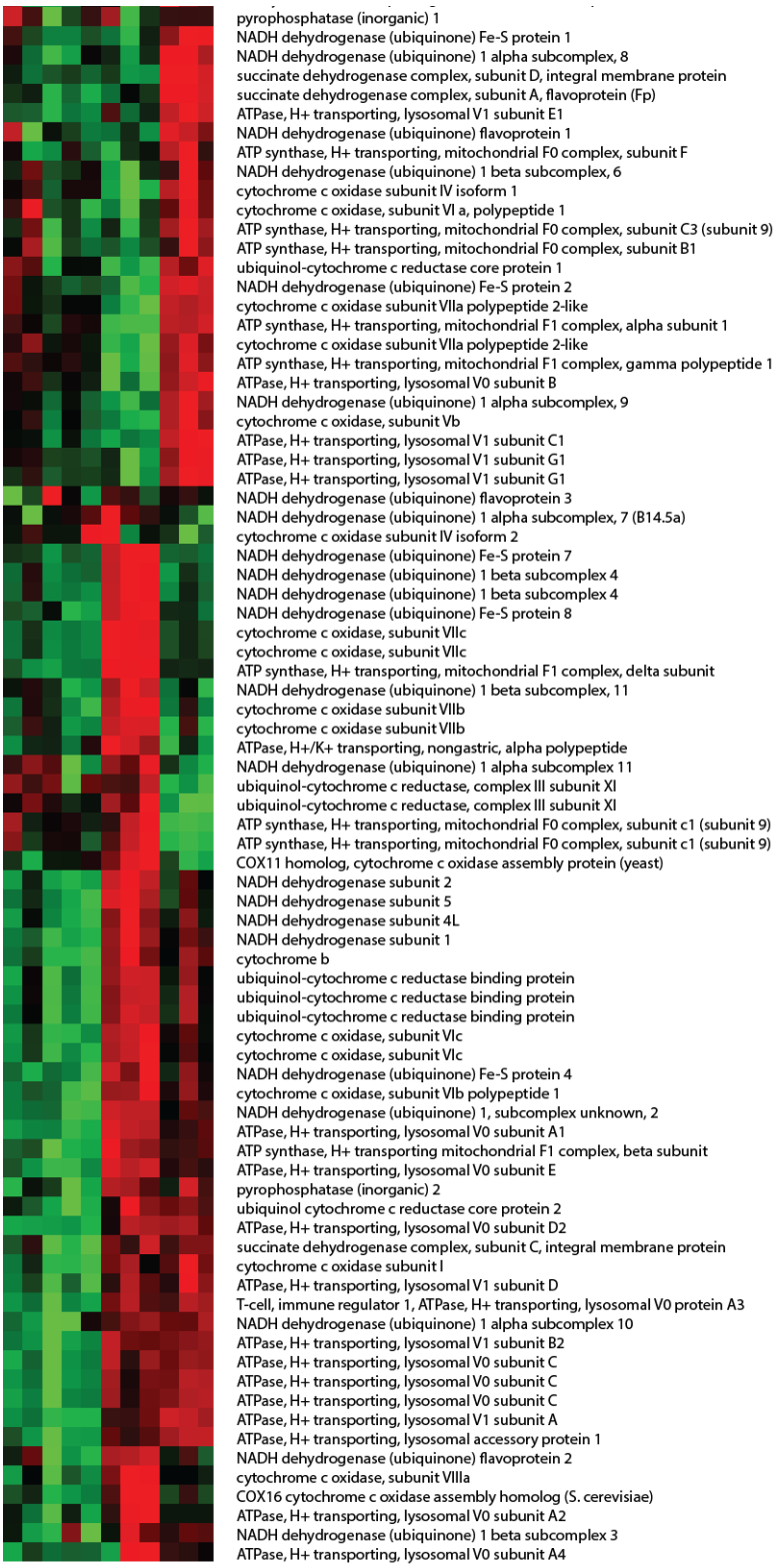

Figure 4.25. Pancreas specific *Ikkα* deletion alters the expression of several genes related with oxidative phosphorylation in p48-Kras animals. Gene expression profiles were shown as a heat-map for 3-4 weeks old Ikkα$^{F/F}$ (G1, n:3), p48-Kras (G2, n:2), Ikkα$^{F/F}$-p48-Kras (G4, n:3) and 7-14 months old p48-Kras mice (G3, n:3). Red color displays up-regulation of the genes whereas green color shows down-regulation.

Tricarboxylic acid cycle (TCA cycle) is one of the main metabolic pathways. In eukaryotic cells, TCA cycle progress in mitochondrial matrix and Acetly-CoA, which is an end product of pyruvate, is used in this cycle to produce adenosine triphosphate (ATP) and several intermediate molecules that are used to synthesize macromolecules that are needed by proliferating cells (DeBerardinis and Thompson, 2008; Levine and Puzio-Kuter, 2010). It is known that cancer cells perform TCA cycle less (Levine and Puzio-Kuter, 2010). Due to its importance, expression of 31 genes related to TCA cycle was checked. Interestingly, TCA gene signature for Ikk$\alpha^{F/F}$-p48-Kras mice appeared distinct compared to that of p48-Kras animals suggesting that pancreas restricted *Ikkα* loss led to altered expression of genes involved in TCA cycle in p48-Kras mice. Importantly expression of the subunits of pyruvate dehydrogenase complex (PDC), pyruvate dehydrogenase E1 alpha1 and dihydrolipoamide dehydrogenase (E3 component of PDC, also known as dihydrolipoyl dehydrogenase) was increased in Ikk$\alpha^{F/F}$-p48-Kras mice in comparison to 7-14 months old p48-Kras mice, whereas dihydrolipoamide S-acetyltransferase (E2 component of PDC) showed an increase in both animal groups. Since PDC is responsible for Acetyl-CoA production from pyruvate and the E1 alpha subunit has the key role in the function of PDC, it suggested that Acetyl-CoA production that is used in TCA cycle might be elevated in Ikk$\alpha^{F/F}$-p48-Kras animals (Figure 4.26). Supporting this notion, expression of other genes involved in TCA cycle including succinate dehydrogenase complex subunit A and D, fumarate hydratase 1 and malate dehydrogenase 1 (NAD, soluble) were further elevated in Ikk$\alpha^{F/F}$-p48-Kras mice. Expression of another enzyme encoding ATP citrate lyase, which is an enzyme functioning in metabolism of carbohydrates and fatty acid production by catalyzing the conversion of citrate and CoA into cytoplasmic acetyl-CoA and oxaloacetate, was highly elevated in Ikk$\alpha^{F/F}$-p48-Kras mice proposing that cytoplasmic acetyl-CoA production, which is used in fatty acid production, might be increased in these animals (Figure 4.26). This finding is consistent with the fact that in tumor cells, a truncated form of TCA cycle is being used in which the intermediates of the cycle such as citrate are taken out from mitochondria and processed in the cytoplasm to produce other molecules including fatty acids or cholesterol that are necessary for the synthesis of cell membrane (DeBerardinis and Thompson, 2008).

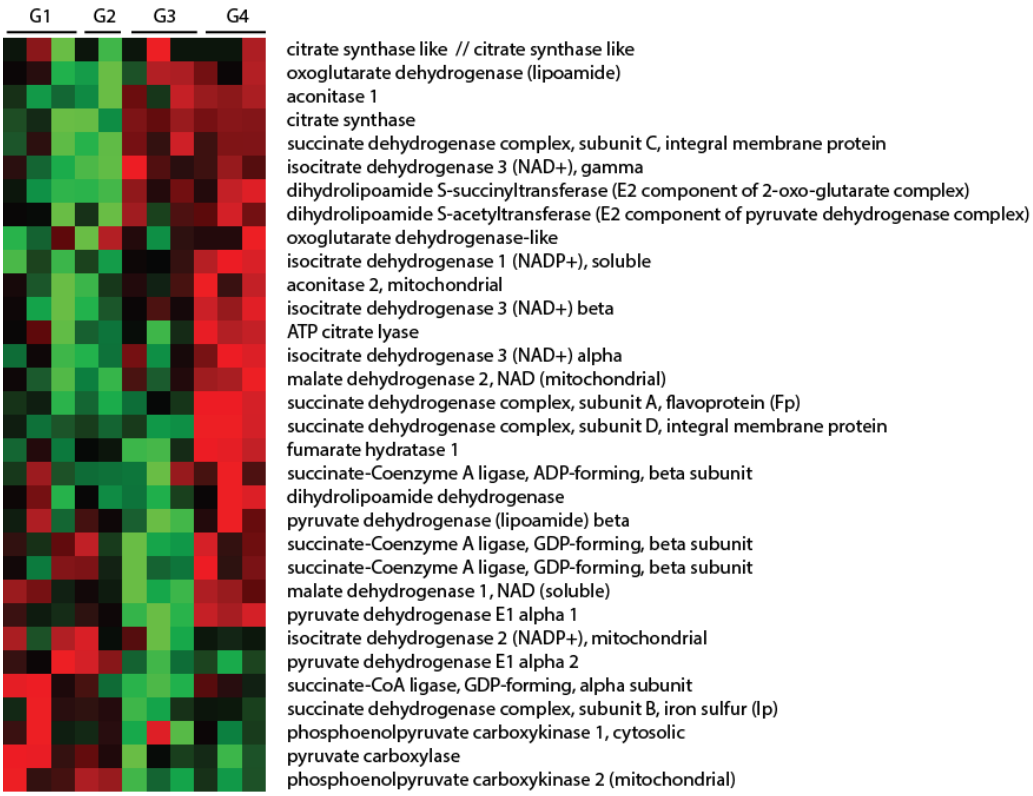

Figure 4.26. ***Ikkα*** **deletion in pancreas causes different expression of some genes involved in TCA cycle in tumor bearing p48-Kras animals.** Gene expression profiles are shown as a heat-map for 3-4 weeks old Ikkα$^{F/F}$ (G1, n:3), p48-Kras (G2, n:2), Ikkα$^{F/F}$-p48-Kras (G4, n:3) and 7-14 months old p48-Kras mice (G3, n:3). Red color displays up-regulation of the genes whereas green color shows down-regulation.

Pentose Phosphate Pathway (PPP), which uses phosphorylated glucose (Glucose-6-P) as a substrate, generates ribose-5-phosphate and nicotinamide adenine dinucleotide phosphate (NADPH). PPP is an important pathway for cancer cells since Ribose-5-phosphate is necessary for nucleic acid and nucleotide synthesis, whereas NADPH is essential for fatty acid metabolism and reactive oxygen species (ROS) balance in the cells. In microarray analysis, expression of PPP related genes was determined. Considerably, expression of three essential enzymes of PPP, ribose 5-phosphate isomerase A (*Rpia*) and the catalyzers of the non-oxidative branch of PPP, transketolase (*Tkt*) and transaldolase 1 (*Taldo1*), was increased in Ikkα$^{F/F}$-p48-Kras mice in comparison to 7-14 months old p48-Kras mice. Among these p48-Kras mice, only one sample, which had liver metastasis in addition to pancreas tumor, displayed significant increase in transketolase expression similar to Ikkα$^{F/F}$-p48-Kras animals. Comparable to transketolase, other enzymes including 2-deoxyribose-5-phosphate aldolase homolog (C. elegans), phosphoglucomutase 2, aldolase A, and phosphofructokinase (both platelet and liver, B type) also displayed increased expression in Ikkα$^{F/F}$-p48-Kras mice and 7-14 months old mouse with pancreas tumor and liver metastasis, whereas the rest of p48-Kras mice did not show an increase.

Further, expression of fructose bisphosphatase 2 (FBPase2; also known as phosphofructokinase 2 (PFK2)) and aldolase B, the enzymes that also function in glycolytic-gluconeogenic pathway, was elevated in Ikkα$^{F/F}$-p48-Kras mice in comparison to 7-14 months old p48-Kras animals. Altogether this data suggest that pancreas specific *Ikkα* deletion alters the expression of several crucial enzymes involved in PPP and glucose metabolism in the pancreas of p48-Kras mice (Figure 4.27).

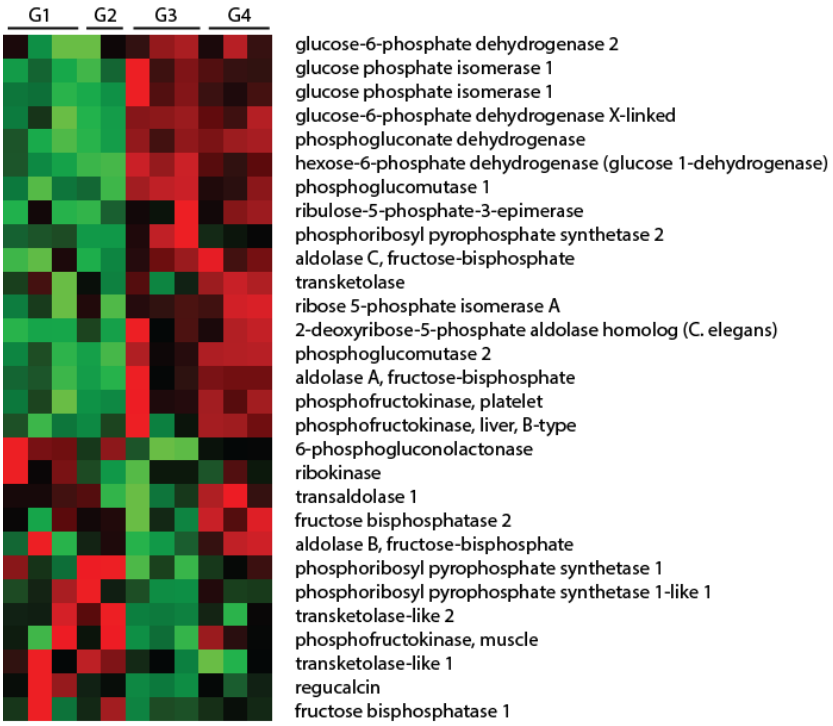

Figure 4.27. Pancreas specific *Ikkα* deletion leads to elevated ribose 5-phosphate isomerase A, transketolase and transaldolase 1 expression in p48-Kras animals. Gene expression profiles are shown as a heat-map for 3-4 weeks old Ikkα$^{F/F}$ (G1, n:3), p48-Kras (G2, n:2), Ikkα$^{F/F}$-p48-Kras (G4, n:3) and 7-14 months old p48-Kras mice (G3, n:3). Red color displays up-regulation of the genes whereas green color shows down-regulation.

Since Otto Warburg realized that tumor cells consume more glucose and produce lactate in the presence of oxygen, a lot of studies confirmed this observation and today it is known that tumor cells prefer to use aerobic glycolysis to generate energy (DeBerardinis and Thompson, 2008). Thus, expression of 58 genes related to glycolysis and gluconeogenesis was checked. Interestingly, although there were variations in gene expression levels, tumor bearing p48-Kras and Ikkα$^{F/F}$-p48-Kras animals displayed similar expression patterns and tendency for increased expression in several important genes suggesting that both tumor mouse groups might majorly rely on glycolysis and gluconeogenesis for energy production. Especially, expressions of Hexokinase 1 and 2 (HK1, HK2) were increased in Ikkα$^{F/F}$-p48-Kras mice. Hexokinases are very

important since they catalyze the first step of glycolysis, in which a charged phosphate group is added at the 6th position of glucose molecule leading to the generation of Glucose 6-Phosphate. After phosphorylation, glucose or 2-deoxy glucose molecules can be kept within the cells and processed in glycolysis or PPP. Among hexokinases, HK2 is particularly important since glycolytic pathway is primarily induced by this enzyme and it was further shown to inhibit cancer cell death via its mitochondrial location (Mathupala *et al*., 2008). Expression of another enzyme, Enolase, displayed differences between animal groups. Enolase 1, alpha non-neuron subunit expression was increased in 7-14 months old p48-Kras and Ikkα$^{F/F}$-p48-Kras mice, whereas enolase 2, gamma neuronal stayed unaltered in these groups. Interestingly, enolase 3, beta muscle expression was similarly decreased in Ikkα$^{F/F}$-p48-Kras mice as well as 3-4 weeks old Ikkα$^{F/F}$-p48-Kras animals, whereas 2 tumor bearing p48-Kras mice displayed an increase for this gene suggesting that although Ikkα$^{F/F}$-p48-Kras mice also had tumors, *Ikkα* deletion might lead to a particular decrease in the expression of this gene (Figure 4.28). In addition, expression of aldolase B, fructose biphosphatase 2 (FBPase2), pyruvate dehydrogenase E1 alpha 1, aldehyde dehydrogenase 1 family member B1 and 2,3-biphosphoglycerate mutase displayed an increase in Ikkα$^{F/F}$-p48-Kras mice but not in 7-14 months old p48-Kras mice proposing that *Ikkα* deletion causes alterations in the expression of glycolysis and gluconeogenesis related genes in p48-Kras animals (Figure 4.28).

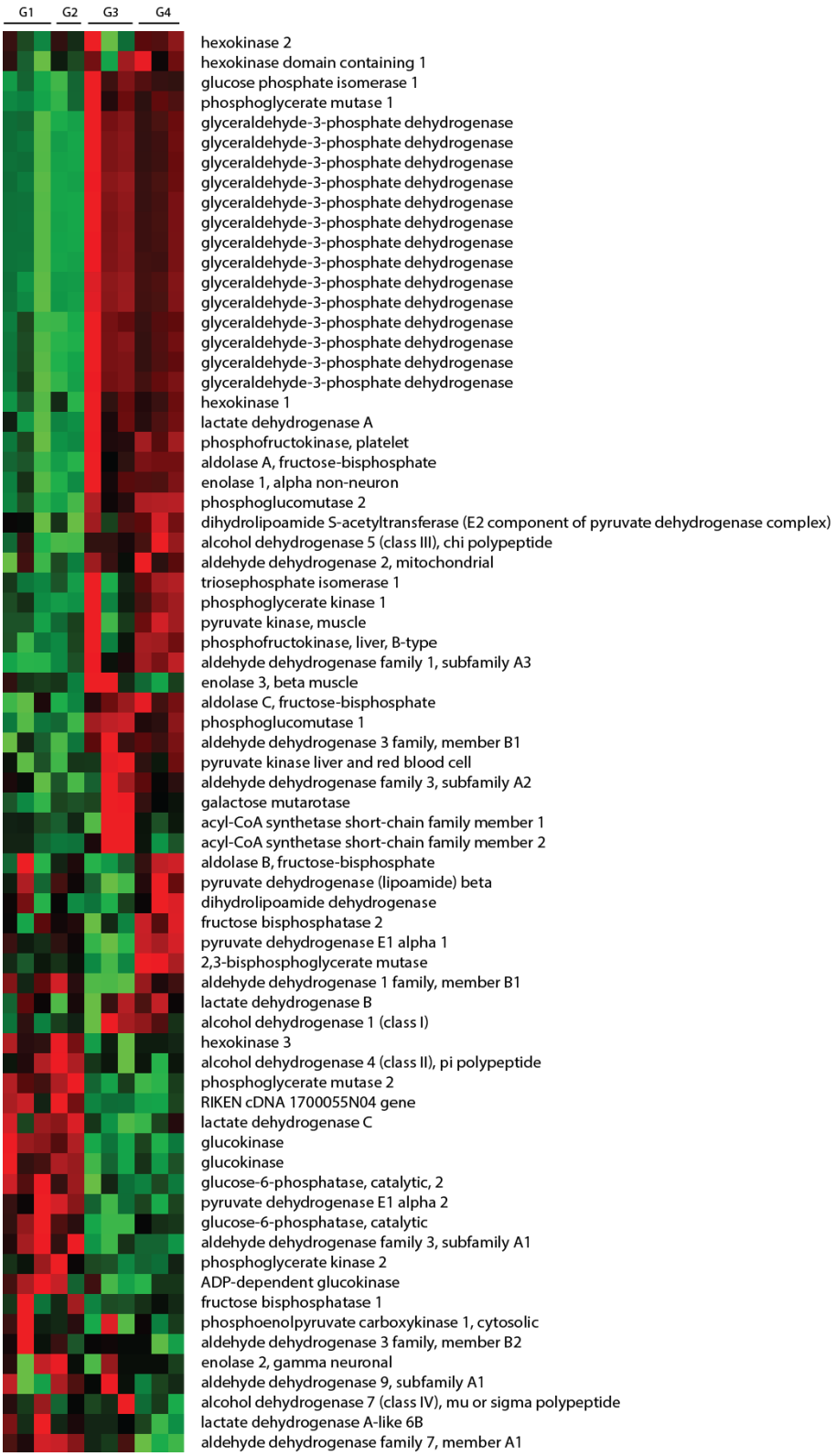

Figure 4.28. Although tumor bearing mouse models seem to rely on glycolytic pathways for energy production, still *Ikkα* loss results in altered expression of glycolysis-gluconeogenesis related genes in p48-Kras mice. Gene expression profiles are displayed as a heat-map for 3-4 weeks old Ikkα$^{F/F}$ (G1, n:3), p48-Kras (G2, n:2), Ikkα$^{F/F}$-p48-Kras (G4, n:3) and 7-14 months old p48-Kras mice (G3, n:3). Red color displays up-regulation of the genes whereas green color shows down-regulation.

To further elucidate expression of the complexes involved in electron transport chain in mitochondria, WB was performed using an antibody cocktail that detects only one subunit of the Complex I-V. Complex II, which is involved in both electron transfer chain and TCA cycle was decreased in Ikkα$^{F/F}$-p48-Kras mice in comparison to 7-14 months old p48-Kras mice (Figure 4.29 A). Moreover, in order to see whether *Ikkα* deficiency has a direct effect on the expression of mitochondrial complexes, we knocked *Ikkα* down by siRNA in mouse pancreatic cancer cell line and checked Complex I-V. The expression of Complex V, which is the ATP synthase, was higher in *Ikkα*$^{-/-}$ cells in comparison to the cells treated with scrambled siRNA (Figure 4.29 B).

Since the antibody cocktail detects only one component of the each complex, which normally consists of many subunits, it was not enough to explore the activity of electron transport chain in the mitochondria in detail. Thus, Clark Electrode was employed to measure the respiration of alive mitochondria from pancreas. Importantly, mitochondrial respiratory rates were significantly decreased in Ikkα$^{F/F}$-p48-Kras mice in comparison to p48-Kras animals (Figure 4.29 C). In order to check whether decreased oxidative phosphorylation was associated with decreased mitochondria content, relative mitochondria copy numbers were checked using the isolated DNA from the pancreata. Indeed, Ikkα$^{F/F}$-p48-Kras mice had relatively lower number of mitochondria than age-matched Ikkα$^{F/F}$ and p48-Kras, whereas there was no difference when compared to 7-14 months old p48-Kras group (Figure 4.29 D). These data suggest a decrease in oxidative phosphorylation and a possible switch to glycolysis in Ikkα$^{F/F}$-p48-Kras mice.

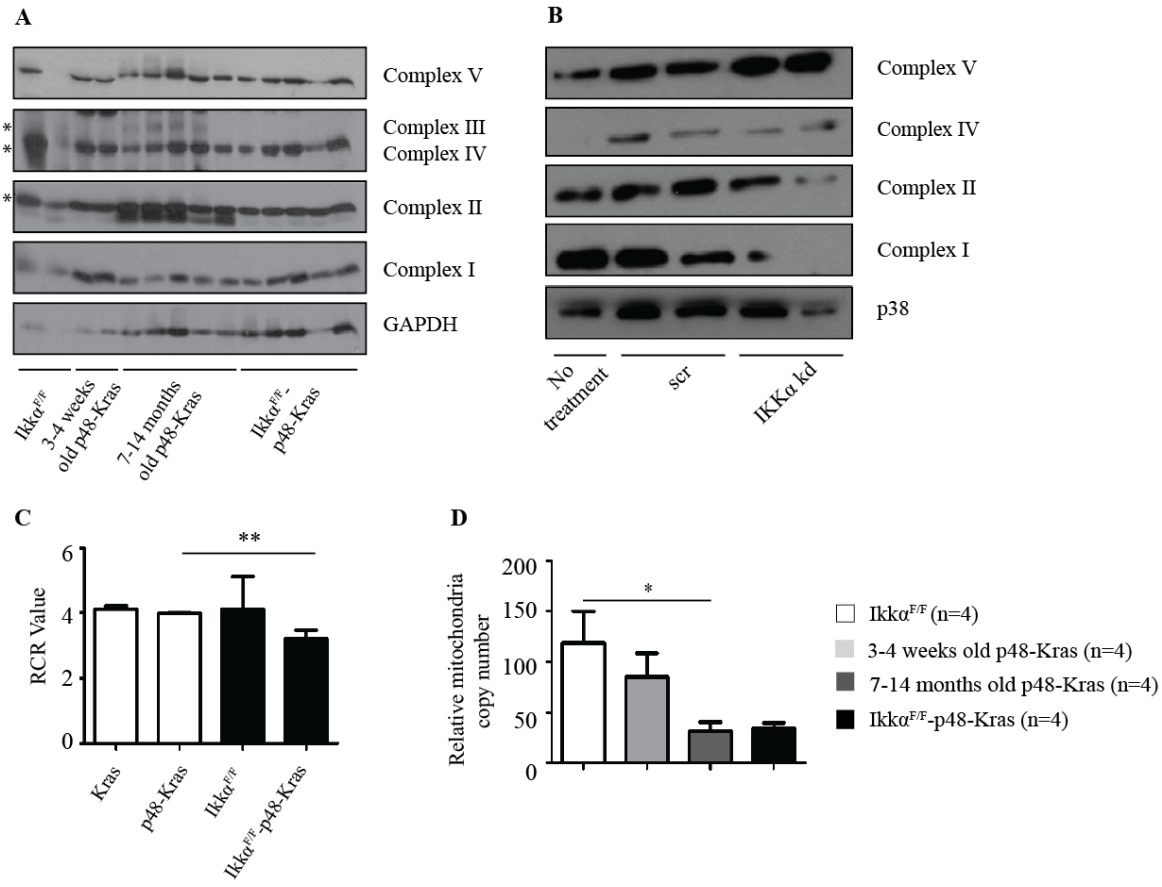

Figure 4.29. ***Ikkα*** **deletion alters the expression and activity of respiratory rates in the pancreata of p48-Kras mice.** (A) WB analysis showing the expression of oxidative phosphorylation complexes in the pancreas of 3-4 weeks old Ikkα$^{F/F}$, p48-Kras, Ikkα$^{F/F}$-p48-Kras and 7-14 weeks old p48-Kras mice, and (B) in mouse pancreatic cancer cell lines. (C) Clark electrode measurements displaying the respiratory chain activity of living mitochondria isolated from the pancreas of 26 weeks old Kras and p48-Kras mice, 3-4 weeks old Ikkα$^{F/F}$ and Ikkα$^{F/F}$-p48-Kras mice. (D) Mitochondria copy numbers were detected using DNA from 3-4 weeks old Ikkα$^{F/F}$, p48-Kras, Ikkα$^{F/F}$-p48-Kras and 7-14 months old p48-Kras mice. GAPDH and p38 was used as loading control of WB analysis. Asterisks indicate the corresponding bands. For Clark electrode; n≥2. Data are mean values ± SEM, *p ≤ 0.05, **p ≤ 0.01.

4.13. Ikkα$^{F/F}$-p48-Kras mice show a shift towards glycolytic pathway during tumor progression

Although energy production by oxidative phosphorylation is higher than glycolysis, tumor cells prefer to produce energy via glycolysis instead of oxidative phosphorylation of pyruvate in mitochondria. Accordingly, it is highly possible that energy is produced preferably via glycolysis rather than oxidative phosphorylation in the pancreas of Ikkα$^{F/F}$-p48-Kras mice. To test this possibility, RT-PCR was performed to check the expression of HK1 and HK2, the enzymes involved in glycolysis, as well as Glucose-6-phosphatase (*G6Pase*), and Fructose 1,6-bisphosphatase (*FBPase1*), which are involved in gluconeogenesis. Confirming our microarray result, although HK1 expression was increased in tumor-bearing mice, however, no significant

difference was observed between 7-14 months old p48-Kras and 3-4 weeks old Ikkα$^{F/F}$-p48-Kras mice. On the other hand, HK2 expression could not be confirmed by RT-PCR since no significant alteration was detected between animal groups. Furthermore, decreased expression of FBPase1 was verified for Ikkα$^{F/F}$-p48-Kras mice in comparison to age-matched Ikkα$^{F/F}$ animals (Figure 4.30).

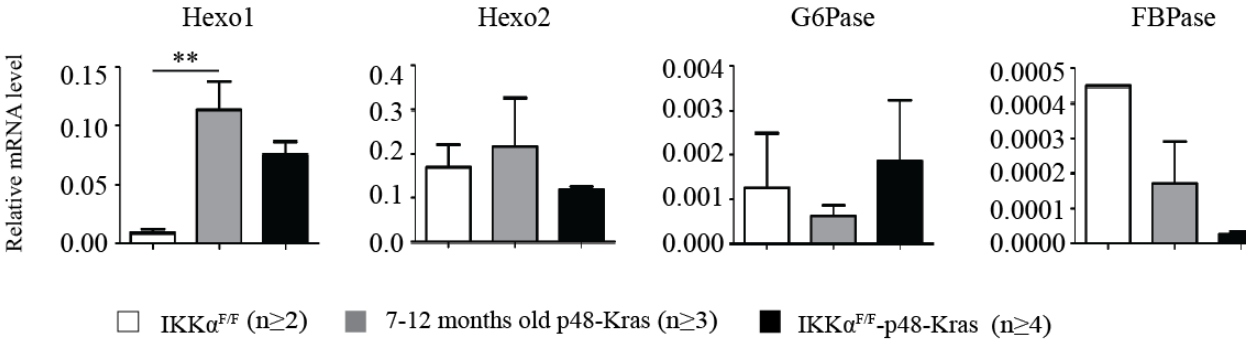

Figure 4.30. Glycolysis is increased in tumor bearing p48-Kras mice with or without IKKα deletion. Relative mRNA levels of the HK1, HK2, G6Pase and FBPase1 genes were detected by RT-PCR for 3-4 weeks old Ikkα$^{F/F}$, Ikkα$^{F/F}$-p48-Kras and 7-14 months old p48-Kras mice. P value was determined by one-way ANOVA followed by Bonferroni`s multiple comparison test. **$p \leq 0.01$.

4.14. Pancreas-specific *Ikkα* deletion leads to significant alteration in the expression of genes involved in Pentose Phosphate Pathway (PPP) in CD11b^{+} cells

De novo synthesis of nucleotides is very important for transformed cells because they must supply enough material to keep up with increased DNA replication. Thus, the metabolic pathways, in which metabolic intermediates provided by the TCA cycle and glycolysis are used, are essential for neoplastic cells. Among these metabolic pathways, the PPP is especially important since it produces NADPH, which is necessary for the production of five carbon nucleotides such as ribose-5-phosphate (Tong *et al*., 2009). Thus, the expression of the genes involved in PPP including glucose phosphate isomerase 1 (*Gpi1*), glucose-6-phosphate dehydrogenase 2 (*G6pd2*), ribulose-5-phosphate-3-epimerase (*Rpe*), ribose 5-phosphate isomerase A (*Rpia*), transketolase (*Tkt*), transaldoase 1 (*Taldo1*), ribokinase (*Rbks*), and phosphoribosyl pyrophosphate synthase 1 (*Prps1*) was checked by RT-PCR. Significant decrease in the expression of *Gpi1* was observed in the whole pancreas of Ikkα$^{F/F}$-p48-Kras mice in comparison to 7-14 months old p48-Kras mice, whereas microarray analysis displayed similar increase in both groups. Consistent to microarray result, expression of *G6pd2*, which converts Glucose-6P into 6-Phosphogluconolactone, was increased in Ikkα$^{F/F}$-p48-Kras mice in

comparison to other groups. Furthermore, increased expression of *Tkt* and *Rpia* in tumor bearing mouse groups were verified by RT-PCR (Figure 4.31 A). Expression of these genes was further checked using RNA extracted from pancreas derived $CD11b^+$ cells. Among the genes involved in PPP, *G6pd2*, *Rpe*, *Prps1* and *Tkt* displayed similar expression pattern in $CD11b^+$ cells and whole pancreas from $Ikk\alpha^{F/F}$-p48-Kras mice, which was further consistent with microarray result. Whereas there was no significant difference in the expression of *Rpe* and *Prps1* between different animal groups, expression of *G6pd2* and *Tkt* was increased in $Ikk\alpha^{F/F}$-p48-Kras mice in comparison to 7-14 months old p48-Kras mice. Apart from these genes, expression of *Rpia*, *Taldo1* and *Rbks* was significantly elevated in $CD11b^+$ cells of $Ikk\alpha^{F/F}$-p48-Kras in comparison to 7-14 months old p48-Kras mice, although no significant increase was detected for these genes in whole pancreas. Moreover, an increase was observed for the expression of *Gpi1* in $CD11b^+$ cells from $Ikk\alpha^{F/F}$-p48-Kras animals in comparison to age-matched $Ikk\alpha^{F/F}$ mice. Similar to this result, elevated expression of Gpi1 was previously monitored in the pancreas of tumor-bearing mice by microarray analysis. In total, these data suggests that expression of several genes involved in PPP display higher expression in $CD11b^+$ cells isolated from the pancreas of $Ikk\alpha^{F/F}$-p48-Kras mice, although the same increase was not observed in whole pancreas (Figure 4.31 A).

In addition to PPP, the expression of genes related to glutamine and glutamate metabolism including glutamate transporter 1 (*Glt1*), ornithine aminotransferase (*Oat*), glutaminase (*Gls*) and glutamine synthetase (*Gs*) were checked by RT-PCR using RNA extracted from whole pancreas or $CD11b^+$ cells isolated from the pancreas. Among these genes, only GLT1 level showed a sharp decrease in both $CD11b^+$ cells and whole pancreas of $Ikk\alpha^{F/F}$-p48-Kras mice in comparison to $Ikk\alpha^{F/F}$ mice (Figure 4.31 B). On the other hand, expression of OAT, GLS and GS showed similar expression pattern in $CD11b^+$ cells as well as whole pancreas and stayed unaltered between animal groups suggesting that there was no significant alteration in the expression of genes checked for glutamine and glutamate metabolism in 7-14 months old p48-Kras and 3-4 weeks old $Ikk\alpha^{F/F}$-p48-Kras mice (Figure 4.31 B).

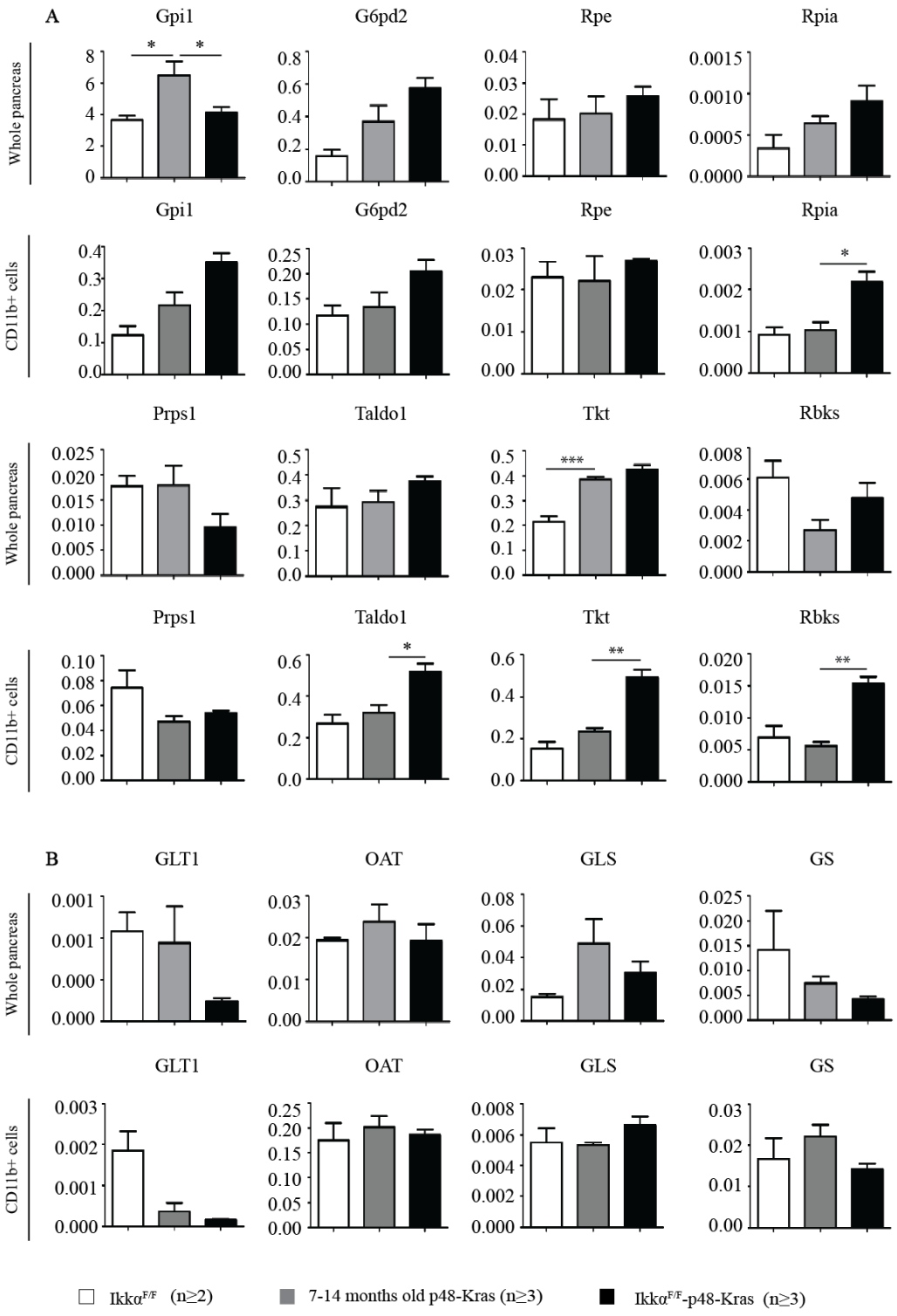

Figure 4.31. Pancreas-specific *Ikkα* deletion causes alterations in the expression of genes involved in Pentose Phosphate Pathway (PPP) and glutamine metabolism in pancreas derived CD11b$^+$ cells and whole pancreas of Ikkα$^{F/F}$-p48-Kras mice (A) Relative mRNA levels of the genes involved in PPP, and (B) glutamine and glutamate metabolism were checked by RT-PCR in whole pancreas and CD11b$^+$ cells isolated from the pancreas of 3-4 weeks old Ikkα$^{F/F}$, Ikkα$^{F/F}$-p48-Kras and 7-14 months old p48-Kras mice. P value was determined by one-way ANOVA followed by Bonferroni`s multiple comparison test. *p ≤ 0.05, **p ≤ 0.01, ***p ≤ 0.001.

4.15. The expression of genes involved in oxidative phosphorylation and glycolysis is altered in CD11b^{+} cells isolated from the pancreas of Ikkα$^{F/F}$-p48-Kras mice

The connection between energy metabolism and macrophages is only recently becoming accepted (Biswas and Mantovani, 2012). In our study, FACS analysis showed increased percentages of CD11b^{+} cells in the pancreas of 3-4 weeks old Ikkα$^{F/F}$-p48-Kras mice in comparison to 7-14 months old p48-Kras mice. Moreover, the expression of M2 polarized macrophage markers were elevated in these CD11b^{+} cells. Thus, it was worth to elucidate the metabolic profiles of myeloid cells during cancer progression to see whether M2 polarized macrophages are involved in the alteration of energy metabolism in Ikkα-p48-Kras mice. To that end, expression of genes involved in glycolysis, TCA cycle and oxidative phosphorylation including hexokinase 1 (*Hk1*), hexokinase 2 (*Hk2*), pyruvate dehydrogenase (lipoamide) beta (*PHDb*) and glucose-6-phosphatase (*G6Pase*) were checked by RT-PCR. Importantly, consistent to microarray data, HK2 expression was significantly increased in CD11b^{+} cells isolated from the pancreas of Ikkα$^{F/F}$-p48-Kras in comparison to 7-14 months old p48-Kras. On the other hand, there was no significant changes in the expression of HK1, G6Pase and PDHb was detected. In addition, no significant alterations in the expression of genes, which are involved in electron transport chain, including NADH dehydrogenase (ubiquinone) 1 beta subcomplex 9 (*Ndufb9*) (Complex I), NADH dehydrogenase (ubiquinone) 1 beta subcomplex 10 (*Ndufb10*) (Complex I), succinate dehydrogenase complex subunit A, flavoprotein (Fp) (*Sdha*) (Complex II), cytochrome c oxidase subunit VIIa polypeptide I (muscle) (*Cox7*) (Complex IV) related genes was observed between mouse groups (Figure 4.32A). However this does not rule out a role for other subunits of the ETC.

Additionally, expression of the genes involved in electron transport chain complexes of mitochondria was detected in protein level and it was observed that Complex I, II and IV were decreased in all oncogenic *K-ras* expressing groups regardless of the age or tumor incidence (Figure 4.32 B). Taken together this data suggest a decrease in mitochondrial respiratory chain and an increase in glycolytic rates in myeloid cells, similar to that seen in the whole pancreas.

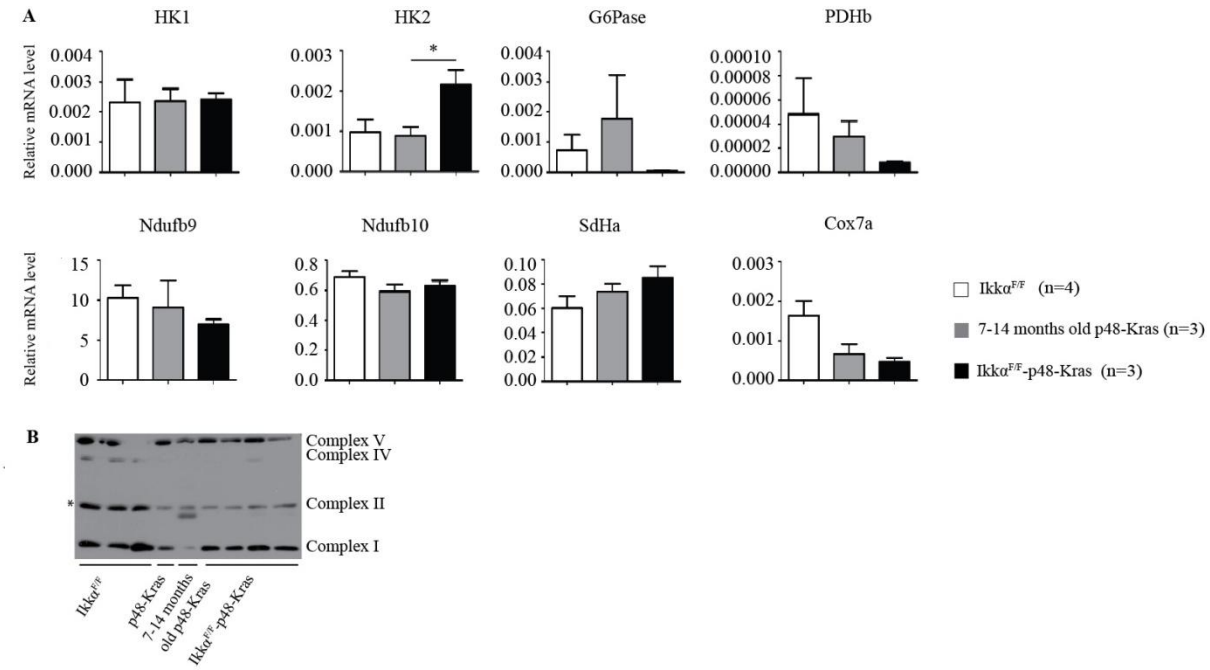

Figure 4.32. CD11b$^+$ cells from the pancreas of Ikkα$^{F/F}$-p48-Kras show differences in the expression of genes involved in energy metabolism. (A) Determination of the relative mRNA levels of the genes involved in glycolysis, gluconeogenesis and oxidative phosphorylation by RT-PCR in the CD11b$^+$ cells from the pancreas of 3-4 weeks old Ikkα$^{F/F}$, p48-Kras, Ikkα$^{F/F}$-p48-Kras and 7-14 months old p48-Kras mice. (B) WB analysis showing the expression of Complex I-V in the CD11b$^+$ cells from the pancreas of 3-4 weeks old Ikkα$^{F/F}$, p48-Kras, Ikkα$^{F/F}$-p48-Kras and 7-14 months old p48-Kras mice. Data are mean values ± SEM, *p ≤ 0.05.

4.16. Fibroblasts isolated from the pancreas of Ikkα$^{F/F}$-p48-Kras animals display altered expression of the genes that are related to glycolysis and PPP

One of the main components of tumor microenvironment is fibroblasts, which are found abundantly in the stroma of especially breast, prostate and pancreatic cancer (Kalluri *et al.*, 2006; Pietras and Ostman, 2010). Fibroblasts have a multifaceted role in tumor progression since they can act as inhibitor or promoter of tumorigenesis depending on the stage of disease. However, the role of fibroblasts in energy metabolism alterations in tumor cells is not known. In order to investigate this possible correlation in our animal model, fibroblasts were isolated from the pancreas of animals and expression of the genes involved in glycolysis and PPP including G6pd2, Taldo1, Rpia, Rbks and HK2 were determined by RT-PCR. Similar to CD11b$^+$ cells, fibroblasts displayed increased expression of glycolysis enzyme HK2 and PPP related enzymes G6pd2 and Taldo1. This finding suggests that similar to CD11b$^+$ cells, fibroblasts might also employ glucose in high ranges for enery production and synthesis of the components that are needed by proliferating cells (Figure 4.33).

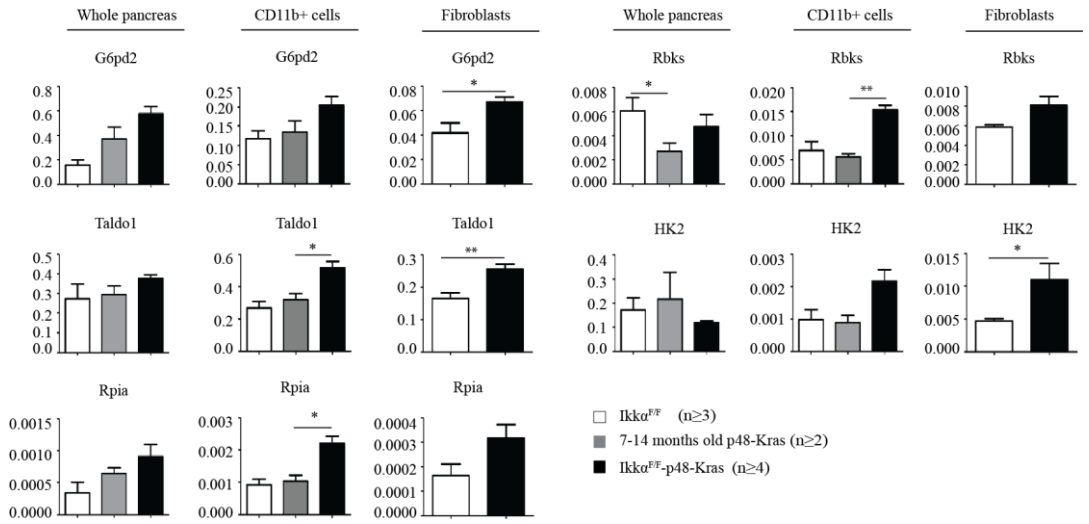

Figure 4.33. Expression of G6pd2, Taldo1 and HK2 is significantly elevated in the fibroblasts isolated from the pancreas of Ikkα$^{F/F}$-p48-Kras mice. RT-PCR was performed to determine the relative mRNA expressions of G6pd2, Taldo1, Rpia, Rbks and HK2 in the whole pancreas and pancreas derived CD11b^{+} cells and fibroblasts of 3-4 weeks old Ikkα$^{F/F}$, Ikkα$^{F/F}$-p48-Kras mice and 7-14 months old p48-Kras mice animals. P value was determined by one-way ANOVA followed by Bonferroni`s multiple comparison test and student`s t-test. *$p \leq 0.05$, **$p \leq 0.01$.

4.17. 2-Deoxy Glucose (2-DG) treatment has a partial effect on cancer progression in Ikkα$^{F/F}$-p48-Kras mice

To provide further proof for a possible role of a switch in bioenergetic pathways towards glycolysis, Ikkα$^{F/F}$-p48-Kras mice and control littermates were treated with a modified glucose molecule 2-Deoxy Glucose (2-DG) in which the 2-hydroxyl group is replaced by a hydrogen molecule. 2-DG can inhibit glucose metabolism and ATP production in cells by inhibiting hexokinase, which is an important enzyme in glycolysis that was also significantly increased in the pancreatic CD11b^{+} cells of Ikkα$^{F/F}$-p48-Kras mice. Since it can block energy production in tumor cells, it is suggested as an anti-cancer drug (Aft *et al*., 2002; Sahra *et al*., 2010).

To that end, 3 mM/gr mouse 2-DG was administered to two weeks old Ikkα$^{F/F}$ and Ikkα$^{F/F}$-p48-Kras mice by intra-peritoneal (IP) injection once every 3 days. Similar to untreated mice, the acinar distortion was 99-100% in the pancreas of 2-DG treated Ikkα$^{F/F}$-p48-Kras mice. Apart from this, 2-DG treatment did not show the same effect on Ikkα$^{F/F}$-p48-Kras mice. Whereas 5 mice still had pancreas cancer after treatment, 3 other mice displayed differences in pancreas histology. One of these mice showed no cancer in the pancreas, whereas 2 others displayed small solid cell nests that might be evaluated as the beginning of cancer (Figure 4.34), suggesting that 2-DG treatment has partial effects on Ikkα$^{F/F}$-p48-Kras mice.

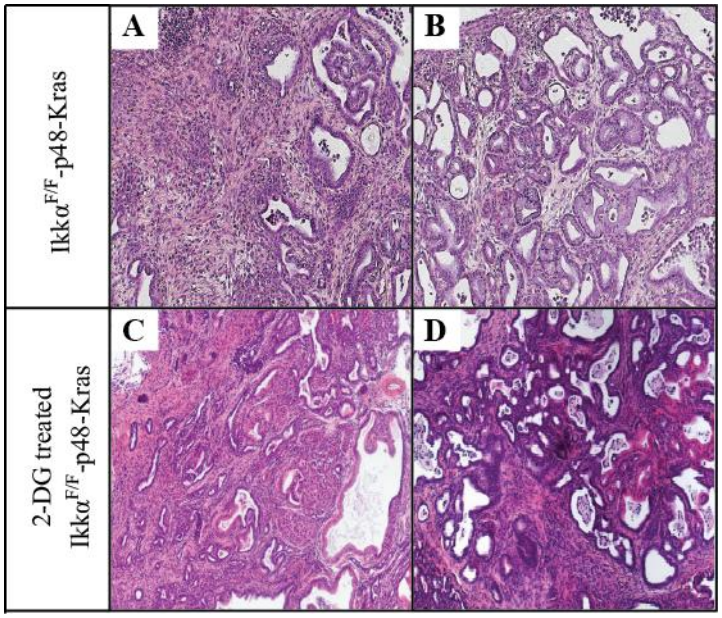

Figure 4.34. Inhibition of glycolysis by 2-DG administration decreases tumor incidence in the pancreas of Ikkα$^{F/F}$-p48-Kras mice. (A, B) H&E-stained pancreas sections of Ikkα$^{F/F}$-p48-Kras mice, and (C, D) 2-DG treated Ikkα$^{F/F}$-p48-Kras mice. 10X magnification.

In order to see if this partial effect of 2-DG treatment on Ikkα$^{F/F}$-p48-Kras mice was related with altered macrophage profiles in 2-DG treated mice, expression of M1 and M2 macrophage markers was checked by RT-PCR for the whole pancreas and pancreas derived CD11b^{+} cells. However, no difference was detected for the expression of M1 and M2 markers between treated and untreated Ikkα$^{F/F}$-p48-Kras in the whole pancreas. Similar to untreated Ikkα$^{F/F}$-p48-Kras mice, increase in the expression of M1 markers and pro-inflammatory cytokines IL1β, IL6, SPP1, IFNGR (Figure 4.35 A) and M2 markers IL13Rα1, IL4Rα, ARG-1, MRC-1, DECTIN-1 (Figure 4.35 B) was observed in 2-DG treated Ikkα$^{F/F}$-p48-Kras in comparison to age-matched 2-DG treated Ikkα$^{F/F}$ animals. Interestingly, expression of M2 markers IL13Rα1, MRC-1, DECTIN-1 was also slightly elevated in 2-DG treated Ikkα$^{F/F}$ animals in comparison to untreated Ikkα$^{F/F}$ suggesting that 2-DG might increase the expression of these genes (Figure 4.35 B). On the other hand, importantly, expression of the pro-inflammatory cytokines IL1β, IL6, TNFα was increased and M2 macrophage markers IL4Rα, ARG-1, MRC-1 was decreased in CD11b^{+} cells from the pancreas of 2-DG treated Ikkα$^{F/F}$-p48-Kras in comparison to age-matched untreated Ikkα$^{F/F}$-p48-Kras mice. This suggests that 2-DG treatment results in a decrease in M2 macrophage infiltration and increased secretion of pro-inflammatory cytokines by CD11b^{+} cells, which might be related with the partial effect of 2-DG treatment on pancreas tumors in treated Ikkα$^{F/F}$-p48-Kras mice (Figure 4.35).

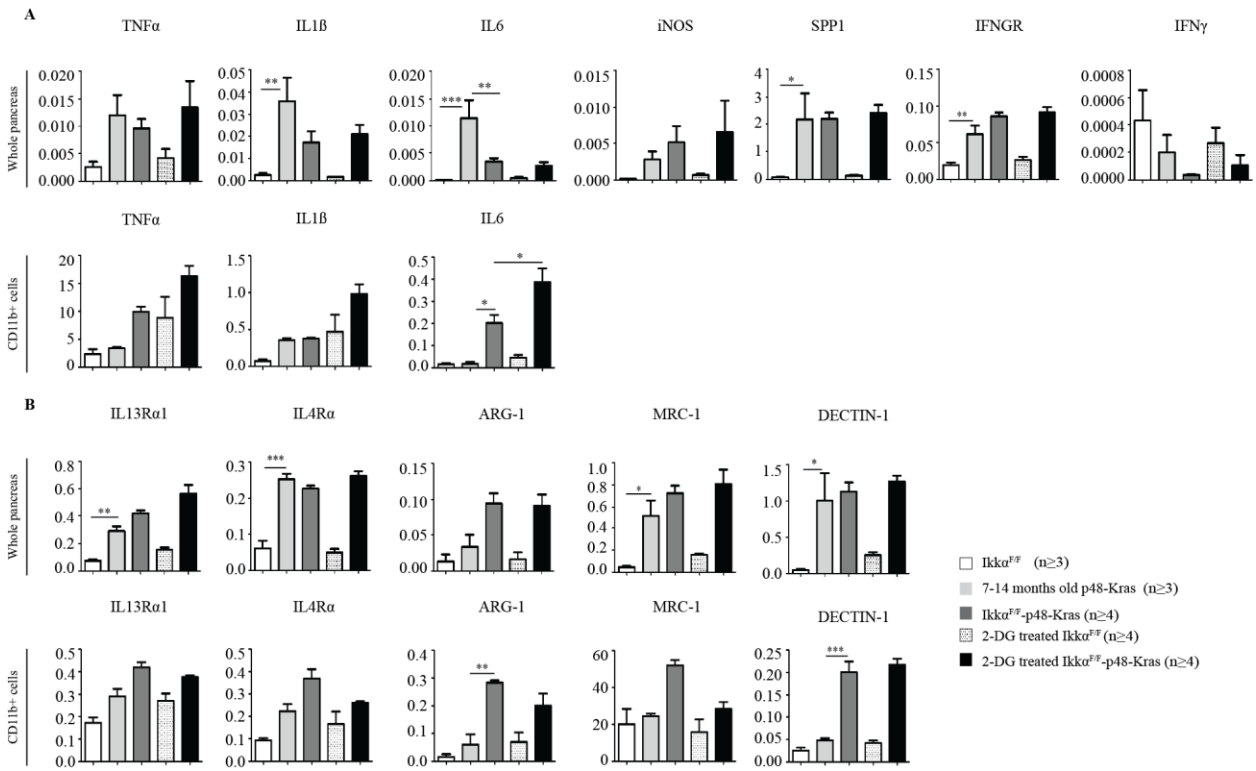

Figure 4.35. 2-DG treatment alters macrophage profiles in the pancreas of Ikkα$^{F/F}$-p48-Kras mice. (A) Relative expression of M1 and (B) M2 macrophage markers were determined by RT-PCR in whole pancreas and CD11b^{+} cells from the pancreas of 3-4 weeks old untreated Ikkα$^{F/F}$ and Ikkα$^{F/F}$-p48-Kras, 2-DG treated Ikkα$^{F/F}$ and Ikkα$^{F/F}$-p48-Kras and 7-14 months old p48-Kras mice. P value was determined by one-way ANOVA followed by Bonferroni`s multiple comparison test. *p ≤ 0.05, **p ≤ 0.01, ***p ≤ 0.001.

Expression of the genes involved in energy metabolism was further determined by RT-PCR using RNA extracted from whole pancreas to see if alterations in energy metabolism might be correlated with decreased tumor incidence in 2-DG treated Ikkα$^{F/F}$-p48-Kras mice. As 2-DG blocks glycolysis, the enzymes that are involved in glycolysis and gluconeogenesis were checked firstly. However, no significant difference was detected between treated and untreated Ikkα$^{F/F}$-p48-Kras mice (Figure 4.36 A). Further, expression of PPP related genes were checked. Whereas the expression of *Tkt*, *Gpi* and *Taldo1* was increased in 2-DG treated Ikkα$^{F/F}$-p48-Kras mice, there was no significant change between 2-DG treated Ikkα$^{F/F}$-p48-Kras and untreated Ikkα$^{F/F}$-p48-Kras animals. Since *Gpi* encodes for the enzyme that converts Glucose 6-phosphate to Fructose 6-phosphate, which is used in glycolysis and directs the glucose into glycolysis rather than PPP (Figure 4.36 B), this suggests that in 2-DG treated animals, glucose might be used less in PPP.

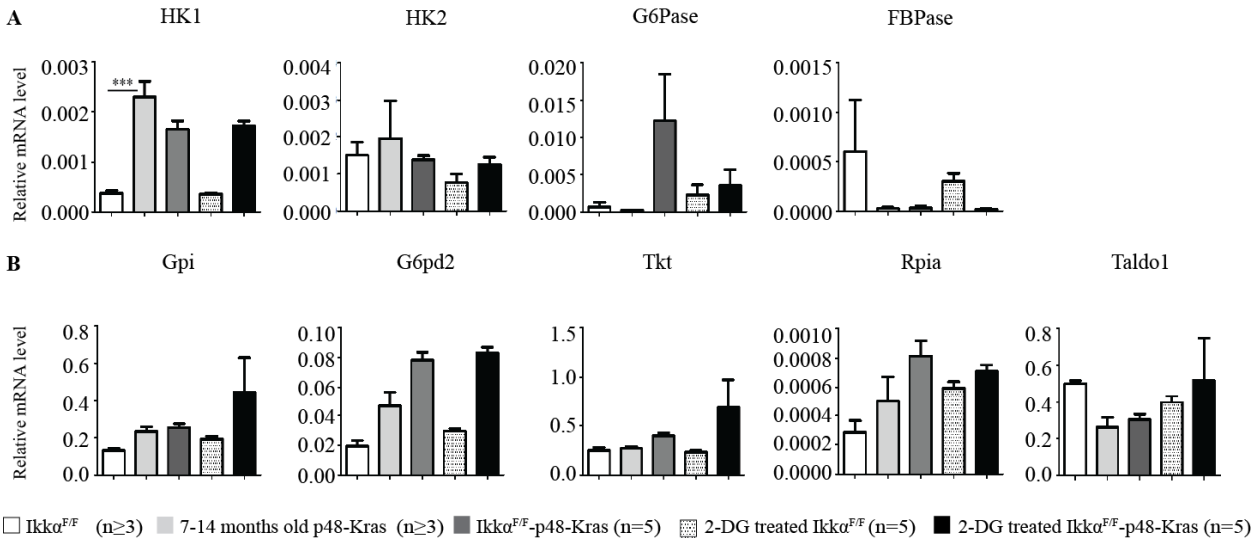

Figure 4.36. 2-DG treatment increases the expression of *Gpi* in Ikkα$^{F/F}$-p48-Kras mice. (A) Relative expression of the genes involved in glycolysis and gluconeogenesis, and (B) in PPP was checked by RT-PCR in whole pancreas of 3-4 weeks old untreated Ikkα$^{F/F}$ and Ikkα$^{F/F}$-p48-Kras, 2-DG treated Ikkα$^{F/F}$ and Ikkα$^{F/F}$-p48-Kras and 7-14 months old untreated p48-Kras mice. P value was determined by one-way ANOVA followed by Bonferroni`s multiple comparison test. ***p ≤ 0.001.

Additionally, expression of the important enzymes of glycolysis and PPP including HK2, Rpia, Taldo1 and Rbks was checked by RT-PCR in CD11b^{+} cells extracted from pancreas. Similar to whole pancreas results, expression of HK2, Rpia and Taldo1 did not change significantly between 2-DG treated and untreated Ikkα$^{F/F}$-p48-Kras mice. However, decreased expression of Rbks was observed in CD11b^{+} cells from 2-DG treated Ikkα$^{F/F}$-p48-Kras mice in comparison to untreated Ikkα$^{F/F}$-p48-Kras animals (Figure 4.37).

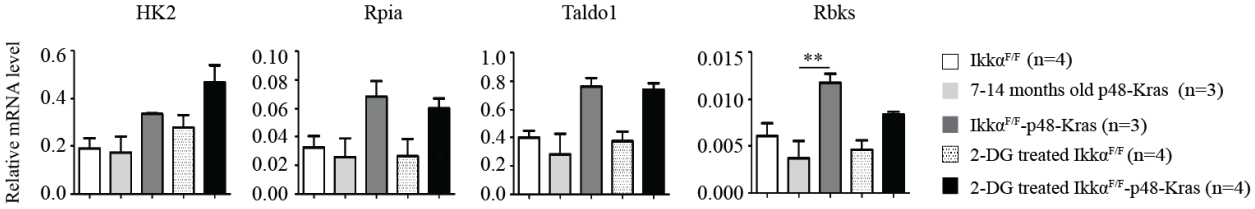

Figure 4.37. 2-DG treatment reduces the expression of *Rbks* in CD11b^{+} cells from Ikkα$^{F/F}$-p48-Kras mice. Relative expression of the genes involved in glycolysis and PPP was checked by RT-PCR in CD11b^{+} cells extracted from the pancreas of 3-4 weeks old untreated Ikkα$^{F/F}$ and Ikkα$^{F/F}$-p48-Kras, 2-DG treated Ikkα$^{F/F}$ and Ikkα$^{F/F}$-p48-Kras and 7-14 months old untreated p48-Kras mice. P value was determined by one-way ANOVA followed by Bonferroni`s multiple comparison test. **p ≤ 0.01.

5. DISCUSSION

Pancreatic ductal adenocarcinoma (PDAC) is a lethal cancer type and every year it causes death of 30000 cancer patients in United States. 5-year survival rate is less than 5% and the median survival is 6 months. Only 15% of PDAC patients can get operation and receive adjuvant chemotherapy, which might increase the 5-year survival up to 20%, exhibiting the importance of early PDAC detection in prolonging the life duration. However, the detection of PDAC is not very easy due to the location of pancreas and the asymptomatic feature of the disease. Moreover, PDAC progress very fast and people are not able to get medication properly due to fibrotic structure of pancreas. Due to these reasons, it is highly important to find out the molecular mechanisms involved in PDAC progression in order to develop better treatment options.

Previous studies established that genetic and epigenetic alterations are crucial in different steps of PDAC development. Importantly, activating mutations of *K-ras* are necessary for the initiation of PanINs, which lead to tumor development. In addition, NF-κB pathway has been shown to be involved in mutant *K-ras* driven PDAC (Ling *et al*., 2012), lung adenocarcinoma and melanoma development (Meylan *et al*., 2009; Yang *et al*., 2010) suggesting that NF-κB family members may play an essential role during PDAC development. However, signaling pathways that connect NF-κB to mutant *K-ras* activity are not known.

In the present study, the function of IkB kinase α (IKKα), which is a member of canonical and non-canonical pathways of NF-κB, in *K-ras* induced PDAC development was elucidated. It is shown that IKKα is involved in PDAC progression by modulating macrophage polarization and energy metabolism *in vivo*.

5.1. Pancreas specific *Ikkα* loss accelerated PDAC development in p48-Kras mice

As a member of NF-κB family, the importance of IKKα in cancer development was investigated and found out that reduced *Ikkα* expression and its mutations resulted in poorly differentiated human squamous cell carcinomas (SCCs) (Liu *et al*, 2006). Furthermore, IKKα ablation has been observed to induce keratinocyte proliferation and papilloma formation, thereby facilitates the development of chemical carcinogen induced skin cancer in mice (Park *et al*.,

2007). Keratinocyte specific IKKα deletion was displayed to induce the EGFR pathway while inactivation of this pathway inhibited epidermal hyperplasia and tumor progression in a SCC mouse model (Liu *et al*., 2008). On the other hand, recently published study about head and neck squamous cell carcinoma cancer (HNSCC) showed that IKKα expression, phosphorylation and nuclear localization was enhanced in human HNSCC patients and in contrast to Liu and collegues' results, together with IKKβ and RelA, IKKα enhanced EGFR and AP1 induced gene expression (Nottingham *et al*., 2013). These contrary results suggest that function of IKKα in cancer progression may vary based on the tissue and organism.

Based on its NF-κB dependent, independent functions in the cells and importance for cancer development, the role of IKKα in mutant *K-ras* induced PDAC development has been elucidated using *Ikkα*$^{F/F}$-*p48*^{Cre}-*K-ras*$^{LSL-G12D/+}$ mouse model (termed Ikkα$^{F/F}$-p48-Kras), which have a Cre knock-in at the *p48* locus. By using p48-Cre system, it was possible to induce mutant *K-ras* expression and deletion of *Ikkα* in pancreatic acinar cells during prenatal period. Ikkα$^{F/F}$-p48 and Ikkα$^{F/F}$-p48-Kras mice were born in normal Mendelian ratio and the pups did not show any phenotypic abnormalities, suggesting that pancreas restricted *Ikkα* deletion is not crucial for the development of mice in prenatal period. It has been published that *Ikkα* ablation caused fetal mortality of mice and defective skin and limb development in fetuses proposing that IKKα is essential during embryonic development in mice (Takeda *et al.,* 1999; Park *et al*., 2011). However, pancreas specific *Ikkα* loss resulted in architectural distortion of pancreas in p48-Kras mice, which was completely transformed and accompanied by inflammatory cells, fibroblasts, pre-neoplastic lesions and tumors at 3-4 weeks of age. It has been published that p48-Kras mice do not show pancreatic tumors before 7,5 months unless they are challenged with chronic inflammation (Guerra *et al*., 2007; Khasawneh *et al*., 2008), suggesting that loss of *Ikkα* accelerates PDAC development.

Importantly, our study pointed out that not only prenatal deletion but also postnatal *Ikkα* deletion induces PanIN development in ElaCre-Kras mice. As previously published, ElaCre-Kras mice occasionally show low-grade PanINs between the age of 6-18 months but no PDAC (Grippo *et al*., 2003; Hruban *et al*., 2006). This data suggests that postnatal *Ikkα* deletion in pancreas is sufficient to accelerate PanIN development in ElaCre-Kras mice.

In contrast to IKKα, pancreas specific inactivation of IKKβ has been found to inhibit NF-κB activation and *K-ras* induced PDAC development *in vivo* (Ling *et al*., 2012). Furthermore, it

has been shown to be required for oncogenic *K-ras* mediated NF-κB activation in lung cancer cells (Basseres *et al.*, 2010) and *H-ras* driven melanoma (Yang *et al*., 2010). Conversely, loss of IKKβ was found to promote inflammation and tumor development in hepatocytes (He *et al*., 2010; Maeda *et al*., 2005), proposing that cancer-related IKKβ functions differ depending on the tissue type. Importantly, since IKKβ is involved in canonical NF-κB pathway and deletion of IKKβ inhibits *K-ras* driven PDAC development (Ling *et al*., 2012), activation of canonical NF-κB pathway seems to enhance pancreatic cancer progression in the presence of mutant *K-ras*. However, IKKβ has also been reported to regulate p100/p52 gene expression and processing (Madge *et al*., 2008; Savinova *et al*., 2009; Scheidereit *et al*., 2012), thus most probably inactivation of IKKβ further affected the activation of non-canonical NF-κB pathway. However, since this possibility was not controlled in the study of Ling and colleagues, the contribution of non-canonical pathway in PDAC in the absence of IKKβ is not known. In the present study, we showed that pancreas specific IKKα accelerated mutant *K-ras* induced PDAC development. Consistently, Liu and colleagues have published that keratinocyte specific IKKα deficiency promotes skin carcinogenesis via activating RAS and EGFR in keratinocytes (Liu *et al*., 2008), suggesting that IKKα deficiency cooperates with mutant *K-ras* to enhance tumorigenesis.

5.1.1. Does IKKα function as a tumor suppressor in the cells?

Our study showed that in the presence of mutant *K-ras* activation, pancreas specific homozygous deletion of *Ikkα* resulted in accelerated PDAC development *in vivo*, whereas heterozygous *Ikkα* deletion caused PanIN-1 and abnormal ductal structure formation in the pancreas of mice, which was similar to age matched p48-Kras mice. This observation suggests that allele number of *Ikkα* is important for the suppression of mutant *K-ras* induced tumor development in pancreas. Consistently, IKKα was previously proposed to behave as tumor suppressor in malignant human squamous cell carcinoma (SCC) since it was detected to be down-regulated in 78% of skin SCCs and in 82% of SCCs derived from several stratified epithelia including oral cavity, larynx, lung and esophagus. It was proposed to shuttle into nucleus upon TGF-β stimulation and thereby starts an anti-proliferative program in keratinocytes (Marinari *et al*., 2008). Furthermore, decreased expression of IKKα due to promoter hypermethylation and genetic instability was observed in human oral carcinomas. Furthermore, nuclear IKKα was proposed to inhibit cancer development via affecting carcinoma cell differentiation in a canonical NF-κB pathway independent manner (Maeda *et al*., 2007). Similarly, Liu and colleagues detected mutations and decreased expression of IKKα in human

skin squamous cell carcinoma and showed that over-expression of *Ikkα* in null mouse inhibited chemically induced tumor development (Liu *et al*., 2006). These findings propose that IKKα might behave as a tumor suppressor gene in the cells. On the other hand, another study using $Ikk\alpha^{AA}$/TRAMP mouse model, which had SV40T antigen expression in the prostate epithelium and IKKα with no kinase activity, showed that kinase activity of IKKα was essential for metastasis but not for primary tumor development while it regulates the expression of metastasis inhibitor maspin gene (Lu *et al*., 2009). This finding suggests that although IKKα might suppress tumor development in several tissues, yet it is involved in metastasis in prostate cancer.

5.1.2. IKKα regulates cell proliferation in p48-Kras mice

Our results displayed increased rate of cell proliferation in the pancreas of $Ikk\alpha^{F/F}$-p48-Kras mice, which seems similar to 7-14 months old p48-Kras mice having advanced pancreas distortion together with PanINs and tumors. Furthermore, pancreas specific IKKα loss enhanced Cyclin D1 expression in p48-Kras mice bearing tumor, proposing that IKKα regulates Cyclin D1 expression. This notion is supported by Kwak and colleagues who have found out that Cyclin D1 expression is higher in $Ikk\alpha^{-/-}$ mouse embryonic fibroblast (MEF) cells in comparison to wild type MEFs (Kwak *et al*., 2011). Further it has already been established that IKKα can promote the degradation of CyclinD1 via directly phosphorylating it (Kwak *et al*., 2005), or IKKα can activate cyclin D1 expression by phosphorylating and stabilizing the transcription factor β-catenin (Albanese *et al*., 2003). Direct phosphorylation effect IKKα on Cyclin D1 was not checked in this study, however higher expression levels of β-catenin was detected in $Ikk\alpha^{F/F}$-p48-Kras mice in comparison to age-matched p48-Kras mice.

5.2. Expression of canonical and non-canonical NF-κB pathway components are increased in $Ikk\alpha^{F/F}$-p48-Kras mice

The present study displays increased canonical and non-canonical NF-κB pathway in the pancreas of $Ikk\alpha^{F/F}$-p48-Kras mice. This finding was surprising since IKKα was deleted in pancreatic cells. However, based on the increased infiltration of IKKα intact fibroblasts and immune cells, it is possible that these cells might be responsible for the enhanced levels of these proteins. Consistent to our findings, RelA and p50 was found to be constitutively activated in nearly 70% of pancreatic cancer cells (Fujioka *et al*., 2003; Wang *et al*., 1999) and deletion of RelA resulted in less lung tumors in the presence of oncogenic *K-ras* activation (Basseres *et al*.,

2010). Furthermore, our data showed higher RelB and cRel levels in Ikk$\alpha^{F/F}$-p48-Kras mice in comparison to tumor bearing p48-Kras mice.

Interestingly, in our study, decreased IKKα level was also observed in human PDAC samples. Consistently, Liu and colleagues previously detected lower IKKα expression and mutations in human differentiated squamous cell carcinoma (SCC) patients, proposing that similar to murine PDAC model, IKKα loss might correlate with PDAC development in humans (Liu *et al*., 2006; Park *et al*., 2011). Furthermore, similar to mouse model, elevated protein levels of RelA, cRel, p100, p50/p105 was detected. Previously, nuclear co-localization of p52 and RelB was displayed in human PDAC cell lines showing the activation of this pathway in human PDAC cell lines (Wharry *et al*., 2009). In our study, cellular localization of these proteins was not controlled. However, decreased RelB and no increase in p52 protein levels were observed in CP and PDAC human samples.

5.2.1. RelB deficiency did not affect tumor progression in Ikk$\alpha^{F/F}$-p48-Kras mice

Our study indicated increased expression of non-canonical NF-κB pathway component RelB in the pancreas of Ikk$\alpha^{F/F}$-p48-Kras mice. Similar to what we observed, increased levels of nuclear RelB and p52 were previously shown in human tumors including oral cancers, prostate cancer, and in tumor cells lines including pancreas and prostate cancer (Chandler *et al*., 2004; Dejardin *et al*., 1995; Dejardin *et al*., 1999; Lessard *et al*., 2007; Mishra *et al*., 2006; Xu *et al*., 2008). Furthermore, inhibition of RelB and p52 in human prostate cancer cells resulted in increased sensitivity to radiation (Xu *et al*., 2008) suggesting that abnormal activation of non-canonical NF-κB pathway induce tumorigenesis in humans. However, contrary to this hypothesis, pancreas specific deletion of RelB did not decelerate fast PDAC development in Ikk$\alpha^{F/F}$-p48-Kras mouse model. Furthermore, RelB deletion resulted in more inflammation with increased macrophage and less dendritic cell infiltration, together with cell rich stroma in the pancreas of Ikk$\alpha^{F/F}$-p48-Kras mice, suggesting that ablation of non-canonical NF-κB pathway accelerates tumor development via modulating immune responses in murine PDAC model.

5.3. IKKα deletion induces inflammation and desmoplasia in p48-Kras mice

Our study displayed strong fibrotic response and increased infiltration of inflammatory cells including macrophages, neutrophils and dendritic cells in the pancreas of Ikk$\alpha^{F/F}$-p48-Kras

mice. This data confirms a previous study showing an increase in macrophages ($F4/80^+$ cells) in IKKα null keratinocytes in comparison to wild type keratinocytes (Liu *et al*., 2008), suggesting that IKKα loss enhances infiltration of immune cells. Furthermore, expression of M2 polarized macrophage markers including IL4Rα, ARG-1, MRC-1 and DECTIN-1 was elevated in $CD11b^+$ positive cells isolated from the pancreas of $Ikk\alpha^{F/F}$-p48-Kras mice, in comparison to tumor bearing p48-Kras animals proposing that IKKα loss induces macrophage polarization into M2 phenotype. On the other hand, since expression of pro-inflammatory cytokines, which are secreted by M1 polarized macrophages, including IL1β, IL6 and TNFα was still high, it was concluded that M1 polarized macrophages still exist in the pancreas of $Ikk\alpha^{F/F}$-p48-Kras mice. This observation was supported by other studies suggesting that M1 and M2 polarized macrophages may co-exist in tumors of cancer mouse models, however tumor development is often related with abundant amounts of M2 polarized macrophages (Squadrito and De Palma, 2011; Qian and Pollard, 2010). M2 polarized macrophages are involved in the resolution of inflammation and wound healing. Furthermore, they show similar characteristics to tumor associated macrophages, which are suggested to be related with tumor progression, especially in breast cancer (Mantovani, 2008; Pollard, 2004). Additionally, it is not surprising that IKKα deletion regulated macrophage polarization in $Ikk\alpha^{F/F}$-p48-Kras animals since NF-κB family has been already published to modulate macrophage polarization (Hagemann *et al*., 2008; Biswas *et al*., 2006; Saccani *et al*., 2006; Porta *et al*., 2009).

Importantly, increase in M2 macrophage markers including IL4Rα, IL13Rα1, MRC-1 was observed, whereas pro-inflammatory cytokine IL1β and IL6 levels showed a tendency to increase in human PDAC samples. This data propose that similar to our murine model, M2 polarization may be a common feature of PDAC progression in human although pro-inflammatory cytokine secreting M1 macrophages still exist in the pancreas.

In the present study, contribution of another tumor microenvironment components, fibroblasts, was also checked and pancreas derived fibroblasts were observed to display a similar phenotype to pancreas derived $CD11b^+$ cells, suggesting that fibroblasts might also function in the acceleration of mutant *K-ras* induced PDAC development upon IKKα deletion. Supporting this hypothesis, Erez *et al.* previously proposed that NF-κB can induce fibroblasts to enhance increase pro-inflammatory gene expression, macrophage recruitment and eventually tumor growth (Erez *et al*., 2010). However, in order to define their roles in our mouse model, further analyzes are necessary.

It is already known that cytokines and chemokines secreted by tumor cells or the cells forming tumor microenvironment enhance tumor growth, cancer cell survival, and modulate cell differentiation (Hanahan and Weinberg, 2011; Cavallo *et al*., 2011). Although M2 polarized macrophages are known to support tumor growth, there are contradictory results in the literature about the tumor-growth promoting effects of IL4 and IL13 (OuYang *et al*., 2008; Toi *et al*., 1992; Uchiyama *et al*., 1996; Kanai *et al*., 2000; Todaro *et al*., 2008; Formentini *et al*., 2009). However, due to fact that M2 polarized macrophage numbers were increased in Ikkα$^{F/F}$-p48-Kras mice, IL4, IL13 and IL13Rα1 expressing cells were investigated and myeloid cells, together with fibroblasts were determined as the major sources of IL4, IL13 and IL13Rα1. Since fibroblasts and immune cells are the major components of tumor microenvironment, this data suggests that tumor microenvironment might have importance in tumor acceleration in Ikkα$^{F/F}$-p48-Kras animals.

5.3.1. Stat6 deletion did not inhibit accelerated tumor progression in Ikkα$^{F/F}$-p48-Kras mice

IL4 and IL13 induced Stat6 signaling has been found to be essential for normal mammary development *in vivo* (Khaled *et al*., 2007). It is already known that abnormal regulation and/or activation of developmental pathways can lead to epithelial tumor cell formation. Consistently, IL4 and IL13 have been established to induce fibrosarcoma tumor formation *in vivo* (Li *et al*., 2008), and PDAC development *in vitro* (Formentini *et al*., 2009), respectively. Furthermore, although contradictory results exist (Ko *et al*., 2008), over-expression of IL4R and IL13R has been published to be related with colitis associated cancer, PDAC development and lung cancer (Koller *et al*., 2010; Formentini *et al*., 2009; Kawakami *et al*., 2002). However, our data pointed out that Stat6 signaling is not crucial in acceleration of PDAC development in Ikkα$^{F/F}$-p48-Kras mice, since pancreas specific *Stat6* deletion did not inhibit tumor development in our mouse model. This data suggests that either IL4Rα signaling does not take part in the acceleration of PDAC development in Ikkα$^{F/F}$-p48-Kras mice, or other signaling proteins, which are phosphorylated upon IL4R stimulation, including Jak1, IRS2, and Fes (Zamarano and Keegan, 1998; Nelms *et al*., 1999; Izuhara *et al*., 1994) might have importance in IKKα loss induced PDAC development in p48-Kras mice.

5.4. Pancreas specific *Ikkα* loss causes alterations in energy metabolism in p48-Kras mice

In the present study, we aimed to figure out how energy metabolism pathways were altered in tumor cells and affected tumorigenesis. Moreover, we would like to reply the question whether metabolic pathways themselves can change immune system modulation, for instance macrophage polarization and their effector functions.

Glycolysis has been suggested to be the main energy production pathway in cancer cells since Otto Warburg observed that tumor cells prefer aerobic glycolysis to produce energy. He suggested that due to defective mitochondria activity, cancer cells use glycolysis although it produces less energy than oxidative phosphorylation (Warburg, 1956). Following studies revealed that not only cancer cells but also proliferating lymphocytes prefer glycolysis for energy production. This shows that aerobic glycolysis is not special for tumor cells and even there is no impairment in the oxidative phosphorylation, it can be preferred by other cells to produce energy (Brand, 1985; Hedeskov, 1968; Roos and Loos, 1973; Wang *et al*., 1976). Moreover, although ATP yield of glycolysis is less than oxidative phosphorylation, high glycolytic influx can result in abundant amount of ATP production in the cells that might be more than produced by oxidative phosphorylation (Guppy *et al*., 1993; Warburg *et al*., 1956b). Furthermore, following studies displayed that tumor cells do not necessarily have to show abnormal oxidative metabolism (Moreno-Sanchez *et al*., 2007), but still decreased mitochondrial metabolism and respiratory rate was proposed to be important for tumor cell growth and proliferation (Denko, 2008). Consistently, decreased respiration rate of mitochondria was shown in Ikkα$^{F/F}$-p48-Kras mice in comparison to p48-Kras mice. This decrease in mitochondrial respiration can be due to the lower mitochondria numbers in the cells and/or impairment in the complexes that are involved in oxidative respiration in mitochondria. Supporting this notion, tumor bearing Ikkα$^{F/F}$-p48-Kras and p48-Kras mice displayed decreased mitochondria number in comparison to 3-4 weeks old Ikkα$^{F/F}$ and p48-Kras animals indicating that number of mitochondria is reduced in tumor bearing mice. On the other hand, expression of oxidative phosphorylation related genes were also altered in these mouse groups. Although it has been already published that catalytic subunit of the mitochondrial ATP synthase (β-F1-ATPase) was down-regulated in most human carcinomas (Gogvadze *et al*., 2008), in our study, expression of ATP synthase mitochondrial F1 complex β subunit was detected as up-regulated in tumor bearing animal groups. Moreover, *Ikkα* knock-down resulted in increase of Complex V in protein level *in vitro*, suggesting that gene

expressions might differ depending on different organisms and pancreas specific IKKα deletion causes alterations in the expression of oxidative phosphorylation related genes. In addition, mutations of the genes involved in mitochondrial energy pathways also might lead to abnormal mitochondria function. For instance, mutations of the enzymes of tricarboxylic acid (TCA) cycle including fumarate hydratase (FH) and succinate dehydrogenase (SDH) was detected in tumor cells, which had abnormal mitochondria activation (Gottlieb and Tomlinson, 2005).

Since mitochondrial respiration rate is decreased, tumor cells might prefer glycolysis as the main energy metabolism in our animal model. Supporting this hypothesis, increased expression of glycolytic enzymes, HK1 and HK2, was determined in $Ikk\alpha^{F/F}$-p48-Kras mice. Since *K-ras* oncogene has been shown to promote glycolysis (Racker *et al*., 1985), this data concluded that IKKα deficiency might strengthen the effect of *K-ras* on glycolysis in pancreatic cancer. Similarly, Ying and colleagues published that $Kras^{G12D}$ induced pancreatic tumors displayed increased glucose uptake and glycolytic intermediate production (Ying *et al*., 2012). Moreover, PDAC cells were shown to display increased aerobic glycolysis (Zhou *et al*., 2011). On the other hand, metabolic switch in favor of glycolysis may vary depending on the cell type or oncogenic RAS isoform since H-Ras transformed mesenchymal stem cells did not show elevated glycolysis for ATP production during transformation (Funes *et al*., 2007). Moreover, $Kras^{G12D}$ extinction was shown to result in decreased levels of glycolytic intermediates including Glucose 6-phosphate (G6P), Fructose 6-phosphate (F6P) and Fructose 1,6-bisphosphate (F1,6BP) (Ying *et al*., 2012). Our data shows that the expression of the enzymes including phosphoglucomutase (PGM) and glucose phosphate isomerase 1 (Gpi1), which are responsible from the production of G6P and F6P respectively, was increased in $Ikk\alpha^{F/F}$-p48-Kras and 7-14 months old p48-Kras mice, confirming that presence of oncogenic *K-ras* induces the expression of glycolytic enzymes. Additionally expression of phosphofructokinase (PFK) platelet and liver, which catalyzes the production of F1,6BP was higher in $Ikk\alpha^{F/F}$-p48-Kras in comparison to tumor bearing p48-Kras mice proposing that IKKα absence induces PFK expression.

Metabolic switch in favor of glycolysis in cancer cells is not important just for energy production. Glycolysis further serves as one of the source of glycolytic intermediates for biosynthetic pathways. It is important because proliferating cells need metabolic intermediates to synthesize other components including nucleotides or lipids (Vander Heiden *et al*., 2009; DeBerardinis *et al.,* 2008). However, glycolysis is not the only pathway which provides metabolic intermediates. Instead, another mitochondrial energetic pathway, TCA cycle, is also

essential since cells use precursors derived from TCA cycle intermediates to synthesize lipids, proteins and amino acids. In proliferating cells, TCA cycle provides abundant amount of carbon molecules to biosynthetic pathways leading to a continous efflux of intermediates, which is called cataplerosis. One of the major yields of cataplerosis is lipid synthesis and the main lipogenic substrate in this pathway is glucose. One of the end products of glucose, mitochondrial citrate, is transferred to the cytosol and is converted by ATP citrate lyase to oxaloacetate (OAA) and lipogenic precursor acetyl-CoA (DeBerardinis *et al*., 2008). The export of citrate to the cytosol for lipid synthesis causes a 'truncated' cycle because the level of mitochondrial citrate oxidization is decreased (Hatzivassiliou *et al*., 2005; Parlo and Coleman, 1984). In tumor cells and proliferating hematopoietic cells, activity of lipogenic enzymes ATP citrate lyase and fatty acid synthase has been shown to be enhanced and necessary for proliferation (Bauer *et al*., 2004; Hatzivassiliou *et al*., 2005; Kuhajda *et al.,* 1994; Pizer *et al*., 1996). Consistently, expression of ATP citrate lyase was up-regulated in Ikk$\alpha^{F/F}$-p48-Kras mice suggesting that TCA cycle might be truncated in this tumor bearing mouse model.

On the other hand, in order to reverse the effect of truncated TCA cycle, cells must find metabolic intermediates to compensate lost oxaloacetate (OAA). The metabolic influx which is required to maintain TCA cycle function is called anaplerosis and one of the main player of anaplerosis is pyruvate carboxylase (PC) that produces OAA directly from pyruvate (DeBerardinis *et al*., 2008). Interestingly, expression of PC enzyme was decreased in tumor bearing p48-Kras and Ikk$\alpha^{F/F}$-p48-Kras mice in comparison to other animal groups. PC activity was previously shown to be increased by mitogens in proliferating lymphocytes (Curi *et al*., 1988). On the other hand, estrogen stimulation promoted proliferation of MCF-7 breast carcinoma cells, whereas PC activity was inhibited (Forbes *et al*., 2006). Comparably, lower PC expression was detected in hepatomas in comparison to normal liver (Chang and Morris, 1973; Hammond and Balinsky, 1978), suggesting that necessity of PC activity in anaplerotic flux alters depending on the tissue types. On the other side, L-malate is oxidized to OAA by malate dehydrogenase in TCA cycle and the expression of mitochondrial malate dehydrogenase 1 and 2 was increased in Ikk$\alpha^{F/F}$-p48-Kras mice. In addition to OOA, another TCA intermediate that can be used for biosynthesis of other components such as proteins and nucleic acids is α-ketoglutarate (α-KG). In TCA cycle, isocitrate is converted to α-KG by isocitrate dehyrogenase (IDH) enzyme. Our data showed increased expression of all 3 subunits of Ikk$\alpha^{F/F}$-p48-Kras mice suggesting that IKKα absence enhances the expression of this enzyme.

Pentose Phosphate Pathway (PPP) is an important biosynthesis pathway consisting of oxidative and non-oxidative branches in which glucose is used as substrate. In PPP, NADPH and ribose 5-phosphate is formed for the synthesis of fatty acids and DNA/RNA for nucleotides, respectively. Thus PPP is proposed to have importance in tumorigenesis (Boros *et al*., 1998; DeBerardinis *et al*., 2008). It has been shown that oncogenically activated *K-ras* induces the oxidative arm of the PPP to enhance cell proliferation (Vizan *et al*., 2005; Weinberg *et al*., 2010). Contrarily, Ying and colleagues found no correlation between *K-ras* oncogene and the oxidative arm of PPP, but showed that in the presence of oncogenic *K-ras,* glycolytic flux was the main source for the non-oxidative PPP for ribose biogenesis and tumorigenic activity was inhibited by the blockage of the non-oxidative PPP (Ying *et al*., 2012). Additionally, non-oxidative PPP branch was displayed to be up-regulated in tumor cells including pancreatic cancer (Boros *et al*., 2005; Tong *et al*., 2009) showing the importance of non-oxidative branch of PPP for pancreatic cancer. Supporting these findings, enhanced activity of the catalyzer enzymes of the non-oxidative branch of the PPP, transketolase (Tkt) and transaldolase 1 (Taldo1) was detected in tumor cells (Heinrich *et al*., 1976; Coy *et al*., 2005). Consistently, expression of these enzymes was also increased in Ikk$\alpha^{F/F}$-p48-Kras mice.

Non-oxidative branch of PPP consists of reversible reactions meaning that direction of the reactions is regulated by the relative level of metabolic substrates and products (Schenk *et al*., 1998). Thus, tumor cells have to keep high levels of fructose 6-phosphate (F6P) and/or glyceraldehyde 3-phosphate (GAP) to use glycolysis metabolites in the non-oxidative branch of PPP. For this reason, Fructose 1,6-bisphosphate (F1,6BP) an essential control point in glycolysis and most tumors have already been shown to generate abundant amounts of F1,6BP, which is converted to GAP by aldolase (Mazurek *et al*., 2002). Consistently, expression of aldolase A, B and C was found to be up-regulated in Ikk$\alpha^{F/F}$-p48-Kras mice. As mentioned before, F6P is converted to F1,6BP by PFK. Thus, activity of this enzyme is important for tumorigenesis and increased PFK-1 activity has already been shown in primary tumor tissues and cancer cell lines (Hennipman *et al*., 1987; Sanchez-Martinez *et al*., 1997). Similarly, expression of PFK1 subunits, liver and platelet, was also enhanced in Ikk$\alpha^{F/F}$-p48-Kras mice in comparison to tumor bearing p48-Kras mice, suggesting that pancreas specific IKKα absence induces the expression of genes related to non-oxidative arm of PPP in the pancreas of p48-Kras mice.

Another glycolysis related enzyme that also directs the carbon atoms from glycolysis to PPP is pyruvate kinase M2 (PK-M2). In mammalian organisms, it has 4 isoenzymes of (type L,

R, M1 and M2). Among them, PK-M2 expression has been shown to increase in tumor cells (Mazurek *et al*., 2002). Consistently, increased expression of pyruvate kinase muscle was detected in the pancreas of Ikk$\alpha^{F/F}$-p48-Kras mice showing that IKKα deletion induces glycolytic enzymes.

5.4.1. Macrophage Polarization and Energy Metabolism

In the literature, there is not abundant data about the connection between energy metabolism and immune system modulation. It is still not completely understood whether immune system is regulated by altered metabolic pathways or immune system components employ different metabolic pathways under certain conditions. Previously macrophages were shown to produce abundant amount of lactate and activate PPP after phagocytosis, suggesting that glycolysis and PPP might be important for their activation (Drapier and Hibbs, 1988; Schnyder and Baggiolini, 1978). However, recent studies implied that metabolic pathways are not only crucial for the activation of immune cells but also for their differentiation and it has been shown that metabolic-reconfiguration regulates the differentiation of Th17 cells and activation of dendritic cells (Beurel *et al*., 2011; Krawczyk *et al*., 2010; Shi *et al*., 2011). Furthermore, IFNγ or TLR ligands activated M1 macrophages were shown to prefer anaerobic glycolytic pathway (Rodriguez-Prados *et al*., 2010), whereas IL4 activated M2 macrophages use oxidative glucose metabolism (fatty acid oxidation) for energy production (Odegaard and Chawla, 2011). Recently, Haschemi and colleagues showed that down-regulation of carbohydrate kinase-like (CARKL) protein, which is a kinase and catalyzes the production of a PPP intermediate sedoheptulose-7-phosphate (S7P), resulted in decreased M2 macrophage polarization and induced M1 metabolic rearrangement showing that glucose intermediates are involved in the regulation of macrophage metabolism and macrophage polarization (Haschemi *et al*., 2012). However, in our study, increased numbers of $CD11b^+$ cells in the pancreas of Ikk$\alpha^{F/F}$-p48-Kras mice were determined. Interestingly, expression of the enzymes involved in non-oxidative branch of PPP, Rpia, Taldo1 and Tkt, and oxidative branch of PPP, Gpi1 and G6pd2, was significantly elevated in pancreas derived $CD11b^+$ cells in Ikk$\alpha^{F/F}$-p48-Kras mice although a significant increase was only detected for G6pd2 and Tkt in whole pancreas of these mice. This finding suggests that PPP pathway might be activated only in $CD11b^+$ cells, which were infiltrated to pancreas.

5.4.2. 2-Deoxy Glucose (2-DG) application has partial effects on PDAC development in Ikkα$^{F/F}$-p48-Kras mice

In the present study, 2-DG was applied to Ikkα$^{F/F}$-p48-Kras mice to determine if the blockage of glycolysis has any effects on PDAC development in this mouse model. 2-DG is a modified glucose molecule, which is used to block one of the main glycolytic enzyme hexokinase and thereby blocks glycolysis in the cells. Thus, it is proposed as an anti-cancer drug (Aft *et al*., 2012; Sahra *et al*., 2010). Indeed 2-DG application displayed a partial effect on PDAC development in Ikkα$^{F/F}$-p48-Kras mice. Whereas five treated Ikkα$^{F/F}$-p48-Kras mice displayed advanced PDAC, one mouse did not have cancer and two mice displayed small solid cell nests, which might be evaluated as the beginning of cancer. This suggests that although 2-DG treatment does not block the development of PDAC in all Ikkα$^{F/F}$-p48-Kras mice, it is effective for some animals and decreases the tumor incidence. However, the reason why 2-DG has a partial effect on animals is not known.

Detailed analysis in our study showed no difference in the expression of glycolytic enzymes in the whole pancreas of 2-DG treated and untreated Ikkα$^{F/F}$-p48-Kras mice. However, CD11b^{+} cells isolated from the pancreas of 2-DG treated Ikkα$^{F/F}$-p48-Kras mice displayed a tendency to be higher for HK2 expression in comparison to untreated Ikkα$^{F/F}$-p48-Kras animals. Since previously IFNγ or TLR ligand induced M1 macrophages were shown to use anaerobic glycolytic pathway (Rodriguez-Prados *et al*., 2010), this data suggested that 2-DG application might induce the infiltration of M1 polarized macrophages. Supporting this hypothesis, expression of pro-inflammatory cytokines TNFα and IL1β was increased, whereas expression of M2 macrophage markers IL4Rα, ARG-1 and MRC-1 were decreased in CD11b^{+} cells derived from the pancreas of 2-DG treated Ikkα$^{F/F}$-p48-Kras in comparison to untreated Ikkα$^{F/F}$-p48-Kras mice. This finding is particularly important since M2 macrophages are known to show tumor promoting effects. Moreover, pro-inflammatory cytokines TNFα and IL1β are mainly secreted by M1 macrophages, which have pro-inflammatory, anti-tumor effects. Thus, decrease in M2 macrophage infiltration and increase in M1 macrophage infiltration, together with the elevated secretion of pro-inflammatory cytokines in the pancreas may play an essential role for the decreased incidence of PDAC in 2-DG treated Ikkα$^{F/F}$-p48-Kras animals. However, it is not completely illuminated if metabolic switch firstly happens in Ikkα$^{F/F}$-p48-Kras animals upon 2-DG treatment and afterwards the polarization of macrophages switches from M2 to M1 that might lead to decreased tumor incidence in the pancreas or tumor progression is already slowed

down via 2-DG treatment in several animals and thus other metabolic pathways becomes activated for energy production and also infiltration of M2 macrophages decreases in 2-DG treated animals. Most probably, altered tumor incidence is a result of combinatory effect of glycolysis inhibition and altered macrophage profiles in the pancreas. However, it is very crucial to increase the efficiency of 2-DG treatment, find out the sequential events during this process and differentiate the contribution of altered energy metabolism and tumor microenvironment in the development of pancreatic cancer in mice since the answer of these questions might open a door to find out an effective treatment for PDAC patients in the future.

6. CONCLUSION

Constitutively activated *K-ras* and Nuclear Factor kappa B (NF-κB) family members have already been shown to co-operate during the development of several types of cancers. Importantly, in the present study, we showed that pancreas specific loss of IκB kinase α (IKKα) accelerates the development of pancreatic ductal adenocarcinoma (PDAC) in the presence of constitutively active mutant *K-ras* oncogene. Whereas p48-Kras (*p48*^{Cre}-*K-ras*$^{LSL-G12D/+}$) mice display high heterogeneity in pancreas histology and do not have pancreatic tumors before 7,5 months, unless they are treated with chemical agents to induce chronic pancreatitis, Ikkα$^{F/F}$-p48-Kras (*Ikkα*$^{F/F}$-*p48*^{Cre}-*K-ras*$^{LSL-G12D/+}$) mice have completely transformed pancreas and PDAC with 100 % incidence at the age of 3-4 weeks. In the pancreas of Ikkα$^{F/F}$-p48-Kras mice, we determined higher proliferation rates and increased expression of Cyclin D1 during PDAC formation.

Furthermore, with the advantage of using Elastase-Cre system, we were able to verify that not only embryonic deletion of IKKα but also post-natal IKKα deletion in pancreas led to the acceleration of pancreatic intraepithelial neoplasm (PanIN) formation in Ikkα$^{F/F}$-p48-Kras mice.

In Ikkα$^{F/F}$-p48-Kras mouse model, although IKKα is deleted, both canonical and non-canonical NF-κB was shown to be activated. In order to emphasize the role of non-canonical NF-κB pathway, RelB$^{F/F}$-Ikkα$^{F/F}$-p48-Kras mice generated. However, *Relb* deletion in the pancreas of Ikkα$^{F/F}$-p48-Kras animals did not improve the pancreas histology of these animals. Moreover, it resulted in completely altered pancreas structure and exacerbated inflammatory response. Macrophage numbers were increased in these mice in comparison to Ikkα$^{F/F}$-p48-Kras, whereas dendritic cell numbers were decreased, proposing that RELB deficiency could accelerate cancer progression in Ikkα$^{F/F}$-p48-Kras mice, possibly through an increase in macrophages and a decrease in dendritic cells that present tumor antigens to adaptive immune cells

We showed that accelerated PDAC development in Ikkα$^{F/F}$-p48-Kras mice is partly related with increased infiltration of immune cells and fibroblasts, which points out the importance of tumor microenvironment during PDAC in this mouse model. We found out that pancreas specific IKKα deletion resulted in increased infiltration of M2 macrophages, which are

expressing ARG-1, IL4Rα, MRC-1 and Dectin-1. On the other hand, elevated expression of pro-inflammatory cytokines including IL1β, IL6, TNFα and decreased expression of IFNγ and IL12 by $CD11b^{+}$ cells in the pancreas of $Ikk\alpha^{F/F}$-p48-Kras mice was detected. These findings show that whereas M2 polarized macrophages infiltrate in the pancreas abundantly, there is still the infiltration of M1 polarized macrophages that continue to secrete pro-inflammatory cytokines. Furthermore, the percentage of IL13Rα1 expressing and IL4, IL13 secreting myeloid cells and fibroblasts were increased in the pancreas of $Ikk\alpha^{F/F}$-p48-Kras mice, suggesting a critical role for M2 macrophage related cytokines IL4, IL13 and its receptor, IL13Rα1, during enhanced cancer progression. In order to see whether IL4/IL13 signaling is the main player in the acceleration of PDAC, $Ikk\alpha^{F/F}$-p48-Kras mice were crossed to whole body *Stat6* knock-out animals. However, $Stat6^{-/-}$-$Ikk\alpha^{F/F}$-p48-Kras mice displayed similar phenotypic and histological features with $Ikk\alpha^{F/F}$-p48-Kras animals, proving that M2 associated inflammation induced tumor promotion in this mouse model does not rely on Stat6 signaling.

Pancreas specific IKKα ablation led to the alterations in the expression of metabolism related genes in $Ikk\alpha^{F/F}$-p48-Kras animals. Among them, especially the expression of glycolytic enzymes HK1 and H2 were elevated. Moreover, decreased respiration rate of mitochondria and mitochondria numbers were detected in the pancreas of these mice. Altogether this data indicates the possibility of glycolytic switch during tumor development in $Ikk\alpha^{F/F}$-p48-Kras mice, which might be a potential inducer of PDAC development. In order to test this hypothesis, $Ikk\alpha^{F/F}$-p48-Kras animals were treated with 2-Deoxy Glucose (2-DG), a modified glucose molecule that can inhibit glucose metabolism and ATP production in the cells by inhibiting hexokinase. This treatment displayed partial effects on animals. Although pancreas distortion was similar to untreated animals at the age of 3-4 weeks, tumor incidence was reduced in $Ikk\alpha^{F/F}$-p48-Kras mice. Detailed analysis showed that 2-DG treatment caused an increase in the expression of pro-inflammatory cytokines IL1β, TNFα and a decrease in the expression of M2 macrophage markers IL4Rα, ARG-1, MRC-1 in pancreas derived $CD11b^{+}$ cells of $Ikk\alpha^{F/F}$-p48-Kras animals. This data proves that 2-DG treatment causes decreased M2 polarized macrophage infiltration and increased secretion of pro-inflammatory cytokines by $CD11b^{+}$ cells, which might be related with the partial effect of 2-DG treatment during tumor development in treated $Ikk\alpha^{F/F}$-p48-Kras mice. Additionally, 2-DG treated $Ikk\alpha^{F/F}$-p48-Kras animals displayed a tendency to express HK2 and decreased expression of PPP related enzyme Rbks in pancreas derived $CD11b^{+}$ cells, suggesting that the treatment does not only affect macrophage polarization but also energy metabolism in these mice.

As a result of this study, we proved the importance of tumor microenvironment and alterations in energy metabolism during accelerated tumor progression in Ikk$\alpha^{F/F}$-p48-Kras mice. However, these findings were not enough to explain why *K-ras* induced PDAC progression is very fast in the absence of IKKα in this mouse model. Thus, the main mechanism lying behind the accelerated tumor progression in Ikk$\alpha^{F/F}$-p48-Kras mice could not be understood completely and further research is necessary to elucidate the whole mechanism.

7. REFERENCES

A

Aft, R.L., Zhang, F.W., and Gius, D. (2002). Evaluation of 2-deoxy-D-glucose as a chemotherapeutic agent: mechanism of cell death. *British journal of cancer 87*, 805-812.

Aguirre, A.J., Bardeesy, N., Sinha, M., Lopez, L., Tuveson, D.A., Horner, J., Redston, M.S., and DePinho, R.A. (2003). Activated Kras and Ink4a/Arf deficiency cooperate to produce metastatic pancreatic ductal adenocarcinoma. *Genes & development 17*, 3112-3126.

Aguirre, A.J., Brennan, C., Bailey, G., Sinha, R., Feng, B., Leo, C., Zhang, Y., Zhang, J., Gans, J.D., Bardeesy, N., Cauwels, C., Cordon-Cardo, C., Redston, M.S., DePinho, R.A., and Chin, L. (2004). High-resolution characterization of the pancreatic adenocarcinoma genome. *Proceedings of the National Academy of Sciences of the United States of America 101*, 9067-9072.

Akakura N., Kobayashi M., Horiuchi I., Suzuki A., Wang J., Chen J., Niizeki H., Kawamura K., Hosokawa M., and Asaka M. (2001). Constitutive expression of hypoxia-inducible factor-1alpha renders pancreatic cancer cells resistant to apoptosis induced by hypoxia and nutrient deprivation. *Cancer Research 61*, 6548-6554.

Al-Aynati, M.M., Radulovich, N., Riddell, R.H., and Tsao, M.S. (2004). Epithelial-cadherin and beta-catenin expression changes in pancreatic intraepithelial neoplasia. *Clinical cancer research : an official journal of the American Association for Cancer Research 10*, 1235-1240.

Albanese, C., Wu, K., D'Amico, M., Jarrett, C., Joyce, D., Hughes, J., Hulit, J., Sakamaki, T., Fu, M., Ben-Ze'ev, A., Bromberg, J.F., Lamberti, C., Verma, U., Gaynor, R.B., Byers, S.W., and Pestell, R.G. (2003). IKKalpha regulates mitogenic signaling through transcriptional induction of cyclin D1 via Tcf. *Molecular biology of the cell 14*, 585-599.

Alguacil J., and Silverman D. T. (2004). Smokeless and other noncigarette tobacco use and pancreatic cancer: a case control study based on direct interviews. *Cancer Epidemiol Biomarkers Prev 13*, 55–58.

Almand B., Resser J. R., Lindman B., Nadaf S., Clark J. I., Kwon, E. D., Carbone D. P., and Gabrilovich D. I. (2000). Clinical significance of defective dendritic cell differentiation in cancer. *Clinical Cancer Research 6*, 1755–1766.

Almholt, K., Lund, L.R., Rygaard, J., Nielsen, B.S., Dano, K., Romer, J., and Johnsen, M. (2005). Reduced metastasis of transgenic mammary cancer in urokinase-deficient mice. *International journal of cancer Journal international du cancer 113*, 525-532.

Annunziata, C.M., Davis, R.E., Demchenko, Y., Bellamy, W., Gabrea, A., Zhan, F., Lenz, G., Hanamura, I., Wright, G., Xiao, W., Dave, S., Hurt, E.M., Tan, B., Zhao, H., Stephens, O., Santra, M., Williams, D.R., Dang, L., Barlogie, B., Shaughnessy, J.D., Jr., Kuehl, W.M., and Staudt, L.M. (2007). Frequent engagement of the classical and alternative NF-kappaB pathways by diverse genetic abnormalities in multiple myeloma. *Cancer cell 12*, 115-130.

B

Bader, A.G., Kang, S., Zhao, L., and Vogt, P.K. (2005). Oncogenic PI3K deregulates transcription and translation. *Nature reviews Cancer 5*, 921-929.

Baker F., Ainsworth S. R., Dye J. T., Crammer C., Thun M. J., Hoffmann D., Repace J. L., Henningfield J. E., Slade J., Pinney J., Shanks T., Burns D. M., Connolly G. N., and Shopland D. R. (2000). Health risks associated with cigar smoking. *JAMA 284*, 735–740.

Balkwill F., and Mantovani A. (2001). Inflammation and cancer: back to Wirchow? *Lancet, 357*, 539-545.

Banchereau J., Steinman R. M. (1998) Dendritic cells and the control of immunity. *Nature 392*, 245–52.
Bardeesy, N., Aguirre, A.J., Chu, G.C., Cheng, K.H., Lopez, L.V., Hezel, A.F., Feng, B., Brennan, C., Weissleder, R., Mahmood, U., Hanahan, D., Redston, M.S., Chin, L., and Depinho, R.A. (2006a). Both p16(Ink4a) and the p19(Arf)-p53 pathway constrain progression of pancreatic adenocarcinoma in the mouse. *Proceedings of the National Academy of Sciences of the United States of America 103*, 5947-5952.

Bardeesy, N., Cheng, K.H., Berger, J.H., Chu, G.C., Pahler, J., Olson, P., Hezel, A.F., Horner, J., Lauwers, G.Y., Hanahan, D., and DePinho, R.A. (2006b). Smad4 is dispensable for normal pancreas development yet critical in progression and tumor biology of pancreas cancer. *Genes & development 20*, 3130-3146.

Bashyam, M.D., Bair, R., Kim, Y.H., Wang, P., Hernandez-Boussard, T., Karikari, C.A., Tibshirani, R., Maitra, A., and Pollack, J.R. (2005). Array-based comparative genomic hybridization identifies localized DNA amplifications and homozygous deletions in pancreatic cancer. *Neoplasia 7*, 556-562.

Basseres, D.S., Ebbs, A., Levantini, E., and Baldwin, A.S. (2010). Requirement of the NF-kappaB subunit p65/RelA for K-Ras-induced lung tumorigenesis. *Cancer research 70*, 3537-3546.

Bauer D. E., Harris M. H., Plas D. R., Lum J. J., Hammerman P. S., Rathmell J. C., Riley J. L., Thompson C. B. (2004) Cytokine stimulation of aerobic glycolysis in hematopoietic cells exceeds proliferative demand. *Faseb J 18*, 1303–1305.

Bell D., Chomarat P., Broyles D., Netto G., Harb G. M., Lebecque S., Valladeau J., Davoust J., Palucka K. A., and Banchereau J. (1999). In breast carcinoma tissue, immature dendritic cells reside within the tumor, whereas mature dendritic cells are located in peritumoral areas. *The Journal of Experimental Medicine 190*, 1417–1426.

Ben Sahra, I., Laurent, K., Giuliano, S., Larbret, F., Ponzio, G., Gounon, P., Le Marchand-Brustel, Y., Giorgetti-Peraldi, S., Cormont, M., Bertolotto, C., Deckert, M., Auberger, P., Tanti, J.F., and Bost, F. (2010). Targeting Cancer Cell Metabolism: The Combination of Metformin and 2-Deoxyglucose Induces p53-Dependent Apoptosis in Prostate Cancer Cells. *Cancer research 70*, 2465-2475.

Berg JM, Tymoczko JL, Stryer L. Biochemistry. 5th edition. New York: W H Freeman; 2002.

Berrington de Gonzalez, A., Sweetland, S., and Spencer, E. (2003). A meta-analysis of obesity and the risk of pancreatic cancer. *British journal of cancer 89*, 519-523.

Bensaad K., Tsuruta A., Selak M. A., Vidal M. N., Nakano K., Bartrons R., Gottlieb E., and Vousden K. H. (2006). TIGAR, a p53-inducible regulator of glycolysis and apoptosis. *Cell 126*, 107-120.

Berry E., Guergova-Kuras M., Huang L., and Crofts A. (2000). Structure and function of cytochrome bc complexes. Annu Rev Biochem 69, 1005–75.

Beurel, E., Yeh, W.I., Michalek, S.M., Harrington, L.E., and Jope, R.S. (2011). Glycogen synthase kinase-3 is an early determinant in the differentiation of pathogenic Th17 cells. *J. Immunol. 186*, 1391–1398.

Bingle, L., Brown, N. J., and Lewis, C. E. (2002). The role of tumour-associated macrophages in tumour progression: implications for new anticancer therapies. *J Pathol. 196*, 254-65.

Bissell, M.J., and Radisky, D. (2001). Putting tumours in context. *Nature reviews Cancer 1*, 46-54.

Biswas, S.K., Gangi, L., Paul, S., Schioppa, T., Saccani, A., Sironi, M., Bottazzi, B., Doni, A., Vincenzo, B., Pasqualini, F., Vago, L., Nebuloni, M., Mantovani, A., and Sica, A. (2006). A distinct and unique transcriptional program expressed by tumor-associated macrophages (defective NF-kappaB and enhanced IRF-3/STAT1 activation). *Blood 107*, 2112-2122.

Biswas S. K., and Mantovani A. (2010). Macrophage plasticity and interaction with lymphocyte subsets: cancer as a paradigm. *Nat Immunol. 11*, 889-96.

Biswas S. K.,and Mantovani A. (2012). Orchestration of metabolism by macrophages. *Cell Metab. 15*, 432-437.

Boffetta P., Aagnes B., Weiderpass E., and Andersen A. (2005). Smokeless tobacco use and risk of cancer of the pancreas and other organs. *Int J Cancer 114*, 992–995.

Boffetta P., Hecht S., Gray N., Gupta P., and Straif K. (2008) Smokeless tobacco and cancer. *Lancet Oncol. 9*, 667-675.

Boire, A., Covic, L., Agarwal, A., Jacques, S., Sherifi, S., and Kuliopulos, A. (2005). PAR1 is a matrix metalloprotease-1 receptor that promotes invasion and tumorigenesis of breast cancer cells. *Cell 120*, 303-313.

Bollrath, J., Phesse, T.J., von Burstin, V.A., Putoczki, T., Bennecke, M., Bateman, T., Nebelsiek, T., Lundgren-May, T., Canli, O., Schwitalla, S., Matthews, V., Schmid, R.M., Kirchner, T., Arkan, M.C., Ernst, M., and Greten, F.R. (2009). gp130-mediated Stat3 activation in enterocytes regulates cell survival and cell-cycle progression during colitis-associated tumorigenesis. *Cancer cell 15*, 91-102.

Borg, C., Terme, M., Taïeb, J., Ménard, C., Flament, C., Robert, C., Maruyama, K., Wakasugi, H., Angevin, E., Thielemans, K., Cesne, A.L., Chung-Scott, V., Lazar, V., Tchou, I., Crépineau, F., Lemoine, F., Bernard, J., Fletcher, J.A., Turhan, A., Blay, J.-Y., Spatz, A., Emile, J.-F., Heinrich, M.C., Mécheri, S., Tursz, T., and Zitvogel, L. (2004). Novel mode of action of c-kit tyrosine kinase inhibitors leading to NK cell–dependent antitumor effects. *Journal of Clinical Investigation 114*, 379-388.

Boros L. G., Torday J. S., Lim S., Bassilian S., Cascante M., and Lee W. N. (2000) Transforming growth factor beta2 promotes glucose carbon incorporation into nucleic acid ribose through the nonoxidative pentose cycle in lung epithelial carcinoma cells. *Cancer Res.* 60, 1183–1185.

Boros L. G., Lee P. W. N., Brandes J. L., Cascande M., Muscarella P., Schirmer W.J., Melvin W.S., and Ellison E.C. (1998). Nonoxidative pentose phosphate pathways and their direct role in ribose synthesis in tumors: is cancer a disease of cellular glucose metabolism? *Medical Hypotheses 50*, 55-59.

Brahimi-Horn M. C., Chiche J., and Pouyssegur J. (2007). Hypoxia signaling controls metabolic demand. *Current Opinions in Cell Biology 19*, 223-229.

Brand, K. (1985). Glutamine and glucose metabolism during thymocyte prolif-eration. Pathways of glutamine and glutamate metabolism. *Biochem. J. 228*, 353–361.

Brinkmann, V., and Zychlinsky, A. (2012). Neutrophil extracellular traps: Is immunity the second function of immunity? *The Journal of Cell Biology 198*, 773-783.

By Russell G. Jones, Michael Parsons, Madeleine Bonnard, Vera S.F. Chan, Wen-Chen Yeh, James R. Woodgett, and Ohashi, P.S. (2000). Protein Kinase B Regulates T Lymphocyte Survival, Nuclear Factor KB Activation, and Bcl-X L Levels In Vivo. *J Exp Med 191*, 1721-1733.

C

Cairns, R.A., Harris, I.S., and Mak, T.W. (2011). Regulation of cancer cell metabolism. *Nature reviews Cancer 11*, 85-95.

Carlos Caldas, and Kern, S.E. (1995). K-ras mutation and pancreatic adenocarcinoma. *International Journal of Pancreatology 18*, 1-6.

Cavallo, F., De Giovanni, C., Nanni, P., Forni, G., and Lollini, P.L. (2011). 2011: the immune hallmarks of cancer. *Cancer immunology, immunotherapy : CII 60*, 319-326.

Chaffer, C.L., and Weinberg, R.A. (2011). A perspective on cancer cell metastasis. *Science 331*, 1559-1564.

Chandler, N.M., Canete, J.J., and Callery, M.P. (2004). Increased expression of NF-κB subunits in human pancreatic cancer cells. *Journal of Surgical Research 118*, 9-14.

Chang L. O., and Morris H.P. (1973). Enzymatic and immunological studies on pyruvate carboxylase in livers and liver tumors. *Cancer Res 33*, 2034–2041.

Chaput N., Conforti R., Viaud S., Spatz A., and Zitvogel L. (2008). The Janus face of dendritic cells in cancer. *Oncogene 27*, 5920–5931.

Chen J., Zhao S., Nakada K., Kuge Y., Tamaki N., Okada F., Wang J., Shindo M., Higashino F., Takeda K., Asaka M., Katoh H., Sugiyama T., Hosokawa M., and Kobayashi M. (2003). Dominant-negative hypoxia-inducible factor-1 alpha reduces tumorigenicity of pancreatic cancer cells through the suppression of glucose metabolism. *American Journal of Pathology 162*, 1283-1291.

Cheng, F., Wang, H.W., Cuenca, A., Huang, M., Ghansah, T., Brayer, J., Kerr, W.G., Takeda, K., Akira, S., Schoenberger, S.P., Yu, H., Jove, R., and Sotomayor, E.M. (2003). A critical role for Stat3 signaling in immune tolerance. *Immunity 19*, 425-436.

Cheng, J., Huo, D.H., Kuang, D.M., Yang, J., Zheng, L., and Zhuang, S.M. (2007). Human macrophages promote the motility and invasiveness of osteopontin-knockdown tumor cells. *Cancer research 67*, 5141-5147.

Chomarat P., Banchereau J., Davoust J., and Palucka A. K. (2000). IL-6 switches the differentiation of monocytes from dendritic cells to macrophages. *Nature Immunology 1*, 510-514.

Cirri, P., and Chiarugi, P. (2011). Cancer associated fibroblasts: the dark side of the coin. *American journal of cancer research 1*, 482-497.

Colotta, F., Allavena, P., Sica, A., Garlanda, C., and Mantovani, A. (2009). Cancer-related inflammation, the seventh hallmark of cancer: links to genetic instability. *Carcinogenesis 30*, 1073-1081.

Condeelis J., and Pollard J.W. (2006). Macrophages: obligate partners for tumor cell migration, invasion, and metastasis. *Cell 124*, 263-266.

Coussens, L. M. and Werb, Z. (2002). Inflammation and cancer. *Nature*, 420, 860-867.

Coventry B. J., Lee P. L., Gibbs D., and Hart D. N. J. (2002). Dendritic cell density and activation status in human breast cancer-CD1a, CMRF-44, CMRF-56 and CD-83 expression. *British Journal of Cancer 86*, 546–551.

Cowgill S. M., and Muscarella P. (2003). The genetics of pancreatic cancer. *Am J Surg 186*, 279–286.

Coy J. F., Dressler D., Wilde J., and Schubert P. (2005). Mutations in the transketolase-like gene TKTL1: clinical implications for neurodegenerative diseases, diabetes and cancer. *Clin Lab 51*, 257–273.

Crowe N. Y., Smyth M. J., and Godfrey D. I. (2002). A critical role for natural killer T cells in immunosurveillance of methylcholanthrene-induced sarcomas. *J Exp Med 196*, 119–127.

Curi, R., Newsholme, P., Pithon-Curi, T.C., Pires-de-Melo, M., Garcia, C., Homem-de-Bittencourt Junior, P.I., and Guimaraes, A.R. (1999). Metabolic fate of glutamine in lymphocytes, macrophages and neutrophils. *Brazilian journal of medical and biological research = Revista brasileira de pesquisas medicas e biologicas / Sociedade Brasileira de Biofisica [et al] 32*, 15-21.

Courtois G., and Gilmore T. D. (2006) Mutations in the NF-kappaB signaling pathway: implications for human disease. Oncogene 25, 6831-6843.

Crofts A. R. (2004). The cytochrome bc1 complex: function in the context of structure. Annu. Rev. Physiol. 66, 689–733.

Curiel, T.J., Coukos, G., Zou, L., Alvarez, X., Cheng, P., Mottram, P., Evdemon-Hogan, M., Conejo-Garcia, J.R., Zhang, L., Burow, M., Zhu, Y., Wei, S., Kryczek, I., Daniel, B., Gordon, A., Myers, L., Lackner, A., Disis, M.L., Knutson, K.L., Chen, L., and Zou, W. (2004). Specific recruitment of regulatory T cells in ovarian carcinoma fosters immune privilege and predicts reduced survival. *Nature medicine 10*, 942-949.

D

Dan, H.C., Cooper, M.J., Cogswell, P.C., Duncan, J.A., Ting, J.P., and Baldwin, A.S. (2008). Akt-dependent regulation of NF-{kappa}B is controlled by mTOR and Raptor in association with IKK. *Genes & development 22*, 1490-1500.

Daniel Kahneman, Amos Tversky and Paul Slovic, eds. (1982) *Judgment under Uncertainty: Heuristics & Biases*. Cambridge, UK, Cambridge University Press ISBN 0-521-28414-7.
Deberardinis, R.J., Sayed, N., Ditsworth, D., and Thompson, C.B. (2008). Brick by brick: metabolism and tumor cell growth. *Current opinion in genetics & development 18*, 54-61.

Deberardinis R. J., Lum J. J., Hatzivassiliou G., and Thompson C. B. (2008). The biology of cancer: metabolic reprogramming fuels cell growth and proliferation. *Cell Metab*. *7*, 11-20.

Denko, N.C. (2008). Hypoxia, HIF1 and glucose metabolism in the solid tumour. *Nature reviews Cancer 8*, 705-713.

Dejardin E., Bonizzi G., Bellahcene A., Castronovo V., Merville M. P., and Bours V. (1995) . Highly-expressed p100/p52 (NFKB2) sequesters other NFkappaB-related proteins in the cytoplasm of human breast cancer cells. *Oncogene 11*, 1835–1841.

Dejardin E., Deregowski V., Chapelier M., Jacobs N., Gielen J., Merville M. Pç, Bours V. (1999). Regulation of NFkappaB activity by IkappaB-related proteins in adenocarcinoma cells. *Oncogene 18*, 2567–2577.

Deramaudt, T., and Rustgi, A.K. (2005). Mutant KRAS in the initiation of pancreatic cancer. *Biochimica et biophysica acta 1756*, 97-101.

Descargues, P., Sil, A.K., and Karin, M. (2008). IKKalpha, a critical regulator of epidermal differentiation and a suppressor of skin cancer. *EMBO J 27*, 2639-2647.

Doedens, A.L., Stockmann, C., Rubinstein, M.P., Liao, D., Zhang, N., DeNardo, D.G., Coussens, L.M., Karin, M., Goldrath, A.W., and Johnson, R.S. (2010). Macrophage expression of hypoxia-inducible factor-1 alpha suppresses T-cell function and promotes tumor progression. *Cancer research 70*, 7465-7475.

Doerks, T., Copley, R.R., Schultz, J., Ponting, C.P., and Bork, P. (2002). Systematic identification of novel protein domain families associated with nuclear functions. *Genome research 12*, 47-56.

Doi K., Horiuchi T., Uchinami M., Tabo T., Kimura N., Yokomachi J., Yoshida M., and Tanaka K. (2002). Neutrophil elastase inhibitor reduces hepatic metastases induced by ischaemia-reperfusion in rats. Eur J Surg. 168, 507-510.

Drapier J. C., and Hibbs Jr, J. B. (1988). Differentiation of murine macrophages to express nonspecific cytotoxicity for tumor cells results in L-arginine-dependent inhibition of mitochondrial iron-sulfur enzymes in the macrophage effector cells. *The Journal of Immunology* 140, 2829-2838.

Du, R., Lu, K.V., Petritsch, C., Liu, P., Ganss, R., Passegue, E., Song, H., Vandenberg, S., Johnson, R.S.,Werb, Z., and Bergers, G. (2008). HIF1alpha induces the recruitment of bone marrow-derived vascular modulatory cells to regulate tumor angiogenesis and invasion. *Cancer cell 13*, 206-220.

E

Egeblad, M., and Werb, Z. (2002). New functions for the matrix metalloproteinases in cancer progression. *Nature reviews Cancer 2*, 161-174.

Erez, N., Truitt, M., Olson, P., Arron, S.T., and Hanahan, D. (2010). Cancer-Associated Fibroblasts Are Activated in Incipient Neoplasia to Orchestrate Tumor-Promoting Inflammation in an NF-kappaB-Dependent Manner. *Cancer cell 17*, 135-147.

Eyden B., Banerjee S. S., Shenjere P., and Fisher C. (2009). The myofibroblast and its tumours. J Clin Pathol. 62, 236-249.

F

Falk Weih, Daniel Carrasco, Stephen K. Durham, Debra S, B., Cheryl A, R., Rolf-Peter Ryseck, Sergio A. Lira, and Bravo, R. (1995). Multiorgan inflammation and hematopoietic abnormalities in mice with a targeted disruption of RelB, a member of NFkB family. *Cell 80*, 331-340.

Fantin V. R., St-Pierre J., and Leder P. (2006). Attenuation of LDH-A expression uncovers a link between glycolysis, mitochondrial physiology, and tumor maintenance. *Cancer Cell 9*, 425-434.

Ferlay, J., Shin, H.R., Bray, F., Forman, D., Mathers, C., and Parkin, D.M. (2010). Estimates of worldwide burden of cancer in 2008: GLOBOCAN 2008. *International journal of cancer Journal international du cancer 127*, 2893-2917.

Finco, T. S., Westwick, J. K., Norris, J. L., Beg, A. A., Der, C. J. and Baldwin, A.S. (1997). Oncogenic Ha-Ras-induced Signaling Activates NF-KB Transcriptional Activity, Which Is Required for Cellular Transformation. *The Journal of biological chemistry 272*, 24113–24116.

Fleming, J.B., Shen, G.L., Holloway, S.E., Davis, M., and Brekken, R.A. (2005). Molecular consequences of silencing mutant K-ras in pancreatic cancer cells: justification for K-ras-directed therapy. *Molecular cancer research : MCR 3*, 413-423.

Forbes, N.S., Meadows, A.L., Clark, D.S., and Blanch, H.W. (2006). Estradiol stimulates the biosynthetic pathways of breast cancer cells: detection by metabolic flux analysis. *Metabolic engineering 8*, 639-652.

Formentini, A., Braun, P., Fricke, H., Link, K.H., Henne-Bruns, D., and Kornmann, M. (2012). Expression of interleukin-4 and interleukin-13 and their receptors in colorectal cancer. *International journal of colorectal disease 27*, 1369-1376.

Formentini, A., Prokopchuk, O., Strater, J., Kleeff, J., Grochola, L.F., Leder, G., Henne-Bruns, D., Korc, M., and Kornmann, M. (2009). Interleukin-13 exerts autocrine growth-promoting effects on human pancreatic cancer, and its expression correlates with a propensity for lymph node metastases. *International journal of colorectal disease 24*, 57-67.

Franco, O.E., Shaw, A.K., Strand, D.W., and Hayward, S.W. (2010). Cancer associated fibroblasts in cancer pathogenesis. *Seminars in cell & developmental biology 21*, 33-39.

Frank, A.K., Leu, J.I., Zhou, Y., Devarajan, K., Nedelko, T., Klein-Szanto, A., Hollstein, M., and Murphy, M.E. (2011). The codon 72 polymorphism of p53 regulates interaction with NF-{kappa}B and transactivation of genes involved in immunity and inflammation. *Molecular and cellular biology 31*, 1201-1213.

Frezza, C., and Gottlieb, E. (2009). Mitochondria in cancer: not just innocent bystanders. *Seminars in cancer biology 19*, 4-11.

Fridlender, Z.G., and Albelda, S.M. (2012). Tumor-associated neutrophils: friend or foe? *Carcinogenesis 33*, 949-955.

Fridlender, Z.G., Sun, J., Mishalian, I., Singhal, S., Cheng, G., Kapoor, V., Horng, W., Fridlender, G., Bayuh, R., Worthen, G.S., and Albelda, S.M. (2012). Transcriptomic analysis comparing tumor-associated neutrophils with granulocytic myeloid-derived suppressor cells and normal neutrophils. *PloS one 7*, e31524.

Fujioka, S., Sclabas, G.M., Schmidt, C., Frederick, W.A., Dong, Q.G., Abbruzzese, J.L., Evans, D.B., Baker, C., and Chiao, P.J. (2003a). Function of nuclear factor kappaB in pancreatic cancer metastasis. *Clinical cancer research : an official journal of the American Association for Cancer Research 9*, 346-354.

Fujioka, S., Sclabas, G.M., Schmidt, C., Niu, J., Frederick, W.A., Dong, Q.G., Abbruzzese, J.L., Evans, D.B., Baker, C., and Chiao, P.J. (2003b). Inhibition of constitutive NF-kappa B activity by I kappa B alpha M suppresses tumorigenesis. *Oncogene 22*, 1365-1370.

Funes, J.M., Quintero, M., Henderson, S., Martinez, D., Qureshi, U., Westwood, C., Clements, M.O., Bourboulia, D., Pedley, R.B., Moncada, S., and Boshoff, C. (2007). Transformation of human mesenchymal stem cells increases their dependency on oxidative phosphorylation for energy production. *Proceedings of the National Academy of Sciences of the United States of America 104*, 6223-6228.

Furihata M., Ono Y., Ichikawa K., Tomita S., Fujimori T., and Kubota K. (2005). Prognostic significance of CD83 positive, mature dendritic cells in the gall bladder carcinoma. *Oncology Reports 14*, 353–356.

G

Gabrilovich, D. I., Ciemik, I. F., and Carbone, D.P. (1996). Dendritic Cells in Antitumor Immune Responses: I. Defective Antigen Presentation in Tumor-Bearing Hosts. *Cellular Immunology 170*, 101-110.

Gambhir, S. S. (2002). Molecular imaging of cancer with positron emission tomography. *Nature Rev. Cancer 2*, 683–693.

Gao, Y., Yang, W., Pan, M., Scully, E., Girardi, M., Augenlicht, L.H., Craft, J., and Yin, Z. (2003). Gamma delta T cells provide an early source of interferon gamma in tumor immunity. *The Journal of experimental medicine 198*, 433-442.

Gapstur, S.M., Gann, P.H., Lowe, W., Liu, K., Colangelo, L., and Dyer, A. (2000). Abnormal glucose metabolism and pancreatic cancer mortality. *JAMA : the journal of the American Medical Association 283*, 2552-2558.

Genkinger, J.M., Spiegelman, D., Anderson, K.E., Bergkvist, L., Bernstein, L., van den Brandt, P.A., English, D.R., Freudenheim, J.L., Fuchs, C.S., Giles, G.G., Giovannucci, E., Hankinson, S.E., Horn-Ross, P.L., Leitzmann, M., Mannisto, S., Marshall, J.R., McCullough, M.L., Miller, A.B., Reding, D.J., Robien, K., Rohan, T.E., Schatzkin, A., Stevens, V.L., Stolzenberg-Solomon, R.Z., Verhage, B.A., Wolk, A., Ziegler, R.G., and Smith-Warner, S.A. (2009). Alcohol intake and pancreatic cancer risk: a pooled analysis of fourteen cohort studies. *Cancer epidemiology, biomarkers & prevention : a publication of the American Association for Cancer Research, cosponsored by the American Society of Preventive Oncology 18*, 765-776.

Giannelli, G., Falk-Marzillier, J., Schiraldi, O., Stetler-Stevenson, W.G., and Quaranta, V. (1997). Induction of cell migration by matrix metalloprotease-2 cleavage of laminin-5. *Science 277*, 225-228.

Giardiello F. M., Offerhaus G. J., Lee D. H., Krush A. J., Tersmette A. C., Booker S. V., Kelley N. C., and Hamilton S. R. (1993). Increased risk of thyroid and pancreatic carcinoma in familial adenomatous polyposis. *Gut 34*, 1394–1396.

Giardiello F. M., Brensinger J. D., Tersmette A. C., Goodman S. N., Petersen G. M., Booker S. V., Cruz-Correa M., and Offerhaus J. A. (2000). Very high risk of cancer in familial Peutz-Jeghers syndrome. *Gastroenterology 119*, 1447–1453.

Gilmore, T.D. (2006). Introduction to NF-kappaB: players, pathways, perspectives. *Oncogene 25*, 6680-6684.

Gilmore TD (2006). NF-kB: from basic research to human disease. *Oncogene (Reviews) 51*, 6679-6899.

Giovannucci, E., and Michaud, D. (2007). The role of obesity and related metabolic disturbances in cancers of the colon, prostate, and pancreas. *Gastroenterology 132*, 2208-2225.

Giraudo, E., Inoue, M., and Hanahan, D. (2004). An amino-bisphosphonate targets MMP-9–expressing macrophages and angiogenesis to impair cervical carcinogenesis. *Journal of Clinical Investigation 114*, 623-633.

Goggins M., Schutte M., Lu J., Moskaluk C. A., Weinstein C. L., Petersen G. M., Yeo C. J., Jackson C. E., Lynch H. T., Hruban R. H., and Kern S. E. (1996). Germline BRCA2 gene mutations in patients with apparently sporadic pancreatic carcinomas. *Cancer Res. 56*, 5360-5364.

Gogvadze, V., Orrenius, S., and Zhivotovsky, B. (2008). Mitochondria in cancer cells: what is so special about them? *Trends in cell biology 18*, 165-173.

Goldman R. D., Kaplan N. O., and Hall T. C. (1964). Lactic dehydrogenase in human neoplastic tissues. *Cancer Research 24*, 389-399.

Gordon S. (2003). Alternative activation of macrophages. Nat Rev Immunol. 3, 23-35.

Gottlieb E., and Tomlinson I. P. (2005). Mitochondrial tumour suppressors: a genetic and biochemical update. *Nat Rev Cancer 5*, 857-866.

Green D. R., and Chipuk J. E. (2006). p53 and metabolism: Inside the TIGAR. *Cell 126*, 30-32.

Grippo, P.J., Nowlin, P.S., Demeure, M.J., Longnecker, D.S., and Sandgren, E.P. (2003). Preinvasive pancreatic neoplasia of ductal phenotype induced by acinar cell targeting of mutant Kras in transgenic mice. *Cancer research 63*, 2016-2019.

Grivennikov, S.I., Greten, F.R., and Karin, M. (2010). Immunity, inflammation, and cancer. *Cell 140*, 883-899.

Guerra, C., Schuhmacher, A.J., Canamero, M., Grippo, P.J., Verdaguer, L., Perez-Gallego, L., Dubus, P., Sandgren, E.P., and Barbacid, M. (2007). Chronic pancreatitis is essential for induction of pancreatic ductal adenocarcinoma by K-Ras oncogenes in adult mice. *Cancer cell 11*, 291-302.

Guido M. Sclabas, Shuichi Fujioka, Christian Schmidt, Douglas B. Evans, and Chiao, P.J. (2003). NF-κB in Pancreatic Cancer. *International Journal of Gastrointestinal Cancer 33*, 15-26.

Guppy M., Greiner E., and Brand K. (1993). The role of the Crabtree effect and an endogenous fuel in the energy metabolism of resting and proliferatingthymocytes. *Eur. J. Biochem. 212*, 95–99.

H

Hagemann, T., Lawrence, T., McNeish, I., Charles, K.A., Kulbe, H., Thompson, R.G., Robinson, S.C., and Balkwill, F.R. (2008). "Re-educating" tumor-associated macrophages by targeting NF-kappaB. *The Journal of experimental medicine 205*, 1261-1268.

Hammond K. D., and Balinsky D. (1978). Activities of key gluconeogenic enzymes and glycogen synthase in rat and human livers, hepatomas, and hepatoma cell cultures. *Cancer Res 38*, 1317–1322.

Hanahan, D., and Coussens, L.M. (2012). Accessories to the crime: functions of cells recruited to the tumor microenvironment. *Cancer cell 21*, 309-322.

Hanahan, D., and Weinberg, R.A. (2000). The hallmarks of cancer. *Cell 100*, 57-70.

Hanahan, D., and Weinberg, R.A. (2011). Hallmarks of cancer: the next generation. *Cell 144*, 646-674.

Haq, S., Ali, S., Mohammad, R., and Sarkar, F.H. (2012). The complexities of epidemiology and prevention of gastrointestinal cancers. *International journal of molecular sciences 13*, 12556-12572.

Haschemi, A., Kosma, P., Gille, L., Evans, C.R., Burant, C.F., Starkl, P., Knapp, B., Haas, R., Schmid, J.A., Jandl, C., Amir, S., Lubec, G., Park, J., Esterbauer, H., Bilban, M., Brizuela, L., Pospisilik, J.A., Otterbein, L.E., and Wagner, O. (2012). The sedoheptulose kinase CARKL directs macrophage polarization through control of glucose metabolism. *Cell metabolism 15*, 813-826.

Hassan M. M., Abbruzzese J. L., Bondy M. L., Wolff R. A., Vauthey J. N., Pisters P.W., Evans D.B., Khan R., Chou T. H., Lenzi R., Jiao L., and Li D. (2007). Passive smoking and use of noncigarette tobacco products and risk for pancreatic cancer: case-control study. *Cancer 109*, 2547–2556.

Hatzivassiliou G., Zhao F., Bauer D. E., Andreadis C., Shaw A. N., Dhanak D., Hingorani S. R., Tuveson D. A., and Thompson C. B. (2005). ATP citrate lyase inhibition can suppress tumor cell growth. *Cancer Cell 8*, 311–321.

He, G., Yu, G.Y., Temkin, V., Ogata, H., Kuntzen, C., Sakurai, T., Sieghart, W., Peck-Radosavljevic, M., Leffert, H.L., and Karin, M. (2010). Hepatocyte IKKbeta/NF-kappaB inhibits tumor promotion and progression by preventing oxidative stress-driven STAT3 activation. *Cancer cell 17*, 286-297.

Hedeskov, C. J. (1968). Early effects of phytohaemagglutinin on glucose me-tabolism of normal human lymphocytes. *Biochem. J. 110*, 373–380.

Heinrich P. C., Morris H. P., and Weber G. (1976). Behavior of transaldolase (EC 2.2.1.2) and transketolase (EC2.2.1.1) Activities in normal, neoplastic, differentiating, and regenerating liver. *Cancer Res. 36*, 3189–3197.

Henley S. J., Thun M. J., Chao A., and Calle E. E. (2004). Association between exclusive pipe smoking and mortality from cancer and other diseases. *J Natl Cancer Inst 96*, 853–861.

Hennipman A., Smits J., van Oirschot B., van Houwelingen J. C., Rijksen G., Neyt J. P., Van Unnik J. A., and Staal G. E. (1987) Glycolytic enzymes in breast cancer, benign breast disease and normal breast tissue. *Tumour Biol. 8*, 251–263.

Henry Q. Xiong, and Abbruzzese, J.L. Molecular Pathogenesis of Pancreatic Adenocarcinoma.

Hildner, K., Edelson, B.T., Purtha, W.E., Diamond, M., Matsushita, H., Kohyama, M., Calderon, B., Schraml, B.U., Unanue, E.R., Diamond, M.S., Schreiber, R.D., Murphy, T.L., and Murphy, K.M. (2008). Batf3 deficiency reveals a critical role for CD8alpha+ dendritic cells in cytotoxic T cell immunity. *Science 322*, 1097-1100.

Hingorani, S.R., Petricoin, E.F., Maitra, A., Rajapakse, V., King, C., Jacobetz, M.A., Ross, S., Conrads, T.P., Veenstra, T.D., Hitt, B.A., Kawaguchi, Y., Johann, D., Liotta, L.A., Crawford, H.C., Putt, M.E., Jacks, T., Wright, C.V., Hruban, R.H., Lowy, A.M., and Tuveson, D.A. (2003). Preinvasive and invasive ductal pancreatic cancer and its early detection in the mouse. *Cancer cell 4*, 437-450.

Hoberg, J.E., Popko, A.E., Ramsey, C.S., and Mayo, M.W. (2006). IkappaB kinase alpha-mediated derepression of SMRT potentiates acetylation of RelA/p65 by p300. *Molecular and cellular biology 26*, 457-471.

Hoshino K., Sugiyama T., Matsumoto M., Tanaka T., Saito M., Hemmi H., Ohara O., Akira S., Kaisho T. (2006). IkappaB kinase-alpha is critical for interferon-alpha production induced by
Toll-like receptors 7 and 9. *Nature 440*, 949-953.

Houghton A. M., Rzymkiewicz D. M., Ji H., Gregory A. D., Egea E. E., Metz H. E., Stolz D. B., Land S. R., Marconcini L. A., Kliment C. R., Jenkins K. M., Beaulieu K. A., Mouded M., Frank S. J., Wong K. K., and Shapiro S. D. (2010). Neutrophil elastase-mediated degradation of IRS-1 accelerates lung tumor growth. *Nat Med. 16*, 219-223.

Howe, G.R., and Burch, J.D. (1996). Nutrition and pancreatic cancer. *Cancer Causes and Control 7*, 69-82.

Hruban, R.H., Adsay, N.V., Albores-Saavedra, J., Anver, M.R., Biankin, A.V., Boivin, G.P., Furth, E.E., Furukawa, T., Klein, A., Klimstra, D.S., Kloppel, G., Lauwers, G.Y., Longnecker, D.S., Luttges, J., Maitra, A., Offerhaus, G.J., Perez-Gallego, L., Redston, M., and Tuveson, D.A. (2006). Pathology of genetically engineered mouse models of pancreatic exocrine cancer: consensus report and recommendations. *Cancer research 66*, 95-106.

Hruban, R.H., Wilentz, R.E., and Kern, S.E. (2000). Genetic progression in the pancreatic ducts. *The American journal of pathology 156*, 1821-1825.

Hsu, P.P., and Sabatini, D.M. (2008). Cancer cell metabolism: Warburg and beyond. *Cell 134*, 703-707.
Huang, W.C., and Hung, M.C. (2013). Beyond NF-kappaB activation: nuclear functions of IkappaB kinase alpha. *Journal of biomedical science 20*, 3.

Huh, S.J., Liang, S., Sharma, A., Dong, C., and Robertson, G.P. (2010). Transiently entrapped circulating tumor cells interact with neutrophils to facilitate lung metastasis development. *Cancer research 70*, 6071-6082.

Hunte C., Palsdottir H., and Trumpower B. L. (2003). Protonmotive pathways and mechanisms in the cytochrome bc1 complex. FEBS Lett. 545, 39–46.

Huxley, R., Ansary-Moghaddam, A., Berrington de Gonzalez, A., Barzi, F., and Woodward, M. (2005). Type-II diabetes and pancreatic cancer: a meta-analysis of 36 studies. *British journal of cancer 92*, 2076-2083.

I

Ijichi, H., Chytil, A., Gorska, A.E., Aakre, M.E., Fujitani, Y., Fujitani, S., Wright, C.V., and Moses, H.L. (2006). Aggressive pancreatic ductal adenocarcinoma in mice caused by pancreas-specific blockade of transforming growth factor-beta signaling in cooperation with active Kras expression. *Genes & development 20*, 3147-3160.

Iliopoulos, D., Jaeger, S.A., Hirsch, H.A., Bulyk, M.L., and Struhl, K. (2010). STAT3 activation of miR-21 and miR-181b-1 via PTEN and CYLD are part of the epigenetic switch linking inflammation to cancer. *Molecular cell 39*, 493-506.

Iodice, S., Gandini, S., Maisonneuve, P., and Lowenfels, A.B. (2008). Tobacco and the risk of pancreatic cancer: a review and meta-analysis. *Langenbeck's archives of surgery / Deutsche Gesellschaft fur Chirurgie 393*, 535-545.

Isaacs, J.S., Jung, Y.J., Mole, D.R., Lee, S., Torres-Cabala, C., Chung, Y.L., Merino, M., Trepel, J., Zbar, B., Toro, J., Ratcliffe, P.J., Linehan, W.M., and Neckers, L. (2005). HIF overexpression correlates with biallelic loss of fumarate hydratase in renal cancer: novel role of fumarate in regulation of HIF stability. *Cancer cell 8*, 143-153.

Iwata, S. (1998). Complete Structure of the 11-Subunit Bovine Mitochondrial Cytochrome bc1 Complex. *Science 281*, 64-71.

Izuhara, K., Feldman, R.A., Greer, P., and Harada, N. (1994). Interaction of the c-fes proto-oncogene product with the interleukin-4 receptor. *The Journal of biological chemistry 269*, 18623-18629.

J

James E., and Wright D. (1995). Diabetes Mellitus as a Risk Factor for Pancreatic Cancer a Meta-analysis. *JAMA 273*, 1605-1609.

Jiao, L., and Li, D. (2010). Epidemiology and Prospects for Prevention of Pancreatic Cancer. 3-25.

Johnson, L., Mercer, K., Greenbaum, D., Bronson, R.T., Crowley, D., Tuveson, D.A., and Jacks, T. (2001). Somatic activation of the K-ras oncogene causes early onset lung cancer in mice. *Nature 410*, 1111-1116.

Jonathan J. Keats, Rafael Fonseca, Marta Chesi, Roelandt Schop, Angela Baker, Wee-Joo Chng, Scott Van Wier, Rodger Tiedemann, Chang-Xin Shi, Michael Sebag, Esteban Braggio, Travis Henry, Yuan-Xiao Zhu, Homer Fogle, Tammy Price-Troska, Gregory Ahmann, Catherine Mancini, Leslie A. Brents, Shaji Kumar, Philip Greipp, Angela Dispenzieri, Barb Bryant, George Mulligan, Laurakay Bruhn, Michael Barrett, Riccardo Valdez, Jeff Trent, A. Keith Stewart, John Carpten, and Bergsagel, P.L. (2007). Promiscuous Mutations Activate the Non-Canonical NF-kB Pathway in Multiple Myeloma. *Cancer cell 12*, 131-144.

José Zamorano, and Keegan, A.D. (1998). Regulation of Apoptosis by Tyrosine-Containing STAT6-Docking Tyrosines, Signal Protection Domains of IL-4R α : Y497 and Y713, But Not the from apoptosis. *Journal of immunology 161*, 859-867.

K

Kallio P. J., Wilson P. J., O'Brien S., Makino Y., and Poellinger L. (1990). Regulation of the hypoxia inducible transcription factor 1α by the ubiquitin-proteasome pathway. *J Biol Chem 274*, 6519-6525.

Kalluri, R., and Zeisberg, M. (2006). Fibroblasts in cancer. *Nature reviews Cancer 6*, 392-401.

Kanai, T., Watanabe, M., Hayashi, A., Nakazawa, A., Yajima, T., Okazawa, A., Yamazaki, M., Ishii, H., and Hibi, T. (2000). Regulatory effect of interleukin-4 and interleukin-13 on colon cancer cell adhesion. *British journal of cancer 82*, 1717-1723.

Kaplan M. H., Sun Y-L, Hoey T., and Grusby M. J. (1996). Impaired IL-12 responses and enhanced development of Th2 cells in Stat4-deficient mice. *Nature* 382, 174 – 177.

Karin, M. (2006). Nuclear factor-kappaB in cancer development and progression. *Nature 441*, 431-436.

Karin, M., and Greten, F.R. (2005). NF-kappaB: linking inflammation and immunity to cancer development and progression. *Nature reviews Immunology 5*, 749-759.

Kawaguchi, Y., Cooper, B., Gannon, M., Ray, M., MacDonald, R.J., and Wright, C.V. (2002). The role of the transcriptional regulator Ptf1a in converting intestinal to pancreatic progenitors. *Nature genetics 32*, 128-134.

Kawakami, M., Kawakami, K., Stepensky, V.A., Maki, R.A., Robin, H., Muller, W., Husain, S.R., and Puri, R.K. (2002). Interleukin 4 receptor on human lung cancer: a molecular target for cytotoxin therapy. *Clinical cancer research : an official journal of the American Association for Cancer Research 8*, 3503-3511.

Kawauchi K., Araki K., Tobiume K., and Tanaka N. (2008). p53 regulates glucose metabolism through an IKK-NF-kappaB pathway and inhibits cell transformation. Nat Cell Biol. 10, 611-618.

Kessenbrock, K., Plaks, V., and Werb, Z. (2010). Matrix metalloproteinases: regulators of the tumor microenvironment. *Cell 141*, 52-67.

Khaled, W.T., Read, E.K., Nicholson, S.E., Baxter, F.O., Brennan, A.J., Came, P.J., Sprigg, N., McKenzie, A.N., and Watson, C.J. (2007). The IL-4/IL-13/Stat6 signalling pathway promotes luminal mammary epithelial cell development. *Development 134*, 2739-2750.

Khasawneh, J., Schulz, M.D., Walch, A., Rozman, J., Hrabe de Angelis, M., Klingenspor, M., Buck, A., Schwaiger, M., Saur, D., Schmid, R.M., Kloppel, G., Sipos, B., Greten, F.R., and Arkan, M.C. (2009). Inflammation and mitochondrial fatty acid beta-oxidation link obesity to early tumor promotion. *Proceedings of the National Academy of Sciences of the United States of America 106*, 3354-3359.

Kim, J.W., Tchernyshyov, I., Semenza, G.L., and Dang, C.V. (2006). HIF-1-mediated expression of pyruvate dehydrogenase kinase: a metabolic switch required for cellular adaptation to hypoxia. *Cell metabolism 3*, 177-185.

Klein A. P., Hruban R. H, Brune K. A., Petersen G. M., and Goggins M. (2001). Familial pancreatic cancer. *Cancer J 7*, 266–273.

Ko, C.W., Cuthbert, R.J., Orsi, N.M., Brooke, D.A., Perry, S.L., Markham, A.F., Coletta, P.L., and Hull, M.A. (2008). Lack of interleukin-4 receptor alpha chain-dependent signalling promotes azoxymethane-induced colorectal aberrant crypt focus formation in Balb/c mice. *The Journal of pathology 214*, 603-609.

Koller, F.L., Hwang, D.G., Dozier, E.A., and Fingleton, B. (2010). Epithelial interleukin-4 receptor expression promotes colon tumor growth. *Carcinogenesis 31*, 1010-1017.

Kondoh H., Lleonart M. E., Gil J., Wang J., Degan P., Peters G., Martinez D., Carnero A., and Beach D. (2005). Glycolytic enzymes can modulate cellular life span. *Cancer Research 65*, 177-185.

Kortylewski M., Kujawski M., Wang T., Wei S., Zhang S., Pilon-Thomas S., Niu G., Kay H., Mulé J., Kerr W. G., Jove R., Pardoll D., and Yu H. (2005). Inhibiting Stat3 signaling in the hematopoietic system elicits multicomponent antitumor immunity. *Nat Med. 11*, 1314-1321.

Krawczyk C.M., Holowka T., Sun J., Blagih J., Amiel E., DeBerardinis R.J., Cross J.R., Jung E., Thompson C.B., Jones R.G., and PearceE.J. (2010). Toll-like receptor-induced changes in glycolyticmetabolism regulate dendritic cell activation. *Blood 115*, 4742–4749.

Kuang D. M., Zhao Q., Wu Y., Peng C., Wang J., Xu Z., Yin X. Y., and Zheng L. (2011). Peritumoral neutrophils link inflammatory response to disease progression by fostering angiogenesis in hepatocellular carcinoma. *J Hepatol. 54*, 948-55.

Kubota, Y., Takubo, K., Shimizu, T., Ohno, H., Kishi, K., Shibuya, M., Saya, H., and Suda, T. (2009). M-CSF inhibition selectively targets pathological angiogenesis and lymphangiogenesis. *The Journal of experimental medicine 206*, 1089-1102.

Kuhajda F. P., Jenner K., Wood F. D., Hennigar R. A., Jacobs L. B., Dick J. D., and Pasternack GR. (1994). Fatty acid synthesis: a potential selective target for antineoplastic therapy. *Proc Natl Acad Sci USA 91*, 6379–6383.

Kwak, Y.T., Li, R., Becerra, C.R., Tripathy, D., Frenkel, E.P., and Verma, U.N. (2005). IkappaB kinase alpha regulates subcellular distribution and turnover of cyclin D1 by phosphorylation. *The Journal of biological chemistry 280*, 33945-33952.

Kwak, Y.T., Radaideh, S.M., Ding, L., Li, R., Frenkel, E., Story, M.D., Girard, L., Minna, J., and Verma, U.N. (2011). Cells lacking IKKalpha show nuclear cyclin D1 overexpression and a neoplastic phenotype: role of IKKalpha as a tumor suppressor. *Molecular cancer research : MCR 9*, 341-349.

L

Lamberti, C., Lin, K.M., Yamamoto, Y., Verma, U., Verma, I.M., Byers, S., and Gaynor, R.B. (2001). Regulation of beta-catenin function by the IkappaB kinases. *The Journal of biological chemistry 276*, 42276-42286.

Larsson, S.C., Orsini, N., and Wolk, A. (2007). Body mass index and pancreatic cancer risk: A meta-analysis of prospective studies. *International journal of cancer Journal international du cancer 120*, 1993-1998.

Lawrence, T., Bebien, M., Liu, G. Y., Nizet, V., and Karin, M. (2005). IKKa limits macrophage NF-kB activation and contributes to the resolution of inflammation. *Nature 434*, 1138-1143.

Lederle, W., Hartenstein, B., Meides, A., Kunzelmann, H., Werb, Z., Angel, P., and Mueller, M.M. (2010). MMP13 as a stromal mediator in controlling persistent angiogenesis in skin carcinoma. *Carcinogenesis 31*, 1175-1184.

Lee, P.N., and Hamling, J. (2009). Systematic review of the relation between smokeless tobacco and cancer in Europe and North America. *BMC medicine 7*, 36.

Lessard L., Begin L. R., Gleave M. E., Mes-Masson A. M., and Saad F. (2005). Nuclear localisation of nuclear factor-kappaB transcription factors in prostate cancer: an immunohistochemical study. *Br J Cancer 93*, 1019–1023.

Lessard L., Saad F., Le Page C., Diallo J. S., Peant B., Delvoye N., and Mes-Masson A.M. (2007). NFkappaB2 processing and p52 nuclear accumulation after androgenic stimulation of LNCaP prostate cancer cells. *Cell Signal 19*, 1093–1100.

Levine A. J., and Puzio-Kuter A. M. (2010). The control of the metabolic switch in cancers by oncogenes and tumor suppressor genes. *Science 330*, 1340-1344.

Li, D., Morris, J.S., Liu, J., Hassan, M.M., Day, R.S., Bondy, M.L., and Abbruzzese, J.L. (2009). Body mass index and risk, age of onset, and survival in patients with pancreatic cancer. *JAMA : the journal of the American Medical Association 301*, 2553-2562.

Li, Z., Jiang, J., Wang, Z., Zhang, J., Xiao, M., Wang, C., Lu, Y., and Qin, Z. (2008). Endogenous interleukin-4 promotes tumor development by increasing tumor cell resistance to apoptosis. *Cancer research 68*, 8687-8694.

Liao D., and Johnson R.S. (2007). Hypoxia: A key regulator of angiogenesis in cancer. *Cancer Metastasis Reviews 26*, 281-290.

Lim W., Olschwang S., Keller J. J., Westerman A. M., Menko F. H., Boardman L. A., Scott R. J., Trimbath J., Giardiello F. M., Gruber S. B., Gille J. J., Offerhaus G. J., de Rooij F. W., Wilson J. H., Spigelman A. D., Phillips R. K., and Houlston R. S. (2004). Relative frequency and morphology of cancers in STK11 mutation carriers. *Gastroenterology 126*, 1788–1794.

Lin, E.Y., Nguyen, A.V., Russell, R.G., and Pollard, J.W. (2001). Colony-stimulating factor 1 promotes progression of mammary tumors to malignancy. *The Journal of experimental medicine 193*, 727-740.

Ling, J., Kang, Y., Zhao, R., Xia, Q., Lee, D.F., Chang, Z., Li, J., Peng, B., Fleming, J.B., Wang, H., Liu, J., Lemischka, I.R., Hung, M.C., and Chiao, P.J. (2012). KrasG12D-induced IKK2/beta/NF-kappaB activation by IL-1alpha and p62 feedforward loops is required for development of pancreatic ductal adenocarcinoma. *Cancer cell 21*, 105-120.

Liu, B., Park, E., Zhu, F., Bustos, T., Liu, J., Shen, J., Fischer, S.M., and Hu, Y. (2006). A critical role for I kappaB kinase alpha in the development of human and mouse squamous cell carcinomas. *Proceedings of the National Academy of Sciences of the United States of America 103*, 17202-17207.

Liu, B., Xia, X., Zhu, F., Park, E., Carbajal, S., Kiguchi, K., DiGiovanni, J., Fischer, S.M., and Hu, Y. (2008). IKKalpha is required to maintain skin homeostasis and prevent skin cancer. *Cancer cell 14*, 212-225.

Lobov, I.B., Rao, S., Carroll, T.J., Vallance, J.E., Ito, M., Ondr, J.K., Kurup, S., Glass, D.A., Patel, M.S., Shu, W., Morrisey, E.E., McMahon, A.P., Karsenty, G., and Lang, R.A. (2005). WNT7b mediates macrophage-induced programmed cell death in patterning of the vasculature. *Nature 437*, 417-421.

Loeffler, M., Kruger, J.A., Niethammer, A.G., and Reisfeld, R.A. (2006). Targeting tumor-associated fibroblasts improves cancer chemotherapy by increasing intratumoral drug uptake. *The Journal of clinical investigation 116*, 1955-1962.

Lohr, M., Schmidt, C., Ringel, J., Kluth, M., Muller, P., Nizze, H., and Jesnowski, R. (2001). Transforming growth factor-beta1 induces desmoplasia in an experimental model of human pancreatic carcinoma. *Cancer research 61*, 550-555.

Lowenfels A.B., Maisonneuve P., Whitcomb D. C., Lerch M. M., and DiMagno E. P. (2001) Cigarette Smoking as a Risk Factor for Pancreatic Cancer in Patients With Hereditary Pancreatitis. *JAMA 286*, 169-170.

Lu, P., Takai, K., Weaver, V.M., and Werb, Z. (2011a). Extracellular matrix degradation and remodeling in development and disease. *Cold Spring Harbor perspectives in biology 3*.

Lu, T., Ramakrishnan, R., Altiok, S., Youn, J.I., Cheng, P., Celis, E., Pisarev, V., Sherman, S., Sporn, M.B., and Gabrilovich, D. (2011b). Tumor-infiltrating myeloid cells induce tumor cell resistance to cytotoxic T cells in mice. *The Journal of clinical investigation 121*, 4015-4029.

Lynch, S.M., Vrieling, A., Lubin, J.H., Kraft, P., Mendelsohn, J.B., Hartge, P., Canzian, F., Steplowski, E., Arslan, A.A., Gross, M., Helzlsouer, K., Jacobs, E.J., LaCroix, A., Petersen, G., Zheng, W., Albanes, D., Amundadottir, L., Bingham, S.A., Boffetta, P., Boutron-Ruault, M.C., Chanock, S.J., Clipp, S., Hoover, R.N., Jacobs, K., Johnson, K.C., Kooperberg, C., Luo, J., Messina, C., Palli, D., Patel, A.V., Riboli, E., Shu, X.O., Rodriguez Suarez, L., Thomas, G., Tjonneland, A., Tobias, G.S., Tong, E., Trichopoulos, D., Virtamo, J., Ye, W., Yu, K., Zeleniuch-Jacquette, A., Bueno-de-Mesquita, H.B., and Stolzenberg-Solomon, R.Z. (2009). Cigarette smoking and pancreatic cancer: a pooled analysis from the pancreatic cancer cohort consortium. *American journal of epidemiology 170*, 403-413.

Lynch H. T., Brand R. E., Hogg D., Deters C. A., Fusaro R. M., Lynch J. F., Liu L., Knezetic J., Lassam N. J., Goggins M., and Kern S. (2002). Phenotypic variation in eight extended CDKN2A germline mutation familial atypical multiple mole melanoma-pancreatic carcinoma-prone families: the familial atypical mole melanoma-pancreatic carcinoma syndrome. *Cancer 94*, 84–96.

M

Maeda, G., Chiba, T., Kawashiri, S., Satoh, T., and Imai, K. (2007). Epigenetic inactivation of IkappaB Kinase-alpha in oral carcinomas and tumor progression. *Clinical cancer research : an official journal of the American Association for Cancer Research 13*, 5041-5047.

Maeda, S., Kamata, H., Luo, J.L., Leffert, H., and Karin, M. (2005). IKKbeta couples hepatocyte death to cytokine-driven compensatory proliferation that promotes chemical hepatocarcinogenesis. *Cell 121*, 977-990.

Maisonneuve, P., and Lowenfels, A.B. (2010). Epidemiology of pancreatic cancer: an update. *Digestive diseases 28*, 645-656.

Maitra, A., and Hruban, R.H. (2008). Pancreatic cancer. *Annual review of pathology 3*, 157-188.

Manalo, D.J., Rowan, A., Lavoie, T., Natarajan, L., Kelly, B.D., Ye, S.Q., Garcia, J.G., and Semenza, G.L. (2005). Transcriptional regulation of vascular endothelial cell responses to hypoxia by HIF-1. *Blood 105*, 659-669.

Mantovani, A., Allavena, P., Sica, A., and Balkwill, F. (2008). Cancer-related inflammation. *Nature 454*, 436-444.

Mantovani, A., Sica, A., and Locati, M. (2005). Macrophage polarization comes of age. *Immunity 23*, 344-346.

Mantovani A., Schioppa C., Porta C., Allavena P., Sica A. (2006). Role of tumor associated macrophages in tumor progression and invasion. *Cancer Metastasis Reviews 25*, 315-322.

Mantovani A., Sica A., and Locati M. (2000). Macrophage polarization comes of age. *Immunity 23*, 344-346.

Marinari, B., Moretti, F., Botti, E., Giustizieri, M.L., Descargues, P., Giunta, A., Stolfi, C., Ballaro, C., Papoutsaki, M., Alema, S., Monteleone, G., Chimenti, S., Karin, M., and Costanzo, A. (2008). The tumor suppressor activity of

IKKalpha in stratified epithelia is exerted in part via the TGF-beta antiproliferative pathway. *Proceedings of the National Academy of Sciences of the United States of America 105*, 17091-17096.

Mathupala S. P., Rempel A., and Pedersen P. L. (1997). Aberrant glycolytic metabolism of cancer cells: a remarkable coordination of genetic, transcriptional, post-translational and mutational events that lead to a critical role for type II hexokinase. *J. Bioenerg. Biomembr. 29*, 339-343.

Matoba S., Kang J. G., Patino W. D., Wragg A., Boehm M., Gavrilova O., Hurley P. J., Bunz F., Hwang P. M. (2006). p53 regulates mitochondrial respiration. *Science 312*, 1650-1653.

Maxwell P. H., Dachs G. U., Gleadle J. M., Nicholls L. G., Harris A. L., Stratford I. J., Hankinson O., Pugh C. W., and Ratcliffe P. J. (1997). Hypoxia-inducible factor-1 modulates gene expression in solid tumors and influences both angiogenesis and tumor growth. *Proceedings of the National Academy of Sciences of the United States 94*, 8104-8109.

Mayo, M.W. (1997). Requirement of NF-B Activation to Suppress p53-Independent Apoptosis Induced by Oncogenic Ras. *Science 278*, 1812-1815.

Mazurek, S., Boschek, C.B., Hugo, F., and Eigenbrodt, E. (2005). Pyruvate kinase type M2 and its role in tumor growth and spreading. *Seminars in cancer biology 15*, 300-308.

Medema, R.H., and Bos, J.L. (1993). The role of p21ras in receptor tyrosine kinase signaling. *Critical reviews in oncogenesis 4*, 615-661.

Melani, C., Sangaletti, S., Barazzetta, F.M., Werb, Z., and Colombo, M.P. (2007). Amino-biphosphonate-mediated MMP-9 inhibition breaks the tumor-bone marrow axis responsible for myeloid-derived suppressor cell expansion and macrophage infiltration in tumor stroma. *Cancer research 67*, 11438-11446.

Menetrier-Caux, C., Bain, C., Favrot, M.C., Duc, A., and Blay, J.Y. (1999). Renal cell carcinoma induces interleukin 10 and prostaglandin E2 production by monocytes. *British journal of cancer 79*, 119-130.

Meylan, E., Dooley, A.L., Feldser, D.M., Shen, L., Turk, E., Ouyang, C., and Jacks, T. (2009). Requirement for NF-kappaB signalling in a mouse model of lung adenocarcinoma. *Nature 462*, 104-107.

Michaud, D.S., and Fuchs, C.S. (2005). Obesity and pancreatic cancer: overall evidence and latency period. *Cancer epidemiology, biomarkers & prevention : a publication of the American Association for Cancer Research, cosponsored by the American Society of Preventive Oncology 14*, 2678; author reply 2678-2679.

Mishra, A., Bharti, A.C., Varghese, P., Saluja, D., and Das, B.C. (2006). Differential expression and activation of NF-kappaB family proteins during oral carcinogenesis: Role of high risk human papillomavirus infection. *International journal of cancer Journal international du cancer 119*, 2840-2850.

Miyamoto, Y., Maitra, A., Ghosh, B., Zechner, U., Argani, P., Iacobuzio-Donahue, C.A., Sriuranpong, V., Iso, T., Meszoely, I.M., and Wolfe, M.S. (2003). Notch mediates TGFα-induced changes in epithelial differentiation during pancreatic tumorigenesis. *Cancer cell 3*, 565-576.

Molon, B., Ugel, S., Del Pozzo, F., Soldani, C., Zilio, S., Avella, D., De Palma, A., Mauri, P., Monegal, A., Rescigno, M., Savino, B., Colombo, P., Jonjic, N., Pecanic, S., Lazzarato, L., Fruttero, R., Gasco, A., Bronte, V., and Viola, A. (2011). Chemokine nitration prevents intratumoral infiltration of antigen-specific T cells. *The Journal of experimental medicine 208*, 1949-1962.

Moreno-Sanchez, R., Rodriguez-Enriquez, S., Marin-Hernandez, A., and Saavedra, E. (2007). Energy metabolism in tumor cells. *The FEBS journal 274*, 1393-1418.

Morris, J.P.t., Wang, S.C., and Hebrok, M. (2010). KRAS, Hedgehog, Wnt and the twisted developmental biology of pancreatic ductal adenocarcinoma. *Nature reviews Cancer 10*, 683-695.

Mottram, H.X., Chen, L., Weiping Zou, Ilona Kryczek, Shuang Wei, Linhua Zou, and Gefeng Zhu, P. (2006). Cutting Edge: Induction of B7-H4 on APCs through IL-10: Novel Suppressive Mode for Regulatory T Cells. *The Journal of Immunology 177*, 40-44.

Movahedi, K., Laoui, D., Gysemans, C., Baeten, M., Stange, G., Van den Bossche, J., Mack, M., Pipeleers, D., In't Veld, P., De Baetselier, P., and Van Ginderachter, J.A. (2010). Different tumor microenvironments contain functionally distinct subsets of macrophages derived from Ly6C(high) monocytes. *Cancer research 70*, 5728-5739.

Movassagh, M., Spatz, A., Davoust, J., Lebecque, S., Romero, P., Pittet, M., Rimoldi, D., Lienard, D., Gugerli, O., Ferradini, L., Robert, C., Avril, M.F., Zitvogel, L., and Angevin, E. (2004). Selective, accumulation of mature DC-Lamp(+) dendritic cells in tumor sites is associated with efficient T-cell-mediated antitumor response and control of metastatic dissemination in melanoma. *Cancer research 64*, 2192-2198.

Murdoch, C., Tazzyman, S., Webster, S., and Lewis, C.E. (2007). Expression of Tie-2 by human monocytes and their responses to angiopoietin-2. *J Immunol 178*, 7405-7411.

Murphy, K.M., Brune, K.A., Griffin, C., Sollenberger, J.E., Petersen, G.M., Bansal, R., Hruban, R.H., and Kern, S.E. (2002). Evaluation of candidate genes MAP2K4, MADH4, ACVR1B, and BRCA2 in familial pancreatic cancer: deleterious BRCA2 mutations in 17%. *Cancer research 62*, 3789-3793.

N

Nabel G. J., and Verma I. M. (1993). Proposed NF-kappa B/I kappa B family nomenclature. *Genes & Development* 7, 2063.

Naoko Ohtani, Kimi Yamakoshi, Akiko Takahashi, and Hara, E. (2004). The p16INK4a-RB pathway: molecular link between cellular senescence and tumor suppression. *The Journal of Medical Investigation 51*, 146-153.

Ngo, V.N., Young, R.M., Schmitz, R., Jhavar, S., Xiao, W., Lim, K.H., Kohlhammer, H., Xu, W., Yang, Y., Zhao, H., Shaffer, A.L., Romesser, P., Wright, G., Powell, J., Rosenwald, A., Muller-Hermelink, H.K., Ott, G., Gascoyne, R.D., Connors, J.M., Rimsza, L.M., Campo, E., Jaffe, E.S., Delabie, J., Smeland, E.B., Fisher, R.I., Braziel, R.M., Tubbs, R.R., Cook, J.R., Weisenburger, D.D., Chan, W.C., and Staudt, L.M. (2011). Oncogenically active MYD88 mutations in human lymphoma. *Nature 470*, 115-119.

Nelms, K., Keegan, A.D., Zamorano, J., Ryan, J.J., and Paul, W.E. (1999). The IL-4 receptor: signaling mechanisms and biologic functions. *Annual review of immunology 17*, 701-738.

Niinaka, Y., Paku, S., Haga, A., Watanabe, H., and Raz, A. (1998). Expression and secretion of neuroleukin phosphohexose isomerase maturation factor as autocrine motility factor by tumor cells. *Cancer research 58*, 2667-2674.

Nottingham, L.K., Yan, C.H., Yang, X., Si, H., Coupar, J., Bian, Y., Cheng, T.F., Allen, C., Arun, P., Gius, D., Dang, L., Van Waes, C., and Chen, Z. (2013). Aberrant IKKalpha and IKKbeta cooperatively activate NF-kappaB and induce EGFR/AP1 signaling to promote survival and migration of head and neck cancer. *Oncogene*.

Nowak, N.J., Gaile, D., Conroy, J.M., McQuaid, D., Cowell, J., Carter, R., Goggins, M.G., Hruban, R.H., and Maitra, A. (2005). Genome-wide aberrations in pancreatic adenocarcinoma. *Cancer genetics and cytogenetics 161*, 36-50.

Novitskiy S. V., Ryzhov S., Zaynagetdinov R., Goldstein A. E., Huang Y., Tikhomirov O. Y., Blackburn M. R., Biaggioni I., Carbone D. P., Feoktistov I., Dikov M. M. (2008). Adenosine receptors in regulation of dendritic cell differentiation and function. *Blood 112*, 1822–1831.

Nowicki A., Szenajch J., Ostrowska G., Wojtowicz A., Wojtowicz K., Kruszewski A. A., Maruszynski M., Aukerman S. L., Wiktor-Jedrzejczak W. (1996). Impaired tumor growth in colony-stimulating factor 1 (CSF-1)-deficient, macrophage-deficient op/op mouse: evidence for a role of CSF-1-dependent macrophages in formation of tumor stroma. *Int J Cancer 3*, 112-119.

Nozawa, H., Chiu, C., and Hanahan, D. (2006). Infiltrating neutrophils mediate the initial angiogenic switch in a mouse model of multistage carcinogenesis. *Proceedings of the National Academy of Sciences of the United States of America 103*, 12493-12498.

O

Odegaard, J.I., and Chawla, A. (2011). Alternative macrophage activation and metabolism. *Annual review of pathology 6*, 275-297.

Ojalvo, L.S., Whittaker, C.A., Condeelis, J.S., and Pollard, J.W. (2010). Gene expression analysis of macrophages that facilitate tumor invasion supports a role for Wnt-signaling in mediating their activity in primary mammary tumors. *Journal of immunology 184*, 702-712.

Olovnikov I. A., Kravchenko J. E., and Chumakov P. M. (2009). Homeostatic functions of the p53 tumor suppressor: regulation of energy metabolism and antioxidant defense. *Seminars in Cancer Biology 19*, 32-41.

Orimo, A., Gupta, P.B., Sgroi, D.C., Arenzana-Seisdedos, F., Delaunay, T., Naeem, R., Carey, V.J., Richardson, A.L., and Weinberg, R.A. (2005). Stromal fibroblasts present in invasive human breast carcinomas promote tumor growth and angiogenesis through elevated SDF-1/CXCL12 secretion. *Cell 121*, 335-348.

Ostrand-Rosenberg S., and Sinha P. (2009). Myeloid-Derived Suppressor Cells:Linking Inflammation and Cancer, *Journal of Immunology* 182, 4499-4506.

Otsuki, M., and Tashiro, M. (2007). 4. Chronic pancreatitis and pancreatic cancer, lifestyle-related diseases. *Internal medicine 46*, 109-113.

OuYang, Z., Hirota, Y., Osuga, Y., Hamasaki, K., Hasegawa, A., Tajima, T., Hirata, T., Koga, K., Yoshino, O., Harada, M., Takemura, Y., Nose, E., Yano, T., and Taketani, Y. (2008). Interleukin-4 stimulates proliferation of endometriotic stromal cells. *The American journal of pathology 173*, 463-469.

P

Papandreou, I., Cairns, R.A., Fontana, L., Lim, A.L., and Denko, N.C. (2006). HIF-1 mediates adaptation to hypoxia by actively downregulating mitochondrial oxygen consumption. *Cell metabolism 3*, 187-197.

Pardoll D., and Allison J. (2004). Cancer immunotherapy: breaking the barriers to harvest the crop. Nat Med 10, 887–892.

Park, E., Liu, B., Xia, X., Zhu, F., Jami, W.B., and Hu, Y. (2011). Role of IKKalpha in skin squamous cell carcinomas. *Future oncology 7*, 123-134.

Park, E., Zhu, F., Liu, B., Xia, X., Shen, J., Bustos, T., Fischer, S.M., and Hu, Y. (2007). Reduction in IkappaB kinase alpha expression promotes the development of skin papillomas and carcinomas. *Cancer research 67*, 9158-9168.

Park, K.J., Krishnan, V., O'Malley, B.W., Yamamoto, Y., and Gaynor, R.B. (2005). Formation of an IKKalpha-dependent transcription complex is required for estrogen receptor-mediated gene activation. *Molecular cell 18*, 71-82.

Parlo R. A., and Coleman P. S. (1984). Enhanced rate of citrate export from cholesterol-rich hepatoma mitochondria. *J. Biol. Chem. 259*, 9997-10003.

Pasca di Magliano, M., Sekine, S., Ermilov, A., Ferris, J., Dlugosz, A.A., and Hebrok, M. (2006). Hedgehog/Ras interactions regulate early stages of pancreatic cancer. *Genes & development 20*, 3161-3173.

Perkins, N.D. (2007). Integrating cell-signalling pathways with NF-kappaB and IKK function. *Nature reviews Molecular cell biology 8*, 49-62.

Perkins, N.D. (2012). The diverse and complex roles of NF-kappaB subunits in cancer. *Nature reviews Cancer 12*, 121-132.

Pietras, K., and Ostman, A. (2010). Hallmarks of cancer: interactions with the tumor stroma. *Experimental cell research 316*, 1324-1331.

Pirilä E., Ramamurthy N. S., Sorsa T., Salo T., Hietanen J., and Maisi P. (2003). Gelatinase A (MMP-2), collagenase-2 (MMP-8), and laminin-5 gamma2-chain expression in murine inflammatory bowel disease (ulcerative colitis). *Dig Dis Sci. 48*, 93-98.

Pizer E. S., Wood F. D., Heine H. S., Romantsev F. E., Pasternack G. R., and Kuhajda F. P. (1996). Inhibition of fatty acid synthesis delays disease progression in a xenograft model of ovarian cancer. *Cancer Res. 56*, 1189–1193.
Pollard, P.J., Briere, J.J., Alam, N.A., Barwell, J., Barclay, E., Wortham, N.C., Hunt, T., Mitchell, M., Olpin, S., Moat, S.J., Hargreaves, I.P., Heales, S.J., Chung, Y.L., Griffiths, J.R., Dalgleish, A., McGrath, J.A., Gleeson, M.J., Hodgson, S.V., Poulsom, R., Rustin, P., and Tomlinson, I.P. (2005). Accumulation of Krebs cycle intermediates and over-expression of HIF1alpha in tumours which result from germline FH and SDH mutations. *Human molecular genetics 14*, 2231-2239.

Pollard, J. W. (2009). Trophic macrophages in development and disease. *Nature Reviews Immunology 9*, 259-270.

Pollard, J.W. (2004). Tumor-educated macrophages promote tumor progression and metastasis. *Nature Reviews Cancer 4*, 71-78.

Pólya, George (1945) *How to Solve It: A New Aspect of Mathematical Method*, Princeton, NJ: Princeton University Press. ISBN 0-691-02356-5

Polyak, K., and Weinberg, R.A. (2009). Transitions between epithelial and mesenchymal states: acquisition of malignant and stem cell traits. *Nature reviews Cancer 9*, 265-273.

Porta, C., Larghi, P., Rimoldi, M., Totaro, M.G., Allavena, P., Mantovani, A., and Sica, A. (2009a). Cellular and molecular pathways linking inflammation and cancer. *Immunobiology 214*, 761-777.

Porta, C., Rimoldi, M., Raes, G., Brys, L., Ghezzi, P., Di Liberto, D., Dieli, F., Ghisletti, S., Natoli, G., De Baetselier, P., Mantovani, A., and Sica, A. (2009b). Tolerance and M2 (alternative) macrophage polarization are related processes orchestrated by p50 nuclear factor kappaB. *Proceedings of the National Academy of Sciences of the United States of America 106*, 14978-14983.

Q

Qian, B.Z., and Pollard, J.W. (2010). Macrophage diversity enhances tumor progression and metastasis. *Cell 141*, 39-51.

R

Racker, E., Resnick, R.J., and Feldman, R. (1985). Glycolysis and methylaminoisobutyrate uptake in rat-1 cells transfected with ras or myc oncogenes. *Proceedings of the National Academy of Sciences of the United States of America 82*, 3535-3538.

Raimondi, S., Lowenfels, A.B., Morselli-Labate, A.M., Maisonneuve, P., and Pezzilli, R. (2010). Pancreatic cancer in chronic pancreatitis; aetiology, incidence, and early detection. *Best practice & research Clinical gastroenterology 24*, 349-358.

Rasanen, K., and Vaheri, A. (2010). Activation of fibroblasts in cancer stroma. *Experimental cell research 316*, 2713-2722.

Rodriguez-Prados, J.C., Traves, P.G., Cuenca, J., Rico, D., Aragones, J., Martin-Sanz, P., Cascante, M., and Bosca, L. (2010). Substrate fate in activated macrophages: a comparison between innate, classic, and alternative activation. *Journal of immunology 185*, 605-614.

Rolny, C., Mazzone, M., Tugues, S., Laoui, D., Johansson, I., Coulon, C., Squadrito, M.L., Segura, I., Li, X., Knevels, E., Costa, S., Vinckier, S., Dresselaer, T., Akerud, P., De Mol, M., Salomaki, H., Phillipson, M., Wyns, S., Larsson, E., Buysschaert, I., Botling, J., Himmelreich, U., Van Ginderachter, J.A., De Palma, M., Dewerchin, M., Claesson-Welsh, L., and Carmeliet, P. (2011). HRG inhibits tumor growth and metastasis by inducing macrophage polarization and vessel normalization through downregulation of PlGF. *Cancer cell 19*, 31-44.

Roos D., and Loos J.A. (1973). Changes in the carbohydrate metabolism of mitogenically stimulated human peripheral lymphocytes. II. Relative impor-tance of glycolysis and oxidative phosphorylation on phytohaemagglutinin stimulation. *Exp. Cell Res. 77*, 127–135.

Rosen, E.D., and MacDougald, O.A. (2006). Adipocyte differentiation from the inside out. *Nature reviews Molecular cell biology 7*, 885-896.

Ruffell B., Affara N. I., and Coussens L.M. (2012). Differential macrophage programming in the tumor microenvironment. *Trends in Immunology 33*, 119-126.

S

Saccani, A., Schioppa, T., Porta, C., Biswas, S.K., Nebuloni, M., Vago, L., Bottazzi, B., Colombo, M.P., Mantovani, A., and Sica, A. (2006). p50 nuclear factor-kappaB overexpression in tumor-associated macrophages inhibits M1 inflammatory responses and antitumor resistance. *Cancer research 66*, 11432-11440.

Sanchez-Martinez C., and Aragon J. J. (1997). Analysis of phosphofructokinase subunits and isozymes in ascites tumor cells and its original tissue, murine mammary gland. *FEBS Lett 409*, 86–90.

Sangaletti, S., Di Carlo, E., Gariboldi, S., Miotti, S., Cappetti, B., Parenza, M., Rumio, C., Brekken, R.A., Chiodoni, C., and Colombo, M.P. (2008). Macrophage-derived SPARC bridges tumor cell-extracellular matrix interactions toward metastasis. *Cancer research 68*, 9050-9059.

Sato, N., and Goggins, M. (2006). The role of epigenetic alterations in pancreatic cancer. *Journal of hepato-biliary-pancreatic surgery 13*, 286-295.

Schenk G., Duggleby R. G., and Nixon P. F. (1998). Properties and functions of the thiamin diphosphate dependent enzyme transketolase. *Int J Biochem Cell Biol 30*, 1297–1318.

Schmielau, J., and Finn, O.J. (2001). Activated granulocytes and granulocyte-derived hydrogen peroxide are the underlying mechanism of suppression of t-cell function in advanced cancer patients. *Cancer research 61*, 4756-4760.

Schneider, G., Saur, D., Siveke, J.T., Fritsch, R., Greten, F.R., and Schmid, R.M. (2006). IKKalpha controls p52/RelB at the skp2 gene promoter to regulate G1- to S-phase progression. *EMBO J 25*, 3801-3812.

Scian, M.J., Stagliano, K.E., Anderson, M.A., Hassan, S., Bowman, M., Miles, M.F., Deb, S.P., and Deb, S. (2005). Tumor-derived p53 mutants induce NF-kappaB2 gene expression. *Molecular and cellular biology 25*, 10097-10110.

Schnyder J., and Baggiolini M. (1978). Role of phagocytosis in the activation of macrophages. *J. Exp. Med.148*, 1449–1457.

Schwaab T., Weiss J. E., Schned A. R., and Barth, R. J. (2001). Dendritic cell infiltration in colon cancer. *Journal of Immunotherapy 24*, 130–137.

Selak, M.A., Armour, S.M., MacKenzie, E.D., Boulahbel, H., Watson, D.G., Mansfield, K.D., Pan, Y., Simon, M.C., Thompson, C.B., and Gottlieb, E. (2005). Succinate links TCA cycle dysfunction to oncogenesis by inhibiting HIF-alpha prolyl hydroxylase. *Cancer cell 7*, 77-85.

Senftleben, U., Cao, Y., Xiao, G., Greten, F.R., Krahn, G., Bonizzi, G., Chen, Y., Hu, Y., Fong, A., Sun, S.C., and Karin, M. (2001). Activation by IKKalpha of a second, evolutionary conserved, NF-kappa B signaling pathway. *Science 293*, 1495-1499.

Shankaran, V., Ikeda, H., Bruce, A.T., White, J.M., Swanson, P.E., Old, L.J., and Schreiber, R.D. (2001). IFNgamma and lymphocytes prevent primary tumour development and shape tumour immunogenicity. *Nature 410*, 1107-1111.

Shapiro J. A., Jacobs E. J., and Thun M. J. (2000). Cigar smoking in men and risk of death from tobacco-related cancers. *J Natl Cancer Inst 92*, 333–337.

Shi L.Z., Wang R., Huang G., Vogel P., Neale G., Green D.R., and Chi H. (2011). HIF1alpha-dependent glycolytic pathway orchestrates a metabolic checkpoint for the differentiation of TH17 and Treg cells. *J. Exp. Med. 208*, 1367–1376.

Shojaei, F., Singh, M., Thompson, J.D., and Ferrara, N. (2008). Role of Bv8 in neutrophil-dependent angiogenesis in a transgenic model of cancer progression. *Proceedings of the National Academy of Sciences of the United States of America 105*, 2640-2645.

Shortman K., and Liu Y. J. (2002) Mouse and human dendritic cell subtypes. *Nat Rev Immunol 2*, 151–161.

Siegel P. M., and Massagué J. (2003). Cytostatic and apoptotic actions of TGF-beta in homeostasis and cancer. *Nat Rev Cancer. 3*, 807-821.

Sil A. K., Maeda S., Sano Y., Roop D. R., and Karin M. (2004). IkappaB kinase-alpha acts in the epidermis to control skeletal and craniofacial morphogenesis. *Nature. 428*, 660-664.

Smyth M. J., Godfrey D. I., and Trapani J. A. (2001) A fresh look at tumor immunosurveillance and immunotherapy. *Nat Immunol 2*, 293–299.

Solaini G., Baracca A., Lenaz G., Sgarbi G. (2010). Hypoxia and mitochondrial oxidative metabolism. *Biochim Biophys Acta. 1797*, 1171-1177.

Solaini, G., Sgarbi, G., and Baracca, A. (2011). Oxidative phosphorylation in cancer cells. *Biochimica et biophysica acta 1807*, 534-542.

Spaeth, E.L., Dembinski, J.L., Sasser, A.K., Watson, K., Klopp, A., Hall, B., Andreeff, M., and Marini, F. (2009). Mesenchymal stem cell transition to tumor-associated fibroblasts contributes to fibrovascular network expansion and tumor progression. *PloS one 4*, e4992.

Squadrito M. L., and De Palma M. (2011). Macrophage regulation of tumor angiogenesis: implications for cancer therapy. *Mol Aspects Med. 32*, 123-145.

Stanger, B.Z., Stiles, B., Lauwers, G.Y., Bardeesy, N., Mendoza, M., Wang, Y., Greenwood, A., Cheng, K.H., McLaughlin, M., Brown, D., Depinho, R.A., Wu, H., Melton, D.A., and Dor, Y. (2005). Pten constrains centroacinar cell expansion and malignant transformation in the pancreas. *Cancer cell 8*, 185-195.

Stilmann, M., Hinz, M., Arslan, S.C., Zimmer, A., Schreiber, V., and Scheidereit, C. (2009). A nuclear poly(ADP-ribose)-dependent signalosome confers DNA damage-induced IkappaB kinase activation. *Molecular cell 36*, 365-378.

T

Tabata, T., Fujimori, T., Maeda, S., Yamamoto, M., and Saitoh, Y. (1993). The role of Ras mutation in pancreatic cancer, precancerous lesions, and chronic pancreatitis. *International journal of pancreatology : official journal of the International Association of Pancreatology 14*, 237-244.

Tada, M., Ohashi, M., Shiratori, Y., Okudaira, T., Komatsu, Y., Kawabe, T., Yoshida, H., Machinami, R., Kishi, K., and Omata, M. (1996). Analysis of K-ras gene mutation in hyperplastic duct cells of the pancreas without pancreatic disease. *Gastroenterology 110*, 227-231.

Takeda, K. (1999). Limb and Skin Abnormalities in Mice Lacking IKK. *Science 284*, 313-316.

Thayer, S.P., di Magliano, M.P., Heiser, P.W., Nielsen, C.M., Roberts, D.J., Lauwers, G.Y., Qi, Y.P., Gysin, S., Fernandez-del Castillo, C.F., Yajnik, V., Antoniu, B., McMahon, M., Warshaw, A.L., and Hebrok, M. (2003). Hedgehog is an early and late mediator of pancreatic cancer tumorigenesis. *Nature 425*, 851-856.

Todaro M., Lombardo Y., Francipane M. G., Alea M. P., Cammareri P., Iovino F., Di Stefano A. B., Di Bernardo C., Agrusa A., Condorelli G., Walczak H., and Stassi G. (2008). Apoptosis resistance in epithelial tumors is mediated by tumor-cell-derived interleukin-4. *Cell Death Differ. 15*, 762-772.

Toi, M., Bicknell, R., and Harris, A.L. (1992). Inhibition of colon and breast carcinoma cell growth by interleukin-4. *Cancer research 52*, 275-279.

Tong, X., Zhao, F., and Thompson, C.B. (2009). The molecular determinants of de novo nucleotide biosynthesis in cancer cells. *Current opinion in genetics & development 19*, 32-37.

Trumpower B. L. (1990). The protonmotive Q cycle. Energy transduction by coupling of proton translocation to electron transfer by the cytochrome bc1 complex J. Biol. Chem. 26, 11409–11412.

Tsukihara T., Aoyama H., Yamashita E., Tomizaki T., Yamaguchi H., Shinzawa-Itoh K., Nakashima R., Yaono R., and Yoshikawa S. (1996). The whole structure of the 13-subunit oxidized cytochrome c oxidase at 2.8 A. Science 272, 1136–1144.

Tu, Z., Prajapati, S., Park, K.J., Kelly, N.J., Yamamoto, Y., and Gaynor, R.B. (2006). IKK alpha regulates estrogen-induced cell cycle progression by modulating E2F1 expression. *The Journal of biological chemistry 281*, 6699-6706.

U

Uchiyama A., Essner R., Doi F., Nguyen T., Ramming K. P., Nakamura T., Morton D. L., Hoon D. S. (1996). Interleukin 4 inhibits hepatocyte growth factor induced invasion and migration of colon carcinomas. *J Cell Biochem 62*, 443–453.

V

van Kempen L. C., Rhee J. S., Dehne K., Lee J., Edwards D. R., and Coussens L. M. (2002). Epithelial carcinogenesis: dynamic interplay between neoplastic cells and their microenvironment. *Differentiation. 70*, 610-623.

Vander Heiden, M.G., Cantley, L.C., and Thompson, C.B. (2009). Understanding the Warburg effect: the metabolic requirements of cell proliferation. *Science 324*, 1029-1033.

Vasiljeva, O., Papazoglou, A., Kruger, A., Brodoefel, H., Korovin, M., Deussing, J., Augustin, N., Nielsen, B.S., Almholt, K., Bogyo, M., Peters, C., and Reinheckel, T. (2006). Tumor cell-derived and macrophage-derived cathepsin B promotes progression and lung metastasis of mammary cancer. *Cancer research 66*, 5242-5250.

Vermi, W., Bonecchi, R., Facchetti, F., Bianchi, D., Sozzani, S., Festa, S., Berenzi, A., Cella, M., and Colonna, M. (2003). Recruitment of immature plasmacytoid dendritic cells (plasmacytoid monocytes) and myeloid dendritic cells in primary cutaneous melanomas. *The Journal of pathology 200*, 255-268.

Vizan, P., Boros, L.G., Figueras, A., Capella, G., Mangues, R., Bassilian, S., Lim, S., Lee, W.N., and Cascante, M. (2005). K-ras codon-specific mutations produce distinctive metabolic phenotypes in NIH3T3 mice [corrected] fibroblasts. *Cancer research 65*, 5512-5515.

W

Wahi M. M., Shah N., Schrock C. E., Rosemurgy A. S., and Goldin S. B. (2009). Reproductive factors and risk of pancreatic cancer in women: a review of the literature. *Ann Epidemiol. 19*, 103-111.

Wang, S., Yuan, Y., Liao, L., Kuang, S.Q., Tien, J.C., O'Malley, B.W., and Xu, J. (2009). Disruption of the SRC-1 gene in mice suppresses breast cancer metastasis without affecting primary tumor formation. *Proceedings of the National Academy of Sciences of the United States of America 106*, 151-156.

Wang T., Marquardt C., and Foker J. (1976). Aerobic glycolysis during lymphocyte proliferation. *Nature 261*, 702–705.

Warburg, O. (1956a). On respiratory impairment in cancer cells. *Science 124*, 269–270.

Warburg, O. (1956b). On the origin of cancer cells. *Science 123*, 309–331.

Weinberg, F., Hamanaka, R., Wheaton, W.W., Weinberg, S., Joseph, J., Lopez, M., Kalyanaraman, B., Mutlu, G.M., Budinger, G.R., and Chandel, N.S. (2010). Mitochondrial metabolism and ROS generation are essential for Kras-mediated tumorigenicity. *Proceedings of the National Academy of Sciences of the United States of America 107*, 8788-8793.

Weinberg R. The Biology of Cancer. 7th edition. Taylor & Francis; 2007

Weisz, L., Damalas, A., Liontos, M., Karakaidos, P., Fontemaggi, G., Maor-Aloni, R., Kalis, M., Levrero, M., Strano, S., Gorgoulis, V.G., Rotter, V., Blandino, G., and Oren, M. (2007). Mutant p53 enhances nuclear factor kappaB activation by tumor necrosis factor alpha in cancer cells. *Cancer research 67*, 2396-2401.

Weixin Wang, James L. Abbruzzese, Douglas B. Evans, Lillie Larry, Karen R. Cleary, and Chiao, P.J. (1999). The Nuclear Factor-κ B RelA Transcription Factor Is Constitutively Activated in Human Pancreatic Adenocarcinoma Cells. *Clinical Cancer Research 5*, 119-127.

Wharry, C.E., Haines, K.M., Carroll, R.G., and May, M.J. (2009). Constitutive non-canonical NFkappaB signaling in pancreatic cancer cells. *Cancer biology & therapy 8*, 1567-1576.

Wong, E.T., and Tergaonkar, V. (2009). Roles of NF-kappaB in health and disease: mechanisms and therapeutic potential. *Clinical science 116*, 451-465.

Wu, R.C., Qin, J., Hashimoto, Y., Wong, J., Xu, J., Tsai, S.Y., Tsai, M.J., and O'Malley, B.W. (2002). Regulation of SRC-3 (pCIP/ACTR/AIB-1/RAC-3/TRAM-1) Coactivator Activity by I B Kinase. *Molecular and cellular biology 22*, 3549-3561.

Wu, Z.H., and Miyamoto, S. (2007). Many faces of NF-kappaB signaling induced by genotoxic stress. *Journal of molecular medicine 85*, 1187-1202.

Wu, Z.H., Wong, E.T., Shi, Y., Niu, J., Chen, Z., Miyamoto, S., and Tergaonkar, V. (2010). ATM- and NEMO-dependent ELKS ubiquitination coordinates TAK1-mediated IKK activation in response to genotoxic stress. *Molecular cell 40*, 75-86.

Wyckoff J., Wang W., Lin E. Y., Wang Y., Pixley F., Stanley E. R., Graf T., Pollard J. W., Segall J., and Condeelis, J. (2004). A *paracrine loop* between tumor cells and *macrophages* is required for tumor cell migration in mammary tumors. *Cancer Research 64*, 7022-7029.

Wyckoff, J.B., Wang, Y., Lin, E.Y., Li, J.F., Goswami, S., Stanley, E.R., Segall, J.E., Pollard, J.W., and Condeelis, J. (2007). Direct visualization of macrophage-assisted tumor cell intravasation in mammary tumors. *Cancer research 67*, 2649-2656.

X

Xu, Y., Fang, F., St Clair, D.K., Sompol, P., Josson, S., and St Clair, W.H. (2008). SN52, a novel nuclear factor-kappaB inhibitor, blocks nuclear import of RelB:p52 dimer and sensitizes prostate cancer cells to ionizing radiation. *Molecular cancer therapeutics 7*, 2367-2376.

Y

Yang, J., Splittgerber, R., Yull, F.E., Kantrow, S., Ayers, G.D., Karin, M., and Richmond, A. (2010). Conditional ablation of Ikkb inhibits melanoma tumor development in mice. *The Journal of clinical investigation 120*, 2563-2574.

Yeung S. J., Pan J., and Lee M. H. (2008). Roles of p53, Myc and HIF-1 in regulating glycolysis-the seventh hallmark of cancer. *Cellular and Molecular Life Sciences 65*, 3981-3999.

Ying, H., Kimmelman, A.C., Lyssiotis, C.A., Hua, S., Chu, G.C., Fletcher-Sananikone, E., Locasale, J.W., Son, J., Zhang, H., Coloff, J.L., Yan, H., Wang, W., Chen, S., Viale, A., Zheng, H., Paik, J.H., Lim, C., Guimaraes, A.R., Martin, E.S., Chang, J., Hezel, A.F., Perry, S.R., Hu, J., Gan, B., Xiao, Y., Asara, J.M., Weissleder, R., Wang, Y.A.,

Chin, L., Cantley, L.C., and DePinho, R.A. (2012). Oncogenic Kras maintains pancreatic tumors through regulation of anabolic glucose metabolism. *Cell 149*, 656-670.

Yoon D. Y., Buchler P., Saarikoski S. T., Hines O. J., Reber H. A., and Hankinson O. (2001). Identification of genes differentially induced by hypoxia in pancreatic cancer cells. *Biochemical and Biophysical Research Communications. 288*, 882-886.

Yoshikawa S., Muramoto K., Shinzawa-Itoh K., Aoyama H., Tsukihara T., Shimokata K., Katayama Y., and Shimada H. (2006). Proton pumping mechanism of bovine heart cytochrome c oxidase. Biochim. Biophys. Acta 1757, 1110–1116.

Z

Zabuawala, T., Taffany, D.A., Sharma, S.M., Merchant, A., Adair, B., Srinivasan, R., Rosol, T.J., Fernandez, S., Huang, K., Leone, G., and Ostrowski, M.C. (2010). An ets2-driven transcriptional program in tumor-associated macrophages promotes tumor metastasis. *Cancer research 70*, 1323-1333.

Zavoral, M., Minarikova, P., Zavada, F., Salek, C., and Minarik, M. (2011). Molecular biology of pancreatic cancer. *World journal of gastroenterology : WJG 17*, 2897-2908.

Zeng, G., Germinaro, M., Micsenyi, A., Monga, N.K., Bell, A., Sood, A., Malhotra, V., Sood, N., Midda, V., Monga, D.K., Kokkinakis, D.M., and Monga, S.P. (2006). Aberrant Wnt/beta-catenin signaling in pancreatic adenocarcinoma. *Neoplasia 8*, 279-289.

Zhou, W., Capello, M., Fredolini, C., Piemonti, L., Liotta, L.A., Novelli, F., and Petricoin, E.F. (2011). Proteomic analysis of pancreatic ductal adenocarcinoma cells reveals metabolic alterations. *Journal of proteome research 10*, 1944-1952.

Zhu, F., Xia, X., Liu, B., Shen, J., Hu, Y., Person, M., and Hu, Y. (2007). IKKalpha shields 14-3-3sigma, a G(2)/M cell cycle checkpoint gene, from hypermethylation, preventing its silencing. *Molecular cell 27*, 214-227.

Zou, P. (2005). Immunosuppressive networks in the tumor microenvironment and their therapeuticreevance. *Nature Reviews Cancer 5*, 263-274.

ACKNOWLEDGEMENTS

PhD study was a long way and without people who supported me, it would not be possible to finish this study. Thus, I would like to express my special thanks to,

My supervisor Priv.-Doz. Dr. M. Canan Arkan, for giving me a chance to study on this great project. During this time, I always felt her continuous encourage, believe and trust. Moreover, her precious advices for science and life pushed me to see the things from different aspects and so helped me a lot.

My advisor Prof. Dr. Florian R. Greten, for his valuable comments and continuous support.

My advisor Prof. Dr. Jürgen Ruland, for his inspirational suggestions and evaluations.

My advisors Prof. Dr. Florian R. Greten and Prof. Dr. Jürgen Ruland, for also giving me a chance to gain more experience during my laboratory rotations in their laboratories.

Priv.-Doz. Dr. Mert Erkan and Prof. Dr. Jörg Kleef, for providing human samples for my dissertation research and letting me to make a laboratory rotation in their laboratory.

Prof. Dr. Irene Esposito, for improving the quality of the study with her valuable pathology evaluations.

Priv.-Doz. Hana Algül, for providing one of the required mouse model for my dissertation research.

Olivia Prazeres Da Costa, M.Sc. and Silvia Weidner, for performing microarray experiments and analysis of the data.

Prof. Dr. Martin Klingenspor, for his valuable collaboration.

PhD program coordinator Katrin Offe, for her continuous efforts to guide and support us.

Deutsche Forschungsgemeinchaft, for financial support that made this work possible.

My colleague Jessica Heringer and former colleagues Manon Schulz, Dr. Franziska Romrig and Begüm Aydin for their friendship, contributions to my study and sharing the good and the bad moments.

Technical assistants Kerstin Burmeister, Saskia Ettl and Kathleen Mohs for their professional help, support and friendship.

Members of Greten`s lab; Dr. Ozge Canli, Dr. Tiago De Oliviera, Dr. Hsin-Yu Fang, Michaela A. Diamanti, Begüm Alankus, Paul Ziegler, Julia Varga, Charles Pallangyo, Olga Goncharova and Dr. Abdelhamid Beji for the friendship, continuous encourage and help.

Former lab members; Dr. Sarah Schwitalla, Dr. Arun Mankan, Kristin Retzlaff, Dr. Serkan Göktuna, Dr. Moritz Bennecke, Dr. Julia Bollrath, Dr. Tim Nebelsiek, Dr. Michael Willert, Gülfem Öner, Angela Krebs and Julia Kaerlein, for the friendship, support and relief.

My dear friends Seda Salar and Ahu T. Türker-Yasa, for simply being always there for me.

My dear family, especially my mother Findik Atay and my father Bayram Atay. I am proud of being your daughter and always find myself very lucky for being a part of our family. I am thankful to you for everything; without your presence and support, I could never be at this point.